Studies in Computational Intelligence 373

Oleg Okun
Giorgio Valentini
Matteo Re (Eds.)

Ensembles in Machine Learning Applications

Springer

Studies in Computational Intelligence, Volume 373

Editor-in-Chief
Prof. Janusz Kacprzyk
Systems Research Institute
Polish Academy of Sciences
ul. Newelska 6
01-447 Warsaw
Poland
E-mail: kacprzyk@ibspan.waw.pl

Further volumes of this series can be found on our homepage: springer.com

Vol. 352. Nik Bessis and Fatos Xhafa (Eds.)
Next Generation Data Technologies for Collective Computational Intelligence, 2011
ISBN 978-3-642-20343-5

Vol. 353. Igor Aizenberg
Complex-Valued Neural Networks with Multi-Valued Neurons, 2011
ISBN 978-3-642-20352-7

Vol. 354. Ljupco Kocarev and Shiguo Lian (Eds.)
Chaos-Based Cryptography, 2011
ISBN 978-3-642-20541-5

Vol. 355. Yan Meng and Yaochu Jin (Eds.)
Bio-Inspired Self-Organizing Robotic Systems, 2011
ISBN 978-3-642-20759-4

Vol. 356. Slawomir Koziel and Xin-She Yang (Eds.)
Computational Optimization, Methods and Algorithms, 2011
ISBN 978-3-642-20858-4

Vol. 357. Nadia Nedjah, Leandro Santos Coelho, Viviana Cocco Mariani, and Luiza de Macedo Mourelle (Eds.)
Innovative Computing Methods and their Applications to Engineering Problems, 2011
ISBN 978-3-642-20957-4

Vol. 358. Norbert Jankowski, Włodzisław Duch, and Krzysztof Grąbczewski (Eds.)
Meta-Learning in Computational Intelligence, 2011
ISBN 978-3-642-20979-6

Vol. 359. Xin-She Yang, and Slawomir Koziel (Eds.)
Computational Optimization and Applications in Engineering and Industry, 2011
ISBN 978-3-642-20985-7

Vol. 360. Mikhail Moshkov and Beata Zielosko
Combinatorial Machine Learning, 2011
ISBN 978-3-642-20994-9

Vol. 361. Vincenzo Pallotta, Alessandro Soro, and Eloisa Vargiu (Eds.)
Advances in Distributed Agent-Based Retrieval Tools, 2011
ISBN 978-3-642-21383-0

Vol. 362. Pascal Bouvry, Horacio González-Vélez, and Joanna Kolodziej (Eds.)
Intelligent Decision Systems in Large-Scale Distributed Environments, 2011
ISBN 978-3-642-21270-3

Vol. 363. Kishan G. Mehrotra, Chilukuri Mohan, Jae C. Oh, Pramod K. Varshney, and Moonis Ali (Eds.)
Developing Concepts in Applied Intelligence, 2011
ISBN 978-3-642-21331-1

Vol. 364. Roger Lee (Ed.)
Computer and Information Science, 2011
ISBN 978-3-642-21377-9

Vol. 365. Roger Lee (Ed.)
Computers, Networks, Systems, and Industrial Engineering 2011, 2011
ISBN 978-3-642-21374-8

Vol. 366. Mario Köppen, Gerald Schaefer, and Ajith Abraham (Eds.)
Intelligent Computational Optimization in Engineering, 2011
ISBN 978-3-642-21704-3

Vol. 367. Gabriel Luque and Enrique Alba
Parallel Genetic Algorithms, 2011
ISBN 978-3-642-22083-8

Vol. 368. Roger Lee (Ed.)
Software Engineering, Artificial Intelligence, Networking and Parallel/Distributed Computing 2011, 2011
ISBN 978-3-642-22287-0

Vol. 369. Dominik Ryżko, Piotr Gawrysiak, Henryk Rybinski, and Marzena Kryszkiewicz (Eds.)
Emerging Intelligent Technologies in Industry, 2011
ISBN 978-3-642-22731-8

Vol. 370. Alexander Mehler, Kai-Uwe Kühnberger, Henning Lobin, Harald Lüngen, Angelika Storrer, and Andreas Witt (Eds.)
Modeling, Learning, and Processing of Text Technological Data Structures, 2011
ISBN 978-3-642-22612-0

Vol. 371. Leonid Perlovsky, Ross Deming, and Roman Ilin (Eds.)
Emotional Cognitive Neural Algorithms with Engineering Applications, 2011
ISBN 978-3-642-22829-2

Vol. 372. António E. Ruano and Annamária R. Várkonyi-Kóczy (Eds.)
New Advances in Intelligent Signal Processing, 2011
ISBN 978-3-642-11738-1

Vol. 373. Oleg Okun, Giorgio Valentini, and Matteo Re (Eds.)
Ensembles in Machine Learning Applications, 2011
ISBN 978-3-642-22909-1

Oleg Okun, Giorgio Valentini, and Matteo Re (Eds.)

Ensembles in Machine Learning Applications

Springer

Editors

Dr. Oleg Okun
Stora Trädgårdsgatan 20, läg 1601
21128 Malmö
Sweden
E-mail: olegokun@yahoo.com

Dr. Giorgio Valentini
University of Milan
Department of Computer Science
Via Comelico 39
20135 Milano
Italy
E-mail: valentini@dsi.unimi.it
http://homes.dsi.unimi.it/∼valenti/

Dr. Matteo Re
University of Milan
Department of Computer Science
Office: T303
via Comelico 39/41
20135 Milano
Italia
E-mail: re@dsi.unimi.it
http://homes.dsi.unimi.it/∼re/

ISBN 978-3-642-22909-1 e-ISBN 978-3-642-22910-7

DOI 10.1007/978-3-642-22910-7

Studies in Computational Intelligence ISSN 1860-949X

Library of Congress Control Number: 2011933576

Typeset & *Cover Design:* Scientific Publishing Services Pvt. Ltd., Chennai, India.

Printed on acid-free paper

9 8 7 6 5 4 3 2 1

springer.com

Alla piccola principessa Sara, dai bellissimi occhi turchini
– Giorgio Valentini
To Gregory, Raisa, and Antoshka
– Oleg Okun

Preface

This book originated from the third SUEMA (Supervised and Unsupervised Ensemble Methods and their Applications) workshop held in Barcelona, Spain in September 2010. It continues and follows the tradition of the previous SUEMA workshops – small international events. These events attract researchers interested in ensemble methods – groups of learning algorithms that solve a problem at hand by means of combining or fusing predictions made by members of a group – and their real-world applications. The emphasis on practical applications plays no small part in every SUEMA workshop as we hold the opinion that no theory is vital without demonstrating its practical value.

In 2010 we observed significant changes in both workshop audience and scope of the accepted papers. The audience became younger and different topics, such as Error-Correcting Output Codes and Bayesian Networks, emerged that were not common at the previous workshops. These new trends are good signs for us as workshop organizers as they indicate that young researchers consider ensemble methods as a promising R& D avenue, and the shift in scope means that SUEMA workshops preserved the ability to timely react on changes.

This book is composed of individual chapters written by independent groups of authors. As such, the book chapters can be read without following any pre-defined order. However, we tried to group chapters similar in content together to facilitate reading. The book serves to educate both a seasoned professional and a novice in theory and practice of clustering and classifier ensembles. Many algorithms in the book are accompanied by pseudo code intended to facilitate their adoption and reproduction.

We wish you, our readers, fruitful reading!

Malmö, Sweden — Oleg Okun
Milan, Italy — Giorgio Valentini
Milan, Italy — Matteo Re
May 2011

Acknowledgements

We would like to thank the ECML/PKDD'2010 organizers for the opportunity to hold our workshop at the world-class Machine Learning and Data Mining conference in Barcelona. We would like to thank all authors for their valuable contribution to this book as this book would clearly be impossible without your excellent work. We also deeply appreciate the financial support of PASCAL 2 Network of Excellence in organizing SUEMA'2010.

Prof. Janusz Kacprzyk and Dr. Thomas Ditzinger from Springer-Verlag deserved our special acknowledgment for warm welcome to our book and their support and a great deal of encouragement. Finally, we thank all other people in Springer who participated in the publication process.

Contents

List of Contributors

Giuliano Armano
DIEE- Department of Electrical and Electronic Engineering,
University of Cagliari, Piazza d'Armi, I-09123, Italy
E-mail: armano@diee.unica.it

Alex Aussem
Université de Lyon 1, Laboratoire GAMA, 69622 Villeurbanne, France
E-mail: alex.aussem@univ-lyon1.fr

Xavier Baró
Applied Math and Analysis Department at University of Barcelona,
Gran Via 585 08007 Barcelona, Spain
E-mail: xevi@maia.ub.es

Computer Vision Center, Autonomous University of Barcelona, Spain
E-mail: xavier.baro@cvc.uab.es

Universitat Oberta de Catalunya,
Rambla del Poblenou 158, Barcelona, Spain
E-mail: xbaro@uoc.edu

Miguel Ángel Bautista
Applied Math and Analysis Department, University of Barcelona,
Gran Via 585 08007 Barcelona, Spain
E-mail: miguelangelbautistamartin@gmail.com

Computer Vision Center, Autonomous University of Barcelona, Spain
E-mail: mbautista@cvc.uab.es

Paola Campadelli
Dipartimento di Scienze dell'Informazione, Università degli Studi di Milano, Via Comelico 39-41, 20135 Milano, Italy
E-mail: campadelli@dsi.unimi.it

Pierluigi Casale
Computer Vision Center, Barcelona, Spain
E-mail: pierluigi@cvc.uab.es

Elena Casiraghi
Dipartimento di Scienze dell'Informazione, Università degli Studi di Milano, Via Comelico 39-41, 20135 Milano, Italy
E-mail: casiraghi@dsi.unimi.it

Stefano Ceccon
Department of Information Systems and Computing, Brunel University, Uxbridge UB8 3PH, London, UK
E-mail: stefano.ceccon@brunel.ac.uk

David Crabb
Department of Optometry and Visual Science, City University London, London, UK
E-mail: david.crabb.1@city.ac.uk

Saylisse Davila
Arizona State University, Tempe, AZ
E-mail: saylisse@asu.edu

Houtao Deng
Arizona State University, Tempe, AZ
E-mail: hdeng3@asu.edu

José F. Díez-Pastor
University of Burgos, Spain
E-mail: jfdiez@ubu.es

Rakkrit Duangsoithong
Centre for Vision, Speech and Signal Processing, University of Surrey, Guildford GU2 7XH, United Kingdom
E-mail: r.duangsoithong@surrey.ac.uk

Haytham Elghazel
Université de Lyon 1, Laboratoire GAMA, 69622 Villeurbanne, France
E-mail: haytham.elghazel@univ-lyon1.fr

Sergio Escalera
Applied Math and Analysis Department at University of Barcelona, Gran Via 585 08007 Barcelona, Spain
E-mail: sergio@maia.ub.es

Computer Vision Center, Autonomous University of Barcelona, Spain
E-mail: sergio.escalera@cvc.uab.es

César García-Osorio
University of Burgos, Spain
E-mail: cgosorio@ubu.es

David Garway-Heath
Moorfields Eye Hospital NHS Foundation Trust and UCL Institute of Ophthalmology, London, UK
E-mail: David.Garway-Heath@Moorfields.nhs.uk

Nima Hatami
DIEE- Department of Electrical and Electronic Engineering, University of Cagliari, Piazza d'Armi, I-09123, Italy
E-mail: nima.hatami@diee.unica.it

Gabriele Lombardi
Dipartimento di Scienze dell'Informazione, Università degli Studi di Milano, Via Comelico 39-41, 20135 Milano, Italy
E-mail: lombardi@dsi.unimi.it

Matthijs Moed
Department of Knowledge Engineering, Maastricht University, P.O.BOX 616, 6200 MD Maastricht, The Netherlands
m.moed@student.maastricht-university.nl

Katharina Morik
Technische Universitat Dortmund, Deutschland
E-mail: morik@ls8.cs.tu-dortmund.de

Georgi Nalbantov
Faculty of Health, Medicine and Life Sciences, Maastricht University, P.O.BOX 616, 6200 MD Maastricht, The Netherlands
g.nalbantov@maastricht-university.nl

Carlos Pardo
University of Burgos, Spain
E-mail: cpardo@ubu.es

Florence Perraud
Université de Lyon 1, Laboratoire GAMA, 69622 Villeurbanne, France
E-mail: florence.perraud@univ-lyon1.fr

Oriol Pujol
Applied Math and Analysis Department at University of Barcelona, Gran Via 585 08007 Barcelona, Spain
E-mail: oriol@maia.ub.es

Computer Vision Center, Autonomous University of Barcelona, Spain
E-mail: oriol.pujol@cvc.uab.es

Petia Radeva
Applied Math and Analysis Department at University of Barcelona, Gran Via 585 08007 Barcelona, Spain
E-mail: petia@maia.ub.es

Computer Vision Center, Autonomous University of Barcelona, Spain
E-mail: petia.radeva@cvc.uab.es

Matteo Re
Dipartimento di Scienze dell'Informazione, Università degli Studi di Milano, Via Comelico 39-41, 20135 Milano, Italy
E-mail: re@dsi.unimi.it

Juan J. Rodríguez
University of Burgos, Spain
E-mail: jjrodriguez@ubu.es

Alessandro Rozza
Dipartimento di Scienze dell'Informazione, Università degli Studi di Milano, Via Comelico 39-41, 20135 Milano, Italy
E-mail: rozza@dico.unimi.it

George Runger
Arizona State University Tempe, AZ
E-mail: george.runger@asu.edu

Benjamin Schowe
Technische Universitat Dortmund, Deutschland
E-mail:
schowe@ls8.cs.tu-dortmund.de

Evgueni N. Smirnov
Department of Knowledge Engineering, Maastricht University, P.O.BOX 616, 6200 MD Maastricht, The Netherlands
smirnov@maastricht-university.nl

Raymond S. Smith
Centre for Vision, Speech and Signal Processing, University of Surrey, Guildford, Surrey, GU2 7XH, UK
E-mail:
Raymond.Smith@surrey.ac.uk

Ida Sprinkhuizen-Kuyper
Radboud University Nijmegen, Donders Institute for Brain, Cognition and Behaviour, 6525 HR Nijmegen, The Netherlands
E-mail: i.kuyper@donders.ru.nl

Allan Tucker
Department of Information Systems and Computing, Brunel University, Uxbridge UB8 3PH, London, UK
E-mail:
allan.tucker@brunel.ac.uk

Eugene Tuv
Intel, Chandler, AZ
E-mail: eugene.tuv@intel.com

Giorgio Valentini
Dipartimento di Scienze dell'Informazione, Università degli Studi di Milano, Via Comelico 39-41, 20135 Milano, Italy
E-mail: valentini@dsi.unimi.it

Jordi Vitrià
Applied Math and Analysis Department at University of Barcelona, Gran Via 585 08007 Barcelona, Spain
E-mail: jordo@maia.ub.es

Computer Vision Center, Autonomous University of Barcelona, Spain
E-mail: jordi.vitria@cvc.uab.es

Terry Windeatt
Centre for Vision, Speech and Signal Processing, University of Surrey, Guildford GU2 7XH, United Kingdom
E-mail: t.windeatt@surrey.ac.uk

Berrin Yanikoglu
Sabanci University, Tuzla, Istanbul 34956, Turkey
E-mail: berrin@sabanciuniv.edu

Cemre Zor
27AB05, Centre for Vision, Speech and Signal Processing, University of Surrey, Guildford, Surrey, GU2 7XH, UK
E-mail: c.zor@surrey.ac.uk

Indrė Žliobaitė
Smart Technology Research Centre, Bournemouth University Poole House, Talbot Campus, Fern Barrow, Poole, Dorset, BH12 5BB, UK

Eindhoven University of Technology, P.O. Box 513, 5600 MB Eindhoven, the Netherlands
E-mail: izliobaite@bournemouth.ac.uk

Chapter 1
Facial Action Unit Recognition Using Filtered Local Binary Pattern Features with Bootstrapped and Weighted ECOC Classifiers

Raymond S. Smith and Terry Windeatt

Abstract. Within the context face expression classification using the facial action coding system (FACS), we address the problem of detecting facial action units (AUs). The method adopted is to train a single Error-Correcting Output Code (ECOC) multiclass classifier to estimate the probabilities that each one of several commonly occurring AU groups is present in the probe image. Platt scaling is used to calibrate the ECOC outputs to probabilities and appropriate sums of these probabilities are taken to obtain a separate probability for each AU individually. Feature extraction is performed by generating a large number of local binary pattern (LBP) features and then selecting from these using fast correlation-based filtering (FCBF). The bias and variance properties of the classifier are measured and we show that both these sources of error can be reduced by enhancing ECOC through the application of bootstrapping and class-separability weighting.

1.1 Introduction

Automatic face expression recognition is an increasingly important field of study that has applications in several areas such as human-computer interaction, human emotion analysis, biometric authentication and fatigue detection. One approach to

Raymond S. Smith
13AB05, Centre for Vision, Speech and Signal Processing, University of Surrey, Guildford, Surrey, GU2 7XH, UK
E-mail: Raymond.Smith@surrey.ac.uk

Terry Windeatt
27AB05, Centre for Vision, Speech and Signal Processing, University of Surrey, Guildford, Surrey, GU2 7XH, UK
E-mail: T.Windeatt@surrey.ac.uk

O. Okun et al. (Eds.): Ensembles in Machine Learning Applications, SCI 373, pp. 1–20.
springerlink.com

this problem is to attempt to distinguish between a small set of prototypical emotions such as fear, happiness, surprise etc. In practice, however, such expressions rarely occur in a pure form and human emotions are more often communicated by changes in one or more discrete facial features. For this reason the facial action coding system (FACS) of Ekman and Friesen [8, 19] is commonly employed. In this method, individual facial movements are characterised as one of 44 types known as action units (AUs). Groups of AUs may then be mapped to emotions using a standard code book. Note however that AUs are not necessarily independent as the presence of one AU may affect the appearance of another. They may also occur at different intensities and may occur on only one side of the face. In this chapter we focus on recognising six AUs from the region around the eyes, as illustrated in Fig. 1.1.

AU1 + AU2 + AU5

AU4

AU4 + AU6 + AU7

Fig. 1.1 Some example AUs and AU groups from the region around the eyes. AU1 = inner brow raised, AU2 = outer brow raised, AU4 = brows lowered and drawn together, AU5 = upper eyelids raised, AU6 = cheeks raised, AU7 = lower eyelids raised. The images are shown after manual eye location, cropping, scaling and histogram equalisation.

Initial representation methods for AU classification were based on measuring the relative position of a large number of landmark points on the face [19]. It has been found, however, that comparable or better results can be obtained by taking a more holistic approach to feature extraction using methods such as Gabor wavelets or principal components analysis (PCA) [5]. In this chapter we compare two such methods, namely PCA [20] and local binary pattern (LBP) features [1, 14]. The latter is a computationally efficient texture description method that has the benefit that it is relatively insensitive to lighting variations. LBP has been successfully applied to facial expression analysis [16] and here we take as features the individual histogram bins that result when LBP is applied over multiple sub-regions of an image and at multiple sampling radii.

One problem with the holistic approach is that it can lead to the generation of a very large number of features and so some method must be used to select only those features that are relevant to the problem at hand. For PCA a natural choice is to use only those features that account for most of the variance in the set of training images. For the LBP representation, AdaBoost has been used to select the most relevant features [16]. In this chapter, however, we adopt the very efficient fast correlation-based filtering (FCBF) [23] algorithm to perform this function. FCBF operates by

repeatedly choosing the feature that is most correlated with class, excluding those features already chosen or rejected, and rejecting any features that are more correlated with it than with the class. As a measure of classification, the information-theoretic concept of symmetric uncertainty is used.

To detect the presence of particular AUs in a face image, one possibility is to train a separate dedicated classifier for each AU. Bartlett et. al. for example [2], have obtained good results by constructing such a set of binary classifiers, where each classifier consists of an AdaBoost ensemble based on selecting the most useful 200 Gabor filters, chosen from a large population of such features. An alternative approach [16] is to make use of the fact that AUs tend to occur in distinct groups and to attempt, in the first instance, to recognise the different AU groups before using this information to infer the presence of individual AUs. This second approach is the one adopted in this chapter; it treats the problem of AU recognition as a multiclass problem, requiring a single classifier for its solution. This classifier generates confidence scores for each of the known AU groups and these scores are then summed in different combinations to estimate the likelihood that each of the AUs is present in the input image.

One potential problem with this approach is that, when the number positive indicators for a given AU (i.e. the number of AU groups to which it belongs) differs from the number of negative indicators (i.e. the number of AU groups to which it does not belong), the overall score can be unbalanced, making it difficult to make a correct classification decision. To overcome this problem we apply Platt scaling [15] to the total scores for each AU. This technique uses a maximum-likelihood algorithm to fit a sigmoid calibration curve to a 2-class training set. The re-mapped value obtained from a given input score then represents an estimate of the probability that the given point belongs to the positive class.

The method used in this chapter to perform the initial AU group classification step is to construct an Error-Correcting Output Code (ECOC) ensemble of Multi-Layer Perceptron (MLP) Neural Networks. The ECOC technique [4, 10] has proved to be a highly successful way of solving a multiclass learning problem by decomposing it into a series of 2-class problems, or dichotomies, and training a separate base classifier to solve each one. These 2-class problems are constructed by repeatedly partitioning the set of target classes into pairs of super-classes so that, given a large enough number of such partitions, each target class can be uniquely represented as the intersection of the super-classes to which it belongs. The classification of a previously unseen pattern is then performed by applying each of the base classifiers so as to make decisions about the super-class membership of the pattern. Redundancy can be introduced into the scheme by using more than the minimum number of base classifiers and this allows errors made by some of the classifiers to be corrected by the ensemble as a whole.

In addition to constructing vanilla ECOC ensembles, we make use of two enhancements to the ECOC algorithm with the aim of improving classification performance. The first of these is to promote diversity among the base classifiers by

training each base classifier, not on the full training set, but rather on a bootstrap replicate of the training set [7]. These are obtained from the original training set by repeated sampling with replacement and this results in further training sets which contain, on average, 63% of the patterns in the original set but with some patterns repeated to form a set of the same size. This technique has the further benefit that the out-of-bootstrap samples can also be used for other purposes such as parameter tuning.

The second enhancement to ECOC is to apply weighting to the decoding of base-classifier outputs so that each base classifier is weighted differently for each target class (i.e. AU group). For this purpose we use a method known as class-separability weighting (CSEP) ([17] and Sect. 1.2.1) in which base classifiers are weighted according to their ability to distinguish a given class from all other classes.

When considering the sources of error in statistical pattern classifiers it is useful to group them under three headings, namely Bayes error, bias (strictly this is measured as bias) and variance. The first of these is due to unavoidable noise but the latter two can be reduced by careful classifier design. There is often a tradeoff between bias and variance [9] so that a high value of one implies a low value of the other. The concepts of bias and variance originated in regression theory and several alternative definitions have been proposed for extending them to classification problems [11]. Here we adopt the definitions of Kohavi and Wolpert [13] to investigate the bias/variance characteristics of our chosen algorithms. These have the advantage that bias and variance are non-negative and additive. A disadvantage, however, is that no explicit allowance is made for Bayes error and it is, in effect, rolled into the bias term.

Previous investigation [17, 18, 21] has suggested that the combination of bootstrapping and CSEP weighting improves ECOC accuracy and that this is achieved through a reduction in both bias and variance error. In this chapter we apply these techniques to the specific problem of FACS-based facial expression recognition and show that the results depend on which method of feature extraction is applied. When LBP features are used, in conjunction with FCBF filtering, an improvement in bias and variance is observed; this is consistent with the results found on other datasets. When PCA is applied, however, it appears that any reduction in variance is offset by a corresponding increase in bias so that there is no net benefit from using these ECOC enhancements. This leads to the conclusion that the former feature extraction method is to be preferred to the latter for this problem.

The remainder of this chapter is structured as follows. In Sect. 1.2 we describe the theoretical and mathematical background to the ideas described above. This is followed in Sect. 1.3 by a more detailed exposition, in the form of pseudo-code listings, of how the main novel algorithms presented here may be implemented (an appendix showing executable MATLAB code for the calculation of the CSEP weights matrix is also given in Sect. 1.6). Section 1.4 presents an experimental evaluation of these techniques and Sect. 1.5 summarises the main conclusions to be drawn from this work.

1.2 Theoretical Background

This section describes in more detail the theoretical and mathematical principles underlying the main techniques used in this work.

1.2.1 ECOC Weighted Decoding

The ECOC method consists of repeatedly partitioning the full set of N classes $\Omega = \{\omega_i \mid i = 1 \ldots N\}$ into L super-class pairs. The choice of partitions is represented by an $N \times L$ binary *code matrix* $\mathbf{Z}$. The rows $\mathbf{Z}_i$ are unique *codewords* that are associated with the individual target classes ω_i and the columns $\mathbf{Z}^j$ represent the different super-class partitions. Denoting the jth super-class pair by S^j and $\overline{\mathrm{S}^j}$, element Z_{ij} of the code matrix is set to 1 or 0[1] depending on whether class ω_i has been put into S^j or its complement. A separate base classifier is trained to solve each of these 2-class problems.

Given an input pattern vector $\mathbf{x}$ whose true class $c(\mathbf{x}) \in \Omega$ is unknown, let the soft output from the jth base classifier be $s_j(\mathbf{x}) \in [0,1]$. The set of outputs from all the classifiers can be assembled into a vector $\mathbf{s}(\mathbf{x}) = [s_1(\mathbf{x}), \ldots, s_L(\mathbf{x})]^{\mathrm{T}} \in [0,1]^L$ called the *output code* for $\mathbf{x}$. Instead of working with the soft base classifier outputs, we may also first harden them, by rounding to 0 or 1, to obtain the binary vector $\mathbf{h}(\mathbf{x}) = [h_1(\mathbf{x}), \ldots, h_L(\mathbf{x})]^{\mathrm{T}} \in \{0,1\}^L$. The principle of the ECOC technique is to obtain an estimate $\hat{c}(\mathbf{x}) \in \Omega$ of the class label for $\mathbf{x}$ from a knowledge of the output code $\mathbf{s}(\mathbf{x})$ or $\mathbf{h}(\mathbf{x})$.

In its general form, a *weighted* decoding procedure makes use of an $N \times L$ weights matrix $\mathbf{W}$ that assigns a different weight to each target class and base classifier combination. For each class ω_i we may use the L_1 metric to compute a class score $F_i(\mathbf{x}) \in [0,1]$ as follows:

$$F_i(\mathbf{x}) = 1 - \sum_{\mathrm{j}=1}^{\mathrm{L}} \mathbf{W}_{\mathrm{ij}} \left| \mathrm{s}_{\mathrm{j}}(\mathbf{x}) - \mathbf{Z}_{\mathrm{ij}} \right|, \tag{1.1}$$

where it is assumed that the rows of $\mathbf{W}$ are normalized so that $\sum_{j=1}^{L} \mathbf{W}_{ij} = 1$ for $i = 1 \ldots N$. Patterns may then be assigned to the target class $\hat{c}(\mathbf{x}) = \arg\max_{\omega_i} F_i(\mathbf{x})$. If the base classifier outputs $s_j(\mathbf{x})$ in Eq. 1.1 are replaced by hardened values $h_j(\mathbf{x})$ then this describes the weighted Hamming decoding procedure.

In the context of this chapter Ω is the set of known AU groups and we are also interested in combining the class scores to obtain values that measure the likelihood that AUs are present; this is done by summing the $F_i(\mathbf{x})$ over all ω_i that contain the given AU and dividing by N. That is, the score $G_k \in [0,1]$ for $\mathrm{AU_k}$ is given by:

$$G_k(\mathbf{x}) = \frac{1}{N} \sum_{AU_k \in \omega_i} F_i(\mathbf{x}) \,. \tag{1.2}$$

[1] Alternatively, the values +1 and -1 are often used.

The values of $\mathbf{W}$ may be chosen in different ways. For example, if $\mathbf{W}_{ij} = \frac{1}{L}$ for all i, j then the decoding procedure of Eq. 1.1 is equivalent to the standard unweighted L^1 or Hamming decoding scheme. In this chapter we make use of the CSEP measure [17, 21] to obtain weight values that express the ability of each base classifier to distinguish members of a given class from those of any other class.

In order to describe the class-separability weighting scheme, the concept of a correctness function must first be introduced: given a pattern $\mathbf{x}$ which is known to belong to class ω_i, the correctness function for the jth base classifier takes the value 1 if the base classifier makes a correct prediction for $\mathbf{x}$ and 0 otherwise:

$$C_j(\mathbf{x}) = \begin{cases} 1 & \text{if } h_j(\mathbf{x}) = \mathbf{Z}_{ij} \\ 0 & \text{if } h_j(\mathbf{x}) \neq \mathbf{Z}_{ij} \end{cases}. \tag{1.3}$$

We also consider the complement of the correctness function $\overline{C}_j(\mathbf{x}) = 1 - C_j(\mathbf{x})$ which takes the value 1 for an incorrect prediction and 0 otherwise.

For a given class index i and base classifier index j, the class-separability weight measures the difference between the positive and negative correlations of base classifier predictions, ignoring any base classifiers for which this difference is negative:

$$\mathbf{W}_{ij} = \max\left\{0, \frac{1}{K_i}\left[\sum_{\substack{\mathbf{p} \in \omega_i \\ \mathbf{q} \notin \omega_i}} C_j(\mathbf{p}) C_j(\mathbf{q}) - \sum_{\substack{\mathbf{p} \in \omega_i \\ \mathbf{q} \notin \omega_i}} \overline{C}_j(\mathbf{p}) \overline{C}_j(\mathbf{q})\right]\right\}, \tag{1.4}$$

where patterns $\mathbf{p}$ and $\mathbf{q}$ are taken from a fixed training set T and K_i is a normalization constant that ensures that the ith row of $\mathbf{W}$ sums to 1.

1.2.2 Platt Scaling

It often arises in pattern recognition applications that we would like to obtain a probability estimate for membership of a class but that the soft values output by our chosen classification algorithm are only loosely related to probability. Here, this applies to the scores $G_k(\mathbf{x})$ obtained by applying Eq. 1.2 to detect individual AUs in an image. Ideally, the value of the scores would be balanced, so that a value > 0.5 could be taken to indicate that $\mathrm{AU_k}$ is present. In practice, however, this is often not the case, particularly when $\mathrm{AU_k}$ belongs to more than or less than half the number of AU groups.

To correct for this problem Platt scaling [15] is used to remap the training-set output scores $G_k(\mathbf{x})$ to values which satisfy this requirement. The same calibration curve is then used to remap the test-set scores. An alternative approach would have been to find a separate threshold for each AU but the chosen method has the added advantage that the probability information represented by the remapped scores could

be useful in some applications. Another consideration is that a wide range of thresholds can be found that give low training error so some means of regularisation must be applied in the decision process.

Platt scaling, which can be applied to any 2-class problem, is based on the regularisation assumption that the the correct form of calibration curve that maps classifier scores $G_k(\mathbf{x})$ to probabilities $p_k(\mathbf{x})$, for an input pattern $\mathbf{x}$, is a sigmoid curve described by the equation:

$$p_k(\mathbf{x}) = \frac{1}{1+\exp(AG_k(\mathbf{x})+B)}, \tag{1.5}$$

where the parameters A and B together determine the slope of the curve and its lateral displacement. The values of A and B that best fit a given training set are obtained using an expectation maximisation algorithm on the positive and negative examples. A separate calibration curve is computed for each value of k.

1.2.3 Local Binary Patterns

The local binary pattern (LBP) operator [14] is a powerful 2D texture descriptor that has the benefit of being somewhat insensitive to variations in the lighting and orientation of an image. The method has been successfully applied to applications such as face recognition [1] and facial expression recognition [16]. As illustrated in Fig. 1.2, the LBP algorithm associates each interior pixel of an intensity image with a binary code number in the range 0-256. This code number is generated by taking the surrounding pixels and, working in a clockwise direction from the top left hand corner, assigning a bit value of 0 where the neighbouring pixel intensity is less than that of the central pixel and 1 otherwise. The concatenation of these bits produces an eight-digit binary code word which becomes the grey-scale value of the corresponding pixel in the transformed image. Figure 1.2 shows a pixel being compared with its immediate neighbours. It is however also possible to compare a pixel with others which are separated by distances of two, three or more pixel widths, giving rise to a series of transformed images. Each such image is generated using a different radius for the circularly symmetric neighbourhood over which the LBP code is calculated.

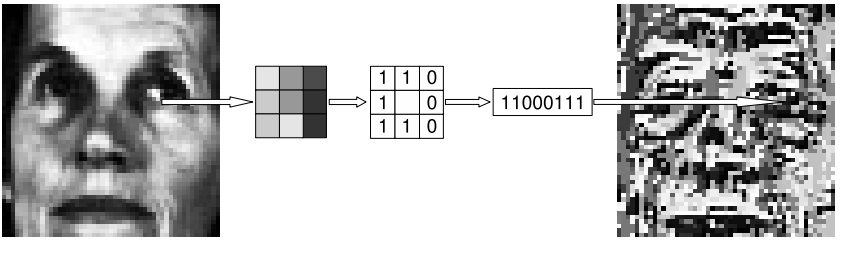

Fig. 1.2 Local binary pattern image production. Each non-border pixel is mapped as shown.

Another possible refinement is to obtain a finer angular resolution by using more than 8 bits in the code-word [14]. Note that the choice of the top left hand corner as a reference point is arbitrary and that different choices would lead to different LBP codes; valid comparisons can be made, however, provided that the same choice of reference point is made for all pixels in all images.

It is noted in [14] that in practice the majority of LBP codes consist of a concatenation of at most three consecutive sub-strings of 0s and 1s; this means that when the circular neighbourhood of the centre pixel is traversed, the result is either all 0s, all 1s or a starting point can be found which produces a sequence of 0s followed by a sequence of 1s. These codes are referred to as uniform patterns and, for an 8 bit code, there are 58 possible values. Uniform patterns are most useful for texture discrimination purposes as they represent local micro-features such as bright spots, flat spots and edges; non-uniform patterns tend to be a source of noise and can therefore usefully be mapped to the single common value 59.

In order to use LBP codes as a face expression comparison mechanism it is first necessary to subdivide a face image into a number of sub-windows and then compute the occurrence histograms of the LBP codes over these regions. These histograms can be combined to generate useful features, for example by concatenating them or by comparing corresponding histograms from two images.

1.2.4 Fast Correlation-Based Filtering

Broadly speaking, feature selection algorithms can be divided into two groups: wrapper methods and filter methods [3]. In the wrapper approach different combinations of features are considered and a classifier is trained on each combination to determine which is the most effective. Whilst this approach undoubtedly gives good results, the computational demands that it imposes render it impractical when a very large number of features needs to be considered. In such cases the filter approach may be used; this considers the merits of features in themselves without reference to any particular classification method.

Fast correlation-based filtering (FCBF) has proved itself to be a successful feature selection method that can handle large numbers of features in a computationally efficient way. It works by considering the classification between each feature and the class label and between each pair of features. As a measure of classification the concept of symmetric uncertainty is used; for a pair random variables X and Y this is defined as:

$$SU(X,Y) = 2\left[\frac{IG(X,Y)}{H(X)+H(Y)}\right] \tag{1.6}$$

where $H(\cdot)$ is the entropy of the random variable and $IG(X,Y) = H(X) - H(X \mid Y) = H(Y) - H(Y \mid X)$ is the information gain between X and Y. As its name suggests, symmetric uncertainty is symmetric in its arguments; it takes values in the range $[0,1]$

where 0 implies independence between the random variables and 1 implies that the value of each variable completely predicts the value of the other. In calculating the entropies of Eq. 1.6, any continuous features must first be discretised.

The FCBF algorithm applies heuristic principles that aim to achieve a balance between using relevant features and avoiding redundant features. It does this by selecting features f that satisfy the following properties:

1. $SU(f,c) \geq \delta$ where c is the class label and δ is a threshold value chosen to suit the application.
2. $\forall g : SU(f,g) \geq SU(f,c) \Rightarrow SU(f,c) \geq SU(g,c)$ where g is any feature other than f.

Here, property 1 ensures that the selected features are relevant, in that they are correlated with the class label to some degree, and property 2 eliminates redundant features by discarding those that are strongly correlated with a more relevant feature.

1.2.5 Principal Components Analysis

Given a matrix of P training patterns $\mathbf{T} \in R^{P \times M}$, where each row consists of a rasterised image of M dimensions, the PCA algorithm [20] consists of finding the eigenvectors (often referred to as eigenimages) of the covariance matrix of the mean-subtracted training images and ranking them in decreasing order of eigenvalue. This gives rise to an orthonormal basis of eigenimages where the first eigenimage gives the direction of maximum variance or scatter within the training set and subsequent eigenimages are associated with steadily decreasing levels of scatter. A probe image can be represented as a linear combination of these eigenimages and, by choosing a cut-off point beyond which the basis vectors are ignored, a reduced dimension approximation to the probe image can be obtained.

More formally, the PCA approach is as follows. The sample covariance matrix of $\mathbf{T}$ is defined as an average outer product:

$$\mathbf{S} = \frac{1}{P} \sum_{i=1}^{P} (\mathbf{T}_i - \mathbf{m})^{\mathrm{T}} (\mathbf{T}_i - \mathbf{m}) \tag{1.7}$$

where $\mathbf{T}_i$ is the ith row of $\mathbf{T}$ and $\mathbf{m}$ is the sample mean row vector given by

$$\mathbf{m} = \frac{1}{P} \sum_{i=1}^{P} \mathbf{T}_i. \tag{1.8}$$

Hence the first step in the PCA algorithm is to find an orthonormal projection matrix $\mathbf{U} = [\mathbf{u}_1, \ldots \mathbf{u}_M]$ that diagonalises $\mathbf{S}$ so that

$$\mathbf{SU} = \mathbf{U}\Lambda \tag{1.9}$$

where Λ is a diagonal matrix of eigenvalues. The columns $\mathbf{u}_q$ of $\mathbf{U}$ then constitute a new orthonormal basis of eigenimages for the image space and we may assume, without loss of generality, that they are ordered so that their associated eigenvalues λ_q form a non-increasing sequence, that is:

$$q < r \Rightarrow \lambda_q \geq \lambda_r \tag{1.10}$$

for $1 \leq q, r \leq M$.

An important property of this transformation is that, with respect to the basis $\{\mathbf{u}_q\}$, the coordinates of the training vectors are de-correlated. Thus each $\mathbf{u}_q$ lies in a direction in which the total scatter between images, as measured over the rows of $\mathbf{T}$, is statistically independent of the scatter in other orthogonal directions. By virtue of Eq. 1.10 the scatter is maximum for $\mathbf{u}_1$ and decreases as the index q increases. For any probe row vector $\mathbf{x}$, the vector $\mathbf{x}' = \mathbf{U}^{\mathrm{T}}(\mathbf{x} - \mathbf{m})^{\mathrm{T}}$ is the projection of the mean-subtracted vector $\mathbf{x} - \mathbf{m}$ into the coordinate system $\{\mathbf{u}_q\}$ with the components being arranged in decreasing order of training set scatter. An approximation to $\mathbf{x}'$ may be obtained by discarding all but the first $K < M$ components to obtain the row vector $\mathbf{x}'' = [x'_1, \ldots, x'_K]$. The value of K is chosen such that the root mean square pixel-by-pixel error of the approximation is below a suitable threshold value. For face data sets it is found in practice that K can be chosen such that $K \ll M$ and so this procedure leads to the desired dimensionality reduction. The resulting linear subspace preserves most of the scatter of the training set and thus permits face expression recognition to be performed within it.

1.3 Algorithms

Section 1.2 presented the theoretical background to the main techniques referred to in this chapter. The aim of this section is to describe in more detail how the novel algorithms used here can be implemented (for details of already established algorithms such as LBP, Platt scaling and FCBF, the reader is referred to the references given in Sect. 1.2). To this end, Fig. 1.3 shows the pseudo-code for the application of bootstrapping to ECOC training, Fig. 1.4 shows how the CSEP weights matrix is calculated and Fig. 1.5 provides details on how the weights matrix is used when ECOC is applied to the problem of calculating AU group membership scores for a probe image.

1.4 Experimental Evaluation

In this section we present the results of performing classification experiments on the Cohn-Kanade face expression database [12]. This dataset contains frontal video clips of posed expression sequences from 97 university students. Each sequence goes from neutral to target display but only the last image has available a ground truth in the form of a manual AU coding. In carrying out these experiments we focused on detecting AUs from the the upper face region as shown in Fig. 1.1. Neutral

Inputs: matrix of training patterns $\mathbf{T} \in R^{P \times M}$, vector of actual class labels $\mathbf{D} \in \{1 \ldots N\}^P$, binary code matrix $\mathbf{Z} \in \{0,1\}^{N \times L}$, base classifier learning algorithm Ψ that, given a training set with binary target labels, outputs a trained base classifier function $B : R^M \mapsto [0,1]$.
Outputs: trained ECOC coding function $E : R^M \mapsto [0,1]^L$.
Create an uninitialised vector $\mathbf{B}$ to hold L base classifier functions.
for i = 1 to L // Loop through all base classifiers
  Create an uninitialised training matrix $\mathbf{T}' \in R^{P \times M}$.
  Create an uninitialised class label vector $\mathbf{D}' \in \{0,1\}^P$.
  for j = 1 to P // Loop through all training patterns
    Let $r \in \{1 \ldots P\}$ be a random integer.
    Set row $\mathbf{T}'_j$ to row $\mathbf{T}_r$ // The feature vector for the rth pattern.
    Let $d = \mathbf{D}_r$ // The true class of the rth pattern.
    Set $\mathbf{D}'_j$ to $Z_{d,i}$ // The modified class for the rth pattern (0 or 1).
  end
  Apply Ψ to $\mathbf{T}'$ and $\mathbf{D}'$ to produce base classifier B_i.
end
Set E to the ECOC coding function that uses $\mathbf{B}$ as base classifiers.

Fig. 1.3 Pseudo-code for training an ECOC ensemble with bootstrapping applied

Inputs: matrix of training patterns $\mathbf{T} \in R^{P \times M}$, vector of actual class labels $\mathbf{D} \in \{1 \ldots N\}^P$, binary code matrix $\mathbf{Z} \in \{0,1\}^{N \times L}$, trained ECOC coding function $E : R^M \mapsto [0,1]^L$.
Outputs: weight matrix $\mathbf{W} \in [0,1]^{N \times L}$ where $\sum_{j=1}^{L} \mathbf{W}_{ij} = 1$, for $i = 1 \ldots N$.
Apply E to each row of $\mathbf{T}$ and round to give prediction matrix $\mathbf{H} \in \{0,1\}^{P \times L}$.
Crate matrix $\mathbf{W} \in [0,1]^{N \times L}$ and initialise to $\mathbf{0}$.
for c = 1 to N // Loop through all class labels
  for i = indices of training patterns where $\mathbf{D}_i = c$
    for j = indices of training patterns where $\mathbf{D}_j \neq c$
      let $d = \mathbf{D}_j$
      for k = 1 to L // Loop through all base classifiers
        if $\mathbf{H}_{ik} = \mathbf{Z}_{ck}$ and $\mathbf{H}_{\mathrm{jk}} = \mathbf{Z}_{\mathrm{dk}}$, add 1 to $\mathbf{W}_{ck}$
          // as the predictions for both patterns $\mathbf{T}_i$ and $\mathbf{T}_j$ are correct.
        if $\mathbf{H}_{ik} \neq \mathbf{Z}_{ck}$ and $\mathbf{H}_{\mathrm{jk}} \neq \mathbf{Z}_{\mathrm{dk}}$, subtract 1 from $\mathbf{W}_{ck}$
          // as the predictions for both patterns $\mathbf{T}_i$ and $\mathbf{T}_j$ are incorrect.
      end
    end
  end
end
Reset all negative entries in $\mathbf{W}$ to 0.
Normalize $\mathbf{W}$ so that each row sums to 1.

Fig. 1.4 Pseudo-code for computing the class-separability weight matrix for ECOC

Inputs: test pattern $\mathbf{x} \in R^M$, binary code matrix $\mathbf{Z} \in \{0,1\}^{N \times L}$, weight matrix $\mathbf{W} \in [0,1]^{N \times L}$ where $\sum_{j=1}^{L} \mathbf{W}_{ij} = 1$ for $i = 1 \ldots N$, trained ECOC coding function $E : R^M \mapsto [0,1]^L$.
Outputs: vector of class label scores $\mathbf{F} \in [0,1]^N$.
Apply E to $\mathbf{x}$ to produce the row vector $\mathbf{s}(\mathbf{x}) \in [0,1]^L$ of base classifier outputs.
Create uninitialised vector $\mathbf{F} \in [0,1]^N$.
for c = 1 to N // Loop through all class labels
Set $\mathbf{F}_c = 1 - \text{abs}(\mathbf{s}(\mathbf{x}) - \mathbf{Z}_c)\,\mathbf{W}_c^T$ where abs $(\bullet)$ is the vector of absolute component values.
// Set $\mathbf{F}_c$ to 1 - the weighted L_1 distance between $\mathbf{s}(\mathbf{x})$ and row $\mathbf{Z}_c$
end

Fig. 1.5 Pseudo-code for weighted ECOC decoding

images were not used and AU groups with three or fewer examples were ignored. In total this led to 456 images being available and these were distributed across the 12 classes shown in Table 1.1. Note that researchers often make different decisions in these areas, and in some cases are not explicit about which choice has been made. This can render it difficult to make a fair comparison with previous results. For example some studies use only the last image in the sequence but others use the neutral image to increase the numbers of negative examples. Furthermore, some researchers consider only images with single AU, whilst others use combinations of AUs. We consider the more difficult problem, in which neutral images are excluded and images contain combinations of AUs. A further issue is that some papers only report overall error rate. This may be misleading since class distributions are unequal, and it is possible to get an apparently low error rate by a simplistic classifier that classifies all images as non-AU. For this reason we also report the area under ROC curve, similar to [2].

Table 1.1 Classes of action unit groups used in the experiments

Class number	1	2	3	4	5	6	7	8	9	10	11	12
AUs present	None	1,2	1,2,5	4	6	1,4	1,4,7	4,7	4,6,7	6,7	1	1,2,4
Number of examples	152	23	62	26	66	20	11	48	22	13	7	6

Each 640 x 480 pixel image we converted to greyscale by averaging the RGB components and the eye centres were manually located. A rectangular window around the eyes was obtained and then rotated and scaled to 150 x 75 pixels. Histogram equalization was used to standardise the image intensities. LBP features were extracted by computing a uniform (i.e. 59-bin) histogram for each sub-window in a non-overlapping tiling of this window. This was repeated with a range of tile sizes (from 12 x 12 to 150 x 75 pixels) and sampling radii (from 1 to 10 pixels).

The histogram bins were concatenated to give 107,000 initial features; these were then reduced to approximately 120 features by FCBF filtering. An FCBF threshold of zero was used; this means that all features were considered initially to be relevant and feature reduction was accomplished by removing redundant features, as described in Sect. 1.2.4.

ECOC ensembles of size 200 were constructed with single hidden-layer MLP base classifiers trained using the Levenberg-Marquardt algorithm. A range of MLP node numbers (from 2 to 16) and training epochs (from 2 to 1024) was tried; each such combination was repeated 10 times and the results averaged. Each run was based on a different randomly chosen stratified training set with a 90/10 training/test set split. The experiments were performed with and without CSEP weighting and with and without bootstrapping. The ECOC code matrices were randomly generated but in such a way as to have balanced numbers of 1s and 0s in each column. Another source of random variation was the initial MLP network weights. When bootstrapping was applied, each base classifier was trained on a separate bootstrap replicate drawn from the complete training set for that run. The CSEP weight matrix was, in all cases, computed from the full training set.

1.4.1 Classifier Accuracy

Table 1.2 shows the mean AU classification error rates and area under ROC figures obtained using these methods (including Platt scaling); the best individual AU classification results are shown in Table 1.3. From Table 1.2 it can be seen that the LBP feature extraction method gives greater accuracy than PCA. Furthermore, LBP is able to benefit from the application of bootstrapping and CSEP weighting, whereas PCA does not. The LBP method thus exhibits behaviour similar to that found on other data sets [17], in that bootstrapping and CSEP weighting on their own each lead to some improvement and the combination improves the results still further. By contrast, PCA performance is not improved by either technique, whether singly or in combination. The reasons for this anomaly, in terms of a bias/variance decomposition of error, are discussed in Sect. 1.4.3.

Table 1.2 Best mean error rates and area under ROC curves for the AU recognition task

Bootstrapping Applied	CSEP Weighting Applied	Error (%)		Area Under ROC	
		PCA	LBP + FCBF	PCA	LBP + FCBF
No	No	9.5	9.0	0.93	0.94
Yes	No	9.8	8.8	0.93	0.94
No	Yes	9.5	9.0	0.93	0.94
Yes	Yes	9.6	**8.5**	0.93	**0.95**

Table 1.3 Best error rates and area under ROC curves for individual AU recognition. LBP feature extraction was used, together with bootstrapping and CSEP weighting. MLPs had 16 nodes and 8 training epochs.

AU no.	1	2	4	5	6	7
Error (%)	8.9	5.4	8.7	4.8	11.2	12.3
Area under ROC	0.94	0.96	0.96	0.97	0.92	0.92

1.4.2 The Effect of Platt Scaling

As noted in Sect. 1.2.2, Platt scaling was used to convert the soft scores G_k from Eq. 1.2 into approximate measures of the probability that AU_k is present. An example of the kind of calibration curves that result from this algorithm is shown in Fig. 1.6 and the effect of applying the mapping to the test set is shown in Fig. 1.7. Note that, before calibration all scores are below 0.5 and hence would be classed as AU not present. After calibration (Fig. 1.7(b)) most of the test patterns that contain AU2 fall to the right hand side of the 0.5 threshold and hence are correctly classified.

Table 1.4 shows the effect on mean error rates and area under ROC curve. It can be seen that AU detection error rates are approximately halved by this procedure but that it has no effect on the area under ROC curve values. The reason for this is that the application of any monotonically increasing function to G_k does not affect the shape of the ROC curve, it only affects the threshold values associated with each point on the ROC curve.

Table 1.4 The effect of applying Platt scaling on error rates and area under ROC curves for AU recognition

Scaling Applied	Error (%)		Area Under ROC	
	PCA	LBP + FCBF	PCA	LBP + FCBF
No	17.5	16.6	0.93	0.95
Yes	9.6	8.5	0.93	0.95

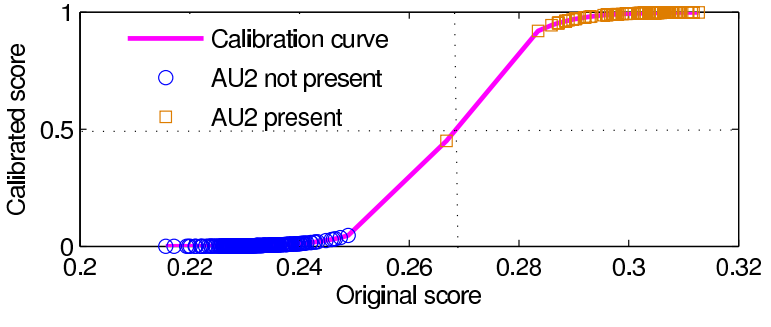

Fig. 1.6 Calibration curve for AU2 training set (bootstrapping plus CSEP weighting applied)

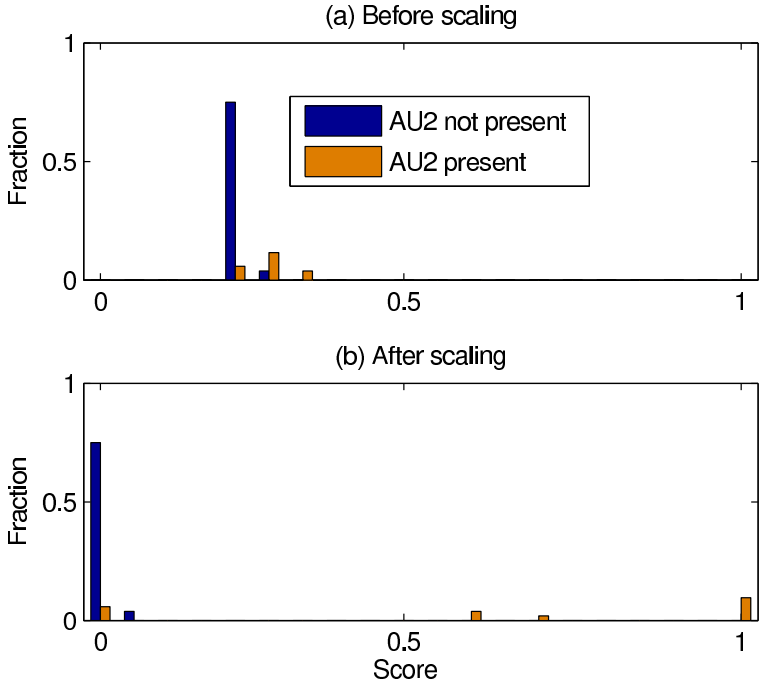

Fig. 1.7 The effect of Platt scaling on the distribution of test-set scores for AU2

1.4.3 A Bias/Variance Analysis

It is instructive to view the performance of these algorithms from the point of view of a bias/variance decomposition of error. Figure 1.8 shows bias and variance curves for AU group recognition when the number of training epochs is varied and other parameter settings are fixed at their respective optimal values. It is notable that, for both types of feature extraction, bias error (which, as noted in Sect. 1.1, includes an unknown amount of Bayes error) predominates. Bias is, however, somewhat higher for PCA (at around 40%) than for LBP (at around 35%). This indicates that LBP is more successful at capturing subtle variations in face expressions than PCA. The downside to this is that LBP feature extraction is more heavily influenced by chance details of the training set and hence shows higher variance (at around 8%) than PCA (at around 4.5%). It is thus evident that these two feature extraction methods are operating at different points on the bias/variance tradeoff curve.

One notable difference between LBP and PCA is that, when ECOC is augmented with bootstrapping and CSEP weighting, the former method benefits by a reduction in both bias and variance; this is consistent with results found on other datasets [18]. For PCA, by contrast, variance is reduced but this is cancelled by an increase in bias so that PCA does not benefit from these methods. This increase in bias appears to be largely due to the application of bootstrapping.

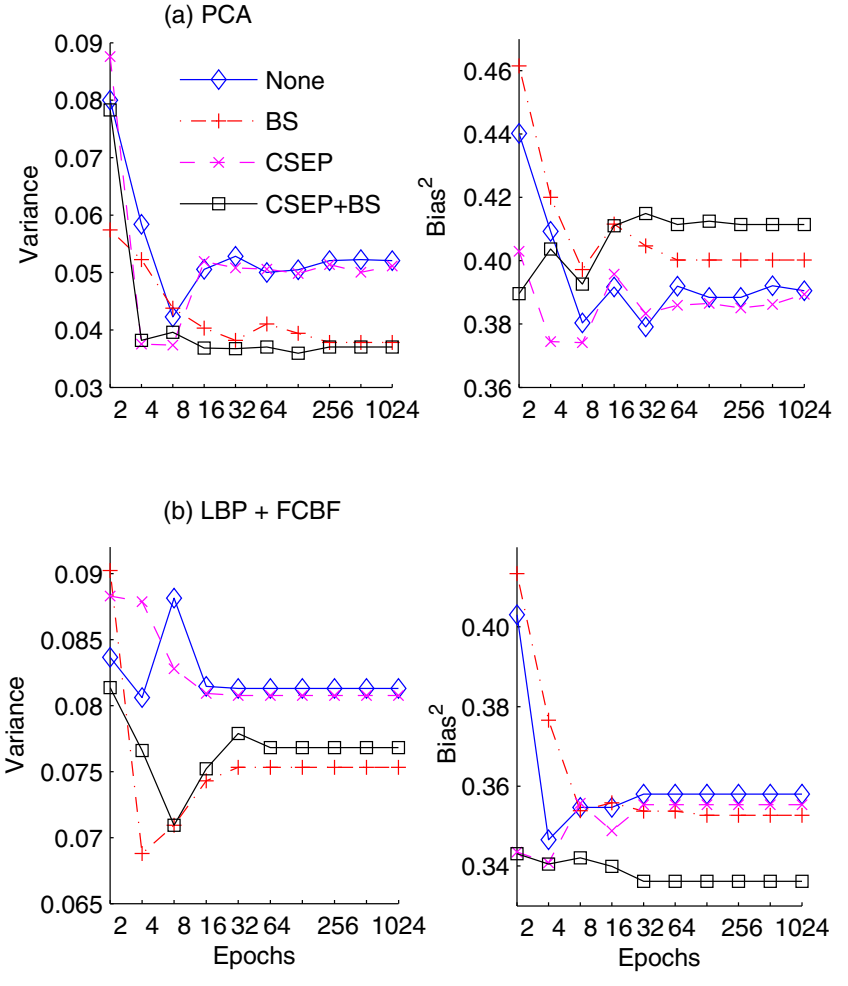

Fig. 1.8 Bias and variance curves for different feature extraction methods using 16-node base classifiers

1.5 Conclusion

In this chapter we have shown that good results on the problem of AU classification can be achieved by using a single multi-class classifier to estimate the probabilities of occurrence of each one of a set of AU groups and then combining the values to obtain individual AU probabilities. An ECOC ensemble of MLP Neural Networks has been shown to perform well on this problem, particularly when enhanced by the application of bootstrapping and CSEP weighting. When combining ECOC outputs

it has been found necessary to apply a score-to-probability calibration technique such as Platt scaling to avoid the bias introduced by different AU group membership numbers.

Two methods of feature extraction have been examined, namely PCA as applied directly to the input images, and the use of LBP to extract a wide range of texture features followed by FCBF filtering to reduce their number. The LBP-based method has been found to be more effective. This is particularly true when combined with bootstrapping and CSEP weighting which lead to a reduction in both bias and variance error.

From an efficiency point of view, it is worth noting that both LBP and FCBF (which is only required during training) are fast lightweight techniques. The use of a single classifier, rather than one per AU, also helps to minimise the computational overheads of AU detection.

Acknowledgements. This work was supported by EPSRC grant E061664/1. The authors would also like to thank the providers of the PRTools [6] and Weka [22] software.

1.6 Code Listings

The following MATLAB code may be used to compute a CSEP weights matrix. Note that this code uses some of the classes and functions from the PRTools [6] toolkit.

```
function wtgMat = computeCsepMatrix(
    trgData,codeMatrix);

% Compute the class-separability weights matrix.
% trgData = training set (a PRTools dataset)
% codeMatrix = the ECOC code matrix of 1's and 0's
% wtgMat = the returned CSEP weights matrix

[numClasses numBase] = size(codeMatrix);
binData=logical(round(getdata(trgData)));
% Weighting requires binarized results
patternNlabs = getnlab(trgData);
% A col vector of per pattern dense class numbers
numPatterns = length(patternNlabs);
ecocErrorMatrix = xor(binData,
codeMatrix(patternNlabs,:));
% Populate matrix which shows where the base
% classifiers went wrong wrt the ECOC targets
ecocCorrectMatrix = ~ecocErrorMatrix;
% The matrix of correct decisons
wtgMat = zeros(size(codeMatrix));
for nlab = 1:numClasses
```

```
  posSet = patternNlabs == nlab;
  % Patterns which belong to the class
  numPosSet = sum(posSet);
  negSet = ~posSet;
  % Patterns which belong to other classes
  numNegSet = numPatterns - numPosSet;
  baseN11s = computePattBaseCounts(posSet,numPosSet,
  negSet,numNegSet,ecocCorrectMatrix);
  % The counts of correct decision pairs
  % per base classifier
  baseN00s = computePattBaseCounts(posSet,numPosSet,
  negSet,numNegSet,ecocErrorMatrix);
  % The counts of bad decison pairs
  % per base classifier
  wtgMat(nlab,:) = baseN11s - baseN00s;
end
wtgMat(wtgMat < 0) = 0;
% Ignore base classifiers with negative counts
wtgMat = wtgMat ./ repmat(sum(wtgMat,2),1,numBase);
% Normalise to sum to 1 along the rows


function counts = computePattBaseCounts(
posSet,numPosSet,negSet,numNegSet,testMatrix)

% Compare a set of patterns divided into positive and
% negative sets by anding together respective pairs of
% matrix rows.
% posSet = logical pattern markers for the positive set
% numPosSet = number of patterns in posSet
% negSet = logical pattern markers for the negative set
% numNegSet = number of patterns in negSet
% testMatrix = logical matrix of values for all
% patterns [numPatterns,numBase]
% counts = returned matrix of pattern pair counts per
% base classifier wrt. the given testMatrix

% Compare each member of group1 with each member of
% group2 and sum over the other group
testMatrix1 = repmat(testMatrix(posSet,:),
[1,1,numNegSet]);
testMatrix1 = permute(testMatrix1,[1 3 2]);
% Dimensions are [posSet,negSet,baseCfrs]
testMatrix2 = repmat(testMatrix(negSet,:),
[1,1,numPosSet]);
testMatrix2 = permute(testMatrix2,[3 1 2]);
```

```
% Dimensions are [posSet,negSet,baseCfrs]
coincidenceMatrix = testMatrix1 & testMatrix2;
counts = squeeze(sum(sum(coincidenceMatrix,2)))';
% Dimensions are [1,baseCfrs]
```

References

1. Ahonen, T., Hadid, A., Pietikainen, M.: Face description with local binary patterns: Application to face recognition. IEEE Trans. Pattern Analysis and Machine Intell. 28, 2037–2041 (2006)
2. Bartlett, M.S., Littlewort, G., Frank, M.G., Lainscsek, C., Fasel, I.R., Movellan, J.R.: Fully automatic facial action recognition in spontaneous behavior. In: Proc. 7th IEEE Int. Conf. Automatic Face and Gesture Recogn., Southampton, UK, pp. 223–230. IEEE Comp. Society, Los Alamitos (2006)
3. Das, S.: Filters, wrappers and a boosting-based hybrid for feature selection. In: Brodley, C.E., Pohoreckyj Danyluk, A. (eds.) Proc. 18th Int. Conf. Machine Learning, Williamstown, MA, pp. 74–81. Morgan Kaufmann, San Francisco (2001)
4. Dietterich, T.G., Bakiri, G.: Solving multiclass learning problems via error-correcting output codes. J. Artif. Intell. Research 2, 263–286 (1995)
5. Donato, G., Bartlett, M.S., Hager, J.C., Ekman, P., Sejnowski, T.J.: Classifying facial actions. IEEE Trans. Pattern Analysis and Machine Intell. 21, 974–989 (1999)
6. Duin, R.P.W., Juszczak, P., Paclik, P., Pekalska, E., de Ridder, D., Tax, D.M.J., Verzakov, S.: PRTools 4.1, A Matlab toolbox for pattern recognition. Delft University of Technology (2007)
7. Efron, B., Tibshirani, R.J.: An introduction to the bootstrap. Chapman & Hall/CRC Press, Boca Raton (1993)
8. Ekman, P., Friesen, W.V.: The facial action coding system: A technique for the measurement of facial movement. Consulting Psychologists Press, Palo Alto (1978)
9. Geman, S., Bienenstock, E.: Neural networks and the bias/variance dilemma. Neural Comp. 4, 1–58 (1992)
10. James, G.: Majority vote classifiers: Theory and applications. PhD Dissertation, Stanford University (1998)
11. James, G.: Variance and bias for general loss functions. Machine Learning 51, 115–135 (2003)
12. Kanade, T., Cohn, J.F., Tian, Y.: Comprehensive database for facial expression analysis. In: Proc. 4th Int. Conf. Automatic Face and Gesture Recognition, Grenoble, France, pp. 46–53. IEEE Comp. Society, Los Alamitos (2000)
13. Kohavi, R., Wolpert, D.: Bias plus variance decomposition for zero-one loss functions. In: Proc. 13th Int. Conf. on Machine Learning, Bari, Italy, pp. 275–283. Morgan Kaufmann, San Francisco (1996)
14. Ojala, T., Pietikäinen, M., Mäenpää, T.: Multiresolution gray-scale and rotation invariant texture classification with local binary patterns. IEEE Trans. Pattern Analysis and Machine Intell. 24, 971–987 (2002)
15. Platt, J.: Probabilistic outputs for support vector machines and comparison to regularized likelihood methods. In: Smola, A.J., Bartlett, P., Scholkopf, B., Schuurmans, D. (eds.) Advances in Large Margin Classifiers, pp. 61–74. MIT Press, Cambridge (1999)
16. Shan, C., Gong, S., McOwan, P.W.: Facial expression recognition based on local binary patterns: A comprehensive study. Image and Vision Comp. 27, 803–816 (2009)

17. Smith, R.S., Windeatt, T.: Class-separability weighting and bootstrapping in error correcting output code ensembles. In: El Gayar, N., Kittler, J., Roli, F. (eds.) MCS 2010. LNCS, vol. 5997, pp. 185–194. Springer, Heidelberg (2010)
18. Smith, R.S., Windeatt, T.: A Bias-variance analysis of bootstrapped class-separability weighting for error-correcting output code ensembles. In: Proc. 22nd IEEE Int. Conf. Pattern Recogn., Istanbul, Turkey, pp. 61–64. IEEE Comp. Society, Los Alamitos (2010)
19. Tian, Y.-I., Kanade, T., Cohn, J.F.: Recognizing action units for facial expression analysis. IEEE Trans. Pattern Analysis and Machine Intell. 23, 97–115 (2001)
20. Turk, M., Pentland, A.: Eigenfaces for recognition. J. Cognitive Neuroscience 3, 71–86 (1991)
21. Windeatt, T., Smith, R.S., Dias, K.: Weighted decoding ECOC for facial action unit classification. In: Okun, O., Valentini, G. (eds.) Proc. 2nd Supervised and Unsupervised Ensemble Methods and their Applications, Patras, Greece, pp. 26–30 (2008)
22. Witten, I.H., Frank, E.: Data mining: Practical machine learning tools and techniques. Morgan Kaufmann, San Francisco (2005)
23. Yu, L., Liu, H.: Feature selection for high-dimensional data: A fast correlation-based filter solution. In: Fawcett, T., Mishra, N. (eds.) Proc. 20th Int. Conf. Machine Learning, Washington DC, pp. 856–863. AAAI Press, Menlo Park (2003)

Chapter 2
On the Design of Low Redundancy Error-Correcting Output Codes

Miguel Ángel Bautista, Sergio Escalera, Xavier Baró, Oriol Pujol, Jordi Vitrià, and Petia Radeva

Abstract. The classification of large number of object categories is a challenging trend in the Pattern Recognition field. In the literature, this is often addressed using an ensemble of classifiers . In this scope, the Error-Correcting Output Codes framework has demonstrated to be a powerful tool for combining classifiers. However, most of the state-of-the-art ECOC approaches use a linear or exponential number of classifiers, making the discrimination of a large number of classes unfeasible. In this paper, we explore and propose a compact design of ECOC in terms of the number of classifiers. Evolutionary computation is used for tuning the parameters of the classifiers and looking for the best compact ECOC code configuration. The results over several public UCI data sets and different multi-class Computer Vision problems show that the proposed methodology obtains comparable (even better) results than the state-of-the-art ECOC methodologies with far less number of dichotomizers.

2.1 Introduction

Nowadays challenging applications of Pattern Recognition deal with changing environments, online adaptations, contextual information, etc. In order to deal with

Miguel Ángel Bautista · Sergio Escalera · Xavier Baró · Oriol Pujol · Jordi Vitrià · Petia Radeva
Applied Math and Analysis Department at University of Barcelona, Gran Via, 585 08007 Barcelona, Spain
E-mail: miguelangelbautistamartin@gmail.com, {sergio,xevi,oriol,petia,jordi}@maia.ub.es

Computer Vision Center, Autonomous University of Barcelona, Edificio O Campus UAB, Cerdanyola, Spain
E-mail: mbautista,sergio.escalera,xavier.baro,oriol.pujol, {petia.radeva,jordi.vitria}@cvc.uab.es

Xavier Baró
Universitat Oberta de Catalunya, Rambla del Poblenou 158, Barcelona, Spain
E-mail: xbaro@uoc.edu

O. Okun et al. (Eds.): Ensembles in Machine Learning Applications, SCI 373, pp. 21–38.
springerlink.com

all these problems, efficient ways for processing huge amount of data are often required. One clear example is the case of general Pattern Recognition algorithms for classification, especially when the number of categories, namely objects, people, brands, etc, is arbitrarily large. Usual Machine Learning strategies are effective for dealing with small number of classes. The choices are limited when the number of classes becomes large. In that case, the natural algorithms to consider are those that model classes in an implicit way, such as instance based learning (i.e. nearest neighbours). However, this choice is not necessarily the most adequate for a given problem. Moreover, we are forgetting many algorithms of the literature such as ensemble learning (i.e. AdaBoost [12]) or kernel based discriminant classifiers (i.e. Support Vector Machines [20]) that have been proven to be very powerful tools.

Most of state-of-the-art multi-class architectures need to deal with the discrimination of each class either by modelling its probability density function, or by storing a classification boundary and using some kind of aggregation/selection function to obtain a final decision. Another way to deal with this kind of problems is to use a divide-and-conquer approach. Instead of extending a method to cope with the multi-class case, one can divide the multi-class problem into smaller binary problems and then combine their responses using some kind of committee strategy, such as voting. In literature, one can roughly find three main lines of research in the last tendency: flat strategies, hierarchical classification , and Error-Correcting Output Codes (ECOC). Flat strategies consist of using some predefined problem partition followed by some kind of voting strategy. Good examples of this line are strategies like one-against-all or all-pairs. Hierarchical classification relies on some similarity metric among classes for creating a binary tree in which at each node a particular partition of the classes is considered. Finally, ECOC encodes different partitions of the problem in a matrix of codewords (one codeword per class) and the final decision is obtained by looking at the most similar codeword at the test step. ECOC can be regarded as a generalization of the former strategies since it allows the inclusion of flat strategies as well as hierarchical classifiers [22]. Moreover, the analysis of the ECOC error evolution has demonstrated that ECOC corrects errors caused by the bias and the variance of the learning algorithm [8][1]. However, note that by construction or in order to obtain the desired performance, most of the strategies need between N and N^2 classifiers, given N different classes. Although this is adequate and acceptable when the number of classes is small, it becomes prohibitive when the number of classes becomes large. This number of classifiers has been recently reduced in some ECOC designs, such as the DECOC approach of [22], that requires $N-1$ classifiers. The Dense Random and Sparse Random designs [2] also reduce this number of classifiers to $15log_2(N)$ and $10log_2(N)$, respectively. However this kind of approaches design the problems without taking into account the underlying distribution of the class characteristics.

[1] The bias term describes the component of the error that results from systematic errors of the learning algorithm. The variance term describes the component of the error that results from random variation and noise in the training samples and random behaviour of the learning algorithm. For more details, see [8].

The goal of this paper is to propose and evaluate different general ways of making the multi-class pattern recognition problem tractable when the number of categories makes most of the models computationally unfeasible. In particular, we are interested in methods that scale sub-linearly with the number of classes, allowing their applicability in general Pattern Recognition problems. The proposal relies on the Error-Correcting Output Codes framework, reducing the number of binary classifiers that have to be trained in the ensemble. Following the Occam razor principle, we propose a compact ECOC design of size $log_2(N)$ in terms of the number of classifiers. An evolutionary approximation, similar to the one proposed in [17] is proposed for tuning the parameters of the classifiers and looking for a compact design with high generalization capability. Moreover, this design is problem dependent in the sense that the evolved ECOC fits the distribution of the object characteristics. The novel compact ECOC is compared with the state-of-the-art ECOC approaches, obtaining comparable (even better results) when classifying several object categories in different Pattern Recognition applications with far less cost.

The paper is organized as follows: Section 2 presents the compact ECOC design. Section 3 evaluates the novel methodology by comparing it with the state-of-the-art approaches on public and challenging Pattern Recognition Applications. Finally, Sect. 4 concludes the paper.

2.2 Compact Error-Correcting Output Codes

In this section, we review the ECOC framework and propose a compact ECOC design in terms of the number of classifiers.

2.2.1 Error-Correcting Output Codes

Given a set of N classes to be learned in an ECOC framework, n different bipartitions (groups of classes) are formed, and n binary problems (dichotomizers) over the partitions are trained. As a result, a codeword of length n is obtained for each class, where each position (bit) of the code corresponds to a response of a given dichotomizer (coded by $+1$ or -1 according to their class set membership). Arranging the codewords as rows of a matrix, we define a *coding matrix* M, where $M \in \{-1,+1\}^{N\times n}$ in the binary case. In Fig. 2.1 we show an example of a binary coding matrix M. The matrix is coded using five dichotomizers $\{h_1,...,h_5\}$ for a 4-class problem $\{c_1,...,c_4\}$ of respective codewords $\{y_1,...,y_4\}$. The hypotheses are trained by considering the labelled training data samples $\{(\rho_1,l(\rho_1)),...,(\rho_m,l(\rho_m))\}$ for a set of m data samples. The white and black regions of the coding matrix M are coded by $+1$ and -1, respectively. For example, the first classifier is trained to discriminate c_3 against c_1, c_2, and c_4; the second one classifies c_2 and c_3 against c_1 and c_4, and so on, as follows:

$$h_1(x) = \begin{cases} 1 & \text{if } x \in \{c_3\} \\ -1 & \text{if } x \in \{c_1,c_2,c_4\} \end{cases}, \ldots, \quad h_5(x) = \begin{cases} 1 & \text{if } x \in \{c_2,c_4\} \\ -1 & \text{if } x \in \{c_1,c_3\} \end{cases} \tag{2.1}$$

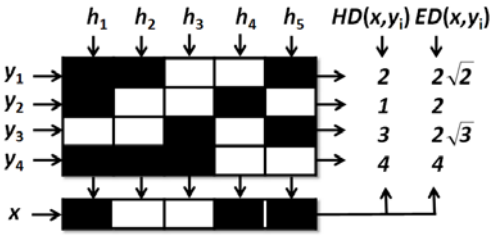

Fig. 2.1 Binary ECOC design for a 4-class problem. An input test codeword x is classified by class c_2 using the Hamming or the Euclidean Decoding.

The standard binary coding designs are the one-versus-all [19] strategy with N dichotomizers and the dense random strategy [2], with $10\log_2 N$ classifiers. In the case of the ternary symbol-based ECOC, the coding matrix becomes $M \in \{-1,0,+1\}^{N\times n}$. In this case, the symbol zero means that a particular class is not considered for a given classifier. In this ternary framework, the standard designs are the one-versus-one strategy [13] and the sparse random strategy [2], with $\frac{N(N-1)}{2}$ and $15\log_2 N$ binary problems, respectively.

During the decoding process, applying n binary classifiers, a code x is obtained for each data sample ρ in the test set. This code is compared to the base codewords $(y_i, i \in [1,..,N])$ of each class defined in the matrix M, and the data sample is assigned to the class with the *closest* codeword. In Fig. 2.1, the new code x is compared to the class codewords $\{y_1,...,y_4\}$ using Hamming [19] and Euclidean Decoding [2]. The test sample is classified by class c_2 in both cases, correcting one bit error.

In the literature, there roughly exists three different lines for decoding [9]: those based on similarity measurements, including the Hamming and Euclidean decoding [19], probabilistic approaches [21], and loss-functions strategies [2].

2.2.2 Compact ECOC Coding

Although the use of large codewords was initially suggested in order to correct as many errors as possible at the decoding step, high effort has been put into improving the robustness of each individual dichotomizer so that compact codewords can be defined in order to save time. In this way, the one-versus-all ECOC has been widely applied for several years in the binary ECOC framework (see Fig. 2.2). Although the use of a reduced number of binary problems often implies dealing with more data per classifier (i.e. compared to the one-versus-one coding), this approach has been defended by some authors in the literature demonstrating that the one-versus-all technique can reach comparable results to the rest of combining strategies if

the base classifier is properly tuned [23]. Recently, this codeword length has been reduced to $N-1$ in the DECOC approach of [22], where the authors codify $N-1$ nodes of a binary tree structure as dichotomizers of a ternary problem-dependent ECOC design. In the same line, several problem-dependent designs have been recently proposed [5, 10, 22, 24]. The new techniques are based on exploiting the problem domain by selecting the representative binary problems that increase the generalization performance while keeping the code length "relatively" small. Figure 2.2 shows the number ofdichotomizers required for the ECOC configurations of the state-of-the-art for different number of classes. The considered codings are: one-versus-all, one-versus-one, Dense random, Sparse random, DECOC and Compact ECOC [2, 10, 13, 19, 22].

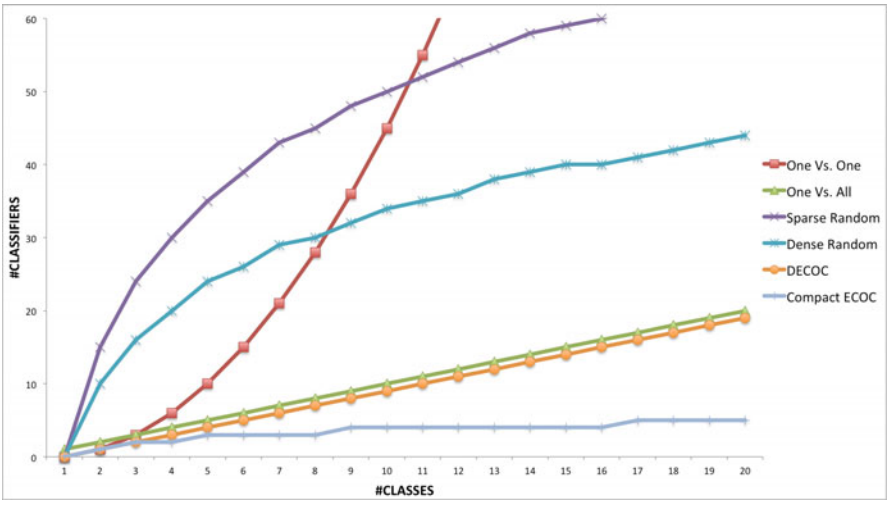

Fig. 2.2 Minimum number of dichotomizers required for each ECOC configuration and different number of classes

Although one-versus-all, DECOC, dense, and sparse random approaches have a relatively small codeword length, we can take advantage of the information theory principles to obtain a more compact definition of the codewords. Having a N-class problem, the minimum number of bits necessary to codify and univocally distinguish N codes is:

$$B = \lceil \log_2 N \rceil, \tag{2.2}$$

where $\lceil . \rceil$ rounds to the upper integer.

For instance, we can think of a codification where the class codewords correspond to the N first Gray or binary code sequences of B bits, defining the Gray or binary compact ECOC designs. Note that this design represents the compact

ECOC codification in terms of the codeword length. An example of a binary compact ECOC, Gray compact ECOC, and one-versus-all ECOC designs for a 8-class problem are shown in Fig. 2.3. The white and black positions correspond to the symbols $+1$ and -1, respectively. The reduced number of classifiers required by this design in comparison with the state-of-the-art approaches is shown in the graphic of Fig. 2.2.

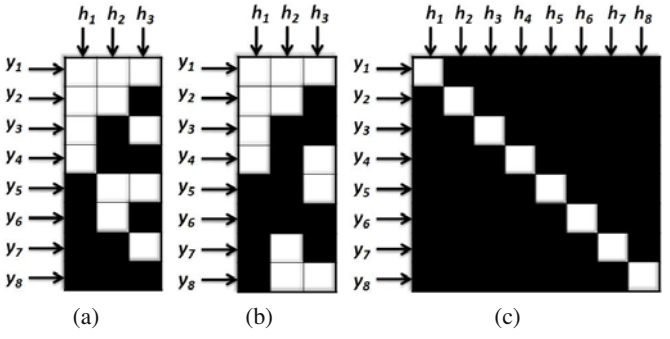

Fig. 2.3 (a) Binary compact, (b) Gray compact, and (c) one-versus-all ECOC coding designs of a 8-class problem

Besides exploring predefined binary or Gray compact coding matrices, we also propose the design of a different compact codification of M based on the distribution of the data and the characteristics of the applied base classifier, which can increase the discrimination capability of the system. However, finding a suitable compact ECOC matrix for an $N-$class problem requires to explore all the possible $N \times B$ binary matrices, where B is the minimum codeword length in order to define a valid ECOC matrix. For this reason, we also propose an evolutionary parametrization of the compact ECOC design.

2.2.2.1 Evolutionary Compact Parametrization

When defining a compact design of an ECOC, the possible loss of generalization performance has to be taken into account. In order to deal with this problem an evolutionary optimization process is used to find a compact ECOC with high generalization capability.

In order to show the parametrization complexity of the compact ECOC design, we first provide an estimation of the number of different possible ECOC matrices that we can build, and therefore, the search space cardinality. We approximate this number using some simple combinatorial principles. First of all, if we have an $N-$class problem and B possible bits to represent all the classes, we have a set CW with 2^B different words. In order to build an ECOC matrix, we select N codewords

from *CW* without replacement. In combinatorics this is represented as $\binom{2^B}{N}$, which means that we can construct $V_{2^B}^N = \frac{2^B!}{(2^B-N)!}$ different ECOC matrices. Nevertheless, in the ECOC framework, one matrix and its opposite (swapping all zeros by ones and vice-versa) are considered as the same matrix, since both represent the same partitions of the data. Therefore, the approximated number of possible ECOC matrices with the minimum number of classifiers is $\frac{V_{2^B}^N}{2} = \frac{2^B!}{2(2^B-N)!}$. In addition to the huge cardinality, it is easy to show that this space is neither continuous nor differentiable, because a change in just one bit of the matrix may produce a wrong coding design.

In this type of scenarios, evolutionary approaches are often introduced with good results. Evolutionary algorithms are a wide family of methods that are inspired on the Darwin's evolution theory, and used to be formulated as optimization processes where the solution space is neither differentiable nor well defined. In these cases, the simulation of natural evolution process using computers results in stochastic optimization techniques which often outperform classical methods of optimization when applied to difficult real-world problems. Although the most used and studied evolutionary algorithms are the Genetic Algorithms (GA), from the publication of the *Population Based Incremental Learning* (PBIL) in 1995 by Baluja and Caruana [4], a new family of evolutionary methods is striving to find a place in this field. In contrast to GA, those new algorithms consider each value in the chromosome as a random variable, and their goal is to learn a probability model to describe the characteristics of good individuals. In the case of PBIL, if a binary chromosome is used, a uniform distribution is learned in order to estimate the probability of each variable to be one or zero.

In this chapter, we report experiments made with the selected evolutionary strategies - i.e. GA and PBIL. Note that for both Evolutionary Strategies, the encoding step and the adaptation function are exactly equivalent.

Problem encoding: The first step in order to use an evolutionary algorithm is to define the problem encoding, which consists of the representation of a certain solution or point in the search space by means of a *genotype* or alternatively a *chromosome* [14]. When the solutions or individuals are transformed in order to be represented in a chromosome, the original values (the individuals) are referred as *phenotypes*, and each one of the possible settings for a phenotype is the *allele*. Binary encoding is the most common, mainly because the first works about GA used this type of encoding. In binary encoding, every chromosome is a string of bits. Although this encoding is often not natural for many problems and sometimes corrections must be performed after crossover and/or mutation, in our case, the chromosomes represent binary ECOC matrices, and therefore, this encoding perfectly adapts to the problem. Each ECOC is encoded as a binary chromosome $\zeta = < h_1^{c_1}, \ldots, h_B^{c_1}, h_1^{c_2}, \ldots, h_B^{c_2}, \ldots, h_1^{c_N}, \ldots, h_B^{c_N} >$, where $h_i^{c_j} \in \{0,1\}$ is the expected value of the $i-th$ classifier for the class c_j, which corresponds to the $i-th$ bit of the class c_j codeword.

Adaptation function: Once the encoding is defined, we need to define the adaptation function, which associates to each individual its adaptation value to the environment, and thus, their survival probability. In the case of the ECOC framework, the adaptation value must be related to the classification error.

Given a chromosome $\zeta =< \zeta_0, \zeta_1, \ldots, \zeta_L >$ with $\zeta_i \in \{0,1\}$, the first step is to recover the ECOC matrix M codified in this chromosome. The elements of M allow to create binary classification problems from the original multi-class problem, following the partitions defined by the ECOC columns. Each binary problem is addressed by means of a binary classifier, which is trained in order to separate both partitions of classes. Assuming that there exists a function $y = f(x)$ that maps each sample x to its real label y, training a classifier consists of finding the best parameters w^* of a certain function $y = f'(x,w)$, in the manner that for any other $w \neq w^*$, $f'(x,w^*)$ is a better approximation to f than $f'(x,w)$. Once the w^* are estimated for each binary problem, the adaptation value corresponds to the classification error. In order to take into account the generalization power of the trained classifiers, the estimation of w^* is performed over a subset of the samples, while the rest of the samples are reserved for a validation set, and the adaptation value ξ is the classification error over that validation subset. The adaptation value for an individual represented by a certain chromosome ζ_i can be formulated as:

$$\varepsilon_i(P,Y,M_i) = \frac{\sum_{j=1}^{s} \delta(\rho_j, M_i) \neq y_j}{s}, \tag{2.3}$$

where M_i is the ECOC matrix encoded in ζ_i, $P = \langle \rho_1, \ldots, \rho_s \rangle$ a set of samples, $Y = \langle y_1, \ldots, y_s \rangle$ the expected labels for samples in P, and δ is the function that returns the classification label applying the decoding strategy.

Evolutionary process: Once the encoding and adaptation functions have been defined, we use standard implementation for GA and PBIL, in order to evolve the compact ECOC matrices. In the case of GA, scattered crossover operator is used, in which we generate a random binary vector, with a binary value assigned to each gene. The first child is created using all the genes from the first parent in those positions with a value of one, and the genes of the second parent with positions with the value zero. The second child is created as the complementary of the first one. That is, taking genes from second parent for values one and from first parent for values zero. In order to introduce variations to the individuals, we use mutation operator that adds a unit Gaussian distributed random value to the chosen gene. The new gene value is clipped if it falls outside the user-specified lower or upper bounds for that gene. For PBIL, the best two individuals of each population are used to update the probability distribution. At each generation, this probability distribution is used to sample a new population of individuals. A uniform random noise is applied to the probability model to avoid convergence to local minima.

Finally, in both evolutionary strategies we adopt an *Island Model* evolution scheme in order to exploit a more coarse grain parallel model. The main idea is to split a population of K individuals into S sub-populations of K/S individuals. If each sub-population is evolved independently from the others, genetic drift will tend to

drive these populations in different directions. By introducing migration, the *Island Model* is able to exploit differences in the various sub-populations (this variation in fact represents a source of genetic diversity). Each sub-population is an island and there is a chance movement of genetic material from one island to another.

Training the binary classifiers: In [23], Rifkin concludes that the number of classifiers in the ECOC problem can be reduced by using more accurate classifiers. Therefore we adopt the Support Vector Machines with Gaussian Radial Basis Functions kernel (SVM-RBF). Training a SVM often implies the selection of a subset of data points (the support vectors), which are used in order to build the classification boundaries. In the specific case of Gaussian RBF kernels, we need to optimize the kernel parameter γ and the regularizer C, which have a close relation to the data distribution. While the support vectors selection is part of the SVM learning algorithm, and therefore, is clearly defined, finding the best C and γ is addressed in the literature with various heuristics or brute-force approaches. The most common approach is the use of cross-validation processes which select the best pair of parameters for a discretization of the parameters space. Nevertheless, this can be viewed as another optimization problem. Therefore, it can be handled using evolutionary algorithms. For each binary problem, defined by one column of the ECOC matrix, we use Genetic Algorithms in order to find good values for C and γ parameters, using the same settings as in [17].

This coding optimization process is computationally more expensive than the standard approaches because for every Compact coding matrix M all the dichotomizers $\{h_1 \dots h_n\}$ have to be optimized. Nevertheless, large-scale multi-classification problems, which are typically computationally unfeasible if using standard coding designs, can be treated with this approach, since this optimization is only applied for a reduced number of dichotomizers.

In order to save time, a historical of column codification and parameter optimization is saved during the evolutionary parametrization process. Let k be a random iteration of the optimization and let $M =< M_1, \dots, M_{ind} >$ be the set of Compact coding matrices to be optimized. Every coding matrix will define a set of bi-partitions $BP =< bp_1, \dots, bp_n >$ to be learned by a set of dichotomizers $H =< h_1, \dots, h_n >$. In fact, we can assume that a certain bi-partition bp_s learned by a certain dichotomizer h_s will be repeated among the coding matrices because of the nature of the evolutionary optimization process.

2.3 Results

In order to present the results, first, we discuss the data, methods, and evaluation measurements of the experiments.

- *Data*: The first data used for the experiments consists of twelve multi-class data sets from the UCI Machine Learning Repository database [3]. The number of training samples, features, and classes per data set are shown in Table 2.1. Then, we apply the classification methodology in five challenging computer vision categorization problems. First, we use the data of the public *Labelled Faces in the Wild* [15]

dataset to perform the multi-class face classification of a large problem consisting of 610 face categories. Second, we use the video sequences obtained from a Mobile Mapping System [1] to test the methods in a real traffic sign categorization problem consisting of 36 traffic sign classes. Third, 20 classes from the ARFaces [18] data set are classified using the present methodology. Fourth, we classify seven symbols from old scanned music scores, and fifth, we classify the 70 visual object categories from the public MPEG7 data set [25].

Table 2.1 UCI repository data sets characteristics

Problem	# Training samples	# Features	# Classes
Dermathology	366	34	6
Iris	150	4	3
Ecoli	336	8	8
Vehicle	846	18	4
Wine	178	13	3
Segmentation	2310	19	7
Glass	214	9	7
Thyroid	215	5	3
Vowel	990	10	11
Balance	625	4	3
Shuttle	14500	9	7
Yeast	1484	8	10

• *Methods*: We compare the one-versus-one [13] and one-versus-all [19] ECOC approaches with the binary and evolutionary compact approaches. For simplicity we omitted the Gray compact design. The Hamming decoding is applied in the decoding step [7]. The ECOC base classifier is the OSU implementation of SVM with Radial Basis Function kernel [20]. The SVM C and γ parameters are tuned via Genetic Algorithms and PBIL for all the methods, minimizing the classification error of a two-fold evaluation over the training sub-set.

• *Evaluation measurements*: The classification performance is obtained by means of a stratified ten-fold cross-validation, and testing for the confidence interval with a two-tailed t-test. We also apply the Friedman test [6] in order to look for statistical significance among the obtained performances.

2.3.1 UCI Categorization

The classification results obtained for all the UCI data sets considering the different ECOC configurations are shown in Table 2.2. In order to compare the performances provided for each strategy, the table also shows the mean rank of each ECOC design considering the twelve different experiments. The rankings are obtained estimating each particular ranking r_i^j for each problem i and each ECOC configuration j, and

Table 2.2 UCI classification results

Data set	Binary C. ECOC		Evol. C. ECOC		One-vs-All ECOC		One-vs-One ECOC	
	Perf.	#C.	Perf.	#C.	Perf.	#C.	Perf.	#C.
Derma	96.0±2.9	3	**96.3±2.1**	3	95.1±3.3	6	94.7±4.3	15
Iris	96.4±6.3	2	**98.2±1.9**	2	96.9±6.0	3	96.3±3.1	3
Ecoli	80.5±10.9	3	**81.4±10.8**	3	79.5±12.2	8	79.2±13.8	28
Vehicle	72.5±14.3	2	76.9±12.4	2	74.2±13.4	4	**83.6±10.5**	6
Wine	95.5±4.3	2	**97.2±2.3**	2	95.5±4.3	3	**97.2±2.4**	3
Segment	96.6±2.3	3	96.6±1.5	3	96.1±1.8	7	**97.2±1.3**	21
Glass	56.7±23.5	3	50.0±29.7	3	53.85±25.8	6	**60.5±26.9**	15
Thyroid	**96.4±5.3**	2	93.8±5.1	2	95.6±7.4	3	96.1±5.4	3
Vowel	57.7±29.4	3	**81.8±11.1**	3	80.7±11.9	8	78.9±14.2	28
Balance	80.9±11.2	2	87.1±9.2	2	89.9±8.4	3	**92.8±6.4**	3
Shuttle	80.9±29.1	3	83.4±15.9	3	**90.6±11.3**	7	86.3±18.1	21
Yeast	50.2±18.2	4	**54.7±11.8**	4	51.1±18.0	10	52.4±20.8	45
Rank & #	2.9	**2.7**	**2.0**	**2.7**	2.7	5.7	2.2	15.9

computing the mean ranking R for each design as $R_j = \frac{1}{N}\sum_i r_i^j$, where N is the total number of data sets. We also show the mean number of classifiers (#) required for each strategy.

In order to analyze if the difference between ranks (and hence, the methods) is statistically significant, we apply a statistical test. In order to reject the null hypothesis (which implies no significant statistical difference among measured ranks and the mean rank), we use the Friedman test. The Friedman statistic value is computed as follows:

$$X_F^2 = \frac{12N}{k(k+1)}\left[\sum_j R_j^2 - \frac{k(k+1)^2}{4}\right]. \tag{2.4}$$

In our case, with $k = 4$ ECOC designs to compare, $X_F^2 = -4.94$. Since this value is rather conservative, Iman and Davenport proposed a corrected statistic:

$$F_F = \frac{(N-1)X_F^2}{N(k-1) - X_F^2}. \tag{2.5}$$

Applying this correction we obtain $F_F = -1.32$. With four methods and twelve experiments, F_F is distributed according to the F distribution with 3 and 33 degrees of freedom. The critical value of $F(3,33)$ for 0.05 is 2.89. As the value of F_F is no higher than 2.98 we can state that there is no statistically significant difference among the ECOC schemes. This means that all four strategies are suitable in order to deal with multi-class categorization problems. This result is very satisfactory and encourages the use of the compact approach since similar (or even better) results can be obtained with far less number of classifiers. Moreover, the GA evolutionary version of the compact design improves in the mean rank to the rest of classical coding strategies, and in most cases outperforms the binary compact approach in the present experiment. This result is expected since the evolutionary version looks for a compact ECOC matrix configuration that minimizes the error over the training

data. In particular, the advantage of the evolutionary version over the binary one is more significant when the number of classes increases, since more compact matrices are available for optimization.

On the other hand, possible reasons why the evolutionary compact ECOC design yields similar or even better performance results than the one-versus-one and one-versus-all approaches can be fewer classifiers considered for tuning and the use of all the classes in balanced binary problems, which can help the system to increase generalization if a good decision boundary can be found by the classifier. Note that the one-versus-one classifier looks for binary problems that split just two classes. In those cases, though good and fast solutions could be found in training time, the use of less data does not assure a high generalization capability of the individual classifiers.

In terms of testing time, since all the trained classifiers spend the same time for testing, classification time is proportional to the number of trained classifiers. The mean number of dichotomizers used for each strategy is shown in the last row of Table 2.2. Observe the great difference in terms of the number of classifiers between the compact approaches and the classical ones. The compact approaches obtain an average speed up improvement of 111% with respect to the one-versus-all approach in testing time. Meanwhile in the case of the one-versus-one technique this improvement is 489%.

In the next section we test if the same behaviour occurs classifying five challenging Computer Vision problems with several object categories.

2.3.2 Computer Vision Applications

In this section, we test the methodology on five challenging Computer Vision problems: faces in the wild, traffic sign, ARface, music scores, and MPEG7 categorization data sets.

2.3.2.1 Labelled Faces in the Wild Categorization

This dataset contains 13000 faces images taken directly from the web from over 1400 people. These images are not constrained in terms of pose, light, occlusions or any other relevant factor. For the purpose of this experiment we used a specific subset, taking only the categories which at least have four or more examples, having a total of 610 face categories. Finally, in order to extract relevant features from the images, we apply an Incremental Principal Component Analysis procedure [16], keeping 99.8% of the information. An example of face images is shown in Fig. 2.4.

The results in the first row of Table 2.3 show that the best performance is obtained by the Evolutionary GA and PBIL compact strategies. One important observation is that Evolutionary strategies outperform the classical one-versus-all approach, with far less number of classifiers (10 instead of 610). Note that in this case we omitted the one-vs-one strategy since it requires 185745 classifiers for discriminating 610 face categories.

Fig. 2.4 Labelled Faces in the Wild dataset

Table 2.3 Computer Vision data sets classification results

Data set	Binary C. ECOC		GA. C. ECOC		PBIL C. ECOC		One-vs-All ECOC		One-vs-One ECOC	
	Perf	#C	Perf	#C	Perf	#C	Perf	#C	Perf	#C
FacesWild	26.4±2.1	10	**30.7±2.3**	10	30.0±2.4	10	25.0±3.1	610	-	185745
Traffic	90.8±4.1	6	90.6±3.4	6	90.7±3.7	6	**91.8±4.6**	36	90.6±4.1	630
ARFaces	76.0±7.2	5	85.8±5.2	5	84.2±5.3	5	84.0±6.3	20	**96.0±2.5**	190
Clefs	81.2±4.2	3	81.8±9.3	3	81.7±8.2	3	80.8±11.2	7	**84.2±6.8**	21
MPEG7	89.3±5.1	7	90.4±4.5	7	90.1±4.9	7	87.8±6.4	70	**92.8±3.7**	2415
Rank & #	3.6	**6.2**	2.2	**6.2**	2.8	**6.2**	3.8	148.6	**1.75**	37800

2.3.2.2 Traffic Sign Categorization

For this second computer vision experiment, we use the video sequences obtained from the Mobile Mapping System of [1] to test the ECOC methodology on a real traffic sign categorization problem. In this system, the position and orientation of the different traffic signs are measured with video cameras fixed on a moving vehicle. The system has a stereo pair of calibrated cameras, which are synchronized with a GPS/INS system. The result of the acquisition step is a set of stereo-pairs of images with their position and orientation information. From this system, a set of 36 circular and triangular traffic sign classes are obtained. Some categories from this data set are shown in Fig. 2.5. The data set contains a total of 3481 samples of size 32×32, filtered using the Weickert anisotropic filter, masked to exclude the background pixels, and equalized to prevent the effects of illumination changes. These feature vectors are then projected into a 100 feature vector by means of PCA.

The classification results obtained when considering the different ECOC configurations are shown in the second row of Table 2.3. The ECOC designs obtain similar classification results with an accuracy of over 90%. However, note that the compact methodologies use six times less classifiers than the one-versus-all and 105 less times classifiers than the one-versus-one approach, respectively.

Fig. 2.5 Traffic sign classes

2.3.2.3 ARFaces Classification

The AR Face database [18] is composed of 26 face images from 126 different subjects (70 men and 56 women). The images have uniform white background. The database has two sets of images from each person, acquired in two different sessions, with the following structure: one sample of neutral frontal images, three samples with strong changes in the illumination, two samples with occlusions (scarf and glasses), four images combining occlusions and illumination changes, and three samples with gesture effects. One example of each type is plotted in Fig. 2.6. For this experiment, we selected all the samples from 20 different categories (persons).

Fig. 2.6 ARFaces data set classes. Examples from a category with neutral, smile, anger, scream expressions, wearing sun glasses, wearing sunglasses and left light on, wearing sun glasses and right light on, wearing scarf, wearing scarf and left light on, and wearing scarf and right light on.

The classification results obtained when considering the different ECOC configurations are shown in the third row of Table 2.3. In this case, the one-versus-one strategy obtains significant superior results to the rest of approaches, and the Evolutionary compact approaches clearly outperforms the one-versus-all ECOC results.

2.3.2.4 Clefs and Accidental Data Set Categorization

The data set of clefs and accidental is obtained from a collection of modern and old musical scores (19th century) of the Archive of the Seminar of Barcelona. The data set contains a total of 4098 samples among seven different types of clefs and accidental from 24 different authors. The images have been obtained from original image documents using a semi-supervised segmentation approach [11]. The main difficulty of this data set is the lack 389 of a clear class separability because of the variation of writer styles and the absence of a standard notation. A pair of segmented samples for each of the seven classes showing the high variability of clefs and accidental appearance from different authors can be observed in Fig. 2.7(a). An example of an old musical score used to obtain the data samples is shown in Fig. 2.7(b). The object images are described using the Blurred Shape Model descriptor (BSM).

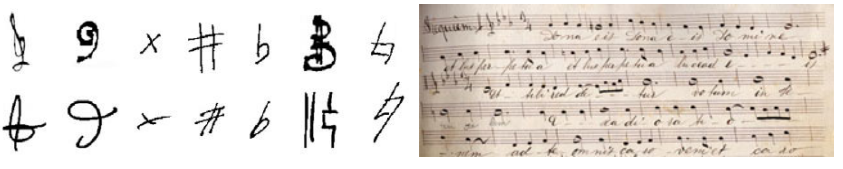

(a) (b)

Fig. 2.7 (a) Object samples, (b) Old music score

The classification results obtained when considering the different ECOC configurations are shown in the fourth row of Table 2.3. In this case, the results are also comparable for all the strategies, with accuracies upon 80%.

2.3.2.5 MPEG7 Categorization

The MPEG7 data set contains 70 classes with 20 instances per class, which represents a total of 1400 object images. All samples are described using the Blurred Shape Model descriptor. Some categories of this data set are shown in Fig. 2.8.

The classification results obtained considering the different ECOC configurations are shown in the fifth row of Table 2.3. These results are very satisfactory since one can see very similar results between the evolutionaries and one-versus-one strategies, taking into account that the last approach requires near 350 times the number of classifiers required by our proposal.

Globally analyzing the results of the Computer Vision classification problems, whose mean ranks are shown in the last row of Table 2.3, one can see that the one-versus-one is the first choice, followed by the evolutionary proposals. The last two positions are for the binary and one-versus-all coding designs.

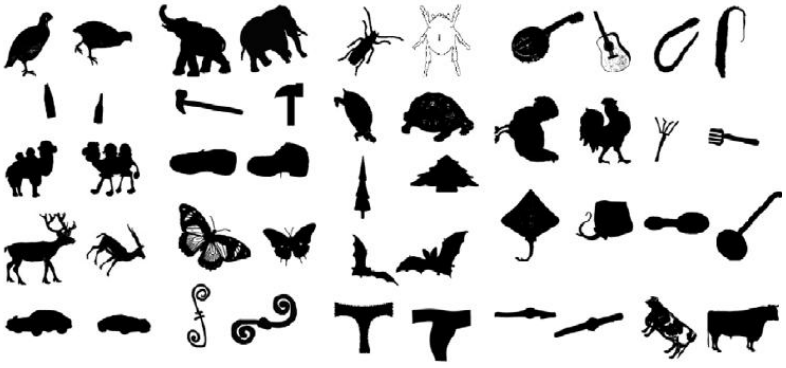

Fig. 2.8 MPEG7 samples

In this case, applying the Friedman statistic, we obtain a value of $X_F^2 = -3.71$, and a corrected value of $F_F = -0.62$. With five methods and five Computer Vision experiments, F_F is distributed according to the F distribution with 4 and 16 degrees of freedom. The critical value of $F(4,16)$ for the 0.05 significance level is 3.01. As the value of F_F is no higher than 3.01 we can state that there is no statistically significant difference among the ECOC schemes. This means that all five strategies are suitable in order to deal with multi-class Computer Vision problems with several categories. This result also encourages the use of the compact approach. Note that for example, in the Faces in the Wild experiment the compact ECOC approach requires 10 classifiers in comparison with the 185745 classifiers required by the one-versus-one ECOC strategy.

2.4 Conclusion

We presented a general methodology for the classification of several object categories, which only requires $\lceil \log_2 N \rceil$ classifiers for a N-class problem. The methodology is defined in the Error-Correcting Output Codes framework, designing a compact coding matrix in terms of dichotomizers which unequivocally distinguish N codes. Moreover, in order to speed up the design of the coding matrix and the tuning of the classifiers, evolutionary computation is also applied.

The results on several public UCI data sets and five multi-class Computer Vision problems with multiple object categories show that the proposed methodology obtains equivalent results than the state-of-the-art ECOC methodologies. However, it achieves this with far less number of dichotomizers. For example, our compact approach trained 10 classifiers to split 610 face categories, meanwhile the one-versus-all and one-versus-one approaches required 610 and 185745 classifiers, respectively.

Acknowledgements. This work has been supported by projects TIN2009-14404-C02 and CONSOLIDER-INGENIO CSD 2007-00018.

References

1. Alamús, R., Baron, A., Bosch, E., Casacuberta, J., Miranda, J., Pla, M., Sànchez, S., Serra, A., Talaya, J.: On the accuracy and performance of the GeoMobil system. In: Proc. the 20th Congress Int. Soc. Photogrammetry and Remote Sens., Istanbul, Turkey, pp. 262–267 (2004)
2. Allwein, E., Schapire, R., Singer, Y.: Reducing multiclass to binary: A unifying approach for margin classifiers. J. Machine Learning Research 1, 113–141 (2002)
3. Asuncion, A., Newman, D.J.: UCI machine learning repository, http://www.ics.uci.edu/~mlearn/MLRepository.html
4. Baluja, S., Caruana, R.: Removing the genetics from the standard genetic algorithm. In: Prieditis, A., Russel, S. (eds.) Proc. the 12th Int. Conf. Machine Learning, Tahoe City, CA, pp. 38–46. Morgan Kaufmann, San Francisco (1995)
5. Crammer, K., Singer, Y.: On the learnability and design of output codes for multi-class problems. Machine Learning 47, 201–233 (2002)
6. Demsar, J.: Statistical comparisons of classifiers over multiple data sets. J. Machine Learning Research 7, 1–30 (2006)
7. Dietterich, T., Bakiri, G.: Solving multiclass learning problems via error-correcting output codes. J. Artif. Intel. Research 2, 263–286 (1995)
8. Dietterich, T., Kong, E.: Error-correcting output codes corrects bias and variance. In: P.A., Russell, S. (eds.) Proc. 12th Int. Conf. Machine Learning, Tahoe City, CA, pp. 313–321. Morgan Kaufmann, San Francisco (1995)
9. Escalera, S., Pujol, O., Radeva, P.: On the decoding process in ternary error-correcting output codes. IEEE Trans. Pattern Analysis and Machine Intel. 32, 120–134 (2010)
10. Escalera, S., Pujol, O., Radeva, P.: Error-correcting output codes library. J. Machine Learning Research 11, 661–664 (2010)
11. Fornés, A., Lladós, J., Sánchez, G.: Primitive segmentation in old handwritten music scores. In: Liu, W., Lladós, J. (eds.) GREC 2005. LNCS, vol. 3926, pp. 279–290. Springer, Heidelberg (2006)
12. Friedman, J., Hastie, T., Tibshirani, R.: Additive logistic regression: a statistical view of boosting. The Annals of Statistics 38, 337–374 (1998)
13. Hastie, T., Tibshirani, R.: Classification by pairwise grouping. In: Jordan, M.I., Kearns, M.J., Solla, S.A. (eds.) Advances in Neural Inf. Proc. Syst., vol. 10, pp. 507–513. MIT Press, Cambridge (1998)
14. Holland, J.H.: Adaptation in natural and artificial systems: An introductory analysis with applications to biology, control, and artificial intelligence. MIT Press, Cambridge (1975)
15. Huang, G.B., Ramesh, M., Berg, T., Miller, E.L.: Labeled faces in the wild: A database for studying face recognition in unconstrained environments. Technical Report, pp. 7–49. University of Massachusets, Amherst (2007)
16. Hwang, W., Weng, J., Zhang, Y.: Candid covariance-free incremental principal component analysis. IEEE Trans. Pattern Analysis and Machine Intel. 25, 1034–1040 (2003)
17. Lorena, A.-C., de Carvalho, A.C.P.L.F.: Evolutionary tuning of svm parameter values in multiclass problems. Neurocomputing 71, 3326–3334 (2008)
18. Martínez, A., Benavente, R.: The AR face database. Computer Vision Center Technical Report 24, University of Barcelona (1998)
19. Nilsson, N.J.: Learning machines: Foundations of trainable pattern-classifying systems. McGraw-Hill, New York (1965)
20. OSU-SVM-TOOLBOX, http://svm.sourceforge.net/
21. Passerini, A., Pontil, M., Frasconi, P.: New results on error correcting output codes of kernel machines. IEEE Trans. Neural Networks 15, 45–54 (2004)

22. Pujol, O., Radeva, P., Vitrià, J.: Discriminant ECOC: A heuristic method for application dependent design of error correcting output codes. IEEE Trans. Pattern Analysis and Machine Intel. 28, 1001–1007 (2006)
23. Rifkin, R., Klautau, A.: In defense of one-vs-all classification. J. Machine Learning Research 5, 101–141 (2004)
24. Utschick, W., Weichselberger, W.: Stochastic organization of output codes in multiclass learning problems. Neural Computation 13, 1065–1102 (2004)
25. http://www.cis.temple.edu/latecki/research.html

Chapter 3
Minimally-Sized Balanced Decomposition Schemes for Multi-class Classification

Evgueni N. Smirnov, Matthijs Moed, Georgi Nalbantov,
and Ida Sprinkhuizen-Kuyper

Abstract. Error-Correcting Output Coding (ECOC) is a well-known class of decomposition schemes for multi-class classification. It allows representing any multi-class classification problem as a set of binary classification problems. Due to code redundancy ECOC schemes can significantly improve generalization performance on multi-class classification problems. However, they can face a computational-complexity problem when the number of classes is large.

In this paper we address the computational-complexity problem of the decomposition schemes. We study a particular class of minimally-sized ECOC decomposition schemes, namely the class of minimally-sized balanced decomposition schemes (MBDSs) [14]. We show that MBDSs do not face a computational-complexity problem for large number of classes. However we also show that MBDSs cannot correct the classification errors of the binary classifiers in MBDS ensembles. Therefore we propose voting with MBDS ensembles (VMBDSs). We show that the generalization performance of the VMBDSs ensembles improves with the number of MBDS classifiers. However this number can become large and thus the VMBDSs ensembles can have a computational-complexity problem as well. Fortunately our experiments show that VMBDSs are comparable with ECOC ensembles and can outperform one-against-all ensembles using only a small number of MBDS ensembles.

Evgueni N. Smirnov · Matthijs Moed
Department of Knowledge Engineering, Maastricht University, P.O. BOX 616,
6200 MD Maastricht, The Netherlands
E-mail: smirnov@maastrichtuniversity.nl,
m.moed@student.maastrichtuniversity.nl

Georgi Nalbantov
Faculty of Health, Medicine and Life Sciences, Maastricht University, P.O. BOX 616,
6200 MD Maastricht, The Netherlands
E-mail: g.nalbantov@maastrichtuniversity.nl

Ida Sprinkhuizen-Kuyper
Radboud University Nijmegen, Donders Institute for Brain, Cognition and Behaviour,
6525 HR Nijmegen, The Netherlands
E-mail: i.kuyper@donders.ru.nl

O. Okun et al. (Eds.): Ensembles in Machine Learning Applications, SCI 373, pp. 39–57.
springerlink.com

3.1 Introduction

A decomposition scheme for a multi-class classification problem is a mapping from a class set Y to a set of binary partitions of Y [4, 13]. It allows for representing the multi-class classification problem as a set of binary classification problems. Thus, the multi-class classification problem can be solved by a set of binary classifiers that corresponds to the set of binary classification problems.

A decomposition scheme is applied on two stages [4, 13]: encoding and decoding. During the encoding stage we first generate binary classification problems according to the decomposition scheme and then train a binary classifier for each problem. During the decoding stage we first apply the binary classifiers for a test instance and then combine the class predictions of these classifiers according to the decomposition scheme to estimate the class of that instance.

The main family of decomposition schemes is that of Error-Correcting Output Coding (ECOC) [4]. Due to redundancy in their codes, ECOC schemes can significantly improve generalization performance on multi-class classification problems. However this code redundancy can cause a computational-complexity problem for ECOC schemes: the number of binary classification problems (and hence the number of classifiers to be trained) can grow exponentially with the number of classes. Several approaches were proposed to deal with this computational-complexity problem of ECOC [1, 4, 18]. In essence these approaches try to maximize the diversity of the binary partitions in ECOC schemes for a fixed scheme size.

In this paper we address the computational-complexity problem of ECOC schemes as well. For that purpose we study ECOC decomposition schemes of minimal size. In this respect our research differs from previous studies which so far have only focused on ECOC schemes of a fixed size [1, 4, 18]. In the paper we show that minimally-sized ECOC decomposition schemes can be viewed as minimally-sized balanced decomposition schemes (MBDSs). We note that MBDSs were suggested in [14] but was never studied in detail. This paper provides a deep analysis of MBDSs. First, we prove that the size of MBDSs equals $\lceil \log_2(|Y|) \rceil$. This property implies that the MBDSs ensembles do not have a computational-complexity problem and thus can be used for classification problems with a large number of classes. Second, we quantify the space of all possible MBDSs. Third, we analyze the error-correction properties of MBDSs. We show that: (a) the minimal Hamming distance between MBDS class code words equals 1, and (b) the Hamming distance between MBDS class-partition code words equals $\frac{|Y|}{2}$. Thus MBDSs cannot correct the classification errors of the binary classifiers in MBDS ensembles.

To enforce error correction, we propose voting with MBDS ensembles, which is denoted as VMBDSs. We show that the VMBDSs ensembles improve generalization performance with the number of MBDS classifiers. However this number can be large and the VMBDSs ensembles can have a computational-complexity problem. Fortunately, our experiments demonstrate that VMBDSs are comparable with ECOC ensembles and can outperform one-against-all ensembles using a small number of MBDS ensembles.

The paper is organized as follows. Section 3.2 formalizes the classification problem. Decomposing multi-class classification problems into binary classification problems is discussed in Sect. 3.3. Section 3.4 introduces balanced decomposition schemes, minimally-sized balanced decomposition schemes, and voting based on these schemes. Experiments are given in Sect. 3.5. Section 3.6 concludes the paper.

3.2 Classification Problem

Let X be a non-empty instance space and Y be a class set of size K greater than 1. A labeled instance is defined as a tuple (x, y) where $x \in X$ and $y \in Y$. Training data D is a multi-set of labeled instances. Given training data D and test instance $x \in X$, the classification problem CP is to find the class of the instance x.

To classify a new instance we need a classifier $h : X \rightarrow Y$ from a hypothesis space H. To identify such a classifier in H we need to search in H. The acceptance criterion is that the final classifier $h \in H$ has to classify correctly future instances iid drawn from the same probability distribution from which D was drawn.

When $K = 2$, the classification problem is said to be a *binary classification problem BCP*. When $K > 2$, the classification problem is said to be a *multi-class classification problem MCP*. Many classifiers are inherently binary for various reasons [7]. However, many real-world classification problems are *multi-class* problems. There are two main approaches for solving a multi-class problem using a binary classifier: direct and indirect. The direct approach is to generalize the binary classifier to a multi-class classifier (e.g., Support Vector Machines [19] and Boosting [6]). The indirect approach is to employ *decomposition schemes* (e.g., ECOC [4, 13]).

3.3 Decomposing Multi-class Classification Problems

This section considers the main elements needed for decomposing a multi-class classification problem into a set of binary problems: the decomposition scheme, the encoding stage, and the decoding stage. More precisely, Sect. 3.3.1 formalizes the concept of *decomposition scheme* and presents two of the most well-known decomposition schemes. Section 3.3.2 provides a detailed explanation of *the encoding and decoding stages*.

3.3.1 Decomposition Schemes

Consider a multi-class classification problem MCP determined on a class set Y of size $K > 2$. To show how to decompose MCP into L binary classification problems BCP_l we define the notion of a *binary class partition* in Definition 3.1.

Definition 3.1. (Binary Class Partition) Given a class set Y, the set $P(Y)$ is said to be a binary class partition of Y iff $P(Y)$ consists of two non-empty sets Y^- and Y^+ such that $Y^- \cup Y^+ = Y$ and $Y^- \cap Y^+ = \emptyset$.

Definition 3.1 allows us to introduce the notion of a *decomposition scheme*. A decomposition scheme describes how to decompose a multi-class classification problem *MCP* into L binary classification problems BCP_l, as given in Definition 3.2.

Definition 3.2. (Decomposition Scheme) Given a multi-class classification problem *MCP* and positive integer L, the *decomposition scheme* of *MCP* is a set $SP(Y)$ of L binary class partitions $P_l(Y)$ such that for any two classes $y_1, y_2 \in Y$ there exists a binary class partition $P_m(Y) \in SP(Y)$ so that $\neg(y_1, y_2 \in Y_m^-) \wedge \neg(y_1, y_2 \in Y_m^+)$ where $Y_m^-, Y_m^+ \in P_m(Y)$.

By Definition 3.2 any decomposition scheme $SP(Y)$ consists of L binary class partitions $P_l(Y)$. The partitions $P_l(Y) \in SP(Y)$ are chosen so that each class $y \in Y$ can be uniquely determined.

A natural representation for a decomposition scheme $SP(Y)$ is a *decomposition matrix* M. The matrix M is defined as a binary matrix $\{-1, +1\}^{K \times L}$. Its encoding is realized according to the following rule:

$$M_{k,l} = \begin{cases} -1 & \text{if class } y_k \in Y \text{ belongs to } Y_l^- \text{ of } P_l(Y); \\ +1 & \text{if class } y_k \in Y \text{ belongs to } Y_l^+ \text{ of } P_l(Y). \end{cases} \tag{3.1}$$

The rows of M form *class code words* w_{y_k} corresponding to the K classes in the class set Y. The columns of M form *class-partition code words* $w_{P_l(Y)}$ corresponding to the L binary class partitions $P_l(Y)$.

Decomposition matrices have certain column and row properties that follow from Definition 3.2. These properties are formulated in Corollary 3.1 and Corollary 3.2 below.

Corollary 3.1. *Any two columns $M_{*,l}$ and $M_{*,m}$ in a matrix M of any decomposition scheme $SP(Y)$ are different if $l \neq m$.*

Proof. By Definition 3.2 the decomposition scheme $SP(Y)$ is a set. This implies that, if $l \neq m$, the columns columns $M_{*,l}$ and $M_{*,m}$ represent different class partitions in $SP(Y)$. Thus, $M_{*,l}$ and $M_{*,m}$ are different. □

Corollary 3.2. *Any two rows $M_{k,*}$ and $M_{o,*}$ of a matrix M of any decomposition scheme $SP(Y)$ are different if $k \neq o$.*

Proof. Given the decomposition scheme $SP(Y)$, by Definition 3.2 for any two classes $y_k, y_o \in Y$ there exists a binary class partition $P_m(Y) \in SP(Y)$ such that $\neg(y_k, y_o \in Y_m^-) \wedge \neg(y_k, y_o \in Y_m^+)$ where $Y_m^-, Y_m^+ \in P_m(Y)$. Thus, the rows $M_{k,*}$ and $M_{o,*}$ differ at least for the position corresponding to the class partition $P_m(Y)$. □

Any two decomposition matrices are equivalent if they represent the same decomposition scheme $SP(Y)$. By Theorem 3.1, given below, any two decomposition matrices M and M' are equivalent iff the columns of M' are a permutation and/or complements of the columns of M.

Theorem 3.1. *Consider decomposition schemes $SP(Y)$ and $SP'(Y)$, both of size L, and their corresponding decomposition matrices M and M'. Then:*

$$SP(Y) = SP'(Y) \leftrightarrow (\forall M_{*,l} \in M)(\exists M'_{*,m} \in M')(M_{*,l} = M'_{*,m} \vee M_{*,l} = -M'_{*,m}).$$

Proof. ($\rightarrow$) Given $SP(Y) = SP'(Y)$, consider an arbitrary column $M_{*,l} \in M$ and its corresponding binary class partition $P_l(Y)$. Since $SP(Y) = SP'(Y)$, $P_l(Y) \in SP'(Y)$. This implies that there exists a column $M'_{*,m} \in M'$ for $P_l(Y)$. Thus, $M_{*,l}$ equals either $M'_{*,m}$ or $-M'_{*,m}$.
($\leftarrow$) Consider an arbitrary column $M_{*,l} \in M$ and its corresponding binary class partition $P(Y)$. There exists a column $M'_{*,m} \in M'$ such that either $M_{*,l} = M'_{*,m}$ or $M_{*,l} = -M'_{*,m}$. Thus, the binary class partition $P'_m(Y) \in SP'(Y)$ represented by $M'_{*,m}$ belongs to $SP(Y)$. Since the latter holds for all $P'_m(Y) \in SP'(Y)$, and $SP(Y)$ and $SP'(Y)$ are sets with equal size L, we conclude $SP(Y) = SP'(Y)$. □

Theorem 3.1 allows us to formulate Corollary 3.3 which determines the number of equivalent decomposition matrices for any decomposition scheme $SP(Y)$.

Corollary 3.3. *For any decomposition scheme $SP(Y)$ there exist $L! \times 2^L$ equivalent decomposition matrices M.*

Proof. Consider a decomposition matrix M that represents the decomposition scheme $SP(Y)$. All possible permutations of the columns of M generate $L!$ matrices M' that represent $SP(Y)$. From each of these matrices we can generate additional 2^L matrices by all possible complements of their columns. □

Several decomposition schemes were proposed, the most well-known being "one-against-all"(OA) [16] and "Error-Correcting Output Coding" (ECOC) [4]. OA is a decomposition scheme $SP(Y)$ that consists of all possible binary class partitions $P(Y) \in SP(Y)$ containing a class set with size equal to 1. In other words, OA decomposes the multi-class classification problem MCP into K binary classification problems BCP_l such that each problem BCP_l consists of discriminating between one particular class and all other classes. Hence any decomposition matrix corresponding to the OA decomposition scheme has dimensions $K \times K$. A OA decomposition matrix for a four-class classification problem is shown in Fig. 3.1.

$$M = \begin{pmatrix} +1 & -1 & -1 & -1 \\ -1 & +1 & -1 & -1 \\ -1 & -1 & +1 & -1 \\ -1 & -1 & -1 & +1 \end{pmatrix}$$

Fig. 3.1 A one-against-all (OA) decomposition matrix for a four-class problem. The i-th row corresponds to class y_i. The first column defines the binary class partition $\{\{y_2, y_3, y_4\}, \{y_1\}\}$, the second column defines the binary class partition $\{\{y_1, y_3, y_4\}, \{y_2\}\}$, and so on.

One of the most successful decomposition schemes is that of exhaustive Error-Correcting Output Coding (eECOC) [4]. The eECOC decomposition scheme $SP(Y)$

consists of all possible binary class partitions $P(Y)$ of the class set Y. This implies that the eECOC decomposition scheme is a superset of the OA decomposition scheme. The number of binary class partitions $P(Y)$ in the eECOC decomposition scheme equals $2^{K-1}-1$. An eECOC decomposition matrix for a four-class classification problem is shown in Fig. 3.2.

$$M = \begin{pmatrix} +1 & -1 & -1 & -1 & +1 & +1 & +1 \\ -1 & +1 & -1 & -1 & +1 & -1 & -1 \\ -1 & -1 & +1 & -1 & -1 & +1 & -1 \\ -1 & -1 & -1 & +1 & -1 & -1 & +1 \end{pmatrix}$$

Fig. 3.2 An eECOC decomposition matrix for four classes. The i-th row corresponds to class y_i.

3.3.2 Encoding and Decoding

To solve a multi-class classification problem MCP according to a decomposition scheme $SP(Y)$ we need to pass two stages: *encoding* and *decoding*. Below we describe each of these stages in detail.

During the encoding stage we first generate binary classification problems BCP_l according to a given decomposition scheme $SP(Y)$. Each BCP_l is uniquely determined by a particular binary class partition $P_l(Y) \in SP(Y)$. BCP_l is defined on the instance space X and a class set given by the binary class partition $P_l(Y)$. The training data D_l for BCP_l consists of instances $(x, Y_l^{\pm}) \in X \times P_l(Y)$ and for any instance $(x, Y_l^{\pm}) \in D_l$ there exists an instance (x, y) from the training data D of the multi-class classification problem MCP such that $y \in Y_l^{\pm}$. Thus, the decomposition scheme $SP(Y)$ reduces the multi-class classification problem MCP to L binary classification problems BCP_l.

Once the binary classification problems BCP_l have been determined, we train a binary classifier $h_{P(Y)} : X \to P(Y)$ for each BCP_l. The binary classifiers $h_{P(Y)}$ together form an ensemble classifier $h_{SP(Y)} : X \to Y$ equal to $\{h_{P(Y)}\}_{P(Y) \in SP(Y)}$.

During the decoding stage, given an instance $x \in X$ to be classified and an ensemble classifier $h_{SP(Y)}$, we need to decode the predictions provided by the binary classifiers $h_{P(Y)} \in h_{SP(Y)}$ to form a class estimate $y \in Y$ for the instance x. The OA and eECOC decomposition schemes both use the same decoding technique. This technique first takes the class score $S(x, y|h_{P(Y)})$ provided by each binary classifier $h_{P(Y)} \in h_{SP(Y)}$ (see Definition 3.3 below) and then computes the final score $S(x, y|h_{SP(Y)})$ of the ensemble classifier $h_{SP(Y)}$ as the sum of scores $S(x, y|h_{P(Y)})$ over all the classifiers $h_{P(Y)} \in h_{SP(Y)}$ (see Definition 3.4 below).

Definition 3.3. Given a binary class partition $P(Y) \in SP(Y)$, a binary classifier $h_{P(Y)} : X \to P(Y)$, an instance $x \in X$ to be classified and a class $y \in Y$, the class score $S(x, y|h_{P(Y)})$ for x and y provided by $h_{P(Y)}$ is defined as follows:

$$S(x, y|h_{P(Y)}) = \begin{cases} 1 & \text{if class } y \in h_{P(Y)}(x); \\ 0 & \text{if class } y \notin h_{P(Y)}(x). \end{cases}$$

Definition 3.4. Given a decomposition scheme $SP(Y)$, an ensemble classifier $h_{SP(Y)}$, an instance $x \in X$ to be classified and a class $y \in Y$, the total class score $S(x,y|h_{SP(Y)})$ for x and y provided by $h_{SP(Y)}$ is defined as follows:

$$S(x,y|h_{SP(Y)}) = \sum_{P(Y)\in SP(Y)} S(x,y|h_{P(Y)}). \tag{3.2}$$

Traditionally, decoding is explained using decomposition matrices [4]. In this case for any test instance $x \in X$ the predictions $h_{P(Y)}(x)$ provided by the binary classifiers are first mapped to either the number -1 or the number +1 according to the column of a decomposition matrix M corresponding to $P(Y)$. Then the resulting numbers are combined into a class code word $\hat{w}$ according to the order of the columns in M. This class code word $\hat{w}$ is compared against each class code word in M and the test instance x receives as final classification the class whose code word is closest according to the Hamming distance. As an example let us consider the eECOC decomposition matrix shown in Fig. 3.2. Assume that the classifiers return the class code word $\hat{w} =$ "`-1 +1 -1 -1 -1 -1 -1`" for a test instance $x \in X$. Then in the matrix M from Fig. 3.2 the class code word nearest to $\hat{w}$ would be "`-1 +1 -1 -1 +1 -1 -1`" with a Hamming distance of 1. Hence, the instance x would be assigned the class y_2.

In order to design an accurate ensemble classifier $h_{SP(Y)}$ a decomposition matrix M has to satisfy two properties [17]:

- **Row separation:** any class code word $M_{k,*}$ in M should be well-separated from all other class code words $M_{m,*}$ in terms of Hamming distance.
- **Column separation:** any class-partition code word $M_{*,l}$ in M should be well-separated from many other class-partition code words $M_{*,n}$ and their complements $-M_{*,n}$ in terms of Hamming distance.

The first property implies that the ensemble classifier $h_{SP(Y)}$ will be capable of correcting the errors of $\lfloor \frac{H_{min}-1}{2} \rfloor$ binary classifiers $h_{P(Y)} \in h_{SP(Y)}$ where H_{min} is the minimum Hamming distance between any pair of class code words in the decomposition matrix M. The second property aims at minimally correlating the errors of the binary classifiers $h_{P(Y)} \in h_{SP(Y)}$, thus minimizing the number of the binary classifiers $h_{P(Y)}$ which predictions have to be corrected. Kong and Dietterich showed experimentally in [9] that the bias and variance components of the error of the ensemble classifier $h_{SP(Y)}$ are reduced by increasing the Hamming distance between all class code words and as many as possible class-partition code words. Increasing the Hamming distance of class code words can be achieved by introducing additional code redundancy, i.e. by increasing the number L of columns in the decomposition matrix M. In the extreme case of the eECOC decomposition scheme this leads to L equal to $2^{K-1} - 1$. Thus, code redundancy can cause a computational-complexity problem for ECOC schemes: the number of binary classification problems (classifiers) can grow exponentially with the number of classes. Several approaches to the

computational-complexity problem of ECOC were proposed [1, 4, 18]. In essence they try to design ECOC schemes that maximize the minimum Hamming distance between class code words and class-partition code words for a fixed scheme size L.

3.4 Balanced Decomposition Schemes and Their Minimally-Sized Variant

In this section we address the computational-complexity problem of ECOC schemes. In contrast with the previous research we focus on ECOC decomposition schemes of minimal size. We show that these schemes belong to the class of balanced decomposition schemes. Therefore, in Subsection 3.4.1 we first introduce balanced decomposition schemes. Then in Subsection 3.4.2 we study minimally-sized ECOC schemes considered as minimally-sized balanced decomposition schemes. Finally in Subsection 3.4.3 we propose voting based on minimally-sized balanced decomposition schemes.

3.4.1 Balanced Decomposition Schemes

Balanced decomposition schemes are a subclass of decomposition schemes that are based on balanced binary class partitions. The concept of *balanced binary class partitions* is provided in Definition 3.5 given below.

Definition 3.5. (Balanced Binary Class Partitions) If the number K of classes in a class set Y is even, then a binary class partition $P(Y) = \{Y^-, Y^+\}$ is said to be balanced iff $|Y^-| = |Y^+|$.

The number of all balanced binary class partitions is provided in Corollary 3.4 given below.

Corollary 3.4. *The number of all balanced binary class partitions* $P(Y)$ *equals* $\frac{K!}{2(\frac{K}{2}!)^2}$.

Proof. The number of all balanced binary class partitions $P(Y)$ is $\frac{1}{2}\binom{K}{\frac{K}{2}} = \frac{K!}{2(\frac{K}{2}!)^2}$.□

Given the concept of balanced binary class partitions we define the concept of *balanced decomposition schemes* in Definition 3.6 below.

Definition 3.6. (Balanced Decomposition Schemes) A decomposition scheme denoted as $SP(Y)$ is said to be *balanced* iff each binary class partition $P(Y) \in SP(Y)$ is balanced.

Theorem 3.2, given below, states that the class of balanced decomposition schemes is non-empty. More precisely we show that by using balanced binary class partitions we can design a decomposition scheme.

Theorem 3.2. *There exists a set $SP(Y)$ of balanced binary class partitions such that $SP(Y)$ is a decomposition scheme.*

Proof. Consider a set $SP(Y)$ of balanced binary class partitions such that for each two classes $y_i, y_j \in Y$ there exists a balanced binary partition $\{Y^+, Y^-\} \in SP(Y)$ for which $\neg(y_i, y_j \in Y^-) \wedge \neg(y_i, y_j \in Y^+)$. By definition 3.2 the set $SP(Y)$ is a decomposition scheme. □

Balanced decomposition schemes have an important practical property: they do not introduce additional imbalance in the training data of the binary classifiers $h_{P(Y)}$ in the ensemble classifier $h_{SP(Y)}$. By Definition 3.5 this is due to the fact that the data of these classifiers are based on balanced class binary partitions $P(Y)$. In this respect balanced decomposition schemes differ from other decomposition schemes (e.g., OA, eECOC).

3.4.2 Minimally-Sized Balanced Decomposition Schemes

Minimally-sized balanced decomposition schemes (MBDSs) are balanced decomposition schemes of minimal size. This type of decomposition schemes was suggested by Mayoraz & Moreira [14] but was never studied in detail. This subsection provides the definition of MBDSs and their properties.

Definition 3.7. (Minimally-Sized Balanced Decomposition Schemes) Given the set $SP^M(Y)$ of all balanced binary class partitions, a balanced decomposition scheme $SP(Y) \subseteq SP^M(Y)$ is said to be minimally-sized iff there does not exist another balanced decomposition scheme $SP'(Y) \subseteq SP^M(Y)$ such that $|SP'(Y)| < |SP(Y)|$.

Notation 1. A minimally-sized balanced decomposition scheme is denoted by $SP^m(Y)$.

Theorem 3.3 below determines the size of MBDSs as a function of the number K of classes.

Theorem 3.3. *A balanced decomposition scheme $SP(Y)$ is minimally-sized iff the size of $SP(Y)$ equals $\lceil \log_2(K) \rceil$.*

Proof. ($\rightarrow$) Consider a minimally-sized balanced decomposition scheme $SP(Y)$. Any decomposition matrix M of $SP(Y)$ represents a minimally-sized binary code for K classes. The size of that code is $\lceil \log_2(K) \rceil$.Thus, the size of $SP(Y)$ equals $\lceil \log_2(K) \rceil$.
($\leftarrow$) Consider a balanced decomposition scheme $SP(Y)$ with size of $\lceil \log_2(K) \rceil$. Any decomposition matrix M of $SP(Y)$ represents a binary code for K classes and the size of this code is $\lceil \log_2(K) \rceil$. Thus, the code is minimally-sized. This implies that $SP(Y)$ is minimally-sized. □

Corollary 3.5. *Any decomposition matrix M of a minimally-sized balanced decomposition scheme $SP(Y)^m$ forms a minimally-sized binary code for K classes.*

For a multi-class classification problem we can define different minimally-sized balanced decomposition schemes MBDSs. To characterize the number of all possible MBDSs, we first determine the number of decomposition matrices of all possible MBDSs (see Corollary 3.6) and then the number of equivalent decomposition matrices for a MBDS (see Corollary 3.7). The ratio of these two numbers is the number of all possible MBDSs stated in Theorem 3.4 below.

Corollary 3.6. *If K is a power of 2, then the number of decomposition matrices of all possible minimally-sized balanced decomposition schemes equals $K!$.*

Proof. This follows from the fact that for K a power of 2 there are exactly K different class code words which can be assigned to the classes in $K!$ different ways. □

Corollary 3.7. *If K is a power of 2, then there exists $\log_2(K)!K$ number of equivalent decomposition matrices M for any minimally-sized balanced decomposition scheme $SP(Y)$.*

Proof. The proof follows from Theorem 3.1. □

Theorem 3.4. *If K is a power of 2, then the number of all possible minimally-sized balanced decomposition schemes $SP^m(Y)$ equals $\frac{(K-1)!}{\log_2(K)!}$.*

Proof. By Corollary 3.6 there exist $K!$ decomposition matrices of all possible MBDSs. By Corollary 3.7 for any MBDS there exist $\log_2(K)!K$ equivalent decomposition matrices. Thus, the number of all possible MBDSs equals:

$$\frac{K!}{\log_2(K)!K} = \frac{(K-1)!}{\log_2(K)!}.$$ □

The decoding stage for the MBDSs is realized according to Definition 3.4. In this context we determine the (minimal) Hamming distance of class code words and class-partition code words in decomposition matrices of MBDSs in Corollary 3.8.

Corollary 3.8. *If the number K of classes is a power of 2, then for any decomposition matrix M of a minimally-sized balanced decomposition scheme $SP^m(Y)$:*

(1) the minimal Hamming distance between different rows $M_{k,*}$ and $M_{o,*}$ of M is equal to 1, and
(2) the Hamming distance between any two different columns $M_{*,l}$ and $M_{*,m}$ of M is equal to $\frac{K}{2}$.

Proof. By Corollary 3.5 the rows of any decomposition matrix M of a minimally-sized balanced decomposition scheme $SP(Y)$ forms a minimally-sized binary code for K classes. The properties (1) and (2) are properties of such a code. □

The results from Corollary 3.8 directly imply that:

- **The row separation property** does not hold for MBDSs. This is due to the fact that the minimum Hamming distance between class code words in any decomposition matrix corresponding to any MBDS equals one. Thus, the ensemble classifiers $h_{SP(Y)}$ based on these decomposition schemes are not capable of correcting errors of the binary classifiers $h_{P(Y)} \in h_{SP(Y)}$.
- **The column separation property** does hold for the MBDSs. This is due to the fact that the Hamming distance of the class-partition code words in any decomposition matrix corresponding to any minimally-sized balanced decomposition scheme equals $\frac{K}{2}$ (the maximal possible distance). Thus, we expect that the errors of the binary classifiers $h_{P(Y)} \in h_{SP(Y)}$ are minimally correlated.

From the above we conclude that MBDSs have an error-correction problem; i.e., MBDSs do not have error-correction capabilities. Nevertheless, when the number of classes is very large, MBDSs can be a viable alternative to the eECOC decomposition scheme. This is due to the fact that they do not have a computational-complexity problem. We note that by Theorem 3.3 the number of the binary classifiers $h_{P(Y)}$ in any MBDS ensemble $h_{SP(Y)}$ equals $\lceil \log_2(K) \rceil$.

3.4.3 *Voting Using Minimally-Sized Balanced Decomposition Schemes*

This subsection addresses the error-correction problem of MBDSs. To enforce error-correction we propose to vote with ensemble classifiers $h_{SP(Y)}$ based on different MBDSs. This approach is called Voting using Minimally-Sized Balanced Decomposition Schemes (VMBDSs) and it is considered below.

Let $SSP(Y)$ be a set of N randomly-chosen minimally-sized balanced decomposition schemes $SP^m(Y)$. Each minimally-sized balanced decomposition scheme $SP^m(Y)$ defines a classifier $h_{SP^m(Y)}$. The classifiers $h_{SP^m(Y)}$ form an ensemble classifier $h_{SSP(Y)} : X \rightarrow Y$ equal to $\{h_{SP^m(Y)}\}_{SP^m(Y) \in SSP(Y)}$. Decoding the predictions of the classifiers $h_{SP^m(Y)}$ into the prediction of $h_{SSP(Y)}$ is realized for any test instance $x \in X$ and class $y \in Y$ by computing an integer score $S(x,y|h_{SSP(Y)})$. This computation is a two-stage process: first we take the class score $S(x,y|h_{SP^m(Y)})$ provided by each classifier $h_{SP^m(Y)}$ (see Definition 3.4) and then compute the score $S(x,y|h_{SSP(Y)})$ as the sum of scores $S(x,y|h_{SP^m(Y)})$ over all the classifiers $h_{SP^m(Y)}$ (see Definition 3.8).

Definition 3.8. Given a set $SSP(Y)$ of minimally-sized balanced decomposition schemes $SP^m(Y)$, a test instance $x \in X$, and a class $y \in Y$, the score $S(x,y|h_{SSP(Y)})$ for x and y provided by the ensemble classifier $h_{SSP(Y)}$ is defined as follows:

$$S(x,y|h_{SSP(Y)}) = \sum_{SP^m(Y) \in SSP(Y)} S(x,y|h_{SP^m(Y)}). \tag{3.3}$$

The rule for the score $S(x,y|h_{SSP(Y)})$ can be further refined. If we combine Eqs. 3.2-3.3 we receive:

$$S(x,y|h_{SSP(Y)}) = \sum_{SP^m(Y)\in SSP(Y)} \sum_{P(Y)\in SP^m(Y)} S(x,y|h_{P(Y)}). \quad (3.4)$$

Thus, the class with the highest score $S(x,y|h_{SSP(Y)})$ will be the class $y \in Y$ that receives most of the votes $S(x,y|h_{P(Y)})$ of the binary classifiers $h_{P(Y)}$.

The class with the highest score according to Eq. 3.4 can be determined by Hamming decoding as well. For that purpose we consider a decomposition matrix $M_{SSP(Y)}$ with dimensions $K \times N\log_2(K)$. The matrix consists of the class-partition code words of the decomposition matrices of the minimally-sized balanced decomposition schemes $SP^m(Y) \in SSP(Y)$ given some order over the class set Y. Classifying any instance $x \in X$ using the decomposition matrix $M_{SSP(Y)}$ is realized using the standard decoding procedure described in Sect. 3.3.2. It is easy to show that the final class for the instance x is exactly that which maximizes the score given in Eq. 3.4.

Since VMBDSs can be explained using the decomposition matrix $M_{SSP(Y)}$, we analyze the properties of class code words and class-partition code words in $M_{SSP(Y)}$.

- **Class code words:** the Hamming distance between class code words in the decomposition matrix $M_{SSP(Y)}$ is computed for non-repeated columns only. Hence, if we have two class code words $M_{i,*}, M_{j,*} \in M_{SSP(Y)}$ that differ in positions o and p, their Hamming distance equals 2 if class-partition code words $M_{*,o}, M_{*,p} \in M_{SSP(Y)}$ are different; otherwise, it is equal to 1. In the case when all minimally-sized balanced decompositions $SP^m(Y) \in SSP(Y)$ are disjointed (i.e., there is no column repetition in $M_{SSP(Y)}$), the minimal Hamming distance between class code words in $M_{SSP(Y)}$ equals N (N times the minimum Hamming distance between class code words of any decomposition matrix M of a MBDS).
- **Class-partition code words:** the Hamming distance between any two class-partition code words in the decomposition matrix $M_{SSP(Y)}$ decreases. If minimally-sized balanced decompositions $SP^m(Y) \in SSP(Y)$ are not disjointed, then the minimal Hamming distance between class-partition code words that belong to different MBDSs is in the range $[0, \frac{K}{2}]$; otherwise, it is in the range $[2, \frac{K}{2}]$. In both cases the errors of the binary classifiers $h_{P(Y)}$ that belong to different classifiers $h_{SP(Y)} \in h_{SSP(Y)}$ can be more correlated compared with an MBDS ensemble.

From the above it follows that the row separation property and column separation property do hold for VMBDSs iff minimally-sized balanced decompositions $SP^m(Y) \in SSP(Y)$ are disjointed. Thus, if we have a VMBDSs ensemble with N MBDS classifiers, then we can correct the errors of $\lfloor \frac{N-1}{2} \rfloor$ binary classifiers $h_{P(Y)} \in \bigcup_{SP^m(Y)\in SSP(Y)} h_{SP^m(Y)}$. However, the errors of some binary classifiers $h_{P(Y)}$ can be more correlated. In this context we note that improving the row separation property and keeping the column separation property in a limit according to [9] allows us reducing the bias and variance components of the error of the VMBDSs ensemble $h_{SSP(Y)}$ compared with the MBDS classifiers $h_{SP(Y)}$. This result for VMDBSs is supported by our experiments provided in the next Section.

Although VMBDS ensembles can correct bias and variance error components, in the extreme case they can contain $\frac{(K-1)!}{\log_2(K)!}$ MBDS classifiers (see Theorem 3.4). Thus, the VMBDSs ensembles can have a computational-complexity problem. Fortunately, our experiments show that the generalization performance of MBDS ensembles is already close to that of eECOC ensembles when N equals two.

3.5 Experiments

To assess the generalization performance of MBDS and VMBDSs ensembles, we performed three sets of experiments. The first set of experiments, provided in Sect. 3.5.1, compares the classification accuracy of MBDS and VMBDS ensembles against that of eECOC and OA on 15 UCI datasets [2]. The second set of experiments, discussed in Sect. 3.5.2, compares the classification accuracy of VMBDS ensembles against OA ensembles on data sets with a large number of classes. The third and final set of experiments, provided in Section 3.5.3, shows the error-reduction capabilities of MBDS and VMBDSs ensembles.

3.5.1 UCI Data Experiments

The purpose of the experiments in this section is to compare the classification accuracy of MBDS, VMBDSs, eECOC, and OA ensembles on 15 UCI datasets [2]. Three types of classifiers were employed as binary base classifiers: the Ripper rule classifier [3], logistic regression [10], and Support Vector Machines [8]. The number of MBDS classifiers in the VMBDSs ensembles varied from 1 to 15. The evaluation method was 10-fold cross validation averaged over 10 runs. The results are given in Table 3.4, Table 3.5, and Table 3.6 in the Appendix. The classification accuracy of the classifiers was compared using the corrected paired t-test [15] at the 5% significance level. Two types of t-test comparisons were realized: eECOC ensembles against all other ensembles and OA ensembles against all other ensembles.

The results in Tables 3.4-3.6 show that:

- The difference in classification accuracy between the MBDS and eECOC ensembles is not statistically significant in 28 out of 45 experiments. In the remaining 17 experiments the classification accuracy of the MBDS ensembles is statistically lower than that of the eECOC ensembles.
- The difference in classification accuracy between the MBDS and OA ensembles is not statistically significant in 34 out of 45 experiments. In the remaining 11 experiments the classification accuracy of the MBDS ensembles is statistically lower than that of the OA ensembles.
- The classification accuracy of the VMBDSs ensembles varies between the accuracy of the MBDS ensembles and the accuracy of the eECOC ensembles. The difference of the classification accuracy of the worst VMBDSs ensembles and the eECOC ensembles is not statistically significant in 28 out of 45 experiments. In the remaining 17 experiments the classification accuracy of the worst

VMBDSs ensembles is statistically lower than that of the eECOC ensembles. The difference of the classification accuracy of the best VMBDSs ensembles and the eECOC ensembles is not statistically significant in 44 out of 45 experiments. In the remaining one experiment the classification accuracy of the best VMBDSs ensembles is statistically greater than that of the eECOC ensembles.

- The difference of the classification accuracy between the worst VMBDSs ensembles and the OA ensembles is not statistically significant in 34 out of 45 experiments. In the remaining 11 experiments the classification accuracy of the worst VMBDSs ensembles is statistically lower than that of the eECOC ensembles. The difference of the classification accuracy of the best VMBDSs ensembles and the OA ensembles is not statistically significant in 38 out of 45 experiments. In the next 6 (1) experiments the classification accuracy of the best VMBDSs ensembles is statistically greater (lower) than that of the OA ensembles. In addition we compare the VMBDSs and OA ensembles when they have an approximately equal number of binary classifiers. In this case we compare the VMBDSs ensembles using two MBDS classifiers with the OA ensembles. The results are that the difference of the classification accuracy of the VMBDSs and OA ensembles is not statistically significant in 41 out of 45 experiments. In the next 2 (2) experiments the classification accuracy of the VMBDSs ensembles is statistically greater (lower) than that of the OA ensembles.

From the above we conclude that:

- The MBDS ensembles are the worst ensembles. The experiments confirm that the MBDS ensembles do not have error-correction capabilities.
- The VMBDSs ensembles perform much better than MBDS ensembles. Their classification accuracy improves with the number of the MBDS classifiers. The results confirm that the VMBDSs ensembles do have error-correction capabilities.
- The VMBDSs ensembles are comparable with the eECOC ensembles in terms of classification accuracy if the number of MBDS ensembles is more than one. In this case VMBDSs ensembles are more preferable, since they require a smaller number of binary classifiers.
- The VMBDSs ensembles are comparable with the OA ensembles in terms of classification accuracy if the number of the MBDS ensembles equals two. VMBDSs ensembles can outperform the OA ensembles if the number of the MBDS ensembles is greater than two.

3.5.2 Experiments on Data Sets with Large Number of Classes

The purpose of this section's experiments is to compare the classification accuracy of the VMBDSs and OA on three datasets with a large number of classes. The datasets chosen are `Abalone` [2], `Patents` [12], and `Faces94` [11]. Several properties of these datasets are summarized in Table 3.1.

Table 3.1 Number of instances and classes for the `Abalone`, `Patents`, and `Faces94` datasets

Name	#instances	#classes
`Abalone`	4177	28
`Patents`	2373	70
`Faces94`	3059	153

The eECOC ensembles were excluded from the experiments, since they require an exponential number of binary classifiers (in our experiments at least $2^{27} - 1$). Support Vector Machines [8] were used as a base classifier. The number of MBDS classifiers in the VMBDSs ensembles was varied from 5 - 25. The evaluation method was 5-fold cross validation averaged over 5 runs. The results are presented in Table 3.2. The classification accuracy of the classifiers is compared using the corrected paired t-test [15] at the 5% significance level. The test compares the OA ensembles against all VMBDSs ensembles.

Table 3.2 Classification Accuracy of SVM-based OA and VMBDSs ensembles on the `Abalone`, `Patents`, and `Faces94` datasets. The numbers in the VMBDSs columns indicate the number of MBDS classifiers in the VMBDSs ensemble. Bold numbers indicate statistically better results with respect to the OA ensembles.

		VMBDSs		
Data set	**OA**	**5**	**10**	**25**
`Abalone`	0.023 ± 0.002	$\mathbf{8.65 \pm 5.31}$	$\mathbf{13.53 \pm 4.58}$	$\mathbf{18.05 \pm 4.29}$
`Patents`	17.23 ± 1.05	19.52 ± 1.81	$\mathbf{21.13 \pm 1.71}$	$\mathbf{21.54 \pm 1.30}$
`Faces94`	73.85 ± 4.29	74.98 ± 2.06	$\mathbf{87.26 \pm 1.21}$	$\mathbf{93.68 \pm 0.80}$

The experimental results from Table 3.2 show that the VMBDSs ensembles can outperform statistically the OA ensembles on these three datasets. In this respect it is important to know whether the VMBDSs ensembles outperform the OA ensembles when both types of ensembles contain the same number of binary classifiers; i.e., when their computational complexities are equal. We show how to organize this experiment for the `Abalone` dataset. This dataset has 28 classes. Thus, the number of binary classifiers in the OA ensemble is 28. This implies that we have to find a configuration for the VMBDSs ensembles so that the total number of binary classifiers is close to 28. In this context we note that the number of binary classifiers in each MBDS ensemble is $\lceil \log_2(28) \rceil = 5$. Thus, in order to have close to 28 number of binary classifiers we need $\lfloor \frac{28}{5} \rfloor = 5$ MBDS classifiers. According to Table 3.2 for this configuration the VMBDSs ensemble outperforms statistically the OA ensemble. Analogously we can do the same computation for the `Patents` and `Faces94` datasets: for the `Patents` dataset we need 10 MBDS classifiers and for the `Faces94` dataset we need 19 MBDS classifiers in the VMBDSs ensemble. According to Table 3.2 for these configurations the VMBDSs ensembles outperform statistically the OA ensemble.

3.5.3 Bias-Variance Decomposition Experiments

The experiments performed in this section aim at obtaining insight into whether eECOC and VMBDSs ensembles are able to reduce the generalization error. For that purpose a bias-variance analysis is performed. We compare the bias, variance and expected loss of three methods: the Ripper classifier, eECOC ensembles, and VMBDSs ensembles. The bias-variance decomposition employed is that of Domingos [5]. The binary base classifier for the ensembles is the Ripper classifier. Four experiments are designed, each for a particular number of classes $K \in [5,8]$. For each experiment, we use a synthetic data set generated as follows. Instances for each class are drawn from a multivariate Gaussian distribution over three variables, with the mean of each distribution located in a fixed octant of the three-dimensional coordinate system such that none of the distribution means are located in the same octant. The distributions have unit covariance. For training, 200 data sets of each 200 instances are used. For testing we use a single data set of 5000 instances [9].

The results are given in Table 3.3. They show that if the base classifier is unstable (e.g. Ripper), the bias and variance components of the error of the VMBDSs ensembles are reduced. More precisely, the expected loss, bias, and variance of the VMBDSs ensembles decrease with the number of MBDS classifiers. If the number of MBDS classifiers in the VMBDSs ensembles is greater than or equal to 5, the expected loss, bias, and variance of the VMBDSs ensembles are significantly better than those for the Ripper classifier. If the number of MBDS classifiers in the VMBDSs ensembles is greater than or equal to 50, the expected loss, bias, and variance of the VMBDSs ensembles become close to those of the eECOC ensembles.

Table 3.3 Results for the bias-variance decomposition for data sets with 5, 6, 7 and 8 classes. The numbers in the VMBDSs headers indicate the number of MBDS classifiers in these ensembles.

# classes		Ripper	eECOC	VMBDSs:1	VMBDSs:5	VMBDSs:50
5	Exp.Loss	0.28	0.20	0.33	0.24	0.21
	Bias	0.02	0.02	0.11	0.04	0.02
	Var.	0.23	0.14	0.24	0.17	0.15
	Noise	0.06	0.06	0.06	0.06	0.06
6	Exp.Loss	0.32	0.21	0.39	0.25	0.23
	Bias	0.04	0.03	0.15	0.04	0.02
	Var.	0.27	0.16	0.28	0.19	0.18
	Noise	0.06	0.06	0.06	0.06	0.06
7	Exp.Loss	0.36	0.21	0.41	0.26	0.22
	Bias	0.05	0.03	0.15	0.06	0.04
	Var.	0.32	0.16	0.31	0.19	0.17
	Noise	0.05	0.05	0.05	0.05	0.05
8	Exp.Loss	0.41	0.24	0.46	0.30	0.25
	Bias	0.05	0.02	0.15	0.05	0.03
	Var.	0.37	0.19	0.37	0.24	0.21
	Noise	0.05	0.05	0.05	0.05	0.05

3.6 Conclusion

In this paper we addressed the computational-complexity problem of the ECOC decomposition schemes. We provided a deep analysis of minimally-sized balanced decomposition schemes (MBDSs). We proved that the size of MBDSs equals $\lceil \log_2(|Y|) \rceil$. This property implies that MBDSs do not have a computational-complexity problem for large number of classes. We quantified the space of all possible MBDSs. We analyzed the error-correction properties of MBDSs and showed that the minimal Hamming distance between MBDS class code words equals 1. Thus, we concluded that MBDSs cannot correct the classification errors of the binary classifiers in MBDS ensembles. To enforce error correction we proposed voting with MBDS ensembles (VMBDSs). We showed that VMBDSs improve generalization performance with the number of MBDS classifiers. However this number can be large and the VMBDSs ensembles can have a computational-complexity problem. Fortunately our experiments demonstrated that the VMBDSs ensembles are comparable with the ECOC ensembles and can outperform the one-against-all ensembles for a small number of the MBDS classifiers.

The practical value of the VMBDSs ensembles stems from the fact that their generalization performance is comparable with that of ECOC schemes and that VMBDSs ensembles require a smaller number of binary classifiers. In practice designing VMBDSs ensembles can be realized as follows. First we estimate the time needed for the learning algorithm employed to train one binary classifier. Then we use this time to estimate the time to train one MBDS ensemble. Finally we decide how many MBDS ensembles need to be included in the resulting VMBDSs ensemble depending on the time restriction imposed.

Future research will focus on two open problems for the MBDSs and VMBDSs ensembles. The first open problem for the MBDSs ensembles is how to design MBDSs schemes so that the generalization performance is maximized. We note that in our current work the MBDSs schemes are chosen randomly. Thus it is possible that classes that are too close (distant) are included too often in different (same) sets of class partitions. This weakens the generalization performance of the binary classifiers and MBDSs ensembles. One possible solution to this problem is to design the MBDSs schemes with respect to the training data so that the classes are included in class partitions depending on their distances to other classes.

The second open problem is that of diversifying the MBDS ensembles in the VMBDSs ensembles. We note that in our current work the MBDSs classifiers are chosen randomly. Thus it is possible to have quite similar MBDSs classifiers in the VMBDSs ensembles. This weakens the generalization performance of the VMBDSs ensembles. Thus we need to develop an approach that can generate the most diverse VMBDSs ensembles.

Software. The Java implementation of the VMBDSs for the Weka environment [20] can be found on: http://www.personeel.unimaas.nl/smirnov/VMBDSs.zip.

References

1. Allwein, E., Schapire, R., Singer, Y.: Reducing multiclass to binary: A unifying approach for margin classifiers. J. Machine Learning Research 1, 113–141 (2002)
2. Asuncion, A., Newman, D.J.: UCI machine learning repository, http://www.ics.uci.edu/~mlearn/MLRepository.html
3. Cohen, W.: Fast effective rule induction. In: Prieditis, A., Russell, R. (eds.) Proc. the 12th Int. Conf. Machine Learning, Tahoe City, CA, pp. 115–123. Morgan Kaufmann, San Francisco (1995)
4. Dietterich, T.G., Bakiri, G.: Solving multiclass learning problems via error-correcting output codes. J. Artif. Intell. Research 2, 263–286 (1995)
5. Domingos, P.: A unified bias-variance decomposition for zero-one and squared loss. In: Kautz, H., Porter, B. (eds.) Proc. the 17th National Conf. Artif. Intell. and 12th Conf. Innovative Applications Artif. Intell., pp. 564–569. AAAI Press, Menlo Park (2000)
6. Freund, Y., Schapire, R.: A decision-theoretic generalization of on-line learning and an application to boosting. J. Comp. Syst. Sci. 55, 119–139 (1997)
7. Fürnkranz, J.: Round robin classification. J. Machine Learning Research 2, 721–747 (2002)
8. Keerthi, S.S., Shevade, S.K., Bhattacharyya, C., Murthy, K.R.K.: Improvements to Platt's SMO algorithm for SVM classifier design. Neural Comp. 13, 637–649 (2001)
9. Kong, E.B., Dietterich, T.G.: Error-correcting output coding corrects bias and variance. In: Prieditis, A., Russell, S.J. (eds.) Proc. the 12th Int. Conf. Machine Learning, Tahoe City, CA, pp. 313–321. Morgan Kaufmann, San Francisco (1995)
10. le Cessie, S., van Houwelingen, J.C.: Ridge estimators in logistic regression. Applied Statistics 41, 191–201 (1992)
11. Libor, S.: Face recognition database (2011), http://cswww.essex.ac.uk/mv/allfaces/index.html
12. Lissoni, F., Llerena, P., Sanditov, B.: Inventors small worlds: academic and CNRS researchers in networks of inventors in France. In: Proc. the DIME Final Conf., Maastricht, The Netherlands (2011)
13. Lorena, A.C., De Carvalho, A.C.P.L.F., Gama, J.M.P.: A review on the combination of binary classifiers in multiclass problems. Artif. Intell. Rev. 30, 19–37 (2008)
14. Mayoraz, E., Moreira, M.: On the decomposition of polychotomies into dichotomies. In: Fisher, D.H. (ed.) Proc. the 14th Int. Conf. Machine Learning, Nashville, TN, pp. 219–226. Morgan Kaufmann, San Francisco (1997)
15. Nadeau, C., Bengio, Y.: Inference for the generalization error. Machine Learning 52, 239–281 (2001)
16. Nilsson, N.: Learning machines: foundations of trainable pattern-classifying systems. McGraw-Hill, New York (1965)
17. Peterson, W., Weldon, J.: Error-correcting codes. MIT Press, Cambridge (1972)
18. Rifkin, R., Klautau, A.: In defense of one-vs-all classification. J. Machine Learning Research 5, 101–141 (2004)
19. Weston, J., Watkins, C.: Support vector machines for multi-class pattern recognition. In: Verleysen, M. (ed.) Proc. the 7th European Symp. Artif. Neural Networks, Bruges, Belgium, pp. 219–224 (1999)
20. Witten, I., Frank, E., Hall, M.: Data mining: Practical machine learning tools and techniques. Morgan Kaufmann, San Francisco (2011)

APPENDIX: Classification Accuracy of eECOC, OA, and VMBDSs Ensembles on 15 UCI Datasets

This appendix contains the experimental results in terms of the classification accuracy of the eECOC, OA, and VMBDSs ensembles based on three base classifiers: Ripper (Table 3.4), logistic regression (Table 3.5), and support vector machines (Table 3.6). The table header numbers in the VMBDSs columns show the number of MBDS classifiers in the VMBDSs ensembles. The numbers after the data-set names indicate the number of classes. The lower-left (upper-left) dots show statistically worse (better) results with respect to the OA ensembles. The lower-right (upper-right) dots indicate statistically worse (better) results with respect to the eECOC ensembles. The statistical test is the corrected paired t-test at the 5% significance level.

Table 3.4 Classification accuracy of the OA, eECOC, and VMBDSs ensembles using the Ripper classifier as a base classifier

			VMBDSs						
Data set	**OA**	**eECOC**	**1**	**2**	**3**	**4**	**5**	**10**	**15**
car(4)	88.5	89.5	◦83.5◦	87.0◦	87.2◦	n/a	n/a	n/a	n/a
hypothy(4)	99.2	99.3	99.1	99.1	99.2	n/a	n/a	n/a	n/a
lymphog(4)	77.8	78.7	73.4	75.3	75.2	n/a	n/a	n/a	n/a
molecul(4)	28.9	26.9	27.7	26.6	26.7	n/a	n/a	n/a	n/a
clevela(5)	79.8	80.4	77.0	78.1	79.2	79.8	80.2	80.2	80.5
hungari(5)	79.8	79.9	77.9	78.6	79.2	79.7	79.8	79.8	80.2
page-bl(5)	97.0◦	•97.4	◦96.5◦	96.7◦	97.0◦	97.1	97.2	97.2	97.3
anneal(6)	98.7	98.5	97.9	98.1	98.2	98.4	98.3	98.4	98.5
bridge1(6)	64.0	66.8	58.4	60.0	62.2	63.4	63.3	64.1	65.0
bridge2(6)	64.1	65.6	58.0	59.2	60.3	61.7	62.3	63.3	64.6
autos(7)	71.9◦	•79.0	67.5◦	72.6	75.0	75.8	76.3	77.1	77.4
glass(7)	67.2◦	•74.9	64.8◦	68.5◦	70.7	70.5	71.3	73.0	73.7
zoo(7)	91.5	93.1	89.0	91.0	91.5	92.4	91.9	92.7	93.0
ecoli(8)	80.7◦	•85.4	◦76.3◦	79.8◦	82.8	84.1	83.7	83.7	84.1
flags(8)	58.3	62.3	51.1◦	56.1	58.4	59.3	60.0	61.2	61.1

Table 3.5 Classification accuracy of the OA, eECOC, and VMBDSs ensembles using logistic regression as a base classifier

			VMBDSs						
Data set	**OA**	**eECOC**	**1**	**2**	**3**	**4**	**5**	**10**	**15**
car(4)	90.1	89.8	∙86.2∙	88.9	90.0	n/a	n/a	n/a	n/a
hypothy(4)	95.1∙	•95.3	95.3	95.5	95.3	n/a	n/a	n/a	n/a
lymphog(4)	78.4	77.7	77.4	77.9	77.4	n/a	n/a	n/a	n/a
molecul(4)	30.0	29.5	27.9	29.1	28.5	n/a	n/a	n/a	n/a
clevela(5)	83.7	83.7	83.7	83.7	83.7	83.7	83.7	83.7	83.7
hungari(5)	84.2	84.2	84.2	84.2	84.2	84.2	84.2	84.2	84.2
page-bl(5)	95.7•	∙95.3	∙94.6∙	∙94.9∙	∙95.1	∙95.2	∙95.2	∙95.3	∙95.3
anneal(6)	99.5	99.6	99.2	99.4	99.5	99.5	99.6	99.7	99.7
bridge1(6)	59.6	63.6	46.6∙	50.1∙	53.6∙	55.9	54.3∙	57.1	58.8
bridge2(6)	55.0	57.8	46.7∙	50.1∙	51.4	52.5	52.3	54.6	54.0
autos(7)	66.9	71.6	∙57.9∙	62.5∙	64.6∙	66.3	66.8	68.8	69.8
glass(7)	64.3	63.9	∙57.2∙	59.7	60.3	60.5	60.0∙	62.0	62.4
zoo(7)	89.5	91.4	82.2∙	88.0	89.6	89.6	90.5	91.7	91.6
ecoli(8)	86.5	86.0	∙76.9∙	∙82.5∙	85.1	86.0	85.8	85.6	85.8
flags(8)	47.1	51.3	∙37.0∙	42.1∙	43.8∙	45.8	46.6	47.9	49.0

Table 3.6 Classification accuracy of the OA, eECOC, and VMBDSs ensembles using SVM as a base classifier

			VMBDSs						
Data set	**OA**	**eECOC**	**1**	**2**	**3**	**4**	**5**	**10**	**15**
car(4)	81.0∙	•86.0	•87.6	•87.1	•86.0	n/a	n/a	n/a	n/a
hypothy(4)	93.3	93.3	93.3	93.4	93.3	n/a	n/a	n/a	n/a
lymphog(4)	85.2	85.6	85.0	84.2	83.0	n/a	n/a	n/a	n/a
molecul(4)	29.0	29.0	28.5	27.9	28.9	n/a	n/a	n/a	n/a
clevela(5)	83.8	83.8	83.8	83.8	83.8	83.8	83.8	83.9	83.9
hungari(5)	82.7	82.7	82.7	82.7	82.7	82.7	82.7	82.7	82.7
page-bl(5)	92.0	92.0	92.1	91.9	92.1	92.2	92.3	92.4	•92.6
anneal(6)	96.6∙	•97.3	96.7	96.9	97.2	97.3	97.4	97.5	97.6
bridge1(6)	58.4∙	•65.9	61.2	61.5	62.9	63.4	64.8	•66.3	•65.4
bridge2(6)	61.5∙	•67.3	64.5	64.6	65.7	66.5	•67.3	66.7	66.7
autos(7)	56.0∙	•64.7	58.3	60.2	•62.6	•62.9	•63.4	•63.9	•64.6
glass(7)	44.4∙	•51.3	48.7	40.6∙	•50.1	•50.0	46.6	51.5	49.9
zoo(7)	93.6	94.7	94.5	94.4	95.0	95.0	95.0	94.7	94.5
ecoli(8)	68.6∙	•81.1	•75.4∙	•76.9∙	•77.7	•79.5	•79.8	•80.1	•80.3
flags(8)	55.1∙	•63.3	53.5∙	56.0∙	58.7	59.4	60.5	•61.3	•61.5

Chapter 4
Bias-Variance Analysis of ECOC and Bagging Using Neural Nets

Cemre Zor, Terry Windeatt, and Berrin Yanikoglu

Abstract. One of the methods used to evaluate the performance of ensemble classifiers is bias and variance analysis. In this chapter, we analyse bootstrap aggregating (Bagging) and Error Correcting Output Coding (ECOC) ensembles using a bias-variance framework; and make comparisons with single classifiers, while having Neural Networks (NNs) as base classifiers. As the performance of the ensembles depends on the individual base classifiers, it is important to understand the overall trends when the parameters of the base classifiers – nodes and epochs for NNs –, are changed. We show experimentally on 5 artificial and 4 UCI MLR datasets that there are some clear trends in the analysis that should be taken into consideration while designing NN classifier systems.

4.1 Introduction

Within Machine Learning research, many techniques have been proposed in order to understand and analyse the success of ensemble methods over single classifiers. One of the main approaches considers tightening the generalization error bounds by using the margin concept [17]. Though theoretically interesting, bounds are not usually tight enough to be used in practical design issues. Another method used to show why ensembles work well is bias and variance analysis. In this chapter, we try to analyse the success of bootstrap aggregating (bagging) [8] and Error Correcting Output Coding (ECOC) [4] as ensemble classification techniques, by using Neural Networks (NNs) as the base classifiers and zero-one loss as the loss function within the bias and variance framework of James [13]. As the characteristics

Cemre Zor · Terry Windeatt
Centre for Vision, Speech and Signal Processing, University of Surrey, UK, GU2 7XH
E-mail: (c.zor,t.windeatt)@surrey.ac.uk

Berrin Yanikoglu
Sabanci University, Tuzla, Istanbul, Turkey, 34956
E-mail: berrin@sabanciuniv.edu

O. Okun et al. (Eds.): Ensembles in Machine Learning Applications, SCI 373, pp. 59–73.
springerlink.com

of the ensemble depend on the specifications of the base classifiers, having a detailed look at the parameters of the base classifiers within the bias-variance analysis is of importance. Comparisons of bagging and ECOC ensembles with single classifiers have been shown through various experiments by changing these parameters, namely nodes and epochs of NN base classifiers. Similar work for bagged Support Vector Machines (SVMs) within Domingos' bias-variance framework [6] can be found in [22].

4.1.1 Bootstrap Aggregating (Bagging)

Bagging [8] is a commonly used ensemble method, which suggests aggregating the decisions of base classifiers trained on bootstrapped training sets.

Using the idea of bootstrapping, i training sets, $D_{1,2,\ldots,i}$, are formed by uniformly sampling elements from the main training set D, with replacement. Note that on average about 37% of each D_i is replicated. By bootstrapping, a close enough approximation to random and independent data generation from a known underlying distribution is expected to be achieved [3]. The training sets created are later used to train the base classifiers; and classification is performed by combining their decisions through majority voting.

4.1.2 Error Correcting Output Coding (ECOC)

ECOC is an ensemble technique [4], in which multiple base classifiers are created and trained according to the information obtained from a pre-set binary *code matrix*. The main idea behind this procedure is to solve the original multi-class problem by combining the decision boundaries obtained from simpler two-class decompositions. The original problem is likely to be more complex compared to the subproblems into which it is decomposed, and therefore the aim is to come up with an easier and/or more accurate solution using the sub-problems rather than trying to solve it by a single complex classifier.

The base classifiers are actually two-class classifiers (dichotomizers), each of which is trained to solve a different bi-partitioning of the original problem. The bi-partitions are created by combining the patterns from some predetermined classes together and relabeling them. An example bi-partitioning of an $N > 2$ class dataset would be by having the patterns from the first 2 classes labeled as $+1$ and the last $N-2$ classes as -1. The training patterns are therefore separated into two superclasses for each base classifier, and the information about how to create these superclasses is obtained from the ECOC matrix.

Consider an ECOC matrix C, where a particular element C_{ij} is an element of the set $(+1,-1)$. Each C_{ij} indicates the desired label for class i, to be used in training the base classifier j; and each row, called a *codeword*, represents the desired output for the whole set of base classifiers for the class it indicates. Figure 4.1 shows an ECOC matrix for a 4-class problem for illustration purposes.

	b1	b2	b3	b4	b5
c1	+1	+1	+1	-1	-1
c2	+1	-1	-1	+1	-1
c3	+1	+1	-1	-1	-1
c4	-1	-1	-1	+1	+1

Fig. 4.1 An example ECOC matrix for a 4-class problem. b1,..., 5 indicate the names of columns to be trained by base classifiers 1,..., 5; and c1,..., 4 indicate names of rows dedicated to classes 1,..., 4.

During testing (decoding), a given test sample is classified by computing the similarity between the output (hard or soft decision) of each base classifier and the codeword for each class, by using a distance metric such as the Hamming or the Euclidean distance. The class with the minimum distance is then chosen as the estimated class label.

As the name of the method implies, ECOC can handle incorrect base classification results up to a certain degree. Specifically, if the minimum Hamming distance (*HD*) between any pair of codewords is d, then up to $\lfloor (d-1)/2 \rfloor$ single bit errors can be corrected. In order to help with the error correction in the testing stage, the code matrix is advised to be designed to have large Hamming distances between the codewords of different classes. Moreover, when deterministic classifiers such as Support Vector Machines (SVMs) are used as base classifiers, the *HD* between a pair of columns should also be large enough so that the outputs of the base classifiers are uncorrelated [4] and their individual errors can be corrected by the ensemble. Many variations of the design of the ECOC matrix, namely *encoding*; and the test stage, namely *decoding*, have been suggested in the literature so far and are still open problems.

While the errors made by individual dichotomizers may be corrected using the ECOC approach, the encoding of the code matrix is also being researched in order to make the method more powerful. A straightforward approach in design is to have an *exhaustive code*, which includes all possible bi-partitionings of the problem. This means that for a problem consisting of n classes, an ECOC matrix of size $n \times (2^{n-1} - 1)$ is created[1]. Apart from the use of exhaustive codes which are computationally expensive and do not guarantee the best performance, some commonly used data-independent techniques such as the one-versus-all, one-versus-one, dense random and sparse random [1] coding schemes have been suggested for the ECOC matrix encoding. Furthermore, data dependent ECOC designs, in which training data is used to create coding matrices meaningful within the input data domain, have

[1] The number of classes is calculated as $2^{n-1} - 1$ after removing the complementary and the all-zero or all-one columns [4].

also gained importance. As an example for the data dependent ECOC design, intelligent creation of binary column classifiers which can better fit the decision boundaries of the problem training set can be given [7]. This is obtained through splitting the original set of classes into sub-classes using the training data. Most importantly, although problem dependent coding approaches provide successful outcomes, it has been theoretically and experimentally proven that the randomly generated long or deterministic equi-distant code matrices are also close to optimum performance when used with strong base classifiers [12, 14]. This is why, *long-random* codes have also been used for the experiments in this chapter. It has also been shown that in real life scenarios that equidistant codes are superior at least for shorter codes; but as length of code word is increased, the coding/decoding strategy becomes less significant [24]. Finally for encoding, note that the use of ternary ECOC matrices [1], where a zero symbol is used to leave a class out of the consideration of a dichotomizer, has also gained interest within the field.

There are many ways used in the decoding of the ECOC matrix apart from the usual *HD* decoding. It is a common convention that the decoding of the problem-dependent ECOC matrices is performed in accordance with their encoding. As common examples of decoding, general weighted decoding approaches, together with Centroid of Classes, Least Squares and Inverse Hamming Distance methods can be listed [24].

As a final point, it should be mentioned that many static and dynamic pruning methods can also be applied to ECOC (e.g., column selection), just like any other ensemble method, so as to increase the efficiency and accuracy.

4.1.3 Bias and Variance Analysis

Bias and variance analysis plays an important role in ensemble classification research due to the framework it provides for classifier prediction error decomposition.

Initially, Geman has decomposed prediction error into bias and variance terms under the regression setting using squared-error loss [10]. This decomposition brings about the fact that a decrease/increase in the prediction error rate is caused by a decrease/increase in bias, or in variance, or in both. Extensions of the analysis have been carried out on the classification setting, and later applied on different ensemble classifiers in order to analyse the reason behind their success over single classifiers. It has been shown that the reason for most of the ensembles to have lower prediction error rates is due to the reductions they offer in sense of both bias and variance.

However, the extension of the original theoretical analysis on regression has been done in various ways by different researchers for classification; and there is no standard definition accepted. Therefore, the results of the analyses also differ from each other slightly. Some of the definitions/frameworks that have gained interest within

the research field are given by Breiman [3], Kohavi and Wolpert [15], Dietterich and Kong [16], Friedman [9], Wolpert [25], Heskes [11], Tibshirani [19], Domingos [6] and James [13].

Although there are dissimilarities in-between the frameworks, the main intuitions behind each are similar. Consider a training set T with patterns (x_i, l_i), where x represents the feature vector and l the corresponding label. Given a test pattern, an optimal classifier model predicts a decision label by assuring the lowest expected loss over all possible target label values. This classifier, which is actually *the Bayes classifier* when used with the zero-one loss function, is supposed to know and use the underlying likelihood probability distribution for the input dataset patterns/classes. If we call the decision of the optimal classifier as the optimal decision (*OD*), then for a given test pattern (x_i, l_i), $OD = argmin_\alpha E_t[L(t, \alpha)]$ where L denotes the loss function used, and l the possible target label values.

The estimator, on the other hand, is actually an averaged classifier model. It predicts a decision label by assuring the lowest expected loss over all labels that are created by classifiers trained on different training sets. The intrinsic parameters of these classifiers are usually the same, and the only difference is the training sets that they are trained on. In this case, instead of minimizing the loss over the target labels using the known underlying probability distribution as happens in the optimal classifier case, the minimization of the loss is carried out for the set of labels which are created by the classifiers trained on various training sets. If the decision of the estimator is named as the expected estimator decision (*EED*); then for a given test pattern (x_i, l_i), $EED = argmin_\alpha E_l[L(l, \alpha)]$ where L denotes the loss function used, and l the label values obtained from the classifiers used. For regression under the squared-error loss setting, the *OD* is the *mean* of the target labels while the *EED* is the *mean* of the classifier decisions obtained via different training sets.

Bias can mainly be defined as the difference or the distance between *OD* and *EED*. Therefore, it emphasizes how effectively the optimal decision can be predicted by the estimator. The type of the distance metric used depends on the loss function of the classification. On the other hand, variance is calculated as the expected loss exposed by the classifiers, which are trained on different training sets, while predicting *OD*. So, it shows how sensible the estimate is, against variations in the training data [9].

The problem with the above mentioned definitions of bias and variance is that most of them are given for specific loss functions such as the zero-one loss. It is difficult to generalize them for the other loss functions; usually new definitions are given for each new loss function. Secondly, as for the definitions which are proposed to be applicable for all loss functions, the problem of failing to satisfy the additive decomposition of the prediction error defined in [10] exists.

The definition of James [13] has advantages over the others as it proposes to construct a bias and variance scheme which is generalizable to any symmetric loss function, while assuring the additive prediction error decomposition by utilizing two new concepts called *systematic effect* (*SE*) and *variance effect* (*VE*). These concepts also help realizing the effects of bias and variance on the prediction error.

Some characteristics of the other definitions which make James' more preferable are as follows:

1. Dietterich allows a negative variance and it is possible for the Bayes classifier to have positive bias.
2. Experimentally, the trends of Breiman's bias and variance closely follow James' *SE* and *VE* respectively. However, for each test input pattern, Breiman separates base classifiers into two sets, as biased and unbiased; and considers each test pattern only to have either bias or variance accordingly.
3. Kohavi and Wolpert also assign a nonzero bias to the Bayes classifier but the Bayes error is absorbed within the bias term. Although it helps avoid the need to calculate the Bayes error in real datasets through making unwarranted assumptions, it is not preferable since the bias term becomes too high.
4. The definitions of Tibshirani, Heskes and Breiman are difficult to generalize and extend for the loss functions other than the ones for which they were defined.
5. Friedman proposes that bias and variance do not always need to be additive.

In addition to all these differences, it should also be noted that the characteristics of bias and variance of Domingos' definition are actually close to James', although the decomposition can be considered as being multiplicative [13].

In the literature, attempts have been made to explore the bias-variance characteristics of ECOC and bagging ensembles. Examples can be found in [3, 5, 13, 16, 18, 22]. In this chapter, a detailed bias-variance analysis of ECOC and bagging ensembles using NNs as base classifiers is given while systematically changing parameters, namely nodes and epochs, based on James' definition.

We start by taking a detailed look at the bias and variance framework of James in the next section.

4.2 Bias and Variance Analysis of James

James [13] extends the prediction error decomposition, which is initially proposed by Geman et al [10] for squared error under regression setting, for all symmetric loss functions. Therefore, his definition also covers zero-one loss under classification setting, which we use in the experiments.

In his decomposition, the terms *systematic effect* (*SE*) and *variance effect* (*VE*) satisfy the additive decomposition for all symmetric loss functions, and for both real valued and categorical predictors. They actually indicate the effect of bias and variance on the prediction error. For example, a negative *VE* would mean that variance actually helps reduce the prediction error. On the other hand, the bias term is defined to show the average distance between the response and the predictor; and the variance term refers to the variability of the predictor. As a result, both the meanings and the additive characteristics of the bias and variance concepts of the original setup have been preserved. Following is a summary of the bias-variance derivations of James:

For any symmetric loss function L, where $L(a,b) = L(b,a)$:

$$\begin{aligned} E_{Y,\tilde{Y}}[L(Y,\tilde{Y})] &= E_Y[L(Y,SY)] + E_Y[L(Y,S\tilde{Y}) - L(Y,SY)] \\ &\quad + E_{Y,\tilde{Y}}[L(Y,\tilde{Y}) - L(Y,S\tilde{Y})] \\ prediction\,error &= Var(Y) + SE(\tilde{Y},Y) + VE(\tilde{Y},Y) \end{aligned} \tag{4.1}$$

where $L(a,b)$ is the loss when b is used in predicting a, Y is the response and $\tilde{Y}$ is the predictor. $SY = argmin_\mu E_Y[L(Y,\mu)]$ and $S\tilde{Y} = argmin_\mu E_Y[L(\tilde{Y},\mu)]$. We see here that prediction error is composed of the variance of the response (irreducible noise), *SE* and *VE*.

Using the same terminology, the bias and variance for the predictor are defined as follows:

$$\begin{aligned} Bias(\tilde{Y}) &= L(SY,S\tilde{Y}) \\ Var(\tilde{Y}) &= E_{\tilde{Y}}[L(\tilde{Y},S\tilde{Y})] \end{aligned} \tag{4.2}$$

When the specific case of classification problems with zero-one loss function is considered, we end up with the following formulations:

$L(a,b) = I(a \neq b)$, $Y\,\varepsilon\,\{1,2,3..N\}$ for an N class problem, $P_i^Y = P_Y(Y=i)$, $P_i^{\tilde{Y}} = P_{\tilde{Y}}(\tilde{Y}=i)$, $ST = argmin_i E_Y[I(Y \neq i)] = argmax_i P_i^Y$

Therefore,

$$\begin{aligned} Var(Y) &= P_Y(Y \neq SY) = 1 - max_i P_i^Y \\ Var(\tilde{Y}) &= P_{\tilde{Y}}(\tilde{Y} \neq S\tilde{Y}) = 1 - max_i P_i^{\tilde{Y}} \\ Bias(\tilde{Y}) &= I(S\tilde{Y} \neq SY) \\ VE(\tilde{Y},Y) &= P(Y \neq \tilde{Y}) - P_Y(Y \neq S\tilde{Y}) = P_{S\tilde{Y}}^Y - \sum_i P_i^Y P_i^{\tilde{Y}} \\ SE(\tilde{Y},Y) &= P_Y(Y \neq S\tilde{Y}) - P_Y(Y \neq SY) = P_{SY}^Y - P_{S\tilde{Y}}^Y \end{aligned} \tag{4.3}$$

where $I(q)$ is 1 if q is a true argument and 0 otherwise.

4.3 Experiments

4.3.1 Setup

In the experiments, 3 classification methods have been analysed: Single classifier, bagging, and ECOC. In each case, 50 classifiers are created for bias-variance analysis. Each of these 50 classifiers is either a single classifier, or an ensemble consisting of 50 bagged classifiers or ECOC matrices of 50 columns. Due to the reasons explained in Sect. 4.1.2, the ECOC matrices are created by randomly assigning binary

values to each matrix cell; and Hamming Distance is used as the metric in the decoding stage. The optimization method used in NNs is the Levenberg-Marquart (LM) technique; the level of training (epochs) varies between 2 and 15; and the number of nodes between 2 and 16.

In artificial dataset experiments, training sets are created by simple random sampling from the infinite data at hand to be used in training 50 classifiers for bias/variance analysis. The number of training patterns per classifier is equal to 300, and the number of test patterns is 18000. Experiments have been repeated 10 times using different test data (also generated via simple random sampling) together with different training data and ECOC matrices in each run, and the results are averaged. In the two-class problem experiments, ECOC has not been used as it is a multi-class classification technique. Applying ECOC in such cases would be nothing different than applying bagging; effect of bootstrapping in bagging would be similar to the effect of the random initial weights of LM in ECOC.

For the UCI datasets having separate test sets, the training sets for each of the 50 classifiers are created from the finite dataset at hand using bootstrapping. Bootstrapping is expected to be a close enough approximation to random and independent data generation from a known underlying distribution [3].The analysis has been performed just once without repetition, as the test set is given/fixed. However, the results of the ECOC setting are averaged over 10 iterations with different matrices.

As for the UCI datasets without separate test sets, the *ssCV* cross-validation method of Webb and Conilione [23], which allows the usage of the whole dataset both in training and test stages, has been implemented. Within a number of iterations, all data is effectively used for both training and testing in each of the 50 classifiers, and the overall results for bias and variance analysis are recorded. The procedure is not repeated as the iterations within *ssCV* already cover the whole dataset. However, 10 different ECOC matrices are again used in ECOC setting, and results are averaged. Note that in *ssCV*, the shortcomings of the hold-out approach like the usage of small training and test sets, and the lack of inter-training variability control between the successive training sets has been overcome. In our experiments, we set the inter-training variability constant δ to $1/2$.

The diagram in Fig. 4.2 visualizes the experimental setup. Experiments have been carried out on 5 artificial and 4 UCI MLR [2] datasets; three of the artificial datasets being created according to Breiman's description in [3]. Detailed information about the sets can be found in Table 4.1.

The Bayes error, namely $Var(Y)$ for the zero-one loss function (see Eq. 4.3), is analytically calculated for the artificial datasets, as the underlying likelihood probability distributions are known. As for the real datasets, usually either the need for the underlying probability distributions has been overcome by assuming zero noise level [6], or some heuristic methods like using nearest neighbours [13] have been proposed to estimate the underlying probability distributions and therefore the Bayes error in the literature. The first approach has the shortcoming of a wrong estimate on bias. Therefore, we also use a heuristic method in our experiments to do the estimation. Our motivation is to find the optimal classifier parameters giving the lowest error rate possible, through cross-fold validation (CV); and then to use these

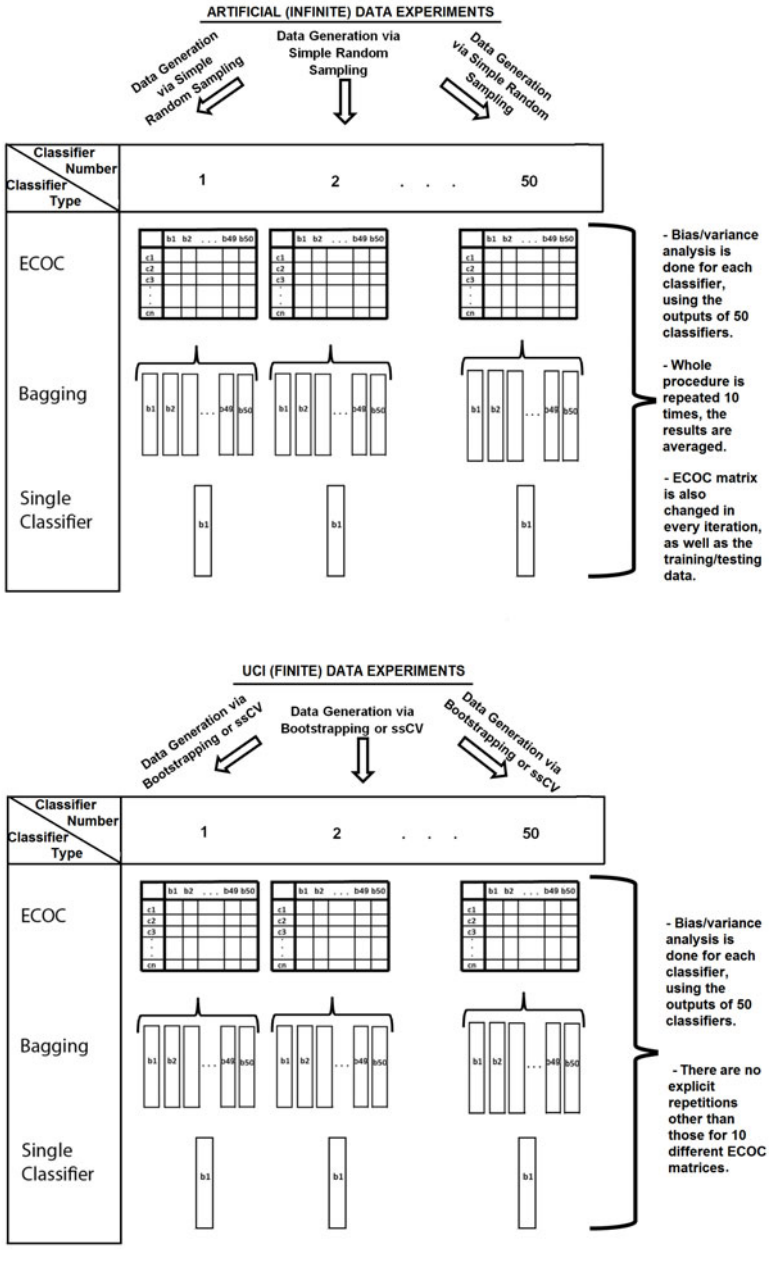

Fig. 4.2 Diagram illustrating the experimental setup for Artificial and Real (UCI MLR) datasets

Table 4.1 Summary of the datasets used

	Type	# Training Samples	# Test Samples	# Attributes	# Classes	Bayes Error (%)
TwoNorm [3]	Artificial	300	18000	20	2	2.28
ThreeNorm [3]	Artificial	300	18000	20	2	10.83
RingNorm [3]	Artificial	300	18000	20	2	1.51
ArtificialMulti1	Artificial	300	18000	2	5	21.76
ArtificialMulti2	Artificial	300	18000	3	9	14.33
Glass Identification	UCI	214*	-	9	6	38.66
Dermatology	UCI	358*	-	33	6	9.68
Segmentation	UCI	210	2100	19	7	4.21
Yeast	UCI	1484*	-	8	10	43.39

*: The total number of the elements of the UCI datasets without separate test sets, are listed under # of training samples.

parameters to construct a classifier which is expected to be close enough to the Bayes classifier. The constructed classifier is then used to calculate the output probabilities per pattern in the dataset. For this, we first find an optimal set of parameters for RBF SVMs by applying 10 fold *CV*; and then, obtain the underlying probabilities by utilizing the leave-one-out approach. Using the leave-one-out approach instead of training and testing with the whole dataset using the previously found *CV* parameters helps us avoid overfitting. It is assumed that the underlying distribution stays almost constant for each fold of the leave-one-out procedure.

4.3.2 Results

In this section, some clear trends found in the analysis are discussed under three subsections: the prediction error, convergence to the prediction error, and bias/variance versus *SE*/*VE*. In the first sub-section, the comparison of the prediction error rates is made for the bagging, ECOC and single classifiers, while in the second one the convergence points in sense of number of nodes and epochs where the prediction error converges to its optimum are discussed. Finally in the third sub-section, the relationship between bias/variance and SE/VE is analysed.

Although the observations are made using 9 datasets, for brevity reasons we only present a number of representative graphs.

4.3.2.1 The Prediction Error

Prediction errors obtained by bagging and ECOC ensembles are always lower than those of the single classifier, and the reduction in the error is almost always a result of reductions both in *VE* and in *SE*. This observation means that the contributions of bias and (predictor) variance to the prediction error are smaller when ensembles are

used (Figs. 4.3 and 4.4). However, note that reductions in *VE* have greater magnitude, and in two-class problems, the reduction in *SE* is almost zero (Fig. 4.5). As for bias and variance themselves, it has been observed that ECOC and bagging induce reduction in both, especially in variance, in almost all the cases. The fact that NNs are high variance/low bias classifiers also plays a role in these observations, where the high variance is more easily reduced compared to the already lower bias and *VE* is reduced more than *SE*. In [3] and [16], bagging and ECOC are also stated to have low variance in the additive error decomposition, and Kong-Dietterich framework [16] also acknowledges that ECOC reduces variance.

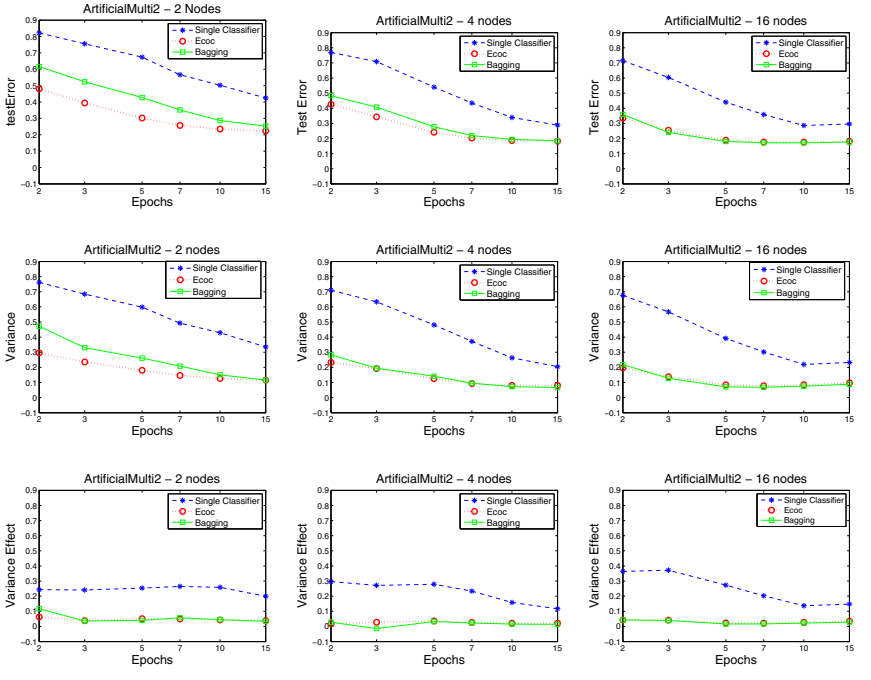

Fig. 4.3 Bias-Variance Analysis for ArtificialMulti2 data. First Row: Overall prediction error. Second Row: Variance. Third Row: Variance effect. First Column: For 2 Nodes. Second Column: For 4 Nodes. Third Column: For 16 Nodes. Dashed blue lines (starred) indicate the results for single classifier, dotted red (circled) for ECOC and solid green (squared) for bagging.

4.3.2.2 Convergence to the Prediction Error

It is observed that the convergence of bagging ensemble to the optimal prediction error is usually achieved at a lower number of epochs compared to those of single classifier; and ECOC ensemble convergence is often at lower epochs than bagging (Figs. 4.3, 4.4, 4.5). The prediction errors are also in the same descending order: single classifier, bagging and ECOC; except when complex networks with high number of nodes and epochs are used. Under these circumstances, *VE*, *SE*, and therefore the

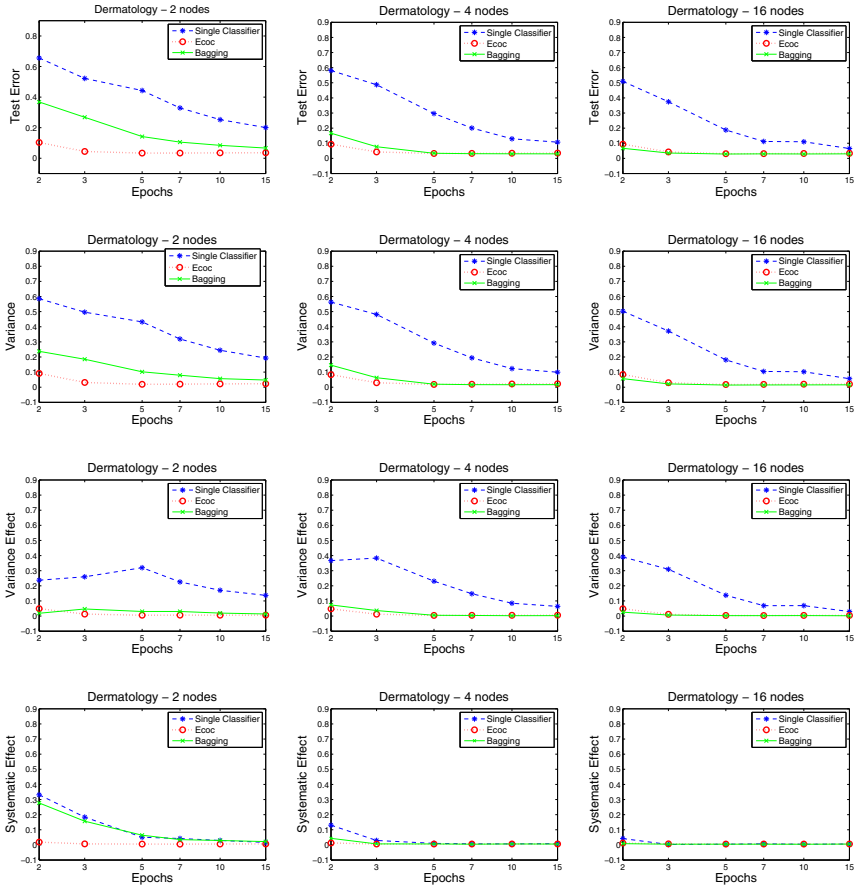

Fig. 4.4 Bias-Variance Analysis for Dermatology data. First Row: Overall prediction error. Second Row: Variance. Third Row: Variance effect. Fourth Row: Systematic effect. First Column: For 2 Nodes. Second Column: For 4 Nodes. Third Column: For 16 Nodes. Dashed blue lines (starred) indicate the results for single classifier, dotted red (circled) for ECOC and solid green (squared) for bagging.

prediction errors of both ECOC and bagging are similar. However, it should also be noted that ECOC outperforms bagging in sense of speed due to the fact that it divides multi-class into multiple two-class problems.

It is also almost always the case that the prediction error of ECOC converges to its optimum in 2 nodes, whereas a single classifier requires higher number of nodes. Moreover, for ECOC, the optimal number of epochs is also lower than or equal to that of the single classifier. In other words, compared to a single classifier trained with high number of epochs and nodes, an ECOC can yield better results with fewer nodes and epochs. The trend is similar when bagging is considered; usually standing between the single classifier and ECOC in sense of accuracy and convergence.

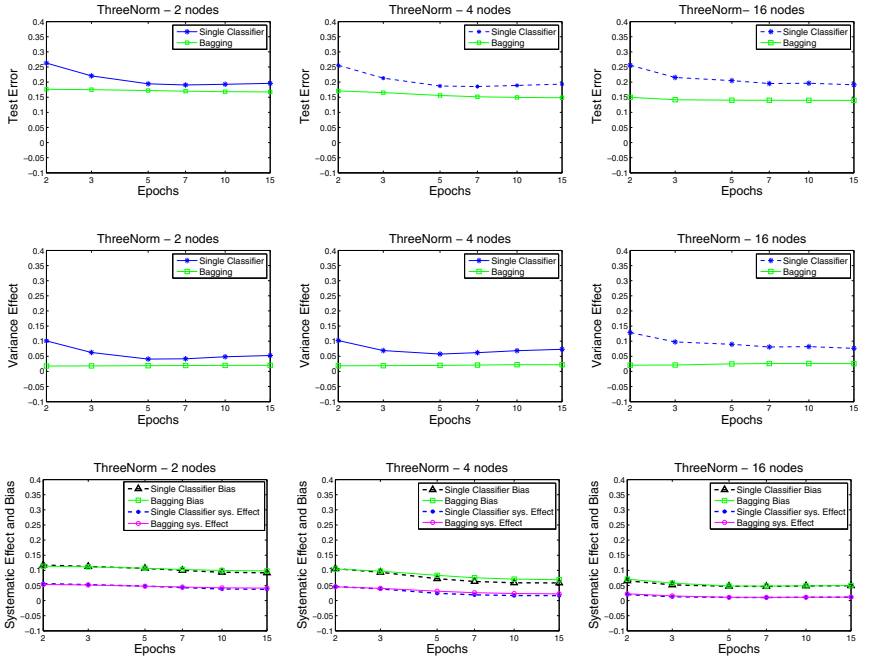

Fig. 4.5 Bias-Variance Analysis for ThreeNorm data. First Row: Overall prediction error. Second Row: Variance effect. Third Row: Systematic effect and Bias. First Column: For 2 Nodes. Second Column: For 4 Nodes. Third Column: For 16 Nodes. In the first two rows, dashed blue lines (starred) indicate the results for single classifier, and solid green (squared) for bagging. In the third row, dashed black (with triangles) & dashed blue (starred) lines indicate the results for single classifier bias and systematic effect respectively; and solid green (squared) & magenta (circled) for those of bagging.

4.3.2.3 Bias/Variance versus SE/VE

For the single classifier we see that *VE* does not necessarily follow the trend of variance. This happens especially when the number of nodes and epochs is small, that is when the network is relatively weak (Figs. 4.3 and 4.4). In this scenario, the variance decreases while *VE* increases. This is actually an expected observation as having high variance helps hitting the right target class when the network is relatively less decisive. However, ensemble methods do not show this property as much as the single classifier. A possible explanation might be that each ensemble classifier already makes use of variance coming from its base classifiers; and this compensates for the decrease in *VE* of single classifiers with high variance, in weak networks. Therefore, more variance among ensemble classifiers does not necessarily help having less *VE*.

In the above mentioned scenario of *VE* showing an opposite trend of variance, the bias-variance trade-off can be observed. At the points where the *VE* increases, SE decreases to reveal an overall decrease in the prediction error. However, these points

are not necessarily the optimal points in terms of the prediction error; the optima are mostly where there is both *VE* and *SE* reduction (Fig. 4.4). Apart from this case, bias and variance are mostly correlated with *SE* and *VE* respectively (Figs. 4.4 and 4.5). This is also pointed out in [13].

4.4 Discussion

By analysing bagging, ECOC and single classifiers consisting of NNs through the bias-variance definition of James, we have found some clear trends and relationships that offer hints to be used in classifier design. For multi-class classification problems, the increase in the overall prediction performance obtained with ECOC makes it preferable over single classifiers. The fact that it converges to the optimum with smaller number of nodes and epochs is yet another advantage. It also outperforms bagging mostly, while in other cases gives similar results. As for the two-class problems, bagging always outperforms the single classifier, and the optimum number of nodes and epochs is relatively smaller.

The increase in the performance of bagging and ECOC is a result of the decrease in both variance effect and systematic effect, although the reductions in the magnitude of the variance effect are bigger. Also, when the NNs are weak, that is when they have been trained with few nodes and epochs, we see that the trends of variance and variance effect might be in opposite directions in the single classifier case. This implies that having high variance might help improve the classification performance in weak networks when single classifiers are used. However, they are still outperformed by ensembles, which have even lower variance effects.

As for further possible advantages of ensembles, the fact that they are expected to avoid overfitting might be shown by using more powerful NNs with higher number of nodes, or other classifiers such as SVMs that are more prone to overfitting. Future work is also aimed at understanding and analysing the bias-variance domain within some mathematical frameworks such as [20, 21] and using the information in the design of ECOC matrices.

References

1. Allwein, E., Schapire, R., Singer, Y.: Reducing multiclass to binary: A unifying approach for margin classifiers. J. Machine Learning Research 1, 113–141 (2002)
2. Asuncion, A., Newman, D.J.: UCI machine learning repository, School of Information and Computer Science. University of California, Irvine (2007)
3. Breiman, L.: Arcing classifiers. The Annals of Stat. 26, 801–849 (1998)
4. Dietterich, T.G., Bakiri, G.: Solving multi-class learning problems via error-correcting output codes. J. Artif. Intell. Research 2, 263–286 (1995)
5. Domingos, P.: Why does bagging work? A Bayesian account and its implications. In: Heckerman, D., Mannila, H., Pregibon, D. (eds.) Proc. the 3rd Int. Conf. Knowledge Discovery and Data Mining, Newport Beach, CA, pp. 155–158. AAAI Press, Menlo Park (1997)

6. Domingos, P.: A unified bias-variance decomposition for zero-one and squared loss. In: Proc. the 17th Natl. Conf. Artif. Intell., Austin, TX, pp. 564–569. MIT Press, Cambridge (2000)
7. Escalera, S., Tax, D.M.J., Pujol, O., Radeva, P., Duin, R.P.W.: Subclass problem-dependent design for error-correcting output codes. IEEE Trans. Pattern Analysis and Machine Intell. 30, 1041–1054 (2008)
8. Freund, Y., Schapire, R.E.: Experiments with a new boosting algorithm. In: Saitta, L. (ed.) Proc. the 13th Int. Conf. Machine Learning, Bari, Italy, pp. 148–156. Morgan Kaufmann, San Francisco (1996)
9. Friedman, J.H.: On bias, variance, 0/1 loss and the curse of dimensionality. Data Mining and Knowledge Discovery 1, 55–77 (1997)
10. Geman, S., Bienenstock, E., Doursat, R.: Neural networks and the bias/variance dilemma. Neural Comp. 4, 1–58 (1992)
11. Heskes, T.: Bias/variance decomposition for likelihood-based estimators. Neural Comp. 10, 1425–1433 (1998)
12. James, G.M.: Majority vote classifiers: Theory and applications. PhD Thesis, Department of Statistics, University of Standford (1998)
13. James, G.: Variance and bias for general loss functions. Machine Learning 51, 115–135 (2003)
14. James, G.M., Hastie, T.: The error coding method and PICT's. Comp. and Graph. Stat. 7, 377–387 (1998)
15. Kohavi, R., Wolpert, D.H.: Bias plus variance decomposition for zero-one loss functions. In: Saitta, L. (ed.) Proc. the 13th Int. Conf. Machine Learning, Bari, Italy, pp. 275–283. Morgan Kaufmann, San Francisco (1996)
16. Kong, E.B., Dietterich, T.G.: Error-correcting output coding corrects bias and variance. In: Prieditis, A., Russell, S.J. (eds.) Proc. the 12th Int. Conf. Machine Learning, Tahoe City, CA, pp. 313–321. ACM Press, New York (1995)
17. Schapire, R.E., Freund, Y., Bartlett, P., Lee, W.S.: Boosting the margin: a new explanation for the effectiveness of voting methods. The Annals of Stat. 26, 1651–1686 (1998)
18. Smith, R.S., Windeatt, T.: The bias variance trade-off in bootstrapped error correcting output code ensembles. In: Benediktsson, J.A., Kittler, J., Roli, F. (eds.) MCS 2009. LNCS, vol. 5519, pp. 1–10. Springer, Heidelberg (2009)
19. Tibshirani, R.: Bias, variance and prediction error for classification rules. Technical Report, University of Toronto, Toronto, Canada (1996)
20. Tumer, K., Ghosh, J.: Analysis of decision boundaries in linearly combined neural classifiers. Pattern Recogn. 29, 341–348 (1996)
21. Tumer, K., Ghosh, J.: Error correlation and error reduction in ensemble classifiers. Connection Science 8, 385–403 (1996)
22. Valentini, G., Dietterich, T.: Bias-variance analysis of support vector machines for the development of SVM-based ensemble methods. J. Machine Learning Research 5, 725–775 (2004)
23. Webb, G.I., Conilione, P.: Estimating bias and variance from data. School of Comp. Science and Software Engineering, Monash University (2005)
24. Windeatt, T., Ghaderi, R.: Coding and decoding strategies for multi-class learning problems. Inf. Fusion 4, 11–21 (2003)
25. Wolpert, D.H.: On bias plus variance. Neural Comp. 9, 1211–1244 (1996)

Chapter 5
Fast-Ensembles of Minimum Redundancy Feature Selection

Benjamin Schowe and Katharina Morik

Abstract. Finding relevant subspaces in very high-dimensional data is a challenging task not only for microarray data. The selection of features is to enhance the classification performance, but on the other hand the feature selection must be stable, i.e., the set of features selected should not change when using different subsets of a population. ensemble methods have succeeded in the increase of stability and classification accuracy. However, their runtime prevents them from scaling up to real-world applications. We propose two methods which enhance correlation-based feature selection such that the stability of feature selection comes with little or even no extra runtime. We show the efficiency of the algorithms analytically and empirically on a wide range of datasets.

5.1 Introduction

The growing dimensionality of recorded data, especially in bioinformatics, demands dimension reduction methods that identify small sets of features leading to a better learning performance. Along with the high dimensionality come small sample size and high variance, which makes it hard to find adequate feature subsets without being kept in local optima. The large number of features challenges the runtime of a selection algorithm. Hence, the main quality criteria are that the algorithm is

- **multivariate** – It takes into account inter-feature-dependencies;
- **stable** – It does not vary much for unseen data of the population;
- **amending learning** – The learning performance is enhanced;
- **fast** – It scales well for very large numbers of features.

Ensemble methods increase stability and, hence, are frequently used in feature selection. However, they usually slow down the procedure. We will present two

Benjamin Schowe · Katharina Morik
Technische Universität Dortmund
E-mail: {schowe,morik}@ls8.cs.tu-dortmund.de

O. Okun et al. (Eds.): Ensembles in Machine Learning Applications, SCI 373, pp. 75–95.
springerlink.com

methods which speed up ensembles in a simple and effective way. A careful evaluation on several real world and simulated data sets investigates the quality of our new methods.

5.2 Related Work

Fast univariate **filter** approaches, like the t-test [5] or SAM-statistics [17], compute a scoring function on the features, disregarding feature interplay. **Wrapper** approaches [13] better solve this problem, at the cost of much longer runtime. Each feature set evaluation demands a cross-validated training of the used learning algorithm. Some learning algorithms provide the user with an implicit feature ranking which can easily be exploited for feature selection. Such **embedded** approaches are using the weight vector of a linear SVM [18] or the frequency of feature use of a *Random Forest* (RF) [3]. They are aware of feature interplay and faster than wrappers but biased towards the learning algorithm used.

A group of new algorithms has come up to bridge the gap between fast but univariate filters on the one hand, and slow but multivariate wrappers on the other hand. Their goal is to find a subset of features which is highly predictive with no or a minimum of redundant information. The *correlation based feature selection* (CFS) [8] performs a *sequential forward search* with a correlation measure in the evaluation step. CFS iteratively adds the feature which has the best ratio between predictive relevance of the feature and its correlation with the already selected features. Both, predictiveness and correlation, are measured by the entropy-based *symmetrical uncertainty*

$$SU(f_i, f_j) = \frac{2IG(f_i|f_j)}{H(f_i)+H(f_j)}, \tag{5.1}$$

where the information gain IG of feature f_i w.r.t. feature f_j is divided by the sum of the entropies of f_i and f_j. Since CFS uses symmetrical uncertainty, it is only suitable for discrete values.

Ding and Peng [4] reinvented CFS with the capability for handling numerical variables calling it *Minimum Redundancy Maximum Relevance FS* (mRMR). For numerical features the *F-test* is used. It reflects the ratio of the variance between classes and the average variance inside theses classes. For a continuous feature X and a nominal class variable Y with C classes, both from a data set with n examples it is defined as

$$F(X,Y) = \frac{(n-C)\sum_c n_c(\bar{X}_c - \bar{X})^2}{(C-1)\sum_c (n_c-1)\sigma_c^2} \tag{5.2}$$

with per-class-variance σ_c^2 and n_c the number of examples in class $c \in \{1,\ldots,C\}$. The redundancy of a numerical feature set is measured by the absolute value of *Pearson's correlation coefficient*

$$R(X,Y) = \frac{Cov(X,Y)}{\sqrt{Var(X)Var(Y)}} \tag{5.3}$$

respectively its estimate

$$r(X,Y) = \frac{\sum_i (x_i - \bar{x})(y_i - \bar{y})}{\sqrt{\sum_i (x_i - \bar{x})^2 \sum_i (y_i - \bar{y})^2}}. \tag{5.4}$$

It detects a linear dependency between X and Y. Another possible measure for the dependency between two nominal variables used by mRMR [4] is the *mutual information*

$$MI(X,Y) = \sum_{x,y} P(x,y) \log_2 \frac{P(x,y)}{P(x)P(y)}, \tag{5.5}$$

where x and y are the possible values of X and Y.

From now on, we will use the term *correlation* and the symbol $Cor(\cdot,\cdot)$ as a synonym for either Pearsons's linear correlation, Eq. (5.3), F-test, Eq. (5.2), or mutual information, Eq. (5.5), depending on the types of variables involved, i.e. numerical or nominal. Instead of the ratio, one can also use the difference between relevance and redundancy [4].

The main algorithmic issue is the computation of the correlations. The set of all features is $\mathbb{F}$ and the dimensionality is $p = \|\mathbb{F}\|$. In the first step, selecting the most relevant feature takes p calculations of $Cor(f_i,y)$ with $i = 1,\ldots,p$. The mRMR/CFS algorithm first picks the feature which has the highest correlation with the label and so is most relevant:

$$F_1 = \arg\max_{f_i} (Cor(f_i,y)) \tag{5.6}$$

with $i \in [1,p]$. This takes p calculations of feature-label-correlation. Let F_j denote the set of selected features in step $j \in \{1,\ldots,k\}$ of mRMR/CFS. The next steps in mRMR/CFS are to repeatedly add the feature which has the best ratio between relevance and redundancy to the already selected features.

$$F_{j+1} = F_j \cup \left\{ \arg\max_{f \in \mathbb{F} \setminus F_j} \frac{Cor(f,y)}{\frac{1}{j}\sum_{g \in F_j} Cor(f,g)} \right\} \tag{5.7}$$

This takes $p-(j-1)$ correlations in each step. For the whole mRMR/CFS process of selecting k from p features

$$p + \sum_{i=1}^{k-1} (p-i) = pk - \frac{k^2-k}{2} \tag{5.8}$$

correlations must be computed.

Variants of the method like, e.g., [7] tried to improve the stability of mRMR by introducing a weighting parameter α for the ratio of relevance and redundancy. Tuning this parameter even increases the overall runtime. The same holds for the approach [15], which evaluates together those pairs of features which are higher correlated than some δ, or for *Fast Correlation-based Filter* (FCBF) [20], which discards all features with relevance $< \delta$. In any case, the measures are based on variance and, hence, are sensitive to outliers and a high variance of the input data, alike. This instability is not suitable, e.g., for biomedical research, where the relevance of features is in the research focus. Hence, mRMR/CFS is promising but suffering from a lack of stability.

5.2.1 Ensemble Methods

A high variance negatively effects prediction algorithms (classification & regression) as well as feature selection schemes. Ensemble methods like *Bagging* [2] or *Boosting* [6] reduce variance. Parallel ensembles, e.g. *Bagging*, do so by repeating the algorithm on different subsamples or bootstrapped samples of the input data. This increases the stability of the set of selected features [10, 11, 16] and - in some cases - even reduces the prediction error [19]. Saeys et al. [16] showed that (bagged) ensembles of *symmetrical uncertainty weighting*, *Relief*, SVM-RFE or RF delivered more stable feature selections than the non-ensembled counterparts, but did not increase classification performance[1]. The major problem with *Bagging* are the e-times repetition for ensembles of cardinality e. This increases runtime considerably [9].

5.3 Speeding Up Ensembles

We now have advantages and shortcomings of the methods which we want to enhance, namely mRMR/CFS (being unstable) and ensemble methods (being too slow). The basis for our algorithm is the "split-sum trick" going back to the parallel axis theorem. The parallel axis theorem helps to compute $Cor(x,y)$ in one pass for any two features.

We use Pearson's linear correlation as an example, but the other measures can be split analogously: The parallel axis theorem allows to rewrite the variance of a feature X

$$Var(X) = E((X - E(X))^2) \tag{5.9}$$

as

$$Var(X) = E(X^2) - (E(X))^2 \tag{5.10}$$

and the covariance of two features X and Y

[1] For *Random Forests* accuracy even decreased.

$$Cov(X,Y) = E((X - E(X))(Y - E(Y))) \tag{5.11}$$

as

$$Cov(X,Y) = E(XY) - E(X)E(Y). \tag{5.12}$$

The benefit is that the expected values of the single variables (their mean) do not have to be estimated before computing the variance or covariance. The variance- and covariance-terms now only contain sums of computationally independent terms.

For n examples the variance can then be estimated by

$$(n-1)\sigma_x^2 = \sum_{i=1}^{n}(x_i - \bar{x})^2 = \left(\sum_{i=1}^{n} x_i^2\right) - n\bar{x}^2 = \left(\sum_{i=1}^{n} x_i^2\right) - \frac{1}{n}\left(\sum_{i=1}^{n} x_i\right)^2. \tag{5.13}$$

Applying this to Eq. (5.4) allows to compute Pearson's linear correlation in only one pass over the data for each feature without prior computation of the mean values of each feature:

$$r(x,y) = \frac{\sum_{i=1}^{n} x_i y_i - \frac{1}{n}\left(\sum_{i=1}^{n} x_i \sum_{i=1}^{n} y_i\right)}{\sqrt{\left[\sum_{i=1}^{n} x_i^2 - \frac{1}{n}\left(\sum_{i=1}^{n} x_i \sum_{i=1}^{n} x_i\right)\right]\left[\sum_{i=1}^{n} y_i^2 - \frac{1}{n}\left(\sum_{i=1}^{n} y_i \sum_{i=1}^{n} y_i\right)\right]}} \tag{5.14}$$

The *F-Test*, Eq. (5.2), and *MI*, Eq. (5.5), can similarly be split into sums of independent terms. This fact is used by our *Inner Ensemble* method and its further enhancement, the *Fast Ensemble*.

5.3.1 Inner Ensemble

correlation measures like Pearson's linear correlation are very sensitive to outliers [12]. This has a negative effect on the stability of the selected feature set. Our first method, the *Inner Ensemble*, increases the robustness of the correlation measure used inside the mRMR/CFS algorithm by performing a parallel *ensemble* of e correlations for every single $Cor(\cdot,\cdot)$ computation. The correlation is calculated for e parts on subsets of the examples, each part leaving out $\frac{1}{e}$ of the data - similar to e-fold cross-validation. In contrast to cross-validation, the left-out fraction of the data is not used. The average of the e correlations gives us a more robust correlation estimate. Usually, for ensembles of size e, this would increase runtime of mRMR/CFS by the factor e to $(epk - (k^2 - k)/2)$ correlations to compute. Now, we use that the Eqs. (5.2), (5.3) and (5.5) can all be split into sums of sums like

$$\sum_{i=1}^{n} h_i = \sum_{i=1}^{m_1} h_i + \sum_{i=m_1+1}^{m_2} h_i + \cdots + \sum_{i=m_{e+1}}^{n} h_i = \sum_{j=1}^{e}\left[\sum_{i=1+(j-1)\frac{n}{e}}^{j\frac{n}{e}} h_i\right] \tag{5.15}$$

for equally sized parts and arbitrary terms h_i. This allows us to compute these sums for all e intervals $\left[(j-1)\frac{n}{e}+1, j\frac{n}{e}\right]$ separately. The final correlation of each part $i \in [1,e]$ of the ensemble is then calculated by using all but the ith partial sums, (cf. Fig. 5.1). There is virtually no extra runtime apart from e times adding up the partial sums within Algorithm 2.

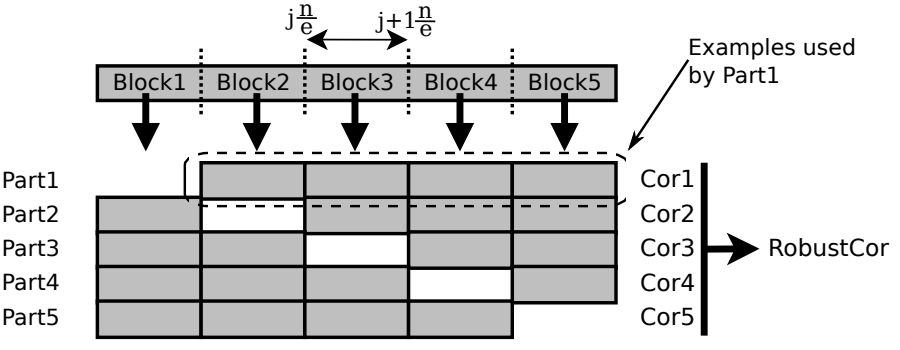

Fig. 5.1 Inner Ensemble: Splitting correlation computation into parts: the $e = 5$ parts calculate the partial sums for the terms used in the different correlation measures. Then for each part i all but the ith sum terms are used for calculating the correlation Cor_i on the subset $X \setminus Block_i$ of the examples. Finally, the average of Cor_1 to Cor_5 becomes *RobustCor*.

The memory need increases by factor e which is very small, because Pearson's linear correlation only needs five accumulator variables for the sums; F-test and mutual information only need $1+3|f_1|$ and $3|f_1||f_2|$ variables, respectively, where $|f_1|$ and $|f_2|$ are the number of distinct values of the features f_1 and f_2. Algorithm 2 shows an implementation for Pearsons's linear correlation returning the average correlation value for all parts in one pass over the data. For *F-Test*, Eq. (5.2), and *MI*, Eq. (5.5), the procedure is similar.

5.3.2 Fast Ensemble

Doing the calculations on diverse subsets of the data and using the split-sum trick in the *Inner Ensemble* way is extremely fast, but it increases the stability of selected feature sets only marginally, when used on each single correlation step, cf. Sect. 5.4. Our second method, *Fast Ensemble*, builds an ensemble of the whole selection process, instead of stabilizing each single correlation (see Algorithm 1). We dramatically reduce runtime of the full ensemble by applying the same split-sum trick.

If a correlation between two features is computed for one part of the ensemble, their correlations can be computed with practically no overhead for all other parts of the ensemble (cf. Algorithm 3). As opposed to the *Inner Ensemble*, here, the partial correlation results are not combined, but cached for later use. Just one pass over the examples is needed: For every ith part of the ensemble, the ith partial sums are left out when aggregating the sums to a correlation measure. Hence, for every two

Algorithm 1. Fast Ensemble of mRMR/CFS

Input: Set of all features $\mathbb{F}$, desired dimension k, size of the ensemble e, label y
for $f \in \mathbb{F}$ **do** {Precompute relevance of every feature}
  Compute $Cor(f,y)[1..e]$ in parallel and store in cache
  maxrel[1,..., e]=$-\infty$
  for $r = 1$ to e **do** {For all parts of the ensemble test if f is most relevant}
    if $Cor(f,y)[r]$ >maxrel[r] **then**
      maxrel[r] = $Cor(f,y)[r]$
      $F_r = \{f\}$
    end if
  end for
end for
for $j = 2$ to k **do** {Iteratively add best feature}
  best_feature[1..e] = $\emptyset$
  best_quality[1..e] = $-\infty$
  for $r = 1$ to e **do** {For all parts of the ensemble}
    for $f \in \mathbb{F} \setminus F_r$ **do**
      relevance = retrieve($Cor(f,y)[r]$) from cache
      redundancy = 0
      for $g \in F_r$ **do**
        redundancy += retrieve($Cor(f,g)[r]$) from cache, when unsuccessful calculate $Cor(f,g)[1..e]$ and store in cache.
      end for
      if (redundancy / relevance) > best_quality[r] **then**
        best_feature[r] = f
        best_quality = (redundancy / relevance)
      end if
    end for
  end for
  for $r = 1$ to e **do** {For all parts of the ensemble}
    $F_r = F_r \cup$ best_feature[r]
  end for
end for
Combine all F_r to a final F
return F

features or a feature-class combination, only one pass over the examples is needed, no matter in how many parts of the ensemble they appear. Where a full ensemble of mRMR/CFS needs ep passes over the examples in order to select a first feature $f_{i,1}$ for e parts of the ensemble, our method does this just once. For every further feature $f_{i,j}$ in all parts of the ensemble, only those feature correlations need a pass over the examples which were not already considered in any other part of the ensemble.

Time-complexity directly depends on the diversity of the ensemble results. If all parts of the ensemble return the same feature set, the needed correlations have all been computed in the first part and the runtime is the same as for a single feature selection. If, in contrast, the resulting feature sets of the feature selections are disjoint, none of the feature pairs has been considered in other parts of the ensemble and thus has not been cached. These extremes are rare.

Algorithm 2. Java implementation of *Inner Ensemble* of Pearson's linear correlation

```
/** Calculates the linear Pearson's correlation between two numerical attributes
  * in one pass over the data, but with a more stable ensemble approach.
  *
  * The parameters:
  * exampleset      An example set  - RapidMiner representation of the dataset
  * x           1st nominal attribute
  * y           2nd nominal attribute
  * ensembleSize    Size of the ensemble - number of parts
  */

double Correlation(ExampleSet exampleset, Attribute x, Attribute y, int e) {
  double result = 0.0;
  double N = exampleset.size();         //Number of examples

  double [] n = new double [e];     // Size of the blocks
  double [] ex = new double [e];    // Blockwise sum over all xi
  double [] exx = new double [e];   // Blockwise sum over all xi^2
  double [] ey = new double [e];    // Blockwise sum over all yi
  double [] eyy = new double [e];   // Blockwise sum over all yi^2
  double [] exy = new double [e];   // Blockwise sum over all yi*xi

  double xi,yi;
  Example example;
  Iterator<Example> iterator = exampleset.iterator();
  int i=0;
  while (iterator.hasNext()) {          // Iterate over all examples once
    example = iterator.next();      // Fetch next example and get values for ...
    xi = example.getValue(x);       // attribute X and ...
    yi = example.getValue(y);       // attribute Y.

    ex[i]  += xi;   // Add example's value for X and Y to the partial sums
    exx[i] += xi * xi;
    ey[i]  += yi;
    eyy[i] += yi * yi;
    exy[i] += xi * yi;
    n[i]++;     // Increase block size counter

    i++;        // Increase block index
    i = i % e;      // To keep i in the range [0..e]. The partial sums are not build up over consecutive
            // blocks, but the blocks are distributed modulo over all examples. The result is the
            // same and reduces the risk of ensemble parts with only one class, should the examples
            // be sorted.
  }

  // Now combine partial sums to partial ensemble results:

  double numerator, denominator;

  for (i=0; i < e; i++) {   // Combine the blockwise sums to the sums the each part of the ensemble
    double EX=0.0, EXX=0.0, EY=0.0, EYY=0.0, EXY=0.0;
    for (j=0; j < e; j++) {
      if (j != i) {     // Leave out the sums of block i
        EX  += ex[j];
        EXX += exx[j];
        EY  += ey[j];
        EYY += eyy[j];
        EXY += exy[j];
      }
    }

    numerator = EXY - (EX * EY) / (N - n[i]);

    denominator = Math.sqrt(
          (EXX - ((EX * EX) / (N - n[i]) )) *
          (EYY - ((EY * EY) / (N - n[i]) )) );

    result += numerator / denominator;  // Add partial correlation result to aggregator variable.
  }

  return result / e;            // Build mor robust correlation as average of partial correlations.
}
```

Algorithm 3. Java implementation of Mutual Information for *Fast Ensemble*

```
/** Ensemble version of mutual information.
  * MI is calculate for each part of the ensemble and an array of MI values is returned.
  *
  * The parameters:
  * exampleset      An example set  - RapidMiner representation of the dataset
  * x           1st nominal attribute
  * y           2nd nominal attribute
  * ensembleSize    Size of the ensemble - number of parts
  */

double [] MutualInformationEnsemble(ExampleSet exampleset, Attribute x, Attribute y, int ensembleSize) {

  double [] result = new double[ensembleSize];      // Will hold the MI-value for each ensemble part.
  int N = exampleset.size();
  if (N == 0)                       // Some sanity checks
    return result;

  if (!x.isNominal() || !y.isNominal())
    throw new OperatorException("Both attributes have to be nominal");

  int num_x = x.getMapping().size();            // The number of distinct values/classes in X
  int num_y = y.getMapping().size();            // The number of distinct values/classes in Y

  double PX[] = new double[num_x];          // Occurence of each of X's values
  double PY[] = new double[num_y];          // Occurence of each of Y's values
  double PXY[][] = new double[num_x][num_y];        // Joint occurence of each X's and Y's values

  double px[][] = new double[num_x][ensembleSize];  // Occurence of each of X's values in each block
  double py[][] = new double[num_y][ensembleSize];  // Occurence of each of Y's values in each block
  double pxy[][][] = new double[num_x][num_y][ensembleSize]; //Joint occ. of X's & Y's values in each block
  double n[] = new double[ensembleSize];        // Size of each Block

  int xi,yi;
  Example example;
  Iterator<Example> iterator = exampleset.iterator();
  int i=0;              // Block index variable, indicating the current block

  while (iterator.hasNext()) {      // Iterate over all examples once
    example = iterator.next();      // Fetch next example and get values for ...
    xi = (int)example.getValue(x);  // attribute x and ...
    yi = (int)example.getValue(y);  // attribute y.

    PX[xi]++;           // Increase overall occurence counter for value xi
    PY[yi]++;           // Increase overall occurence counter for value yi
    PXY[xi][yi]++;      // Increase overall joint occurence counter for value (xi,yi)

    px[xi][i]++;        // Increase occurence counter for value xi in the current block
    py[yi][i]++;        // Increase occurence counter for value yi in the current block
    pxy[xi][yi][i]++;   // Increase joint occurence counter for (xi,yi) in the current block
    n[i]++;             // Increase block size counter

    i++;                // Increase block index
    i = i % ensembleSize;       // To stay in the range [0, e-1] for e blocks
  }

  double temp;
  for (i = 0; i < ensembleSize; i++)
  { // Build MI value for each ensemble part by subtracting the blockwise
    result[i] = 0.0; // occurences from overall occurences and inserting into MI formula.

    for (int k = 0; k < num_x; k++) {   // Iterate over all possible values for X
      for (int j = 0; j < num_y; j++) { //  Iterate over all possible values for Y
        temp = ((N - n[i]) * (PXY[k][j] - pxy[k][j][i])) / ((PX[k]  - px[k][i]) * (PY[j] - py[j][i]));
        if (temp > 0 && !Double.isInfinite(temp) && !Double.isNaN(temp)) {
          result[i] += ((PXY[k][j] - pxy[k][j][i])* Math.log(temp)) / (N - n[i]);
    }
      }
    }

    result[i] *= LOG2INV;   //For scaling from log_e to log_2
  }

  return result;
}
```

A simple example of selecting 3 out of 5 features (X_1 to X_5), label Y, illustrates *Fast Ensemble*, cf. Fig. 5.2.

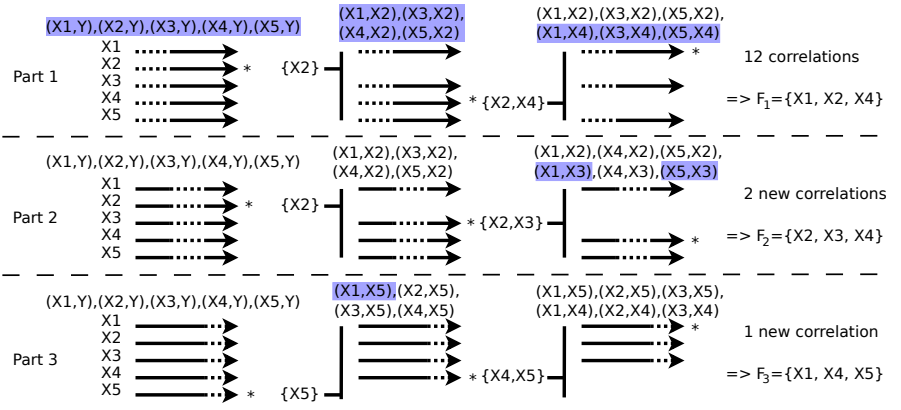

Fig. 5.2 Fast Ensemble: A simple example with $k = 3$, $n = 5$, $e = 3$. The dashed lines in the arrows represent the subset of the examples which is left out when estimating the correlation. The correlation computations demanding a pass over the data for split-sum calculation are highlighted.

The ensemble consists of three parts. After a first calculation of the relevance of each feature, i.e. the correlation of X_i and Y, the relevance values are cached for each ensemble part r. In the first part let feature X_2 be chosen, because it has the highest relevance. To estimate the next feature with the best relevance/redundancy ratio the correlations of X_2 and the remaining four features must be computed, i.e $Cor(X_2, X_1)$, $Cor(X_2, X_3)$, $Cor(X_2, X_4)$ and $Cor(X_2, X_5)$. X_4 is chosen. In the last step the remaining features must be compared to the newly added X_4. The needed correlations are $Cor(X_4, X_1)$, $Cor(X_4, X_3)$ and $Cor(X_4, X_5)$. This is repeated for all other parts. Again the first most relevant feature has to be chosen. Now relevance can be computed from the already cached partial $Cor(X_i, Y)$ values. Let X_2 be chosen again. If X_i, X_j have been compared in an earlier part, the correlation for all subsets $X \setminus X_r$ have already been calculated. So, in the 2nd step of the 2nd part all correlations can be fetched from cache. Let X_3 be chosen. Only in the 3rd round the next $Cor(\cdot, \cdot)$ are due for (X_1, X_3) and (X_3, X_5). In the last part of the ensemble again the relevance values can be fetched from cache. Let X_5 be chosen. Then in the rest of this part only $Cor(X_1, X_5)$ is needed, which has not been computed in an earlier step. The resulting sets are then combined to a final result, e.g. via majority vote. Only 15 passes are needed instead of 36 without the split-sum trick.

5.3.3 Result Combination

After e different feature sets have been selected in the ensemble these sets have to be integrated into one final result. We investigate two very fast and simple approaches.

The first method simply counts how often a feature was selected. The k most often selected features constitute the final set. We call this *Fast Ensemble with sets*.

This method does not regard the fact that features selected in later steps F_j with $j \rightarrow k$ are more unstable and less relevant than those selected in early steps of the mRMR/CFS algorithm. This can be overcome by a rank-combination similar to that proposed by [16]. The mRMR/CFS algorithm implicitly provides a ranking of the first k features (feature f is selected in iteration $j \Rightarrow Rank(f) = j$). For full averaging of all ranks mRMR/CFS would have to be performed e times with $k = p$. This would lead to a runtime of $O(p^2)$ and is thus only feasible for low-dimensional datasets. One could try to average over all k existing ranks in every ensemble part and assume a constant rank $\gg k$ for all $p - k$ unranked features. This has the drawback that features with a relatively high rank of $k + \varepsilon$ are ignored. We instead suggest an intermediate solution. In each part of the ensemble we calculate the ranks only for the top $2k$ features. For all non-selected features assume a rank of $3k$ (or an arbitrary value $> 2k$). Experimentation showed that this yields as good stability results as the combination of fully ranked feature sets. We call this *Fast Ensemble with ranks*.

5.3.4 Benefits

Our algorithms conduct search in feature subset space like wrappers do. Yet, unlike wrappers, the feature sets are not evaluated in long cross-validation runs but with a fast filter approach. Unlike filters, feature interdependencies are still considered. Hence, *Inner* and *Fast Ensemble* combine the advantages of wrapper and filter approaches. Note, that the inherent parallelism of the algorithms speeds up computation additionally. Every correlation computation between two features is independent of the other features. Thus, not only the parts of the ensemble can be computed in parallel, but also all correlation computations. Only completed calculations must be reported to some central instance which conducts the search in feature subset space.

5.4 Evaluation

We evaluated the performance of our algorithm with respect to **stability**, **accuracy**, **runtime** and **low-sample performance** on ten publicly available datasets of a wide range of problem settings and dimensionality (Table 5.1).

All experiments were conducted in the open-source Data Mining system *RapidMiner*. The proposed algorithms are open-source and available as an extension[2] to *RapidMiner*.

[2] https://sourceforge.net/projects/rm-featselext

Table 5.1 Data characteristics and significance of the difference between the stabilities achieved by *Fast Ensemble* and plain mRMR for 10 and 20 features. Values < 0.05 are highly significant.

Dataset	p	n	Classes	Data	$k = 10$	$k = 20$
Sonar	60	208	2	continuous	0.0085	0.0025
Ionosphere	34	351	2	continuous	0.022	0.19951
Musk	166	476	2	continuous	$3.1 \cdot 10^{-6}$	$1.4 \cdot 10^{-8}$
Lung	325	73	7	nominal	$4.1 \cdot 10^{-7}$	$4.0 \cdot 10^{-14}$
H/W Digits	64	3823	10	continuous	0.082	0.0058
Colon	2000	62	2	nominal	$1.4 \cdot 10^{-9}$	$1.1 \cdot 10^{-6}$
Lymphoma	4026	96	9	nominal	$1.2 \cdot 10^{-10}$	$4.4 \cdot 10^{-14}$
Leukemia	7070	72	2	nominal	$2.6 \cdot 10^{-11}$	$1.9 \cdot 10^{-15}$
NCI60	9712	60	9	nominal	$2.4 \cdot 10^{-14}$	0.0
LUCAS	11	2000	2	nominal	-	-

5.4.1 Stability

We analyse how the produced feature sets differ under variation of the input data. We compare our two methods *Inner Ensemble* and *Fast Ensemble* with set- and rank-combination to mRMR/CFS. All ensembles consist of $e = 20$ parts.

The stability of a feature selection method can be measured by the similarity of the resulting feature subset generated by a feature selection method on different data drawn from the same basic population. Different stability indices are available for this similarity of sets. The *Jaccard index* of two feature-sets as used by [16] is defined as

$$S_J(F_a, F_b) = \frac{|F_a \cap F_b|}{|F_a \cup F_b|}. \tag{5.16}$$

A measure very similar to the Jaccard Index was proposed by [14] which we will refer to as Kuncheva's index S_K. For two feature subsets of size k it is defined as

$$S_K(F_a, F_b) = \frac{|F_a \cap F_b| \frac{k^2}{p}}{k - \frac{k^2}{p}}, \tag{5.17}$$

where $S_K(F_a, F_b) \in [-1, 1]$. Its advantage over the Jaccard index is that it also regards the size p of the whole feature set and the number k of selected features.

Similar to [16] we draw ten subsets from the example set like ten-fold cross-validation. On each of these subsets a feature selection is computed. The overall stability is further defined as the average of the stability indices for all combinations of those feature selections:

$$\bar{S} = \frac{2}{l^2 + l} \sum_{i=1}^{l} \sum_{j=i+1}^{l} S(F_i, F_j), \tag{5.18}$$

where l is the number of different feature selection results in the validation scheme. The averages over 10 runs are reported. Fig. 5.3 shows the results for the stability of the four feature selection methods dependent on k, the number of features to select.

Both versions of the *Fast Ensemble* clearly outperform the standard mRMR/CFS, whereas the *Inner Ensemble* shows nearly no visible improvement except for the *Leukemia* dataset in Fig. 5.3h. For the *Leukemia* dataset the *mutual information* was used to measure relevance and redundancy. One can see that the *Inner Ensemble* method only affects nominal datasets. As it increases runtime only in $O(1)$ we suggest using it for nominal datasets. Our new *Fast Ensemble* achieves the same performance as a full ensemble of the same size. The benefit is the much smaller number of computations. For all datasets stability increases with larger k because the (possible) overlap between subsets selected by different parts of the ensemble increases. The visible differences between methods in Fig. 5.3 are significant. We exemplarily report the p-Values for 10 and 20 features in Table 5.1. The only exception in p-values is selecting 20 features from the *ionosphere* dataset, where all methods are about the same (cf. Fig. 5.3f).

We also investigated the effect of our approaches on a data set with a "good" sample/feature ratio. The *Handwritten Digits* datasets contains 3828 examples with 64 features. In this setting ensemble methods did not deliver a significant improvement in stability as 3828 examples allow for stable feature selections, cf. Table 5.1. The Jaccard index and Kuncheva's index were close to 1 for most choices of k.

The effect of the size e of an ensemble on the selection stability was also investigated, cf. Fig. 5.4. Too small an ensemble does not increase performance and too large an ensemble degrades performance for small n. Stability increases with the number of selected features, but in general a mid-sized ensemble with $e \approx 20$ performs best for all k.

In comparison to [16] another question arises. Does the manner in which ensemble diversity is generated affect the stability? Saeys et al. [16] generated diversity by re-sampling the data (Bagging) while our approach demands sub-sampling. Figure 5.5 compares the stability of sub-sampling based *Fast Ensemble with sets* to a re-sampling based ensemble of the same size $e = 20$. Most of the time *Fast Ensemble* performed better than Bagging. The last stability experiments explores whether the joint application of *Inner Ensemble* and *Fast Ensemble* can give further improvement. But as the continuous lines in Fig. 5.5 show, the performance did not differ significantly from that of *Fast Ensemble* alone.

5.4.2 Accuracy

We analyse if a more stable feature selection benefits classification accuracy on five different learning schemes: *Naive Bayes* (NB), *5-Nearest-Neighbors* (5NN), a *Decision Tree* (DT), a linear SVM, and *Linear Discriminant Analysis* (LDA) which all have different strengths and weaknesses. We compare the standard mRMR/CFS approach (Plain) to our *Inner Ensemble* and our *Fast Ensemble* algorithm. SVM and LDA were only applied to two-class problems with continuous variables. The parameter k of selected features was varied from 5 to 50 with step-size 5. Accuracy

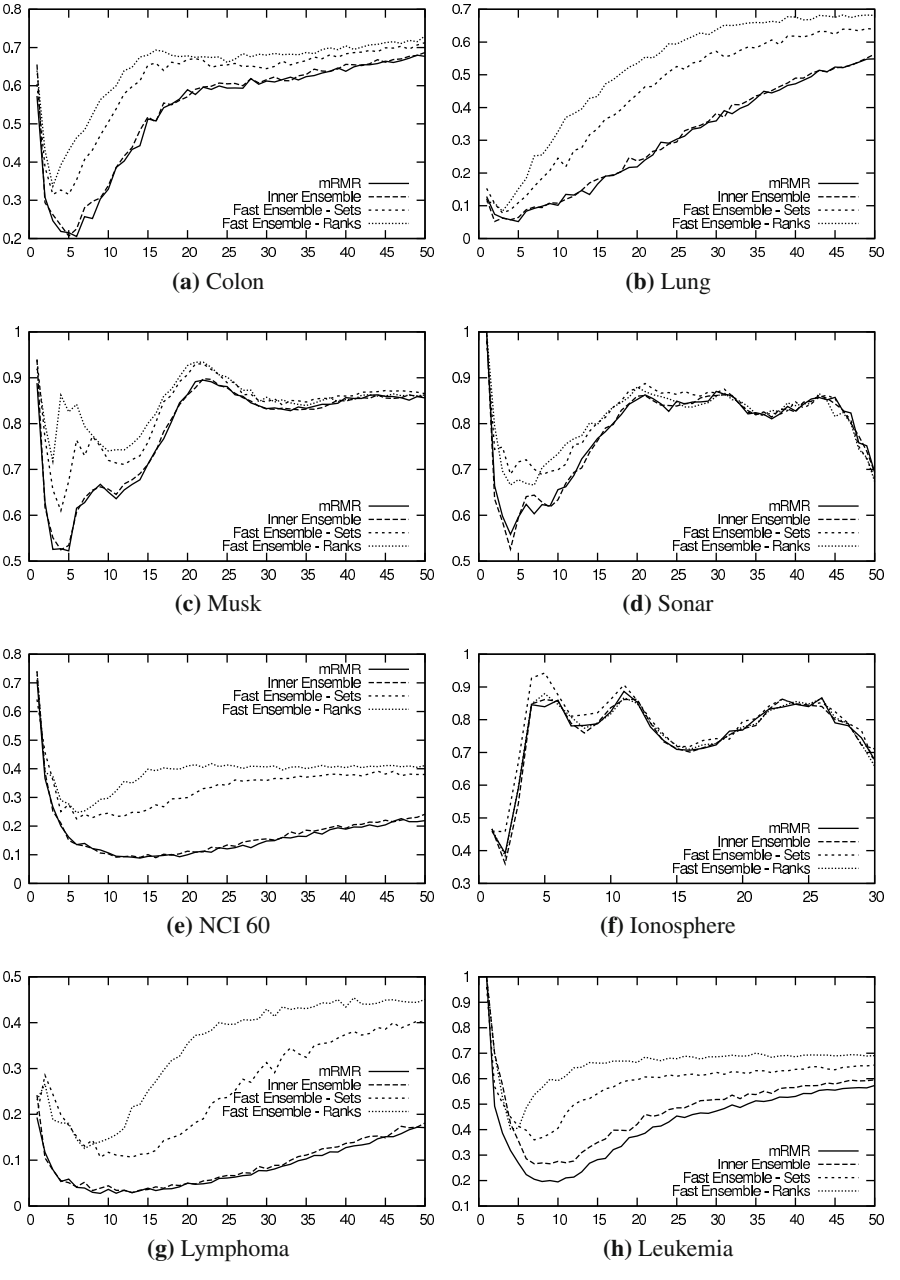

(a) Colon **(b)** Lung

(c) Musk **(d)** Sonar

(e) NCI 60 **(f)** Ionosphere

(g) Lymphoma **(h)** Leukemia

Fig. 5.3 Stability of the four approaches: *Inner Ensemble*, *Fast Ensemble* with averaged sets, *Fast Ensemble* with averaged ranks, and standard mRMR/CFS. The y-axis is the average Kuncheva's index and k, the number of selected features, is the x-axis.

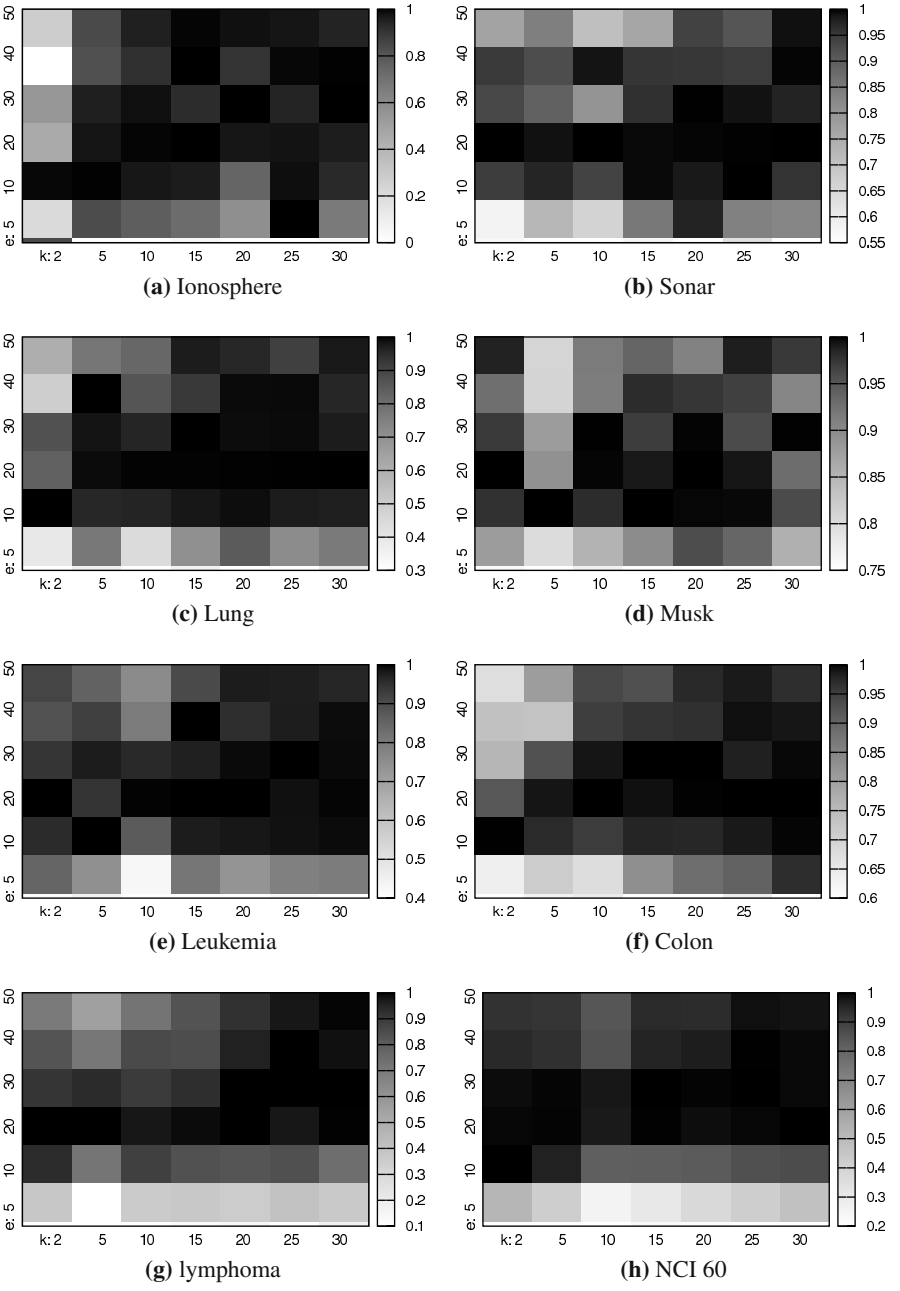

(a) Ionosphere **(b)** Sonar

(c) Lung **(d)** Musk

(e) Leukemia **(f)** Colon

(g) lymphoma **(h)** NCI 60

Fig. 5.4 Stability of the selected feature sets as a function of e (vertical axis) and k (horizontal axis). The values have been normalized to the range of $[0, 1]$ separately for each choice of k, i.e. for each column. Darker equals higher stability.

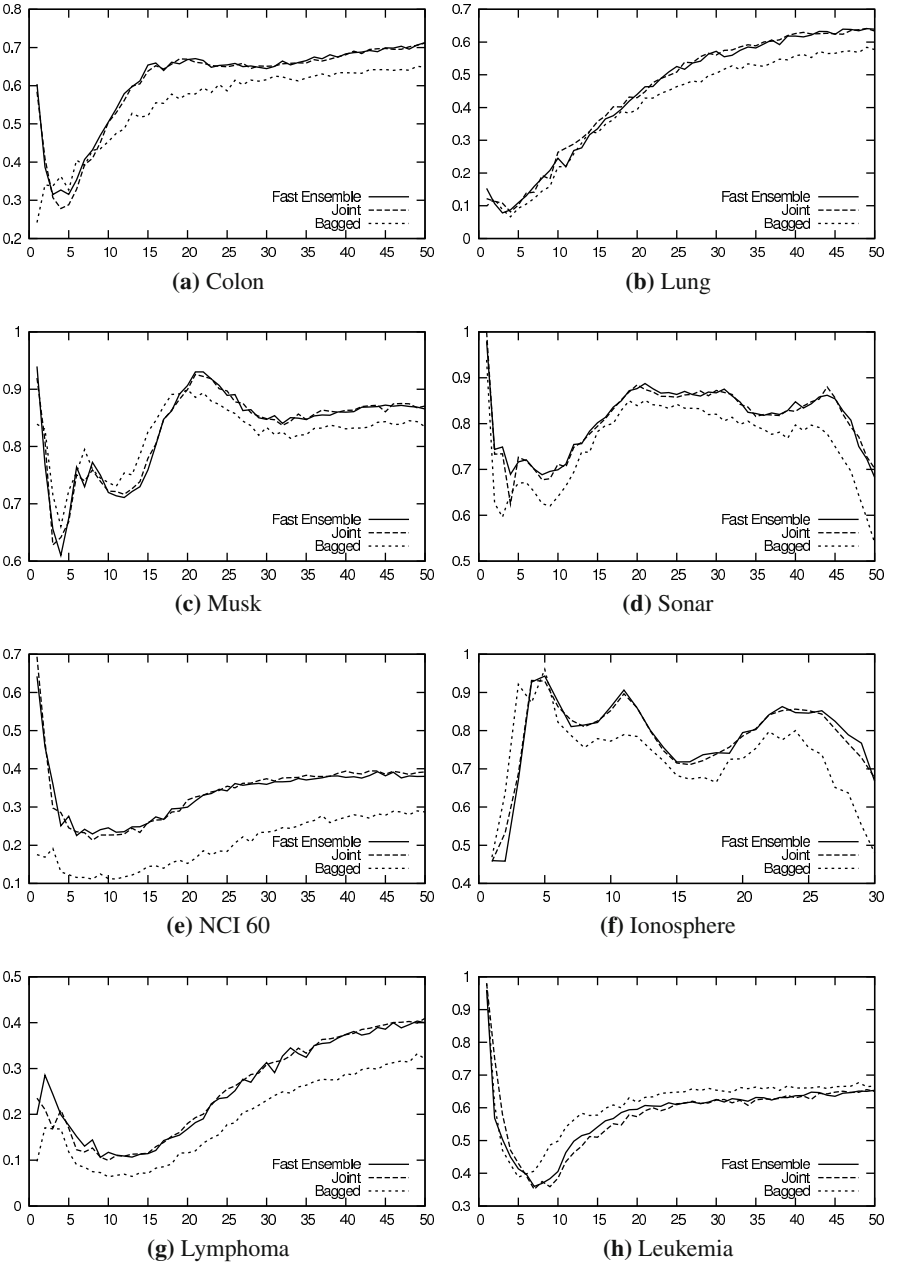

(a) Colon **(b)** Lung

(c) Musk **(d)** Sonar

(e) NCI 60 **(f)** Ionosphere

(g) Lymphoma **(h)** Leukemia

Fig. 5.5 Comparison of the stability of *Fast Ensemble* with averaged sets to a *bagged* ensemble of mRMR/CFS and the *joint* application of *Inner Ensemble* and *Fast Ensemble*. The y-axis is average Kuncheva's index and the x-axis is the number of selected features k.

was averaged over 10 runs of ten-fold cross-validation. Feature selection was only performed on the training set and not on the test set, as this would lead to far too optimistic results.

Table 5.2 shows in detail the effect of more stable feature selection on classification accuracy for all datasets. For each choice of k, dataset and learner we compared the average accuracy results for our methods to standard mRMR/CFS via an analysis of variance (ANOVA) and counted the times that each of our methods performed *significantly* better or worse. On the lower dimensional datasets, i.e. *Sonar* and *Ionosphere*, the increased stability did not result in better prediction. But for the very high-dimensional datasets a small performance increase can be detected, especially for *Naive Bayes* and *Nearest Neighbours*. In total out of the 280 experiments our methods performed *significantly*

	better	worse
Inner Ensemble	11	6
Fast Ensemble - Sets	14	6
Fast Ensemble - Ranks	30	10

than mRMR/CFS. The *Fast Ensemble with Ranks* gave better results than *Fast Ensemble with Sets*. This might be caused by the fact that the rank combination puts more focus on the higher ranked and thus more meaningful features. When looking at the behaviour of the accuracy dependent on k it showed that *Fast Ensemble* delivers better results earlier (with less features) than mRMR/CFS.

Table 5.2 Accuracy: How often was a method significantly *better than/equal to/worse than* the standard mRMR/CFS algorithm

	Naive Bayes			Decision Tree			5NN		
Dataset	Inner	Sets	Ranks	Inner	Sets	Ranks	Inner	Sets	Ranks
Colon	0/10/0	1/9/0	1/9/0	2/8/0	1/9/0	0/10/0	0/10/0	0/10/0	0/10/0
Ionosphere	0/6/0	0/6/0	0/6/0	0/6/0	0/6/0	0/6/0	0/6/0	0/6/0	1/4/1
Leukemia	2/8/0	1/9/0	2/7/1	1/7/2	1/9/0	2/8/0	0/10/0	0/10/0	2/8/0
Lung	0/9/1	1/8/1	3/7/0	0/10/0	0/10/0	0/10/0	0/10/0	0/10/0	1/9/0
Lymphoma	1/9/0	4/6/0	6/4/0	1/8/1	0/10/0	0/10/0	1/9/0	0/10/0	4/6/0
Musk	0/9/1	0/9/1	0/10/0	1/9/0	1/8/1	2/8/0	0/10/0	0/8/2	0/7/3
NCI60	0/7/0	0/7/0	0/6/1	1/5/0	1/5/0	0/6/0	1/5/0	0/6/0	4/2/0
Sonar	0/10/0	1/9/0	1/9/0	0/10/0	0/10/0	1/9/0	0/10/0	0/10/0	0/9/1
Sum	3/68/2	8/63/2	13/58/2	6/63/3	4/67/1	5/67/0	2/70/0	0/70/2	12/55/5

	SVM			LDA		
Dataset	Inner	Sets	Ranks	Inner	Sets	Ranks
Musk	0/9/1	0/9/1	0/9/1	0/10/0	0/10/0	0/10/0
Ionosphere	0/6/0	0/6/0	0/5/1	0/6/0	0/6/0	0/5/1
Sonar	0/10/0	0/10/0	0/10/0	0/9/1	2/8/0	0/10/0
Sum	0/25/1	0/25/1	0/24/2	0/25/1	2/24/0	0/25/1

5.4.3 Runtime

Let us now compare the runtime of our new *Fast Ensemble with sets* to a standard ensemble of the same size. The overlap (number of features which two sets have in common) can be calculated based on their size k and their Jaccard index as

$$ol(\bar{S}_J,k) = 2\bar{S}_J k/(\bar{S}_J+1). \tag{5.19}$$

The average Jaccard index of the sets produced by the parts of the ensemble is similar to the average Jaccard index measured for Plain mRMR/CFS for inspecting stability.

Considering a *Fast Ensemble with sets* of e parts we now sum up the average amount of correlations in the parts of the ensemble. In the first part of the ensemble, all $pk - \frac{k^2-k}{2}$ correlations must be computed. In the second part, there are no correlations needed for relevance estimation, and for the redundancy check, only those $k - ol(\bar{S}_J,k)$ features, which have not been selected in the first part, must be correlated with the all other features. At this point, it is unclear whether these features are added at the end or at the beginning of the selection process, i.e., whether the parts of the ensemble differ at the end or the beginning of the selection process. This determines how many features it is compared to and explains the imprecision of the estimate.

For a rough estimate assume the average probability that a feature f^r in the rth part, $r \in \{1,\ldots,e\}$, has already been correlated to all other features in the part before is

$$P_{k,\bar{S}_J}(f^r) = \sum_{m=1}^{r-1} \frac{ol(\bar{S}_J,k)}{k}\left(1 - P_{k,\bar{S}_J}(f^m)\right) \tag{5.20}$$

which reduces to

$$P_{\bar{S}_J}(f^r) = \frac{2\bar{S}_J}{\bar{S}_J+1} \sum_{m=1}^{r-1} \left(1 - P_{\bar{S}_J}(f^m)\right) \tag{5.21}$$

with $P_{\bar{S}_J}(f^1) = 0$. As seen from Eq. (5.8), in each step of one part, there are on average $p-(k-1)/2$ correlations to compute. When multiplied with the probability of **not** needing to compute the correlation and adding the initial relevance computation this gives a total average runtime of

$$T(p,k,e,\bar{S}_J) = p + \sum_{r=1}^{e}\sum_{j=2}^{k} (p-j)\left(1 - P_{\bar{S}_J}(f_j^r)\right) \tag{5.22}$$

$$= p + (k-1)\left(p - \frac{k-1}{2}\right)\left(e - \sum_{r=1}^{e} P_{\bar{S}_J}(f^r)\right) \tag{5.23}$$

under the assumption $P_{\bar{S}_J}(f_j^r) = P_{\bar{S}_J}(f^r), \forall j \in [1,k]$.

To give an empirical validation of this average case runtime estimation, Table 5.3 shows the number of correlations that must be computed depending on k for four of the datasets. We compare our approach to a standard ensemble of mRMR/CFS, both of size $e = 20$. High variance and large p can decrease the overlap between the ensemble parts, such increasing runtime as it is this overlap which speeds up runtime of our approach. It is not possible to predict in which order features are selected in different parts of the ensemble. This puts more variance to the number of needed correlations and makes it harder to predict those numbers. Nonetheless, Eq. (5.22) seems to give a good estimate on the average case of correlation computations.

Table 5.3 Number of computed correlations for *Fast Ensemble with sets*, the estimated number, number for a standard ensemble of mRMR/CFS and speed gain

k	Fast Ens.	Estimate	Std. Ensemble	Gain	Fast Ens.	Estimate	Std. Ensemble	Gain
	Ionosphere				Lung			
30	595	641	11,700	19.66	30,820	21,158	186,300	6.04
50					33,669	24,109	300,500	8.93
	Musk				Colon			
30	6,111	11,190	90,900	14.87	166,430	95,035	1,191,300	7.16
50	8,505	11,008	141,500	16.64	234,740	142,631	1,975,500	8.42
	Lymphoma				Leukemia			
30	1,296,456	1,086,820	2,406,900	1.86	987,000	430,168	4,233,300	4.29
50	1,631,750	1,091,347	4,001,500	2.45	1,242,707	605,412	7,045,500	5.67
	NCI60				Sonar			
30	2,802,838	1,872,590	5,818,500	2.08	1,577	1,738	27,300	17.31
50	3,515,832	2,085,675	9,687,500	2.76	1,815	1,985	35,500	19.56

5.4.4 LUCAS

A further test was to inspect whether the increased stability could also shed a brighter light on the causality behind the data distribution. Such a test was used by [1] on the LUCAS dataset[3]. This dataset is based on the Bayesian network shown in Fig. 5.6. It consists of eleven binary variables and one binary target variable in 2000 instances. The target variable has two direct causes, the variables 1 and 5. A feature selection method which reflects this causality should select these two features at first. We report the average selection rank of these two features over 1000 runs in Table 5.4.

The optimal value is 1.5. This is never achieved because variable 11 has a higher correlation to the target than 1 and 5, and due to its greedy forward selection, any variant of mRMR/CFS will choose variable 11 first. Nonetheless, it shows, that the performance for large sample sizes does not increase significantly, but for small sample sizes the results of the ensemble version are as good as the results of standard mRMR on the complete dataset. This is beneficial for settings in which only very few samples are available, e.g. microarray data. Again *Fast Ensemble* delivers better results earlier.

[3] http://www.causality.inf.ethz.ch/data/LUCAS.html

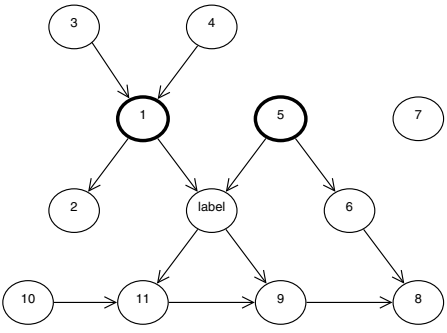

Fig. 5.6 Bayesian network of the LUCAS dataset

Table 5.4 Average combined rank of variables 1 and 5 over 1000 runs dependent on the sample size n

n	mRMR	Inner	Sets	Ranks
10	5.38	5.39	5.12	5.08
20	4.72	4.63	4.46	4.83
50	3.91	3.76	3.57	3.91
100	3.55	3.26	3.19	3.33
200	3.36	3.14	2.99	2.97
500	3.33	3.09	3.02	2.96
1000	3.14	2.96	2.93	2.86
mean	3.91	3.75	3.61	3.71
all	2.5	2.5	2.5	2.5

5.5 Conclusion

We presented two new algorithms towards selecting a maximum relevant and minimum redundant feature set. Our algorithms are more stable than the existing mRMR/CFS approach and much faster than a standard ensemble of mRMR/CFS. The speed-up is due to a faster computation of $Cor(f, f')$ based on the one-pass calculation and due to caching redundancy calculations from partitions. We showed that our method is well suited for feature selection on high-dimensional data as it is more robust against high variance and outliers than the single version. For the choice of $e = 20$ our algorithm is 1.4 to 19.7 times faster than a usual ensemble of mRMR/CFS.

Our methods do not rely on Mutual Information, Pearson's correlation, or the F-Test, alone. They can make use of any measure of similarity which can be split into sums. The split-sum-trick could also speed-up, e.g., Saeys' *bagged* SU [16], which builds upon MI, when replacing BaggingBagging by our subset splits. If a feature selection method implicitly generates a ranking of the features, it can be enhanced by the *Fast Ensemble* method and rank combination. If not, it can at least be enhanced by the *Fast Ensemble* with set combination. Applying ensemble methods is beneficial when only few examples are available and meaningful and robust results are needed.

References

1. Bontempi, G., Meyer, P.E.: Causal filter selection in microarray data. In: Fürnkranz, J., Joachims, T. (eds.) Proc. the 27th Int. Conf. Machine Learning, Haifa, Israel, pp. 95–102. Omnipress, Madison (2010)
2. Breiman, L.: Bagging predictors. Machine Learning 24, 123–140 (1996)
3. Breiman, L.: Random forests. Machine Learning 45, 5–32 (2001)
4. Ding, C.H.Q., Peng, H.: Minimum redundancy feature selection from microarray gene expression data. In: Proc. the 2nd IEEE Comp. Society Bioinformatics Conf., Stanford, CA, pp. 523–529. IEEE Comp. Society, Los Alamitos (2003)
5. Fox, R.J., Dimmic, M.W.: A two-sample Bayesian t-test for microarray data. BMC Bioinformatics 7 (2006)
6. Freund, Y., Schapire, R.E.: A decision-theoretic generalization of on-line learning and an application to boosting. J. Comput. Syst. Sci. 55, 119–139 (1997)
7. Gulgezen, G., Cataltepe, Z., Yu, L.: Stable and accurate feature selection. In: Buntine, W., Grobelnik, M., Mladenić, D., Shawe-Taylor, J. (eds.) ECML PKDD 2009. LNCS, vol. 5781, pp. 455–468. Springer, Heidelberg (2009)
8. Hall, M.A.: Correlation-based feature selection for discrete and numeric class machine learning. In: Langley, P. (ed.) Proc. the 17th Int. Conf. Machine Learning, Stanford, CA, pp. 359–366. Morgan Kaufmann, San Francisco (2000)
9. Han, Y., Yu, L.: A variance reduction framework for stable feature selection. In: Webb, G.I., Liu, B., Zhang, C., Gunopulos, D., Wu, X. (eds.) Proc. the 10th IEEE Int. Conf. Data Mining, Sydney, Australia, pp. 206–215. IEEE Computer Society, Los Alamitos (2010)
10. Jurman, G., Merler, S., Barla, A., Paoli, S., Galea, A., Furlanello, C.: Algebraic stability indicators for ranked lists in molecular profiling. Bioinformatics 24, 258–264 (2008)
11. Kalousis, A., Prados, J., Hilario, M.: Stability of feature selection algorithms: a study on high-dimensional spaces. Knowledge and Inf. Syst. 12, 95–116 (2007)
12. Koh, J.L.Y., Li Lee, M., Hsu, W., Lam, K.-T.: Correlation-based detection of attribute outliers. In: Kotagiri, R., Radha Krishna, P., Mohania, M., Nantajeewarawat, E. (eds.) DASFAA 2007. LNCS, vol. 4443, pp. 164–175. Springer, Heidelberg (2007)
13. Kohavi, R., John, G.H.: Wrappers for feature subset selection. Artif. Intell. 97, 273–324 (1997)
14. Kuncheva, L.I.: A stability index for feature selection. In: Devedzic, V. (ed.) IASTED Int. Conf. Artif. Intell. and Appl., Innsbruck, Austria, pp. 421–427. ACTA Press, Calgary (2007)
15. Michalak, K., Kwasnicka, H.: Correlation-based feature selection strategy in neural classification. In: Proc. the 6th Int. Conf. Intell. Syst. Design and Appl., Jinan, China, pp. 741–746. IEEE Comp. Society, Los Alamitos (2006)
16. Saeys, Y., Abeel, T., Van de Peer, Y.: Robust feature selection using ensemble feature selection techniques. In: Daelemans, W., Goethals, B., Morik, K. (eds.) ECML PKDD 2008, Part II. LNCS (LNAI), vol. 5212, pp. 313–325. Springer, Heidelberg (2008)
17. Tusher, V.G., Tibshirani, R., Chu, G.: Significance analysis of microarrays applied to the ionizing radiation response. Proc. the National Academy of Sciences of the United States of America 98, 5116–5121 (2001)
18. Vapnik, V.: Statistical learning theory. Wiley, Chichester (1998)
19. Xu, X., Zhang, A.: Boost feature subset selection: A new gene selection algorithm for microarray dataset. In: Alexandrov, V.N., van Albada, G.D., Sloot, P.M.A., Dongarra, J. (eds.) ICCS 2006. LNCS, vol. 3992, pp. 670–677. Springer, Heidelberg (2006)
20. Yu, L., Liu, H.: Efficient feature selection via analysis of relevance and redundancy. J. Machine Learning Research 5, 1205–1224 (2004)

Chapter 6
Hybrid Correlation and Causal Feature Selection for Ensemble Classifiers

Rakkrit Duangsoithong and Terry Windeatt

Abstract. PC and TPDA algorithms are robust and well known prototype algorithms, incorporating constraint-based approaches for causal discovery. However, both algorithms cannot scale up to deal with high dimensional data, that is more than few hundred features. This chapter presents hybrid correlation and causal feature selection for ensemble classifiers to deal with this problem. Redundant features are removed by correlation-based feature selection and then irrelevant features are eliminated by causal feature selection. The number of eliminated features, accuracy, the area under the receiver operating characteristic curve (AUC) and false negative rate (FNR) of proposed algorithms are compared with correlation-based feature selection (FCBF and CFS) and causal based feature selection algorithms (PC, TPDA, GS, IAMB).

6.1 Introduction

With rapid development of computer and information technology that can improve a large number of applications such as web text mining, intrusion detection, biomedical informatics, gene selection in micro array data, medical data mining, and clinical decision support systems, many information databases have been created. However, in some applications especially in medical area, data may contain hundreds to thousands of features with small sample size. A consequence of this problem is increased complexity that leads to degradation in efficiency and accuracy by curse of dimensionality and over-fitting. The resulting classifier works very well with training data but very poorly on test data.

Rakkrit Duangsoithong · Terry Windeatt
Centre for Vision, Speech and Signal Processing, University of Surrey,
Guildford, United Kingdom GU2 7XH
E-mail: r.duangsoithong@surrey.ac.uk, t.windeatt@surrey.ac.uk

O. Okun et al. (Eds.): Ensembles in Machine Learning Applications, SCI 373, pp. 97–115.
springerlink.com

To overcome this high dimensional feature spaces degradation problem, number of features should be reduced. Basically, there are two methods to reduce the dimension: feature extraction and feature selection. Feature extraction transforms or projects original features to fewer dimensions without using prior knowledge. Nevertheless, it lacks comprehensibility and uses all original features which may be impractical in large feature spaces. On the other hand, feature selection selects optimal feature subsets from original features by removing irrelevant and redundant features. It has the ability to reduce over-fitting, increase classification accuracy, reduce complexity, speed up computation and improve comprehensibility by preserving original semantic of datasets. Normally, clinicians prefer feature selection because of its understandability and user acceptance.

Feature selection is an important pre-processing step to reduce feature dimensions for classification and generally, can be divided into four categories [9, 15, 18]. Filter method is independent from learning method and uses measurement techniques such as correlation and distance measurement to find a good subset from entire set of features. Wrapper method uses pre-determined learning algorithm to evaluate selected feature subsets that are optimum for the learning process. Hybrid method combines advantage of both Filter and Wrapper method together. It evaluates features by using an independent measure to find the best subset and then uses a learning algorithm to find the final best subset. Finally, Embedded method interacts with learning algorithm but it is more efficient than Wrapper method because the filter algorithm has been built with the classifier.

As has been illustrated by Liu and Yu [15], feature selection has four basic processes: subset generation, subset evaluation, stopping criterion and subset validation. Subset generation produces candidate subset by complete (exhaustive), sequential (heuristic) or random search with three directions: forward (adding feature to selected subset that begin with empty set), backward (eliminate features from selected subset that begins with full original set) and bidirectional (both adding and removing features). After that, the candidate subset is evaluated based on criteria such as distance, dependency and information gain and consistency measurement. The process will stop when it reaches the stopping criterion. Finally, the selected subset is validated with validation data.

Feature selection does not usually take causal discovery into account. However, in some cases such as when training and testing dataset do not conform to i.i.d. assumption, testing distribution is shifted from manipulation by external agent, causal discovery can provide some benefits for feature selection under these uncertainty conditions. Causal relationships are usually uncovered by Bayesian Networks (BNs) which consist of a direct acyclic graph (DAG) that represents dependencies and independencies between variable and joint probability distribution among a set of variables [1]. It also can learn underlying data structure, provide better understanding of the data generation process and better accuracy and robustness under uncertainty [10].

An ensemble classifier or multiple classifier system (MCS) is another well-known technique to improve system accuracy [24]. Ensembles combine multiple base classifiers to learn a target function. It has ability to increase accuracy by combining output of multiple experts to reduce bias and variance [3], improve efficiency by decomposing complex problem into multiple sub problems and improve reliability by reducing uncertainty. To increase accuracy, each classifier in the ensemble should be diverse or unique such as starting with different input, initial weight, random features or random classes [23].

Generally, the number of features in feature selection analysis can be divided into three categories: small scale (the number of features is less than 19), medium scale (the number of features is between 20 and 49) and large scale (the number of features is equal or higher than 50 features) [12, 27]. The main purpose of this research is to find methods that can scale up to deal with hundreds or thousands of features.

The main objective of this chapter is to find approaches that enable PC and TPDA algorithms to deal with high dimensional data. We propose hybrid correlation and causal feature selection for ensemble classifiers and compare number of eliminated features, average percent accuracy, the area under the receiver operating characteristic curve (AUC) and false negative rate (FNR).

The structure of the chapter is the following. Related research is briefly described in Sect. 6.2. Section 6.3 explains theoretical approach of feature selection , causal discovery and ensemble classifiers. The dataset and evaluation procedure are described in Sect. 6.4. Experimental results are presented in Sect. 6.5 and are discussed in Sect. 6.6. Finally, Conclusion is summarized in Sect. 6.7.

6.2 Related Research

Feature selection and ensemble classification have received attention from many researchers in the areas of Statistics, Machine Learning, Neural Networks and Data Mining for many years. Initially, most researchers focused only on removing irrelevant features such as ReliefF [25], FOCUS [2] and Correlation-based Feature Selection(CFS) [8]. Recently, in Yu and Liu (2004) [26], Fast Correlation-Based Filter (FCBF) algorithm was proposed to remove both irrelevant and redundant features by using Symmetrical Uncertainty (SU) measurement and was successful for reducing high dimensional features while maintaining high accuracy.

In the past few years, learning Bayesian Networks (BNs) from observation data has received increasing attention from researchers for many applications such as decision support system, information retrieval, natural language processing, feature selection and gene expression data analysis [21, 22]. The category of BNs can be divided into three approaches: Search-and-Score, Constraint-Based and Hybrid approaches [21, 22]. In Search-and-Score approach, BNs search all possible structures to find the one that provides the maximum score. The standard Scoring functions

that normally used in BNs are Bayesian Dirichlet (BDeu), Bayesian Information Criterion (BIC), Akaike Information Criterion (AIC), Minimum Description Length (MDL) and K2 scoring function [21]. The second approach, Constraint-Based, uses test of conditional dependencies and independencies from the data by estimation using G^2 statistic test or mutual information, etc. This approach defines structure and orientation from results of the tests based on some assumptions that these tests are accurate. Finally, Hybrid approach uses Constraint-Based approach for conditional independence test (CI test) and then identifies the network that maximizes a scoring function by using Search-and-Score approach [22].

Constraint-Based algorithms are computationally effective and suitable for high dimensional feature spaces. PC algorithm [19], is a pioneer, prototype and well-known global algorithm of Constraint-Based approach for causal discovery. Three Phase Dependency Analysis (TPDA or PowerConstructor) [6] is another global Constraint-Based algorithm that uses mutual information to search and test for CI test instead of using G^2 Statistics test as in PC algorithm. However, both PC and TPDA algorithm use global search to learn from the complete network and can not scale up to more than few hundred features (they can deal with 100 and 255 features for PC and TPDA, respectively) [20]. Sparse Candidate algorithm (SC) [7] is one of the prototype BNs algorithm that can deal with several hundreds of features by using local candidate set. Nevertheless, SC algorithm has some disadvantages: it may not identify true set of parents and users have to find appropriate k parameter of SC algorithm [21].

Recently, many Markov Blanket-based algorithms for causal discovery have been studied extensively and they have ability to deal with high dimensional feature spaces such as MMMB, IAMB [20] and HITON [1] algorithms. HITON is a state-of-the-art algorithm that has ability to deal with thousands of features and can be used as an effective feature selection method in high dimensional spaces. However, HITON and all other MB-based algorithms may not specify features in Markov Blanket for desired classes or target (MB(T)) when the data is not faithful [5].

6.3 Theoretical Approach

In our research, hybrid algorithm of correlation and causal feature selection is compared with Fast Correlation-Based Filter (FCBF), Correlation-based Feature Selection with Sequential Forward Floating Search direction (CFS+SFFS), and with causal feature selection algorithms (PC, TPDA, GS and IAMB) using Bagging (described in Sect. 6.3.4).

6.3.1 Feature Selection Algorithms

6.3.1.1 Fast Correlation-Based Filter (FCBF)

FCBF [26] algorithm is a correlation-based filter which has two stages: relevance analysis and redundancy analysis.

Relevance Analysis
Normally, correlation is widely used to analyze relevance in linear system and can be measured by linear correlation coefficient.

$$r = \frac{\sum_i (x_i - \overline{x_i})(y_i - \overline{y_i})}{\sqrt{\sum_i (x_i - \overline{x_i})^2}\sqrt{\sum_i (y_i - \overline{y_i})^2}}. \tag{6.1}$$

However, most systems in real world applications are non-linear. Correlation in non-linear systems can be measured by using Symmetrical Uncertainty (SU).

$$SU(X,Y) = 2\Big[\frac{IG(X|Y)}{H(X)+H(Y)}\Big], \tag{6.2}$$

$$IG(X|Y) = H(X) - H(X|Y), \tag{6.3}$$

$$H(X) = -\sum_i P(x_i) log_2 P(x_i), \tag{6.4}$$

where $IG(X|Y)$ is the Information Gain of X after observing variable Y, $H(X)$ and $H(Y)$ are the entropy of variable X and Y, respectively, and $P(x_i)$ is the probability of variable X.

SU is the modified version of Information Gain that has range between 0 and 1. FCBF removes irrelevant features by ranking correlation (SU) between feature and class. If SU between feature and class equal to 1, it means that this feature is completely related to that class. On the other hand, if SU is equal to 0, the features are irrelevant to this class.

Redundancy analysis
Redundant features can be defined from meaning of predominant feature and approximate Markov Blanket. In Yu and Liu (2004) [26], a feature is predominant (both relevant and non redundant feature) if it does not have any approximate Markov Blanket in the current set.

Approximate Markov Blanket: For two relevant features F_i and F_j $(i \neq j)$, F_j forms an approximate Markov Blanket for F_i if

$$SU_{j,c} \geq SU_{i,c} \; and \; SU_{i,j} \geq SU_{i,c}, \tag{6.5}$$

where $SU_{i,c}$ is a correlation between any feature and the class, $SU_{i,j}$ is a correlation between any pair of feature F_i and F_j $(i \neq j)$.

6.3.1.2 Correlation-Based Feature Selection (CFS)

CFS [8] is one of well-known techniques to rank the relevance of features by measuring correlation between features and classes and between features and other features.

Given number of features k and classes c, CFS defined relevance of features subset by using Pearson's correlation equation

$$Merit_s = \frac{kr_{kc}}{\sqrt{k+(k-1)r_{kk}}}, \tag{6.6}$$

where $Merit_s$ is relevance of feature subset, r_{kc} is the average linear correlation coefficient between these features and classes and r_{kk} is the average linear correlation coefficient between different features.

Normally, CFS adds (forward selection) or deletes (backward selection) one feature at a time, however, in this research, we used Sequential Forward Floating Search (SFFS) [17] as the search direction because of its powerful search scheme which is very fast and does not require any tuning parameters.

Sequential Forward Floating Search (SFFS). SFFS [17] is one of the classic heuristic searching methods. It is a variation of bidirectional search and sequential forward search (SFS) that has dominant direction on forward search. SFFS removes features (backward elimination) after adding features (forward selection). The number of forward and backward steps is not fixed but dynamically controlled depending on the criterion of the selected subset and therefore, no parameter setting is required.

6.3.2 Causal Discovery Algorithm

In this chapter, two standard constraint-based approaches (PC and TPDA) and two Markov Blanket based algorithms (GS, IAMB) are used as causal feature selection methods. In the final output of the causal graph from each algorithm, the unconnected features to classes will be considered as eliminated features.

6.3.2.1 PC Algorithm

PC algorithm [10, 19] is the prototype of constraint-based algorithm. It consists of two phases: Edge Detection and Edge Orientation.

Edge Detection: the algorithm determines directed edge by using conditionally independent condition. The algorithm starts with:

i) Undirected edge with fully connected graph.

ii) Remove a share direct edge between A and B ($A-B$) iff there is a subset F of features that can present conditional independence $(A,B|F)$.

Edge Orientation: The algorithm discovers V-Structure $A-B-C$ in which $A-C$ is missing.

i) If there are direct edges between $A-B$ and $B-C$ but not $A-C$, then orient edge $A \rightarrow B \leftarrow C$ until no more possible orientation.

ii) If there is a path $A \rightarrow B-C$ and $A-C$ is missing, then $A \rightarrow B \rightarrow C$.

iii) If there is orientation $A \rightarrow B \rightarrow ... \rightarrow C$ and $A-C$ then orient $A \rightarrow C$.

6.3.2.2 Three Phase Dependency Analysis Algorithm (TPDA)

TPDA or PowerConstructor algorithm [6] has three phases: drafting, thickening and thinning phases.

Drafting phase: mutual information of each pair of nodes is calculated and used to create a graph without loop.

Thickening phase: edge will be added when that pair of nodes can not be *d-separated* (node A and B are *d-separated* by node C iff node C blocks every path from node A to node B [21]) The output of this phase is called an independence map (*I-map*).

Thinning phase: The edge of *I-map* will be removed in thinning phase, if two nodes of the edge can be *d-separated* and the final output is defined as a *perfect map* [6].

6.3.2.3 Grow-Shrink Algorithm (GS)

GS [16] algorithm consists of two phases: forward and backward phases.

Forward phase: GS statistically ranks features by using the strength of association with target or class (T) given empty set. After that the next ordering feature which is not conditionally independent from class T given current Markov Blanket (CMB) will added into CMB.

Backward phase: Identify false positive nodes and remove them from CMB. At this stage, $CMB = MB(T)$. Finally, a feature X will be removed from CMB one-by-one if that feature X is independent of class T given the remaining CMB.

6.3.2.4 Incremental Association Markov Blanket Algorithm (IAMB)

IAMB [20] is one of Markov Blanket detection algorithms using forward selection followed by removing false positive node. IAMB has two phases: forward and backward.

Forward phase: In forward selection phase, the algorithm starts with empty set in CMB, then adding features which maximize a heuristic function $f(X;T|CMB)$. A feature member in MB(T) will not return zero value of this function.

Backward phase: False positive nodes will be removed from CMB by using condition independent testing of class T given the rest CMB.

6.3.3 Feature Selection Analysis

6.3.3.1 Correlation-Based Redundancy and Relevance Analysis

The concept of selecting the optimal subset from the entire set of features is presented in Fig. 6.1 [26], where I is irrelevant feature, II is weakly relevant and redundant feature, III is weakly relevant but non redundant feature, IV is strongly relevant feature. The combination of III+IV is the optimal feature subset.

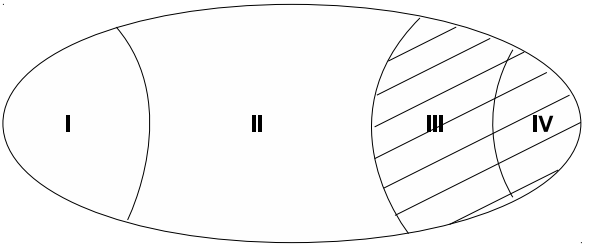

Fig. 6.1 Optimal Subset

Thus, the optimal subset should include all strongly relevant features, subset of weakly relevant features that have no redundancy and none of the irrelevant features.

In 2004, Yu and Liu [26] proposed FCBF algorithm to remove both redundant and irrelevant features.

1) Redundancy: A feature is redundant if it has approximate Markov Blanket ($SU_{j,c} \geq SU_{i,c}$ *and* $SU_{i,j} \geq SU_{i,c}$).

2) Irrelevance: A feature is irrelevant if SU between feature and class is zero.

3) Relevance: A feature is relevant if SU between feature and class is more than zero but less than one.

4) Strong relevance: A feature is strongly relevant if SU between feature and class is equal to one.

6.3.3.2 Causal-Based Relevance Analysis

In Guyon [10], the notion of Markov Blanket is defined in term of Kohavi-John feature relevance:

1) Irrelevance: A feature is irrelevant if it is disconnected from graph (conditional independence).

2) Relevance: A feature is relevant if it has connected path to class (target).

3) Strong relevance: A feature is strongly relevant if it is Markov Blanket of class.

6.3.3.3 Hybrid Correlation-Based Redundancy Causal-Based Relevance Analysis

According to Fig. 6.1 and the above analysis, optimal subset consists of strongly relevant features and weakly relevant features that do not contain redundant and irrelevant features. Therefore, we propose a new analysis for Hybrid Correlation-Based Relevance Causal-Based Redundancy Analysis as follows:

1) Redundancy: A feature is redundant if it has approximate Markov Blanket.

2) Irrelevance: A feature is irrelevant if it is disconnected from the graph (conditional independence).

3) Relevance: A feature is relevant if it has connected path to the target (class).

4) Strong relevance: A feature is strongly relevant if it is Markov Blanket of the target (class).

Table 6.1 Summary analysis of correlation, causal and proposed hybrid correlation and causal feature selection for redundancy and relevance analysis

Relation	Correlation-Based	Causal-Based	Hybrid algorithm
Strongly relevant	$SU_{i,c} = 1$	Features in Markov Blanket	Features in Markov Blanket
Weakly relevant without redundant features	does not has approximate Markov Blanket	connected to classes	connected to classes
Weakly relevant with redundant features	has approximate Markov Blanket	connected to classes	has approximate Markov Blanket
Irrelevant	$SU_{i,c} = 0$	disconnected to classes	disconnected to classes

Table 6.1 shows the summary analysis of redundancy and relevancy analysis for correlation-based [26], causal-based [10] and proposed hybrid correlation and causal feature selection . Markov Blanket (MB(T)) of target or class (T) is the minimal set of conditional features that all other features are probabilistically independent of T. It consists of the set of parents, children and spouses of T.

Figure 6.2 presents the proposed system block diagram. Redundant features are removed by correlation-based feature selection and irrelevant features are eliminated by causal-based feature selection . After that, selected features are passed through ensemble classifier for training and predicting output.

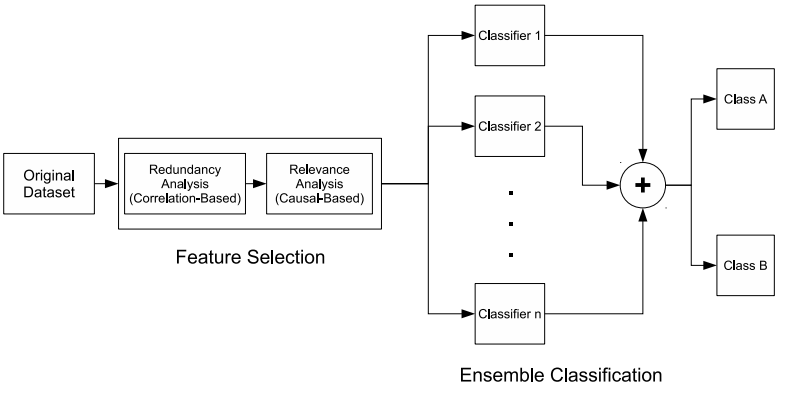

Fig. 6.2 Block Diagram of proposed algorithm

6.3.4 Ensemble Classifier

Bagging [4] or **B**ootstrap **agg**regat**ing** is one of the earliest, simplest and most popular methods for ensemble based classifiers. Bagging uses Bootstrap that randomly samples with replacement and combines with majority vote. The selected data is divided to m bootstrap replicates and randomly sampled with replacement. Each bootstrap replicate contains, on average, 63.2 % of the original dataset. Final output will be selected from majority vote of all classifiers of each bootstrap replicate. Bootstrap is the most well-known strategy for injecting randomness to improve generalization performance in multiple classifier systems and provides out-of-bootstrap estimate for selecting classifier parameters [24]. Randomness is desirable since it increases diversity among the base classifiers, which is known to be a necessary condition for improved performance. However, there is an inevitable trade-off between accuracy and diversity known as the accuracy/diversity dilemma [24].

Nevertheless, in causal discovery, there are some disadvantages for BNs learning using Bagging. Bootstrap method can add many extra edges in graphical model due to more complexity especially in high dimensional features with limited dataset [13]. Moreover, distribution from bootstrap dataset may not satisfy Markov Blanket condition and faithfulness condition [14].

6.3.5 Pseudo-code: Hybrid Correlation and Causal Feature Selection for Ensemble Classifiers Algorithm

Goal : To find optimal subset features for ensemble classifiers by using correlation and causal discovery.

6.3.5.1 Eliminate Redundant Features by Using Correlation

◇ *Input*: Training set (each pattern having features $\{f_1, f_2, ..., f_n\}$ and class $\{C\}$)
◇ *Output*: Selected features without redundant features $\{S_1\}$
• Calculate SU between features and between feature and classes, find and remove redundant features using approximate Markov Blanket.

for $i = 1$ to $n-1$, $j = i+1$
    f_i = first feature, f_j = next feature
    calculate $SU_{i,j}$, $SU_{i,c}$ and $SU_{j,c}$
        if $SU_{i,c} \geq SU_{j,c}$ and $SU_{i,j} \geq SU_{j,c}$
            then remove f_j
        else Append f_j to output selected features list $\{S_1\}$
end for

6.3.5.2 Remove Irrelevant Features by Using Causal Discovery

◇ *Input*: Selected features without redundant features. $\{S_1\}$
◇ *Output*: Optimal features without redundant and irrelevant features.$\{S_2\}$

• Find constructor and direction of graph by using causal discovery algorithm. (PC, TPDA, GS, IAMB or other causal discovery algorithm)
• Remove irrelevant features which are disconnected from class.

- PC Algorithm
Edge Detection: using conditionally independent condition.

Starts with completely connected graph G.
$i = -1$
repeat
$i = i + 1$
repeat
- Select and order pair of features (nodes) A, B in graph G.
- Select adjacent (neighborhood) feature F of A with size i
- if there exists a feature F that presents conditional independence $(A, B|F)$, delete direct edge between A and B.

until all ordered pairs of feature F have been tested.
until all adjacent features have size smaller than i.

Edge Orientation: directed edges using following rules;
• If there are direct edges between $A - B$ and $B - C$ but not $A - C$, then orient edge $A \rightarrow B \leftarrow C$ until no more possible orientation.
• If there is a path $A \rightarrow B - C$ and $A - C$ is missing, then $A \rightarrow B \rightarrow C$.
• If there is orientation $A \rightarrow B \rightarrow ... \rightarrow C$ and $A - C$ then orient $A \rightarrow C$.

- Three Phase Dependency Analysis Algorithm (TPDA).
Drafting phase
• calculated mutual information (MI) of each pair of features.
• create a graph without loop using MI.
Thickening phase
• add edge when that pair of nodes can not be *d-separated*.
• the output of this phase is called an independence map (*I-map*).
Thinning phase
• remove the edge of *I-map*, if two nodes of the edge can be *d-separated*.
• the final output is defined as a *perfect map*.

6.3.5.3 Ensemble Classifiers Using Bagging Algorithm

◇ *Input*:
• Optimal features without redundant and irrelevant features $\{S_2\}$
• Number of bootstrap sample (m) (number of iterations) with 100 percentage setting from original data
• Classifier or Inducer function (I)

for $i = 1$ to m
$\{S_2'\}$ = bootstrap sample from $\{S_2\}$
$C_i = I\{S_2'\}$ //(class output of each bootstrap replicate)
end for

◇ *Output*:
• ensemble classifiers prediction based on majority vote ($C^*(x)$)
• y is one of the class of total Y classes
• count majority vote class from all output of bootstrap replicates

$$C^*(x) = argmax_{y \in Y} \sum_{i:C_i(x)=y} 1$$

6.4 Experimental Setup

6.4.1 Dataset

The datasets used in this experiment were taken from Causality Challenge [11] and details of each dataset are shown as follows:

LUCAS (LUng CAncer Simple set) dataset is toy data generated artificially by causal Bayesian networks with binary features. Both this dataset and the next one (**LUCAP**) are modelling a medical application for the diagnosis, prevention and cure of lung cancer. Lucas has 11 features with binary classes and 2,000 samples.

LUCAP (LUng CAncer set with Probes) is LUCAS dataset with probes which are generated from some functions plus some noise of subsets of the real variables. LUCAP has 143 features, 2,000 samples and binary classes.

REGED (REsimulationed Gene Expression Dataset) is dataset that simulated model from real human lung cancer micro array gene expression data. The target to simulate this data is to find genes which could be responsible of lung cancer. It contains 500 examples with 999 features and binary classes.

CINA (Census Is Not Adult) dataset derived from Census dataset from UCI Machine learning repository. The goal of dataset is to uncover the socio-economic factors affecting high income. It has 132 features which contains 14 original features and distracter features which are artificially generated features that are not causes of the classes, 16,033 examples and binary classes.

SIDO (SImple Drug Operation mechanisms) has 4,932 features, 12,678 samples and 2 classes. Sido dataset consists of molecules descriptors that have been tested against the AIDS HIV virus and probes which artificially generated features that are not causes of the target.

Due to large number of samples and limitation of computer memory during validation in CINA and SIDO datasets, the number of samples of both dataset are reduced to 10 percent (1,603 and 1,264 samples, respectively) from the original dataset.

6.4.2 Evaluation

To evaluate feature selection process we use four widely used classifiers: Naive-Bayes (NB), Multilayer Perceptron (MLP), Support Vector Machines (SVM) and Decision Trees (DT). The parameters of each classifier were chosen as follows. MLP has one hidden layer with 16 hidden nodes, learning rate 0.2, momentum 0.3, 500 iterations and uses backpropagation algorithm with sigmoid transfer function. SVM uses polynomial kernel with exponent 2 and the regularization value set to 0.7. DT uses pruned C4.5 algorithm. The number of classifiers in Bagging is varied from 1, 5, 10, 25 to 50 classifiers. The threshold value of FCBF algorithm in our research is set at zero for LUCAS, REGED, CINA, SIDO and 0.14 for LUCAP dataset, respectively.

The classifier results were validated by 10 fold cross validation with 10 repetitions for each experiment and evaluated by average percent of test set accuracy, False Negative Rate (FNR) and area under the receiver operating characteristic curve (AUC).

In two-class prediction, there are four possible results of classification as shown in Table 6.2.

Table 6.2 Four possible outcomes from two-classes prediction

		Predicted Class	
		Positive	Negative
Actual Class	Positive	True Positive (TP)	False Negative (FN)
	Negative	False Positive (FP)	True Negative (TN)

Accuracy. Accuracy of classification measurement can be calculated from the ratio between number of correct predictions (True Positive(TP) and True Negative (TN)) and total number of all possible outcomes (TP,TN,FP and FN).

$$Accuracy = \left[\frac{TP+TN}{TP+FP+FN+TN}\right] \tag{6.7}$$

The area under the receiver operating characteristic curve (AUC). AUC is a graph of true positive against false positive. AUC has value between 0 and 1. The AUC value of 1 represents a perfect classifier performance while AUC lower than 0.5 represents a poor prediction.

Table 6.3 Number of selected features from each algorithm

Dataset	Original Feature	Correlation-Based		Causal-Based				Hybrid algorithm			
		FCBF	CFS	PC	TPDA	GS	IAMB	H-PC	H-TPDA	H-GS	H-IAMB
LUCAS	11	3	3	9	10	9	11	2	3	2	2
LUCAP	143	7	36	121	121	16	14	21	22	17	13
REGED	999	18	18	N/A	N/A	2	2	18	N/A	2	2
CINA	132	10	15	132	N/A	4	4	5	7	10	9
SIDO	4932	23	25	N/A	N/A	17	17	2	3	1	2

False Negative Rate (FNR) For medical dataset, FNR is the ratio of number of patient with negative prediction (False Negative (FN)) and number with disease condition (FN and TP).

$$FNR = \left[\frac{FN}{FN+TP}\right] \tag{6.8}$$

For causal feature selection , PC algorithm uses mutual information (*MI*) as statistical test with threshold 0.01 and maximum cardinality equal to 2. In TPDA algorithm, mutual information was used as statistic test with threshold 0.01 and data assumed to be monotone faithful. GS and IAMB algorithm use *MI* statistic test with significance threshold 0.01 and provides output as Markov Blanket of the classes.

6.5 Experimental Result

Table 6.3 presents the number of selected features for correlation-based, causal based feature selection and proposed hybrid algorithm. It can be seen that PC and TPDA algorithms are impractical for high dimensional features due to their complexity. However, if redundant features are removed, the number of selected features will enable both algorithms to be practical as shown in proposed hybrid algorithm. Nevertheless, for some datasets such as REGED, TPDA algorithm might not be feasible because of many complex connections between nodes (features).

Figures 6.3-6.6 show the average percent accuracy, AUC and FNR of five datasets from all four classifiers. From average accuracy in Fig. 6.3, correlation-based feature selection (FCBF, CFS) provides the best average accuracy. Hybrid correlation and causal feature selection has better accuracy than original causal feature selection. Hybrid method using PC algorithm (H-PC) has slightly lower average accuracy than correlation-based feature selection but has the ability to deal with high dimensional features. From Fig. 6.4, PC, CFS, TPDA and FCBF algorithms provide the best and comparable AUC. Proposed hybrid algorithm has lower AUC than both correlation and original causal-based algorithms. In Fig. 6.5, H-PC has the lowest FNR. In all experiments, hybrid algorithm provides lower FNR than original causal algorithm but still higher than correlation-based algorithm.

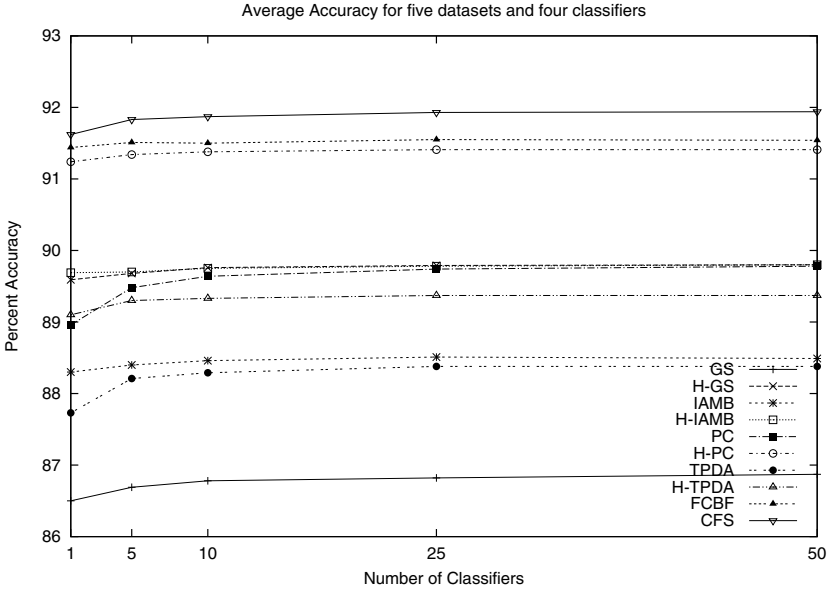

Fig. 6.3 Average Percent Accuracy of five datasets and four classifiers

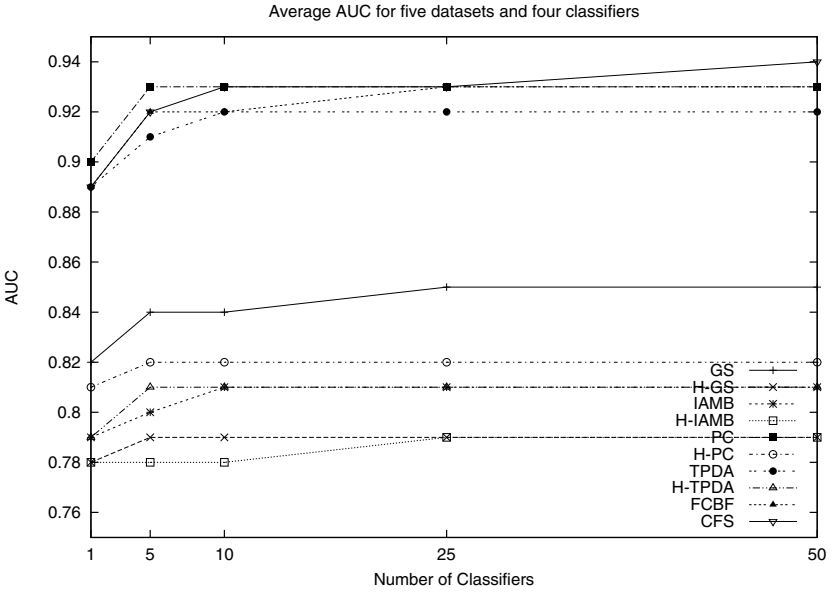

Fig. 6.4 Average AUC of five datasets and four classifiers

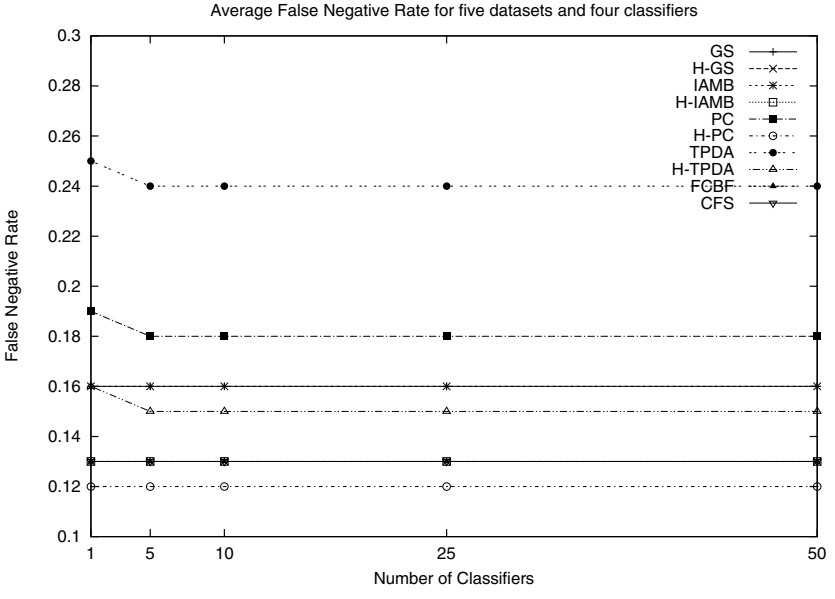

Fig. 6.5 Average FNR of five datasets and four classifiers

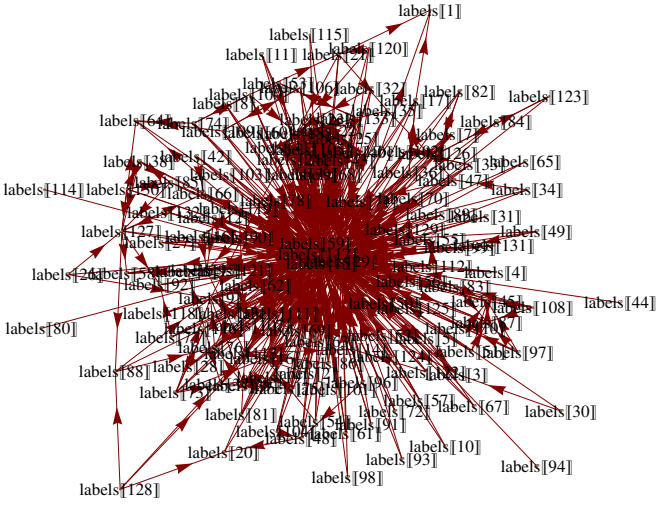

Fig. 6.6 Causal structure of CINA dataset from PC algorithm

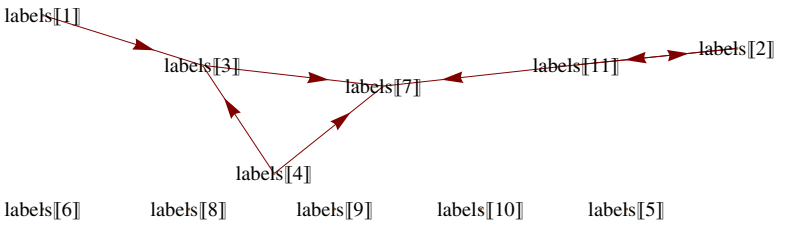

Fig. 6.7 Causal structure of CINA dataset from Hybrid-PC algorithm (class=labels[11])

Figures 6.6-6.7 present examples of the causal structure for CINA dataset using PC and Hybrid-PC algorithms, respectively. The high complexity of original CINA dataset using PC algorithm can be seen in Fig. 6.6 while after removing redundant and irrelevant features of CINA dataset using hybrid PC algorithm as shown in Fig. 6.7, the complexity of system is decreased, easier to understand and higher accuracy (Fig. 6.4), compared to using the original PC algorithm.

Ensemble classifiers using Bagging slightly improves accuracy and AUC for most algorithms. Bagging also reduces FNR for CFS, PC and TPDA algorithm but provides stable FNR for the rest. After increasing number of classifiers to 5-10, the graphs of average accuracy, AUC and FNR all reach saturation point.

6.6 Discussion

In high dimensional features spaces, Bagging algorithm is not appropriate and impractical for Bayesian Networks and its complexity may overestimate extra edges and their distribution might not satisfy Markov Blanket condition and faithfulness condition [13, 14]. Therefore, this chapter proposed to solve this problem by reducing dimensionality before bagging while preserving efficiency and accuracy.

For small and medium number of features, a set of selected features after removing redundancy might be very small (may be only 2-3 features in some datasets and algorithms), however, the result is still comparable to the result before removing redundant features.

PC algorithm has tendency to select all features (all connected such as in CINA dataset) that may be impractical due to computational expense. Therefore, removing redundant features prior to causal discovery would benefit PC algorithm.

In some cases, such as REGED dataset as shown in Table 6.3, TPDA algorithm can have very complex causal relations between features that might be impractical to calculate even for medium number of features.

From the experiment results, Bagging can improve system accuracy and AUC but cannot improve FNR.

6.7 Conclusion

In this chapter, hybrid correlation and causal feature selection for ensemble classifiers is presented to deal with high dimensional features. According to the results, the proposed hybrid algorithm provides slightly lower accuracy, AUC and higher FNR than correlation-based. However, compared to causal-based feature selection, the proposed hybrid algorithm has lower FNR, higher average accuracy and AUC than original causal-based feature selection. Moreover, the proposed hybrid algorithm can enable PC and TPDA algorithms to deal with high dimensional features while maintaining high accuracy, AUC and low FNR. Also the underlying causal structure is more understandable and has less complexity. Ensemble classifiers using Bagging provide slightly better results than single classifier for most algorithms. Future work will improve accuracy of search direction in structure learning for causal feature selection algorithm.

References

1. Aliferis, C.F., Tsamardinos, I., Statnikov, A.: HITON, A novel Markov blanket algorithm for optimal variable selection. In: Proc. American Medical Iinformation Association Annual Symp., Washington DC, pp. 21–25 (2003)
2. Almuallim, H., Dietterich, T.G.: Learning with many irrelevant features. In: Proc. the 9th Natl. Conf. Artif. Intell., San Jose, CA, pp. 547–552. AAAI Press, New York (1991)
3. Bauer, E., Kohavi, R.: An empirical comparison of voting classification algorithms: bagging, boosting, and variants. Machine Learning 36, 105–139 (1999)
4. Breiman, L.: Bagging predictors. Machine Learning 24, 123–140 (1996)
5. Brown, L.E., Tsamardinos, I.: Markov blanket-based variable selection. Technical Report DSL TR-08-01 (2008)
6. Cheng, J., Bell, D.A., Liu, W.: Learning belief networks from data: An information theory based approach. In: Golshani, F., Makki, K. (eds.) Proc. the 6th Int. Conf. Inf. and Knowledge Management, Las Vegas, NV, pp. 325–331. ACM, New York (1997)
7. Friedman, N., Nachman, I., Peer, D.: Learning of Bayesian network structure from massive datasets: The sparse candidate algorithm. In: Laskey, K., Prade, H. (eds.) Proc. the 15th Conf. Uncertainty in Artif. Intell., Stockholm, Sweden, pp. 206–215. Morgan Kaufmann, San Francisco (1999)
8. Hall, M.A.: Correlation-based feature selection for discrete and numeric class machine learning. In: Langley, P. (ed.) Proc. the 17th Int. Conf. Machine Learning, Stanford, CA, pp. 359–366. Morgan Kaufmann, San Francisco (2000)
9. Duangsoithong, R., Windeatt, T.: Relevance and redundancy analysis for ensemble classifiers. In: Perner, P. (ed.) MLDM 2009. LNCS, vol. 5632, pp. 206–220. Springer, Heidelberg (2009)
10. Guyon, I., Aliferis, C., Elisseeff, A.: Causal feature selection. In: Liu, H., Motoda, H. (eds.) Computational Methods of Feature Selection, pp. 63–86. Chapman & Hall/CRC Press, Boca Raton (2007)
11. Guyon, I.: Causality workbench (2008), http://www.causality.inf.ethz.ch/home.php
12. Kudo, M., Sklansky, J.: Comparison of algorithms that select features for pattern classifiers. Pattern Recognition 33, 25–41 (2000)

13. Liu, F., Tian, F., Zhu, Q.: Bayesian network structure ensemble learning. In: Alhajj, R., Gao, H., Li, X., Li, J., Zaïane, O.R. (eds.) ADMA 2007. LNCS (LNAI), vol. 4632, pp. 454–465. Springer, Heidelberg (2007)
14. Liu, F., Tian, F., Zhu, Q.: Ensembling Bayesian network structure learning on limited data. In: Silva, M.J., Laender, A.H.F., Baeza-Yates, R.A., McGuinness, D.L., Olstad, B., Olsen, Ø.H., Falcão, A.O. (eds.) Proc. of the 16th ACM Conf. Inf. and Knowledge Management, Lisbon, Portugal, pp. 927–930. ACM, New York (2007)
15. Liu, H., Yu, L.: Toward integrating feature selection algorithms for classification and clustering. IEEE Trans. Knowledge and Data Engineering 17, 491–502 (2005)
16. Margaritis, D., Thrun, S.: Bayesian network induction via local neighborhoods. In: Solla, S.A., Leen, T.K., Müller, K.-R. (eds.) Proc. Neural Inf. Proc. Conf., Denver, CO., pp. 505–511. MIT Press, Cambridge (2000)
17. Pudil, P., Novovicova, J., Kittler, J.: Floating Search Methods in Feature Selection. Pattern Recognition Letters 15, 1119–1125 (1994)
18. Saeys, Y., Inza, I., Larranaga, P.: A review of feature selection techniques in bioinformatics. Bioinformatics 23, 2507–2517 (2007)
19. Spirtes, P., Glymour, C., Scheines, R.: Causation, prediction, and search. Springer, New York (1993)
20. Tsamardinos, I., Aliferis, C.F., Statnikov, A.: Time and sample efficient discovery of Markov blankets and direct causal relations. In: Getoor, L., Senator, T.E., Domingos, P., Faloutsos, C. (eds.) Proc. the 9th ACM SIGKDD Int. Conf. Knowledge Discovery and Data Mining, Washington DC, pp. 673–678. ACM, New York (2003)
21. Tsamardinos, I., Brown, L.E., Aliferis, C.F.: The max-min hill-climbing Bayesian network structure learning algorithm. Machine Learning 65, 31–78 (2006)
22. Wang, M., Chen, Z., Cloutier, S.: A hybrid Bayesian network learning method for constructing gene networks. J. Comp. Biol. and Chem. 31, 361–372 (2007)
23. Windeatt, T.: Accuracy/diversity and ensemble MLP classifier design. IEEE Trans. Neural Networks 17, 1194–1211 (2006)
24. Windeatt, T.: Ensemble MLP classifier design. In: Lakhmi, J.C., Sato-Ilic, M., Virvou, M., Tsihrintzis, G.A., Balas, V.E., Abeynayake, C. (eds.) Computational Intelligence Paradigms. SCI, vol. 137, pp. 133–147. Springer, Heidelberg (2008)
25. Witten, I.H., Frank, E.: Data mining: Practical machine learning tools and techniques. Morgan Kaufmann, San Francisco (2005)
26. Yu, L., Liu, H.: Efficient feature selection via analysis of relevance and redundancy. J. Machine Learning Research 5, 1205–1224 (2004)
27. Zhang, H., Sun, G.: Feature selection using tabu search. Pattern Recognition 35, 701–711 (2002)

Chapter 7
Learning Markov Blankets for Continuous or Discrete Networks via Feature Selection

Houtao Deng, Saylisse Davila, George Runger, and Eugene Tuv

Abstract. Learning Markov Blankets is important for classification and regression, causal discovery, and Bayesian network learning. We present an argument that ensemble masking measures can provide an approximate Markov Blanket. Consequently, an ensemble feature selection method can be used to learn Markov Blankets for either discrete or continuous networks (without linear, Gaussian assumptions). We use masking measures for redundancy and statistical inference for feature selection criteria. We compare our performance in the causal structure learning problem to a collection of common feature selection methods. We also compare to Bayesian local structure learning. These results can also be easily extended to other casual structure models such as undirected graphical models.

7.1 Introduction

Structure learning in Bayesian Networks is an important step for causal inference and Markov Blanket causal discovery algorithms can be helpful for learning the structure of Bayesian Networks. Here we argue that ensemble masking measures (applied in decision tree ensembles) can provide an approximate Markov Blanket. This result implies that an ensemble feature selection method can effectively learn Markov Blankets for either discrete or continuous networks. Thus, Markov Blanket learning can initialize a causal structure learning algorithm. In particular, the ensemble methods can be used in continuous network structure learning without the

Houtao Deng · Saylisse Davila · George Runger
Arizona State University Tempe, AZ
E-mail: {hdeng3,saylisse@asu.edu,george.runger}@asu.edu

Eugene Tuv
Intel, Chandler, AZ
E-mail: eugene.tuv@intel.com

O. Okun et al. (Eds.): Ensembles in Machine Learning Applications, SCI 373, pp. 117–131.
springerlink.com

strong linear, Gaussian assumptions. There are well-known contexts where the linear and Gaussian assumptions common in continuous Bayesian Networks (BN) do not hold (e.g, fMRI [17]). Mixed BNs provide other examples. The sensitivity of BN learning to linearity assumptions was described by [21]. Also, [16](LIMGAM) considered for the learning of causal structure, along with the inference in such models. More recent work by [7] indicated the importance of relaxed assumptions.

There are few studies that applied feature selection methods to learning causal structure in continuous networks. A linear regression model was extended by [10] to learn structure in a Gaussian undirected graph model. [13] applied SVM-RFE method to discover causal structure and proposed their methods for learning continuous Gaussian Bayesian Networks with linear causal relations. A more related work was by [2](C5C). C5C uses the features selected from C5.0 rules to identify Markov Blankets of a discrete Bayesian Network. However, the C5C algorithm still needs prior specification for the importance threshold. Furthermore, it is based on only one decision tree and the greedy nature of a single tree could lead to local optimum.

The masking measure relationship to approximate Markov Blanket learning suggests an ensemble-based feature selection method such as ACE [20] should be effective to initialize structure learning. Consequently, we compare a set of commonly used minimum relevancy, maximum redundancy feature selection methods to learn Markov Blankets in Bayesian Networks along with ACE. Therefore, the structure learning problem is studied under a collection of feature selection methods. We focus here on continuous learning experiments and illustrate performance without the common strong assumptions. A discrete network example illustrates that an ensemble-based method can also generalize to discrete networks. Finally, our work focuses on learning causal structure in Bayesian Networks. However, it can be easily extended to other causal graphical models such as undirected graphical models.

In Sect. 7.2 we describe the feature selection approach and provide an argument that a masking measure defines an approximate Markov Blanket. In Sect. 7.3 we provide experiments for local structure learning in continuous networks for both linear and nonlinear models and with and without Gaussian assumptions. We also provide an example for one discrete Bayesian network to illustrate that our method can generalize. Section 7.4 provides conclusions.

7.1.1 Learning Bayesian Networks Via Feature Selection

Let F be a full set of variables. Given a target variable Y, let $MB(Y) \subset F$ and $Y \notin MB(Y)$, $MB(Y)$ is said to be a Markov Blanket (MB) for Y if $Y \perp (F - MB)|MB$. That is, Y is conditionally independent of other features given MB.

An MB can be considered the objective of a feature selection algorithm. However, redundant features can replace others in a feature subset. In reality, it is not so straightforward to determine feature redundancy if a feature is partially correlated to a set of features.

An MB is important for learning a Bayesian network structure because an MB is useful for discovering the causal relationship of Y. Under certain conditions (faithfulness to a Bayesian network), MB(Y) is identical to Y's parents, its children, and its children's other parents (co-parents) [18]. Therefore, Markov Blanket causal discovery algorithms can be helpful for learning the structure of Bayesian networks. By [11], MB(Y) for all Y are identified first, and then MB(Y) are used to construct the Bayesian network of the domain. Algorithms (e.g., [18]) have been proposed for identifying Markov Blankets in a Bayesian network.

MB learning is also closely related to feature selection and [9] stated that MB is an optimal solution for a feature selection method. The MB definition is similar to the maximal relevancy and minimal redundancy principle used in [12], and [4]. There are common characteristics between current MB learning and feature selection algorithms. For example, the feature selection methods [4, 5], select relevant features in a forward phase and remove redundant features in a backward phase (similar to the two phases described in a Markov Blanket learning algorithm [18]).

Therefore, those feature selection methods maximizing relevancy and minimizing redundancy could be used for learning Markov Blankets and thus for learning causal structure in networks. [2] and [13] showed the advantages of feature selection methods over a Bayesian network learning algorithm for learning causal structure. Furthermore, most Bayesian network learning algorithms are designed to learn either networks with discrete variables or networks with continuous variables under the Gaussian-distribution, linear-relation assumptions. The ACE feature selection method used here can deal with mixed categorical and continuous variables free of distributions and relations [20]. Therefore, the method can be used to learn local causal structure in both discrete and continuous Bayesian Networks without any distribution and relation assumption.

Current feature selection approaches have been successfully used in ranking the importance of variables [1, 14] or selecting a maximal relevancy and minimal redundancy set [5, 12]. In classification and regression problems, it is well known that selecting a combination of most important individual features can not necessarily produce the best result. Therefore, a feature selection for purpose of supervised learning should be designed to maximize relevancy and minimize redundancy.

7.2 Feature Selection Framework

The framework of our method is outlined in Algorithm 1 (shown for a regression problem) and with notation summarized in Table 7.1. A similar algorithm applies to classification problems. Several iterations of feature selection are considered to include features important, but possibly weaker than a primary set. In each iteration only the important features are used to predict the target and generate residuals (targets minus model predictions for regression). In subsequent iterations the feature selection is applied to the residuals. However, all variables are input to the feature

selection module that builds the ensembles – not only the currently important ones. This is to recover partially masked variables that still contribute predictive power to the model. This can occur after the effect of a masking variable is completely removed, and the partial masking is eliminated. Based on important features, the redundancy elimination module selects a non-redundant feature subset. Brief comments for the functions *SelectFeatures* and *RemoveRedundant* are provided below and further details were provided by [20].

Table 7.1 Notation in Algorithm 1

Algorithm 1: Ensemble-Based Feature Selection

1. Set $\Phi \leftarrow \{\}$; set $F \leftarrow \{X_1, \ldots, X_M\}$; set $I = 0$ $(|I| = M)$
2. Set $[\hat{\Phi}, \Delta I] = SelectFeatures(F, Y)$
3. Set $\hat{\Phi} = RemoveRedundant(\hat{\Phi})$
4. If $\hat{\Phi}$ is empty, then quit
5. $\Phi \leftarrow \Phi \cup \hat{\Phi}$
6. $I(\hat{\Phi}) = I(\hat{\Phi}) + \Delta I(\hat{\Phi})$
7. $Y = Y - g_Y(\hat{\Phi}, Y)$
8. Go to 2.

F	set of original variables
Y	target variable
M	Number of variables
I	cumulative variable importance vector
Φ	set of important variables
ΔI	current vector of variable importance scores from an ensemble
$\Delta I(\hat{\Phi})$	current variable importance scores for the subset of variables $\hat{\Phi}$
$g_Y(F, Y)$	function that trains an ensemble based on variables F and target Y, and returns a prediction of Y

7.2.1 Feature Importance Measure

Relevant feature selection is based on an ensemble of decision tees. Trees handle mixed categorical and numerical data, capture nonlinear interactions, are simple, fast learners. Trees also provide intrinsic feature selection scores through split values. We briefly summarize here and details were provided for the ACE feature

selection algorithm by [20]. For a single decision tree the measure of variable importance is $VI(X_i,T) = \sum_{t \in T} \triangle I(X_i,t)$ where $\triangle I(X_i,t)$ is the impurity decrease due to an actual split on variable X_i at a node t of tree T. Impurity measure $I(t)$ for regression is defined as $\sum_{i \in t}(y_i - \bar{y})^2/N(t)$, where y_i is the response of observation i in node t, and $\bar{y}$ is the average response for all $N(t)$ observations in node t. For classification, $I(t)$ equals the Gini index at node t

$$\text{Gini}(t) = \sum_{i \neq j} p_i^t p_j^t, \tag{7.1}$$

where p_i^t is the proportion of observations with $y = i$ and i and j run through all target class values. The split weight measure $\triangle I(X_i,t)$ can be improved if out-of-bag (OOB) samples are used. The split value for the selected variable is calculated using the training data as usual. However, only the OOB samples are used to select the feature as the primary splitter. The experiments show that this provides a more accurate estimate of variable importance, and mitigates the cardinality problem of feature selection with trees [1] (where features with greater numbers of attributes values are scored higher by the usual metrics). Then, the importance score in a ensemble can be obtained by averaging over the trees

$$E(X_i) = \frac{1}{M} \sum_{m=1}^{M} VI(X_i, T_M). \tag{7.2}$$

Furthermore, a statistical criterion is determined through the use of artificial features (permutations of the actual features). Variable importance scores for actual features are compared to the distribution of scores obtained for the artificial features. Replicates of the ensembles are also used so that a statistical t-test can generate a p-value for the importance score of an actual feature. Further comments are provided below.

7.2.2 Feature Masking Measure and Its Relationship to Markov Blanket

Next we define a feature masking measure and argue the measure can be used to define an approximate Markov Blanket. An important issue for variable importance in tree-based models is how to evaluate or rank variables that were masked by others with slightly higher splitting scores, but could provide as accurate a model if used instead. One early approach in the CART methodology used surrogate splits [1]. The predictive association of a surrogate variable X^s for the best splitter X^* at a tree node T is defined through the probability that X^s predicts the action of X^* correctly and this is estimated as

$$p(X^s, X^*) = p_L(X^s, X^*) + p_R(X^s, X^*), \tag{7.3}$$

where $p_L(X^s, X^*)$ and $p_R(X^s, X^*)$ define the estimated probabilities that both X^s and X^* send a case in T left (right).

The predictive measure of association $\lambda(X^*|X^s)$ between X^s and X^* is defined as [20]:

$$\lambda(X^s|X^*) = \frac{min(\pi_L, \pi_R) - (1 - p(X^s, X^*))}{min(\pi_L, \pi_R)}, \tag{7.4}$$

where $\pi_L(\pi_R)$ are the proportions of cases sent to left(right) by X^*. Here $1 - p(X^s, X^*)$ measures the error using the surrogate X^s for X^*, $min(\pi_L, \pi_R)$ measures the error of the *naive* surrogate that assigns all cases according to $max(\pi_L, \pi_R)$. If $\lambda(X^s, X^*) < 0$, then X^s is disregarded as a surrogate for X^*. Sometimes a small, nonnegative threshold is used instead of 0.

Equation 7.4 only measures the association at a node; we now extend it to define a masking score as follows. Variable i is said to mask variable j in a tree, if there is a split in variable i in a tree with a surrogate on variable j. We define the masking measure for a pair of variables i, j in tree T as

$$M_{ij}(T) = \sum_{\{t \in T, split\ on\ X_i\}} w(X_i, t)\lambda(X_i|X_j), \tag{7.5}$$

where $w(X_i, t) = \Delta I(X_i, t)$ is the decrease in impurity from the primary split on variable X_i, and summation is done over the nodes where primary split was made on variable X_i. Here we take into account both the similarity between variables X_i, X_j at the node, and the contribution of the actual split of variable X_i to the model. For an ensemble the masking measure is simply averaged over the trees. Note that, in general, the measure is not symmetric in the variables, e.g., X_i may mask X_j, but the reverse may not be true (one variable may mask several others, but for a single selected masked variable the reverse may not be true).

In order to show that the masking measure corresponds to the Markov Blanket criterion, we now proceed to show that if masking is strong, that is, if the predictive measure of association λ approaches one, then excluding the masked variable has no effect on the conditional distribution of the target as measured by cross-entropy. Of course, this only determines conditional independence, which is weaker than the Markov Blanket condition, but can well be used to define an approximate Markov Blanket.

Now, it is intuitively sensible that masking variable X_i with globally high predictive association with masked variable X_j might be a good candidate for a Markov Blanket for X_j. We use expected KL-divergence $\delta(X_i|X_j)$ to estimate how close X_i is to being a Markov Blanket for X_j. Consider

$$\delta(X_i|X_j) = \sum_{x_i, x_j} Pr(X_i = x_i, X_j = x_j) \cdot D(Pr(C|X_i = x_i, X_j = x_j), Pr(C|X_i = x_i)), \tag{7.6}$$

where the KL-divergence $D(p, q)$ between two distributions p and q is defined as $\sum_{c \in C} p_c \log \frac{p_c}{q_c}$. In fact, it is easy to see that our masking measure between two

variables computed in a tree node behaves very similar to cross-entropy $\delta(X_i|X_j)$ locally. Specifically $\lambda(X_i|X_j) \to 1$ leads to $\delta(X_i|X_j) \to 0$.

Consider a case when node T has a stronger primary splitter X_i masking a surrogate X_j with a high predictive association $\lambda(X_i|X_j) \sim 1$. Then a four-node tree T^* with a split on X_i followed by splits on X_j locally approximates $P(C|X_i,X_j)$, and a four-node tree T^s with three splits using only X_i approximates $P(C|X_i)$. We will show that $\delta(X_i|X_j) \sim 0$. Because trees T^* and T^s have a common root split, it suffices to demonstrate $\delta(X_i|X_j) \sim 0$ between the left (or right) two-node subtrees of T^* and T^s, constructed using X_i and X_j splitters, correspondingly. For simplicity we keep the same notations T^* and T^s for the corresponding two-node subtrees, and assume that the root nodes of both T^* and T^s have n samples. Note that n samples could be partitioned in four disjoint sets: $n = n_{LL} + n_{LR} + n_{RL} + n_{RR}$ where n_{LL} is a number of samples sent by both X_i and X_j to the left nodes of T^* and T^s correspondingly; n_{LR} is a number of samples sent by X_i to the left node of T^*, but sent to the right node of T^s by X_j; n_{RL} and n_{RR} are defined in the same way. Let also n^*_{Lc} be a number of samples in T^* of class c sent to the left by X_i; quantities n^*_{Rc} , n^s_{Rc} ,n^s_{Lc} are defined similarly. Then

$$\delta(X_i|X_j) = \sum_{c=1}^{C} \left(\frac{n_{LL}}{n} \cdot \frac{n^*_{Lc}}{n} \log \frac{n^*_{Lc}}{n^s_{Lc}} + \frac{n_{RR}}{n} \cdot \frac{n^*_{Rc}}{n} \log \frac{n^*_{Rc}}{n^s_{Rc}} + \frac{n_{LR}}{n} \cdot \frac{n^*_{Lc}}{n} \log \frac{n^*_{Lc}}{n^s_{Rc}} + \frac{n_{RL}}{n} \cdot \frac{n^*_{Rc}}{n} \log \frac{n^*_{Rc}}{n^s_{Lc}}\right). \tag{7.7}$$

For the last two terms in Eq. (7.7) we see that

$$\frac{n_{LR}}{n} \cdot \frac{n^*_{Lc}}{n} \log \frac{n^*_{Lc}}{n^s_{Rc}} + \frac{n_{RL}}{n} \cdot \frac{n^*_{Rc}}{n} \log \frac{n^*_{Rc}}{n^s_{Lc}} \leq \frac{n_{LR}}{n} \cdot \log n + \frac{n_{RL}}{n} \cdot \log n$$

$$= \log n \cdot \left(1 - \frac{n_{LL} + n_{RR}}{n}\right) < log(n) \cdot (1 - \lambda(X_i|X_j)) \to 0 \; as \; \lambda \to 1$$

Denote n_{LLc} a subset of n_{LL} samples that belongs to class c, then for the first term in Eq. (7.7) we have $\frac{n_{LL}}{n} \cdot \frac{n^*_{Lc}}{n} \log \frac{n^*_{Lc}}{n^s_{Lc}} \leq \log \frac{n^*_{Lc}}{n^s_{Lc}} = \log \frac{n_{LLc}+n_{LRc}}{n_{LLc}+n_{RLc}}$, but $\max(n_{LRc}, n_{RLc}) \leq \max(n_{LR}, n_{RL}) \leq n_{LR} + n_{RL} = n - n_{RR} - n_{LL} \to 0$ as $\lambda \to 1$ hence, the upper bound for the first term $\log(n_{LLc} + n_{LRc})/(n_{LLc} + n_{RLc}) \to 0$ as $\lambda \to 1$ The same exact argument applies for the second term in Eq. (7.7), and therefore $\delta(X_i|X_j) \to 0$ as $\lambda(X_i|X_j) \to 1$.

We have just shown that the defined masking measure indeed corresponds to KL-divergence and thus provides an approximately optimal means to remove redundant variables based on the Markov Blanket criterion. We next describe an efficient algorithm to make use of the measure.

7.2.3 Statistical Criteria for Identifying Relevant and Redundant Features

For deleting irrelevant or redundant features, a threshold is needed. Artificial contrasts can be used to construct and specify the threshold in an efficient way. Let the number of variables be M. Denote the variables set as $S_X = \{X_j, j = 1,2,...K\}$. In each replicate $r, r = 1,2,...R$, artificial variables are generated as follows. For every variable X_j in S_X, a corresponding artificial variable Z_j^r is generated from randomly permutating values of X_j, let $S_Z^r = \{Z_j^r, j = 1,2,...K\}$. Then the new variables set can be denoted as $S_{X,Z}^r = \{S_X, S_Z^r\}$.

Consider relevant variables selection. Denote the importance score of $S_{X,Z}^r$ as $I_{X,Z}^r = \{I_X^r, I_Z^r\}$, where $I_X^r = \{I_{X_j}^r, j = 1,2,...M)\}$ and $I_Z^r = \{I_{Z_j^r}, j = 1,2,...K)\}$, $I_{X_j}^r$ and $I_{Z_j^r}$ are the importance scores of X_j and Z_j^r at the r^{th} replicate respectively. Denote $I_{X_j} = \{I_{X_j}^r, r = 1,2,...R\}$. Then $I_{X,Z}^r$ can be obtained by using relevant feature selection methods to $S_{X,Z}^r$. Denote I_α^r as the $1-\alpha$ percentile value of I_Z^r and $I_\alpha = \{I_\alpha^r, r = 1,2,...,R\}$. For each variable X_j, a paired t-test compares I_{X_j} to I_α. A test that results in statistical significance, i.e., a suitably small p-value, identifies an important variable. Therefore, an important variable here needs consistently higher score than the artificial variables over multiple replicates.

Consider redundancy elimination. Let M_{X_i,X_j}^r for $j = 1,2,...i-1,i+1,...,K$ and M_{X_i,Z_j}^r for $j = 1,2,...,K$ denote the masking score of X_i over X_j, and over Z_j^r for replicate $S_{X,Z}^r$ respectively. Denote $M_{X_i,\alpha}^r$ as the $1-\alpha$ percentile value of M_{X_i,Z_j}^r and $M_{X_i,\alpha} = \{M_{X_i,\alpha}^r, r = 1,2,...,R\}$. A paired t-test compares between M_{X_i,X_j}^r and $M_{X_i,\alpha}$. Variable X_j is masked by variable X_i if the outcome is significant.

7.2.4 Residuals for Multiple Iterations

A single iteration in Algorithm 1 can select a relevant and non-redundant feature set, but it may fail to detect some variables important but possibly weaker than a primary set. Thus more iterations are considered here. At the end of each iteration, a subset of features $\hat{\Phi}$ can be obtained. An ensemble model $g_Y(\hat{\Phi})$ is built on $\hat{\Phi}$. Denote $\hat{Y}$ as the OOB prediction of $g_Y(\hat{\Phi})$. Then residuals are calculated and form a new target. For a regression problem, the new target is simply formed by: $Y = Y - \hat{Y}$. For a classification problem, residuals are calculated from a multi-class logistic regression procedure. Log-odds of class probabilities for each class are predicted (typically a gradient boosted tree [3] is used), and then pseudo-residuals are taken as residuals.

In a Bayesian network sometimes non-causal, but relevant variables, can also contribute to the target. Though the contribution from those non-causal but relevant variables could be small compared to causal related variables, ACE adds them into the feature set. Therefore, false alarm rates might be increased. The Bonferroni correction is a multiple-comparison correction used when several statistical tests are performed simultaneously. The Bonferroni correction is used here to reduce the false positive rate. For example, if the p-value of t-test in the previous sections is α, when there are N features, the p-value is reduced to α/N.

7.3 Experiments

The work here focuses on continuous Bayesian Networks but we add an example from a discrete network that also illustrates that the method easily generalizes – the discrete networks results are equally good. We applied our method and the feature selection methods CFS [5], SVM-RFE [4], and FCBF [23] to learn the MB of the target nodes. The performance is also compared to a well-known Bayesian local structure learning algorithm (MMPC) [19]. In the experiments, ACE [20] is programmed in C, while RWeka [6, 22] and bnlearn [15] in R [8] are used to run the other algorithms. The default parameter setting for the methods in the software are used. To evaluate the performance of an algorithm, we measure the sensitivity and specificity for a given task. The sensitivity is the ratio of the number of correctly identified variables in the MB over the size of the true MB. The specificity is the ratio of the number of correctly identified variables as not belonging in the MB over the true number of variables not in MB [19]. To compare different algorithms, we follow the same terminology that was used by [19] and define a combined measure d:

$$d = \sqrt{(1 - \text{sensitivity})^2 + (1 - \text{specificity})^2}. \tag{7.8}$$

A better algorithm implies a smaller d value.

7.3.1 *Continuous Gaussian Local Structure Learning*

There are few available continuous benchmark causal-structure networks (the focus is on discrete networks). Therefore we simulated a causal-structure network with continuous nodes as shown Fig. 7.1. Bayesian structure learning often assumes Gaussian models whereas the ensemble-based ACE method is not limited to the such models. The first experiment uses the common Gaussian distributions for these experiments and a second experiment relaxes this assumption. Because FCBF and SVM-RFE (in RWeka [6, 22]) do not work with continuous target variables, only ACE, MMPC and CFS with best first search (CFSBestFirst) and gene search (CFSGene) are applied to this data.

Consider the network in Fig. 7.1. For the first experiment nodes A, B, C are root nodes and follow normal distributions N(1,1), N(2,1) N(3,1), respectively, where $N(\mu, \sigma^2)$ denotes a normal distribution with mean μ and variance σ^2. Denote a node (not a root node) as N_i, and denote the parent nodes of N_i as $N_i^p(j), j = 1, ..., |N_i^p|$, where $|N_i^p|$ is the number of parent nodes of N_i. The causal relation between N_i and $N_i^p(j)$ is expressed by $N_i = f(N_i^p(j))$. We considered $N_i = \sum_{j=1}^{|N_i^p|}(N_i^p(j)) + \varepsilon$ or $N_i = \prod_{j=1}^{|N_i^p|}(N_i^p(j)) + \varepsilon$ where $\varepsilon \sim N(0,1)$. Therefore, we can investigate both linear and nonlinear causal relationships in the network. For example, in Fig. 7.1, the linear causal relationship between node D and its parent nodes A, C is $D = A + C + \varepsilon$. The nonlinear causal relationship is $D = A * C + \varepsilon$. For each of the continuous Bayesian Networks, 5000 rows of data are simulated. The objective is to learn the MB of the output nodes.

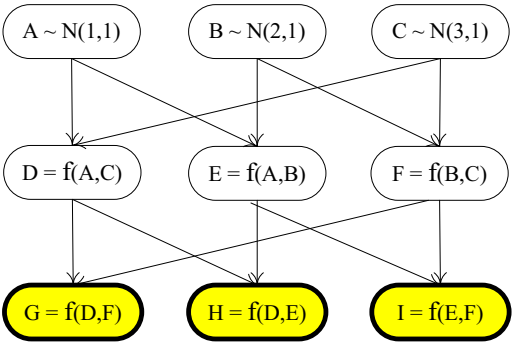

Fig. 7.1 Nodes with thick edges (yellow) are taken as targets. The function f is taken as either an additive or multiplicative function of the inputs.

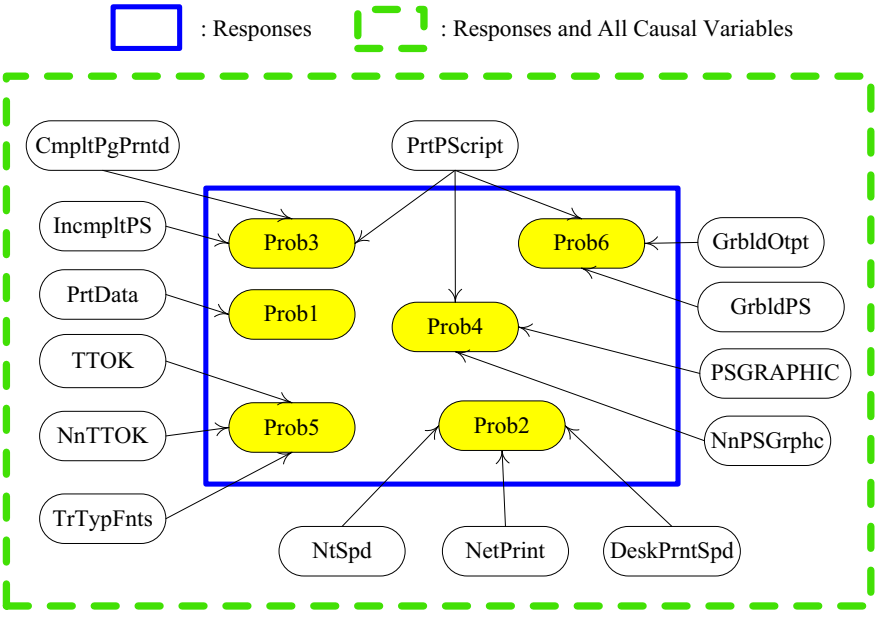

Fig. 7.2 Local structure of the Windows printer network with regard to targets

The sensitivity, specificity and combined measure d for the linear and non-linear cases are shown in Tables 7.2–7.4. For the linear Bayesian network, it is well known that linear relationships are not optimal for a tree representation, but well-suited for correlation-based methods. Still ACE has the lowest d value. The other three methods have the same d value. For the non-linear network the challenge of learning increases, and the d of all methods increase. ACE still produces the smallest d value.

Table 7.2 Sensitivity for each output node from different algorithms, learning continuous Gaussian linear and nonlinear Bayesian networks

	Linear				NonLinear			
	G	H	I	**Average**	G	H	I	**Average**
ACE	1.00	1.00	1.00	**1.00**	1.00	1.00	1.00	**1.00**
CFSBestFirst	1.00	1.00	1.00	**1.00**	1.00	1.00	0.50	**0.83**
CFSGene	1.00	1.00	1.00	**1.00**	1.00	1.00	1.00	**1.00**
MMPC	1.00	1.00	1.00	**1.00**	1.00	1.00	0.50	**0.83**

Table 7.3 Specificity for each output node from different algorithms, learning continuous Gaussian linear and nonlinear Bayesian networks

	Linear				NonLinear			
	G	H	I	**Average**	G	H	I	**Average**
ACE	1.00	1.00	0.83	**0.94**	1.00	0.67	1.00	**0.89**
CFSBestFirst	0.67	0.67	0.67	**0.67**	0.50	0.33	0.33	**0.39**
CFSGene	0.67	0.67	0.67	**0.67**	0.50	0.33	0.33	**0.39**
MMPC	0.67	0.67	0.67	**0.67**	0.00	0.67	0.17	**0.28**

Table 7.4 Combined measure d for each output node from different algorithms, learning continuous Gaussian linear and nonlinear Bayesian networks

	Linear				NonLinear			
	G	H	I	**Average**	G	H	I	**Average**
ACE	0.00	0.00	0.17	**0.06**	0.00	0.33	0.00	**0.11**
CFSBestFirst	0.33	0.33	0.33	**0.33**	0.50	0.67	0.83	**0.67**
CFSGene	0.33	0.33	0.33	**0.33**	0.50	0.67	0.67	**0.61**
MMPC	0.33	0.33	0.33	**0.33**	1.00	0.33	0.97	**0.77**

7.3.2 Continuous Non-Gaussian Local Structure Learning

For the non-Gaussian experiment the distributions for nodes A, B, C were changed to $Normal(0,1)$, $Exponential(1)$, $Uniform(-1,1)$ respectively. Other characteristics of the experiment (including the linear and nonlinear target functions) were the same as in the Gaussian case. The results are shown in Tables 7.5–7.7.

For both non-Gaussian linear and nonlinear networks, ACE is still better than the other three methods. CFSBestFirst outperforms MMPC in the non-Gaussian linear case, while they have similar performance in other cases. Consequently, feature selection methods can provide reasonable alternatives to the MMPC algorithm in continuous networks. Furthermore, it is more difficult for all methods to learn a nonlinear relationship than a linear relationship in the non-Gaussian cases.

Table 7.5 Sensitivity for each output node from different algorithms, learning continuous non-Gaussian linear and nonlinear Bayesian networks

	Linear				NonLinear			
	G	H	I	**Average**	G	H	I	**Average**
ACE	1.00	1.00	1.00	**1.00**	1.00	1.00	1.00	**1.00**
CFSBestFirst	1.00	1.00	1.00	**1.00**	0.00	0.00	0.50	**0.17**
CFSGene	1.00	1.00	1.00	**1.00**	0.00	0.00	0.50	**0.17**
MMPC	1.00	1.00	1.00	**1.00**	0.00	0.00	0.50	**0.17**

Table 7.6 Specificity for each output node from different algorithms, learning continuous non-Gaussian linear and nonlinear Bayesian networks

	Linear				NonLinear			
	G	H	I	**Average**	G	H	I	**Average**
ACE	1.00	1.00	0.67	**0.89**	0.50	0.50	0.33	**0.44**
CFSBestFirst	0.67	0.83	0.83	**0.78**	0.50	0.33	0.50	**0.44**
CFSGene	0.67	0.83	0.83	**0.78**	0.50	0.33	0.50	**0.44**
MMPC	0.50	0.50	0.67	**0.56**	0.50	0.33	0.50	**0.44**

Table 7.7 Combined measure d for each output node from different algorithms, learning continuous non-Gaussian linear and nonlinear Bayesian networks

	Linear				NonLinear			
	G	H	I	**Average**	G	H	I	**Average**
ACE	0.00	0.00	0.33	**0.11**	0.50	0.50	0.67	**0.56**
CFSBestFirst	0.33	0.17	0.17	**0.22**	1.12	1.20	0.71	**1.01**
CFSGene	0.33	0.17	0.17	**0.22**	1.12	1.20	0.71	**1.01**
MMPC	0.50	0.50	0.33	**0.44**	1.12	1.20	0.71	**1.01**

7.3.3 Discrete Local Structure Learning

Although our focus is continuous network structure, a discrete Bayesian network is also considered. The network is Windows printer trouble shooting with 76 features and 10,000 observations were generated with the GeNIe structural modeling tool (http://genie.sis.pitt.edu/). Due to limitations of space, only the local structure with regard to the targets of the network is illustrated in Fig. 7.2. Here 6 nodes (printer problem nodes) are considered as the targets (each with binary classes). ACE, MMPC, FCBF, CFSBestFirst, CFSGene, SVM-RFE are compared based on learning the local structure of the Bayesian networks. Because SVM-RFE requires the number of features to be selected as an input, we assign the number of features in two ways: the size of the correct Markov Blanket and the number of features

Table 7.8 Sensitivity of outputs from different algorithms learning the Windows printer network. SVM(MB) is given the correct number of features, and SVM(ACE) is given the number of features selected by ACE.

	Pro1	Prob2	Prob3	Prob4	Prob5	Prob6	**Average**
ACE	1.00	1.00	0.67	1.00	1.00	0.33	**0.833**
CFSBestFirst	1.00	1.00	0.67	1.00	0.67	0.67	**0.833**
CFSGene	1.00	1.00	0.67	0.67	1.00	1.00	**0.889**
FCBF	1.00	1.00	0.33	1.00	0.67	0.33	**0.722**
MMPC	1.00	1.00	0.33	0.67	1.00	0.33	**0.722**
SVM(ACE)	1.00	1.00	0.33	1.00	1.00	0.33	**0.778**
SVM(MB)	1.00	1.00	0.67	1.00	1.00	0.67	**0.889**

Table 7.9 Specificity of outputs from different algorithms learning the Windows printer network. SVM(MB) is given the correct number of features, and SVM(ACE) is given the number of features selected by ACE.

	Pro1	Prob2	Prob3	Prob4	Prob5	Prob6	**Average**
ACE	1.00	1.00	1.00	1.00	1.00	1.00	**1.000**
CFSBestFirst	0.89	0.97	0.96	0.96	0.94	0.93	**0.943**
CFSGene	0.66	0.81	0.76	0.85	0.75	0.81	**0.772**
FCBF	1.00	0.97	1.00	0.96	0.93	1.00	**0.977**
MMPC	1.00	0.96	1.00	0.99	0.97	1.00	**0.986**
SVM(ACE)	1.00	1.00	0.99	1.00	1.00	1.00	**0.998**
SVM(MB)	1.00	1.00	0.99	1.00	1.00	0.99	**0.995**

Table 7.10 Combined measure: d of outputs from different algorithms learning the Windows printer network. SVM(MB) is given the correct number of features, and SVM(ACE) is given the number of features selected by ACE.

	Pro1	Prob2	Prob3	Prob4	Prob5	Prob6	**Average**
ACE	0.00	0.00	0.33	0.00	0.00	0.67	**0.167**
CFSBestFirst	0.11	0.03	0.34	0.04	0.34	0.34	**0.199**
CFSGene	0.34	0.19	0.41	0.37	0.25	0.19	**0.292**
FCBF	0.00	0.03	0.67	0.04	0.34	0.67	**0.291**
MMPC	0.00	0.04	0.67	0.33	0.03	0.67	**0.289**
SVM(ACE)	0.00	0.00	0.67	0.00	0.00	0.67	**0.222**
SVM(MB)	0.00	0.00	0.33	0.00	0.00	0.33	**0.111**

selected by ACE. We refer the SVM-RFE with these two parameters as SVM(MB) and SVM(ACE), respectively. The results from the Windows printer trouble shooting network are shown in Tables 7.8–7.10.

For the Windows printer network, ACE and SVM(MB) have the lowest d values. SVM(MB) only outperforms ACE for the target Prob6. However, SVM(MB) is given the priori knowledge of the size of true MBs. With the number of variables selected by ACE as input, SVM(ACE) does not perform as well as ACE. Another feature selection method CFSBestFirst also provides better results than MMPC.

7.4 Conclusion

Structure learning is important for both discrete and continuous networks, and relaxed Gaussian assumptions are important for continuous networks. A relationship between ensemble masking and Markov Blankets is argued here and exploited for a generalized feature selection method to handle discrete and continuous cases for local structure learning. Common feature selection methods, along with a Bayesian structure algorithm, are compared for the structure learning problem, and experiments illustrate the strength of an ensemble-based feature selection approach in these cases.

Acknowledgements. This research was partially supported by ONR grant N00014-09-1-0656.

References

1. Breiman, L.: Random forests. Machine Learning 45, 5–32 (2001)
2. Frey, L., Fisher, D., Tsamardinos, I., Aliferis, C., Statnikov, A.: Identifying Markov blankets with decision tree induction. In: Proc. the 3rd IEEE Int. Conf. Data Mining, Melbourne, FL, pp. 59–66. IEEE Comp. Society, Los Alamitos (2003)
3. Friedman, J., Hastie, T., Tibshirani, R.: Additive logistic regression: A statistical view of boosting. Annals of Statistics 28, 832–844 (2000)
4. Guyon, I., Weston, J., Barnhill, S., Vapnik, V.: Gene selection for cancer classification using support vector machines. Machine Learning 46, 389–422 (2002)
5. Hall, M.A.: Correlation-based feature selection for discrete and numeric class machine learning. In: Langley, P. (ed.) Proc. the 17th Int. Conf. Machine Learning, Stanford, CA, pp. 359–366. Morgan Kaufmann, San Francisco (2000)
6. Hornik, K., Buchta, C., Zeileis, A.: Open-source machine learning: R meets Weka. Computational Statistics 24, 225–232 (2009)
7. Hoyer, P., Janzing, D., Mooij, J., Peters, J., Scholkopf, B.: Nonlinear causal discovery with additive noise models. In: Koller, D., Schuurmans, D., Bengio, Y., Bottou, L. (eds.) Advances in Neural Inf. Proc. Syst., pp. 689–696. MIT Press, Cambridge (2009)
8. Ihaka, R., Gentleman, R.: A language for data analysis and graphics. J. Comp. and Graphical Stat. 5, 299–314 (1996)
9. Koller, D., Sahami, M.: Toward optimal feature selection. In: Saitta, L. (ed.) Proc. the 13th Int. Conf. Machine Learning, Bari, Italy, pp. 284–292. Morgan Kaufmann, San Francisco (1996)
10. Li, F., Yang, Y.: Use modified lasso regressions to learn large undirected graphs in a probabilistic framework. In: Veloso, M.M., Kambhampati, S. (eds.) Proc. the 20th Natl. Conf. Artif. Intell. and the 17th Innovative Appl. Artif. Intell. Conf., Pittsburgh, PA, pp. 81–86. AAAI Press, MIT Press (2005)

11. Margaritis, D., Thrun, S.: Bayesian network induction via local neighborhoods. In: Solla, S.A., Leen, T.K., Müller, K.-R. (eds.) Advances in Neural Inf. Proc. Syst., pp. 505–511. MIT Press, Cambridge (2000)
12. Pudil, P., Kittler, J., Novovicová, J.: Floating search methods in feature selection. Pattern Recognition Letters 15, 1119–1125 (1994)
13. Pellet, J.P., Elisseeff, A.: Using Markov blankets for causal structure learning. J. Machine Learning Research 9, 1295–1342 (2008)
14. Robnik-Sikonja, M., Kononenko, I.: Theoretical and empirical analysis of relief and relieff. Machine Learning 53, 23–69 (2003)
15. Scutari, M.: Learning bayesian networks with the bnlearn R package. J. Stat. Software 35, 1–22 (2010)
16. Shimizu, S., Hoyer, P., Hyvärinen, A., Kerminen, A.: A linear non-gaussian acyclic model for causal discovery. J. Machine Learning Research 7, 2003–2030 (2006)
17. Tillman, R., Gretton, A., Spirtes, P.: Nonlinear directed acyclic structure learning with weakly additive noise models. In: Bengio, Y., Schuurmans, D., Lafferty, J., Williams, C.K.I., Culotta, A. (eds.) Advances in Neural Inf. Proc. Syst., pp. 1847–1855. MIT Press, Cambridge (2010)
18. Tsamardinos, I., Aliferis, C., Statnikov, A.: Algorithms for large scale Markov blanket discovery. In: Russell, I., Haller, S.M. (eds.) Proc. the 16th Florida Artif. Intell. Research Society Conference, St. Augustine, FL, pp. 376–381. AAAI Press, New York (2003)
19. Tsamardinos, I., Aliferis, C., Statnikov, A.: Time and sample efficient discovery of Markov blankets and direct causal relations. In: Getoor, L., Senator, T.E., Domingos, P., Faloutsos, C. (eds.) Proc. the 9th ACM SIGKDD Int. Conf. Knowledge Discovery and Data Mining, Washington DC, pp. 673–678. ACM, New York (2003)
20. Tuv, E., Borisov, A., Runger, G., Torkkola, K.: Feature selection with ensembles, artificial variables, and redundancy elimination. J. Machine Learning Research 10, 1341–1366 (2009)
21. Voortman, M., Druzdzel, M.: Insensitivity of constraint-based causal discovery algorithms to violations of the assumption of multivariate normality. In: Wilson, D., Lane, H.C. (eds.) Proc. the 21st Int. Florida Artif. Intell. Research Society Conf., Coconut Grove, FL, pp. 680–695. AAAI Press, New York (2008)
22. Witten, I.H., Frank, E.: Data mining: Practical machine learning tools and techniques. Morgan Kaufmann, San Francisco (2005)
23. Yu, L., Liu, H.: Efficient feature selection via analysis of relevance and redundancy. J. Machine Learning Research 5, 1205–1224 (2004)

Chapter 8
Ensembles of Bayesian Network Classifiers Using Glaucoma Data and Expertise

Stefano Ceccon, David Garway-Heath, David Crabb, and Allan Tucker

Abstract. Bayesian Networks (BNs) are probabilistic graphical models that are popular in numerous fields. Here we propose these models to improve the classification of glaucoma, a major cause of blindness worldwide. We use visual field and retinal data to predict the early onset of glaucoma. In particular, the ability of BNs to deal with missing data allows us to select an optimal data-driven network by comparing supervised and semi-supervised models. An expertise-driven BN is also built by encoding expert knowledge in terms of relations between variables. In order to improve the overall performances for classification and to explore the relations between glaucomatous data and expert knowledge, the expertise-driven network is combined with the selected data-driven network using a BN-based approach. An accuracy-weighted combination of these networks is also compared to the other models. The best performances are obtained with the semi-supervised data-driven network. However, combining it with the expertise-driven network improves performance in many cases and leads to interesting insights about the datasets, networks and metrics.

8.1 Improving Knowledge and Classification of Glaucoma

Glaucoma is the second most common cause of blindness worldwide [21], but its underlying mechanisms are still not clear. However, early treatment has been shown to slow the progression of the disease, thus early diagnosis is desirable [27]. To this purpose, several medical instruments available nowadays provide a large amount of anatomical and functional data, which can be exploited using statistical and A.I. techniques. Our study aims to set up and combine Bayesian Network (BNs) classifiers in order to obtain more precise early diagnosis of glaucoma and to learn insights from the models. BNs are models which seem to be appropriate for this issue,

Stefano Ceccon · Allan Tucker
Department of Information Systems and Computing, Brunel University,
Uxbridge UB8 3PH, London, UK
E-mail: {stefano.ceccon,allan.tucker@brunel.ac.uk}@brunel.ac.uk

O. Okun et al. (Eds.): Ensembles in Machine Learning Applications, SCI 373, pp. 133–150.
springerlink.com

being able to integrate different datasets and model expert knowledge in the field [20]. Moreover, their ability in handling missing data is very useful in the context of glaucoma, because no gold standard disease detection method is available. BNs are white-box models, so it is possible to look at the underlying relations of the model to improve knowledge in the field. BNs have already been successfully tested with glaucoma data in [23].

In the first stage of this study, two different BN models are obtained using the data (i.e. using the Advanced Glaucoma Intervention Study (AGIS) score [8] as the class variable), and imposing an expertise-driven network based on the anatomy of the optic nerve. The AGIS defect scoring system depends on the number and depth of clusters of adjacent depressed test sites in the visual field (VF) test STATPAC-2 analysis. The VF test aims to measure the functional ability of an eye by exposing different stimulus to different locations of the patient field and it's a routine test when screening for glaucoma. The anatomy-based network is obtained by modelling the relations between sectors of the optic nerve head (ONH) and the VF sectors as proposed by [11]. This is a widely used structure-function map which has been proved to be correlated with previous studies. The second stage of this study aims to combine the results of the two BN classifiers in order not only to maximize the results, but also to learn new insights about how the two different approaches interact. Two techniques are explored: a BN combiner with 3 nodes and a more classical weighted vote technique with accuracy-based weights. A BN combiner weighted on accuracy is also proposed. In the last part of the chapter the results of the different models are presented and discussed in terms of performance and qualitative outcome to better understand glaucoma and the associated clinical metrics.

8.2 Theory and Methods

In this section we will describe the datasets available and we will present the techniques used to obtain the BN models and the theory behind them. We will also analyse how the combination of a set of base classifiers can be used to increase the performances of the whole classification system.

8.2.1 Datasets

In this study two independent datasets were used (Table 8.1). Dataset A is a cross-sectional dataset of 78 early glaucomatous patients and 102 healthy control subjects. Inclusion criteria for early glaucomatous patients were Intraocular Pressure (IOP) greater than 21 mmHg and early VF defects on at least 3 occasions. Control subjects had IOP $<$ 21 mmHg and known to be healthy. Dataset B is a longitudinal dataset of 19 controls and 43 patients from Ocular Hypertensive Treatment group, who developed glaucoma in the time span observed. Initial eligibility criteria were in this case IOP $>$ 21 mmHg and negative VF test, and conversion was defined as positive AGIS score on 3 consecutive tests. Control subjects had negative VF test in 2 tests and IOP $<$ 21 mmHg.

Table 8.1 Characteristics of the datasets used in the study

	Dataset A	Dataset B
Control Subjects (values)	102 (102)	19 (155)
Converters (values)	78 (78)	43 (474)
Total Subjects (values)	180 (180)	62 (629)
Mean Age (controls)	67.6 (57.5)	65.7 (66.7)

Data consists of VF point sensibility obtained with Humphrey Field Analyzer II and retinal sector-based parameters data from Heidelberg Retina Tomograph (Fig. 8.1). Retinal data was pre-processed for both datasets by applying the 95% prediction interval MRA regression equation as indicated in [10], [25], which is a linear combination of Age, Optic Disc Area (ODA) and Retinal Rim Area (RRA) into one single parameter. Sensibility values were grouped in six sectors as suggested in [11] for computational and simplicity reasons in correspondence with retinal parameters.

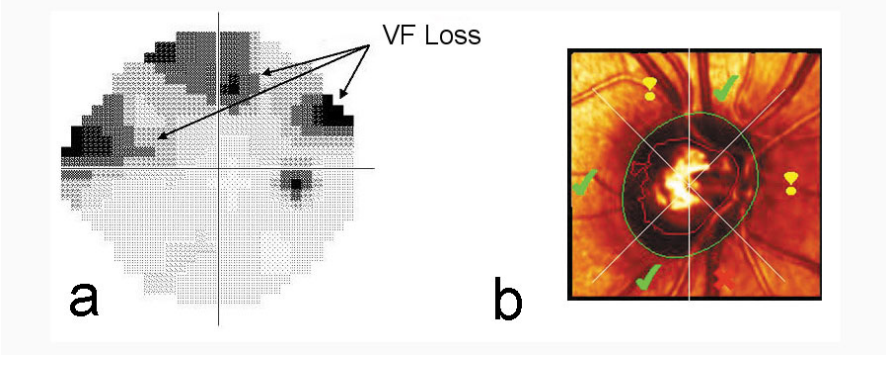

Fig. 8.1 (a) VF Test output for the right eye with VF Loss. (b) HRT output image showing the six sectors of the OD with defects on three sectors. VF pointwise data was grouped in six sectors consistently with [11].

8.2.2 Bayesian Networks

BNs are probabilistic directed graphical models in which each node represents a variable, and a lack of arcs between nodes represents a conditional independence assumption. The arcs are connected from a parent node to a child node and they must form a directed acyclic graph (DAG). In a DAG, there are no closed paths within the graph such that we can move from node to node along links following the direction of the arrows and end up back at the starting node (i.e. no directed cycles).

Each variable is associated with a conditional probability distribution (CPD), so that given the set of all CPDs in the network it is possible to infer about any value of any node. All together, the structure provides an efficient factorization of the joint probability

$$p(\mathbf{x}) = \prod_{i=1}^{n} p(x_i|\mathbf{pa_i}), \tag{8.1}$$

where pa_i are the parents of the node x_i (which denotes both node and variable) [14], [23].

For classification, BNs are used by selecting the most probable value of the class node (i.e. glaucomatous vs healthy) given the values observed for all the other nodes. To build a BN, the CPDs of all the variables need to be estimated from data. This is typically obtained using the Maximum Likelihood Estimation (MLE), which involves maximizing the likelihood of the data given the parameters. In case of missing data, however, this technique cannot be used. Therefore, the Expectation-Maximization algorithm (EM) was used for estimating the parameters in the unsupervised network. This technique iteratively estimates the hidden values for the unobserved data in the first step and maximizes the estimated likelihood function at the next step. When the algorithm converges to a local maximum, the parameters are estimated [4]. In addition, the structure of the network (i.e. the links between nodes) must be chosen: it can be either learned from the data or imposed using expert knowledge. For the former case, the learning algorithm used in this study was a Simulated Annealing (SA) technique, which is a quasi-greedy algorithm that searches through the space of possible structures to obtain the optimal structure [17]. The score used in the structure search is the Bayesian Information Criterion (BIC) score, which is a metric based on the likelihood of the observed data given the structure and the parameters, with a penalizing factor related to the number of parameters that aims to prevent overfitting. The searching algorithm was repeated 100 times using bootstrapping on the dataset [6]. This resampling technique has been widely used in order to reduce noise and obtain more robust results. It involves randomly sampling a subset from the dataset (with replacement) at each iteration. Bayesian Model Averaging was used on the learned structures in order to calculate the posterior probability for each arc as proposed in [7], i.e. by weighting each arc f on the network score in which it is present. Since calculation of the posterior probability on the whole set of possible structures is feasible only for tiny domains, an approximation is made by enumerating only over the learned set of structures (i.e. a set of optimal structures), as proposed by [19]. Thus, the formula used to estimate the relative mass of the structures in G that contains arc f given the data D is shown below:

$$P(f|D) \approx \frac{\sum_{G \in G} P(G|D) f(G)}{\sum_{G \in G} P(G|D)}, \tag{8.2}$$

where $f(G)$ is a binary function equal to 1 when the arc is present in the structure G, and $P(G|D)$ represents the posterior probability of each structure given the data D. The latter function can be calculated as the product of the likelihood of the data and

a prior over the structures, which was in this case assumed to be uniform. The arcs with the highest posterior probability were then selected to obtain the final structure.

8.2.2.1 Data-Driven Bayesian Networks

In the first stage of this study, two structures were learned using dataset A. The first structure was learned using the complete dataset A (Fig. 8.2), and the second was learned using only the control subjects in dataset A (Fig. 8.3). The rationale behind the second network is to model the healthy controls in order to avoid the potential bias introduced by the scoring metric AGIS. In fact, the AGIS score is based only on visual field tests and therefore a bias is introduced by supervising the learning process just on it [3],[12],[27]. Learning the network only on healthy subjects provides a more reliable framework, which can then be combined with the AGIS score by training the parameters of the network on AGIS labeled data. This approach can be seen as a form of semi-supervised learning based on control subjects using the AGIS score (which can be seen to accurately identify controls). From an informative point of view, both these networks are relevant as they can show how the variables interact in the disease process and in control subjects. The

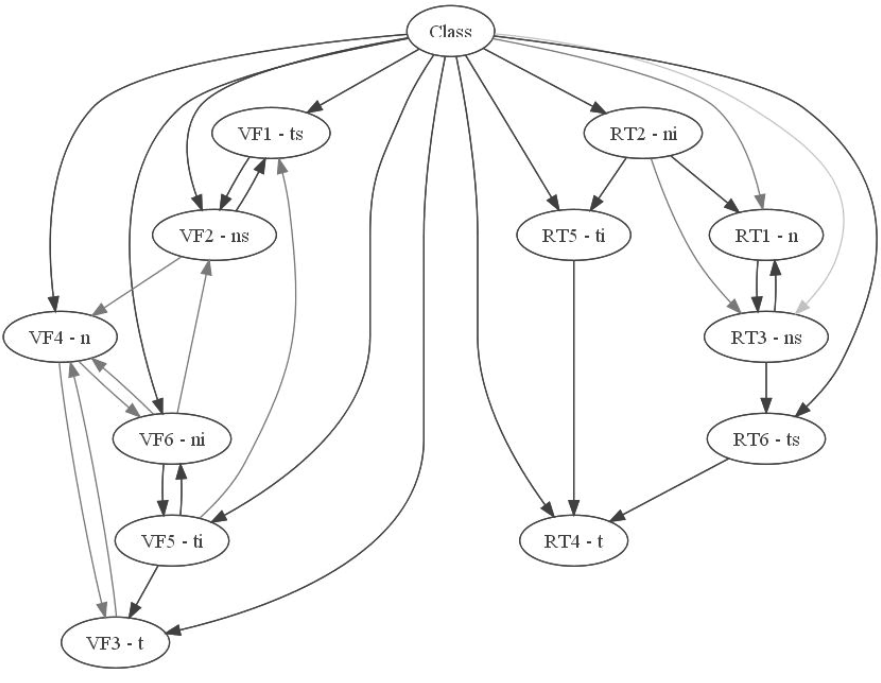

Fig. 8.2 Structure learned on dataset A using Simulated Annealing. Lighter arcs represent lower probabilities (black: $P>0.8$, dark gray: $0.6<P<0.8$, light grey: $0.4<P<0.6$). The identification name of each spatial sector is reported next to each variable name consistently with [11].

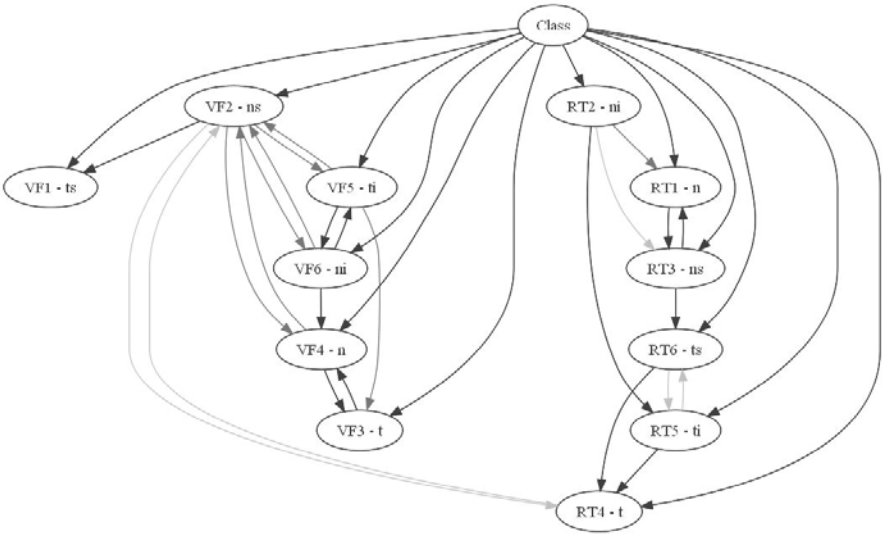

Fig. 8.3 Structure learned on dataset A using Simulated Annealing on controls subjects. Lighter arcs represent lower probabilities (black: $P>0.8$, dark gray: $0.6<P<0.8$, light grey: $0.4<P<0.6$). The identification name of each spatial sector is reported next to each variable name consistently with [11].

structures obtained show relevant differences which will be discussed in the next sections, however from a first glance it can be seen that the relations between the variables are substantially similar but there are some differences especially in the VF variables and in the links between VF nodes and RT nodes.

8.2.2.2 Expertise-Driven Bayesian Networks

The second stage of our experiments involved the exploration of expert knowledge modeling and its performance in classification. To this purpose, we modeled the relations shown in the structure-function map proposed in [11] imposing arcs between corresponding sector-based VF values and retinal values (Fig. 8.4). The retinal variables in this network were not pre-processed, i.e. the raw optic disc and rim size values were used instead of the MRA calculation. In fact, since we are imposing the structure, it's not needed to search and score the network. Therefore, more variables can be used in this case instead of a combination of them. Further, these raw variables could give more diversity in the results and actually shown to perform better than the pre-processed variables with the correspondent expertise-driven structure. The network was then trained on unsupervised data, in order to be independent on all clinical metrics. The aim of using this BN is to assess the different results obtained with a network based only on prior anatomical knowledge, and to explore whether it's possible to understand more about glaucoma and to improve classification performance together with the data-driven network.

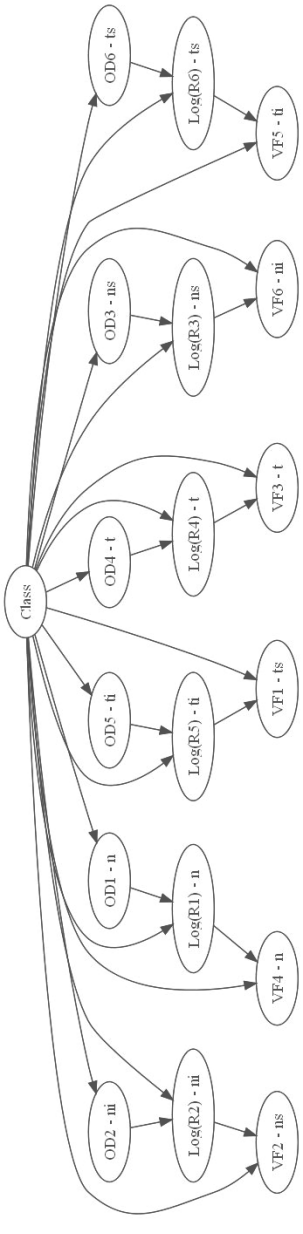

Fig. 8.4 Structure imposed based on expertise knowledge

8.2.3 *Combining Networks*

The natural next step was thus to combine the two networks described above, to exploit base classifier outputs and obtain the best performing and most illustrative results. In fact the data-driven networks seem to be better at excluding negative patients than the expertise based, whilst the latter seems to produce the most different results, having a higher sensitivity at low specificities. There is a broad literature on ensembles of classifiers [18], [22] and given the input available (i.e. probabilistic outputs from base BNs), a non-generative stacked structure ensemble was chosen [5]. Non-generative ensemble methods try to combine existing base classifiers, without acting on the base classifiers structure. Stacked ensembles use Machine Learning techniques on the top of the base learners, using their output as a set of input data for the final combiner. In particular, since the aim is not just in terms of performance but also in understanding how data and anatomy driven networks interacts to improve results, a BN model was chosen. This latter model was built using the base classifiers' outputs as input data for two input nodes linked to a third node, i.e. the final class node (Fig. 8.5a). This type of BN has been proved to be an effective combiner in [9], although improved performances can be obtained only if the individual classifiers disagree with each other [13]. For validation purpose, a combination of the outputs was also performed using a weighted voting approach[26]. The weights were adjusted in relation to the accuracy of the base networks.

A

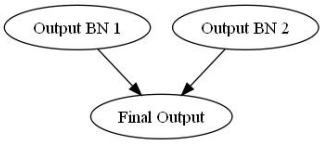

B

Low values → High values

Controls and AGIS BN discretized outputs ↓ High values	Anatomy-based BN discretized outputs							
	0.27	0.15	0.25	0.33	0.33	0.00	0.00	0.00
	0.47	0.33	0.09	0.64	0.50	0.43	0.40	0.00
	0.58	0.75	0.52	0.77	0.67	0.92	1.00	0.00
	1.00	0.60	0.80	0.89	0.85	0.95	0.73	1.00
	1.00	1.00	1.00	0.89	0.94	1.00	0.94	0.75
	1.00	1.00	1.00	1.00	1.00	1.00	0.94	0.79
	1.00	1.00	1.00	1.00	1.00	1.00	1.00	0.88
	0.00	0.00	1.00	1.00	1.00	1.00	1.00	1.00

Fig. 8.5 (a) Combining Bayesian Network. (b) Instance of a raw CPD of the class node. Each value represents the probability of positive output for each combination of base classifiers inputs (i.e. the final output of the combining network).

An optimized combining BN was also set up by weighting its output with the accuracy of the base networks. The probabilistic outputs are in this way biased towards the output provided by the most accurate base classifier.

8.3 Algorithms

The pseudo-code of the main algorithms used to obtain the results are here shown.

8.3.1 Learning the Structure

The SA-like learning algorithm used to obtain the data-driven base classifiers is represented by the following pseudo-code:

```
input init_temp, delta_temp, iterations, data

order = random(n)
Initialise structure(order)
temp = init_temp
result = structure

for i=1 : iterations
   score = score(structure)
   new_structure = operation(structure)
   new_score = score(new_structure)
   diff_score = new_score - score

   if new_score > score

       if new_score > score(result)
          result = new_structure
       end

       structure = new_structure

   elseif rand < exp(diff_score/temp)
       structure = new_structure
   end

   temp = temp * delta_temp

end
```

Here temp is the temperature factor which allows the algorithm to explore even non-optimal links, delta_temp is the "cooling" factor < 1 to decrease the temperature and result is the final output structure. To explore different structures 2100

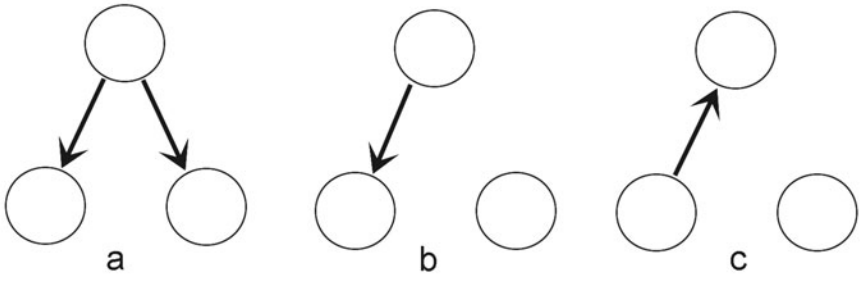

Fig. 8.6 Operations on the structure. a to b: deleting a link, b to c: swapping two nodes, b to a: adding a link

operations were carried by the algorithm, so that in each iteration a randomly chosen link was added, removed or two nodes were swapped (Fig. 8.6): an exhaustive search of the non-linked nodes is found and a link is implemented randomly at each iteration, a link is deleted by choosing it randomly from the available ones and two nodes are swapped without changing the structure of the network (i.e. the data vectors pointing to the node are swapped). Notice that the two different networks were obtained by using different portions of dataset A: in one case the full dataset and in the other only the control subjects. For the latter, the class node pointing to all nodes (i.e. a naive BN structure) was added only after learning.

8.3.2 Combining Two Networks

Once the networks were obtained, the combination with the data-driven and the expertise-based classifiers was obtained by building a third BN which was then imposed to combine the outputs from the other two networks (Fig. 8.5a). Each output was discretized in 8 states and then linked to a 2 states class node. As a result, an 8x8 matrix showing the interactions between the two networks was obtained by observing the CPD of the class node (Fig. 8.5b). In order to optimize the CPD, the matrix was then smoothed using a mean-filter window of size 3. The algorithm can be summarized as:

```
input Output_BN1 Output_BN2 data

discretize(Output_BN1)
discretize(Output_BN2)

Initialise structure
Learn_parameters(structure, data)

CPD = structure(ClassNode).CPD
smoothed_CPD = filter(CPD)
new_structure(ClassNode.CPD) = smoothed_CPD
```

Here BN1 and BN2 represent the two base classifiers' outputs and the CPD is the Conditional Probability Distribution of a node (Fig. 8.5b).

8.3.3 Optimized Combination

An optimized BN was also set up by weighting its output on the accuracy of the base classifiers on the training dataset. In particular, the following algorithm was applied to the final output of the combining BN:

```
input TestDataset output
                  output_BN1 output_BN2
                  accuracy_BN1 accuracy_BN2

align(accuracy_BN1,accuracy_BN2)

Weighted_output = (output_BN1 * accuracy_BN1 +
                   output_BN2 * accuracy_BN2) /
                   sum(accuracy_BN1, accuracy_BN2)

Final_output = mean(output, Weighted_output)

end
```

Here output is the output of the raw combining BN and the suffixes BN1 and BN2 on output and accuracy represent the two base classifiers outputs and accuracies. The align function aligns the base classifiers accuracies using the threshold values, in order to weight each base classifiers output on the corresponding accuracy for each threshold value on the testing dataset.

8.4 Results and Performance Evaluation

8.4.1 Base Classifiers

The base classifiers were compared using dataset A as a training set and dataset B as a testing set. As shown in Table 8.2, the BN model built using only the control subjects performed similarly to the model built using using all subjects. However, at high specificity, it outperformed the others. For glaucoma, which is a relative low frequency disease, high specificities are preferred. This reflects the higher weight put on the False Positive (FP) rate to minimize their occurrence. Therefore, the control-based BN was selected for combining with the expertise-driven classifier.

Another interesting result must be pointed out. Both learned structures show some interesting features which find correspondence in literature. Typical examples are a set of links between spatially adjacent variables and links from inferior temporal sectors (ti sector) to superior temporal sectors (ts sector) which proves the

Table 8.2 Performances of the base classifiers trained using dataset A and tested on dataset B

	AUROC	Sensitivity at 90% specificity	Sensitivity at 80% specificity
AGIS-supervised BN	0.85	0.68	0.82
Semi-supervised BN	0.85	0.71	0.80

hypothesis that early glaucomatous signs often occur on the arcuate sectors of the visual field and the optic nerve [2], [16]. The structure learned on the control subjects only aims to model relations in healthy subjects, which are therefore subject to less variability as the disease process is not present. As expected, more arcs were found with this approach, however substantially similar to those observed on the AGIS supervised structure. This can be explained as the presence of a class node in the AGIS based network learning process "explains away" the relations between sectors, by selecting the most informative relationships for classification as in a feature selection process. Therefore, some links may not be interesting for discrimination between controls and glaucomatous subjects and so they are not captured with this approach. For classification purpose, however, the best performing network is the controls supervised structure combined with AGIS score, which was then selected for combination with the expertise-driven network. This points out the importance to use a conservative approach (i.e. using the structure learned only on control subjects) in the classification of glaucoma.

8.4.2 Ensembles of Classifiers

Results of the ensemble of classifiers were evaluated and compared to base classifiers using 3-fold cross validation on dataset A and 6-fold cross validation on dataset B. Different folds reflect the different sizes of the datasets. The performance of the single and the combined networks are shown in Table 8.3 and Figs. 8.7-8.8. The same tests were performed considering only the pre-diagnosis data subset of dataset B, in order to take into account only patients "converting" to glaucoma. This led to results very similar qualitatively to those in Table 8.3.

Considering the overall performances on the complete datasets A and B, the semi-supervised data-driven BN performs better than the expertise-driven based one and is at least comparable to the combined ones. On dataset A, however, the performances of all the classifiers are comparable. Among the combined classifiers, the Weighted Vote is outperformed only at high specificities, but in dataset B it's outperformed by both the other combined networks. The BN combined networks perform well in both datasets, the accuracy weighted one being better on dataset A but worse on dataset B. Their performances were the best for higher specificities. Looking at the ROC curves in a particular test on dataset B (Fig. 8.7) it can be seen that the performances of the base semi-supervised data-driven BN are the

Table 8.3 Performances of different BNs tested in terms of mean AUROC and total errors at maximum accuracy and at 90% specificity

	Dataset A			Dataset B		
	AUROC	Errors	Errors at 90% spec	AUROC	Errors	Errors at 90% spec
Semi-Supervised BN	0.98	6	13	0.87	84	206
Expertise-Driven BN	0.98	7	13	0.75	110	326
Weighted Vote Combined	0.98	5	13	0.84	90	252
BN-based Combined	0.98	8	12	0.87	93	186
Accuracy Weighted BN	0.98	5	12	0.85	93	118

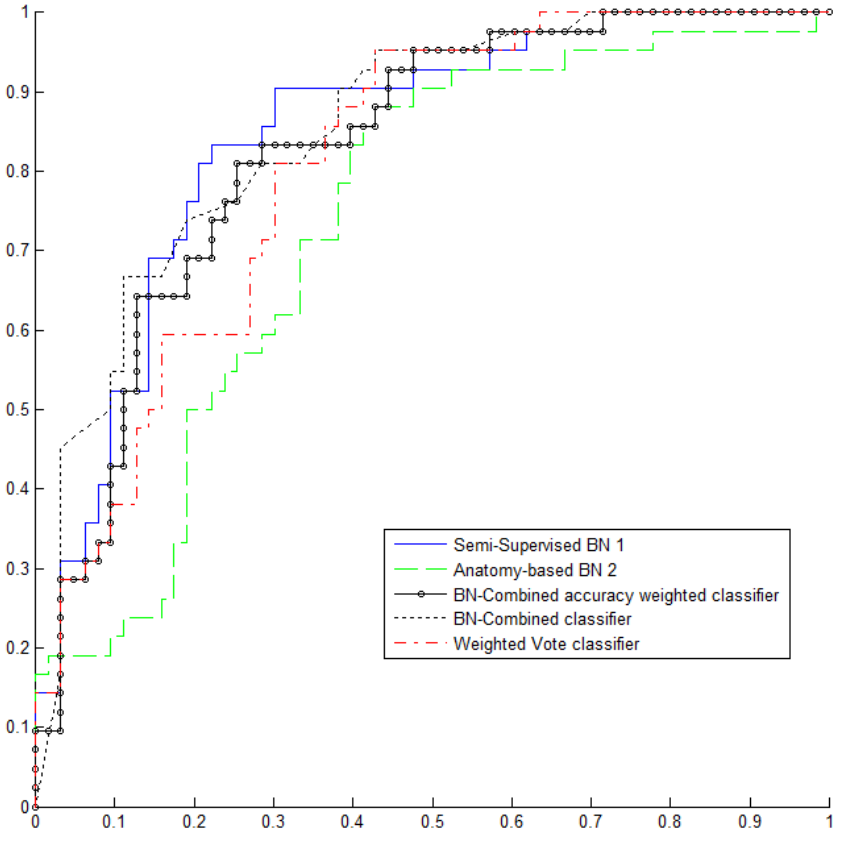

Fig. 8.7 ROC curves of classifiers in a test with 6-fold cross validation on dataset B

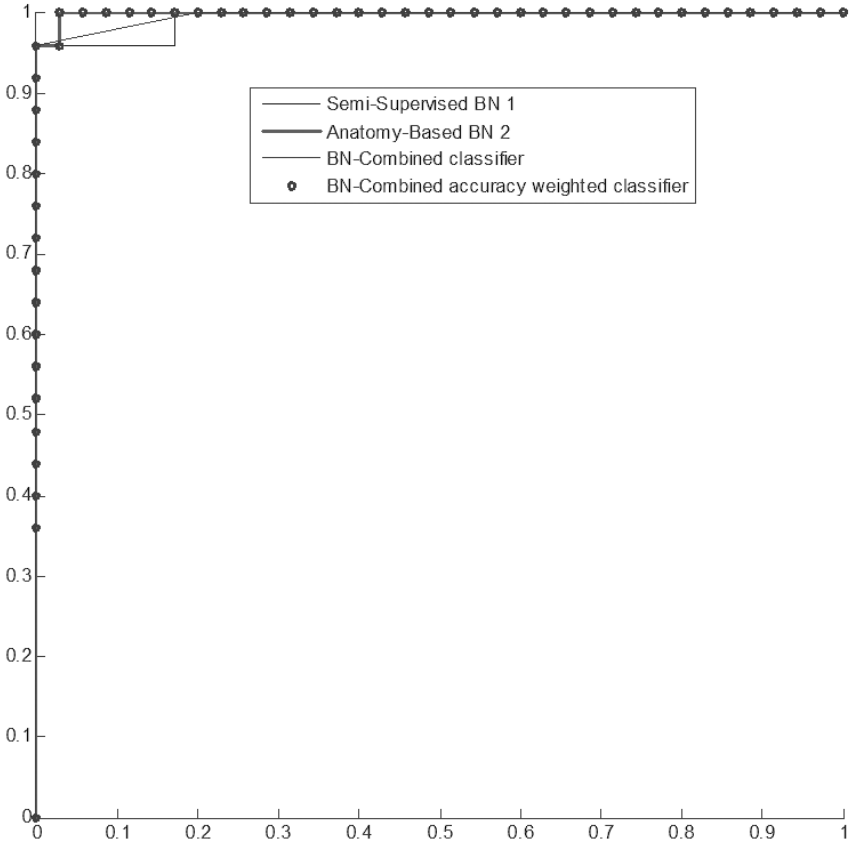

Fig. 8.8 ROC graph for a 3-fold cross validation test on dataset A

highest at mid-specificities. However, at higher specificity, the BN combined networks are comparable or outperform it, as shown also in Table 8.3. On dataset A the performance of the two base BNs are more similar and often the expertise-driven BN outperforms the other (Fig. 8.8). The Weighted Vote classifier performs better at low specificities as pointed out considering the total errors.

Between the two selected base classifiers and their combinations, the semi-supervised network is still clearly performing very well at all specificities. The conservative nature of AGIS metric score and the idea of modeling controls show the effectiveness of data and BNs in classification. However, the bias introduced by using AGIS score in the inclusion criteria and its unreliability must be kept in mind, especially for dataset B where conversion diagnosis is a more difficult task and it's defined using the AGIS score. The expertise-driven network on the other hand seems not to perform as well as the other. However, variability was found in the results

obtained, so that improvements in performances can be theoretically obtained with a combination of them. In fact, as pointed out in [24], diversity and accuracy of base classifiers are key factors for better performing ensembles of classifiers. diversity (and correlated independency) was obtained by using an unsupervised approach on the expertise-network. This consequently decreased the performances of the base classifier but increased those of the combined ones in many cases, especially at higher specificities.

Performances at different specificities are of great interest. The performances of the accuracy Weighted Vote classifier decrease when the specificity increases. This occurs also in the BN combining network weighted on the accuracy, as expected. On the other hand, the simple BN combining classifier is not biased toward the accuracy and this allows the classifier to outperform all the others at high specificities. In fact, looking at the ROC curves it can be seen that with an increase of accuracy of the anatomy-based network there is a decrease in performance of the accuracy weighted ones. In this particular case this is due to the expertise-driven network that doesn't outperform the other at any specificity. However, on dataset A, the opposite situation was observed. In Fig. 8.8 a ROC curve is shown for dataset A, showing the higher performances of the BN Accuracy-Weighted classifier with respect to the non-weighted one.

The higher number of total errors in Dataset A could therefore be explained by the differences in the datasets and the different performances on them: on dataset A the diversity between the results of the base classifiers is lower than in dataset B, leading to worse combined performance. Therefore, a single BN achieved strong results on dataset A (being more easy to classify), so that adding a weaker BN didn't lead to any improvement. This highlights the importance of choosing the most efficient base classifiers, and could lead to further study in generative ensembles of classifiers (i.e. active learning of base classifiers to improve diversity and accuracy of base classifiers) [15]. The difference in performances obtained with the two base classifiers and the two datasets points also out another key aspect about datasets and their combination. Data is very noisy due to the absence of a gold standard and to the high variability of the measurements [27], therefore a generalized algorithm that accords itself to the best performing network independently on the data is desirable. This seems not correctly obtained using accuracy weight, as the training and the testing dataset can be very different: considering an example, if dataset A is used to train an accuracy-based network and dataset B is used to test it, results will be insufficient as the accuracies are not similar for the same networks in both datasets. The idea here would be to use an independent dataset of the same type (cross-sectional or longitudinal) for training and testing: using cross-sectional data to build models used with longitudinal data is often not advisable [1]. Further, a broader search on both datasets for a network that shows more accurate and "diverse" performances than the other could lead in this case to better results for both datasets.

An interesting advantage offered by the BN combining classifiers is the possibility to observe at the CPD for the class node. This gives us interesting insights about how the network works and how the two outputs combine to obtain better results. In Fig. 8.5b a CPD is shown: for each discretized value of the base classifiers a

probability is learned from the data and can be observed. This reflects the output of the final classifier, in particular, the probability of diagnosis of glaucoma for each combination of inputs. Observing the CPDs obtained in an instance of a CPD in Fig. 8.5b, it can be seen that the matrix is slightly skewed towards the bottom-left, i.e. there are more higher probabilities in the bottom-left half than in the other. This shows that the AGIS semi-supervised network is more reliable at high specificities. For example, for all values of the expertise-driven network, if the data-driven network's output is low then the combined output will be low. It must also be noticed that for lower values of the data-driven base network (e.g. value 3), the output of the expertise-driven network increases the probability of glaucoma sensibly, adding its knowledge to the result. Some 0 values are obtained in the corners of the matrix due to the lack of data for these combinations of outputs: these cells are smoothed with the mean-filter application. Several different instances of this matrix have been found in this study, showing again variability between different datasets used. Thus, the exploration of the CPD of the combined network confirms the higher performances at high specificity of semi-supervised data-driven network, but also gives a quantitative measure of the improvement that each single base classifier brings to the final output. Further study using this approach will be carried in the future, for example by acting on the CPDs or averaging on them, as well as using different discretization and more complete datasets.

In conclusion, this preliminary study has shown the possibilities of using BNs for classification and exploration of different datasets in a real problem. Data-driven BN classifier outperformed the expertise-driven one, even if with different magnitude on different datasets. Combining networks have been shown to be both effective in terms of performances and illustrative. In particular, the performances of the combined classifier seem to be better for datasets with more different results for the base classifiers. Given the issues of the datasets, the idea of using simulated data for future work could give a start to more deep analysis of BNs potential in modeling data and combining classifiers, keeping in mind the importance of an effective choice of the base classifiers.

References

1. Artes, P.H., Chauhan, B.C.: Longitudinal changes in the visual field and optic disc in glaucoma. Progress in Retinal and Eye Research 24, 333–354 (2005)
2. Bowd, C., Zangwill, L.M., Medeiros, F.A., Tavares, I.M., Hoffmann, E.M., Bourne, R.R., Sample, P.A., Weinreb, R.N.: Structure-function relationships using confocal scanning laser ophthalmoscopy, optical coherence tomography, and scanning laser polarimetry. Investigative Ophthalmology & Visual Science 47, 2889 (2006)
3. Chauhan, B.C., Drance, S.M., Douglas, G.R.: The use of visual field indices in detecting changes in the visual field in glaucoma. Investigative Ophthalmology & Visual Science 31, 512 (1990)

4. Dempster, A.P., Laird, N.M., Rubin, D.B.: Maximum likelihood from incomplete data via the em algorithm. J. the Royal Stat. Society. Series B (Methodological) 39, 1–38 (1977)
5. Duin, R., Tax, D.: Experiments with classifier combining rules. In: Kittler, J., Roli, F. (eds.) MCS 2000. LNCS, vol. 1857, pp. 16–29. Springer, Heidelberg (2000)
6. Efron, B., Tibshirani, R., Tibshirani, R.J.: An introduction to the bootstrap. Chapman & Hall/CRC Press, Boca Raton (1993)
7. Friedman, N., Koller, D.: Being Bayesian about network structure: A Bayesian approach to structure discovery in Bayesian networks. Machine Learning 50, 95–125 (2003)
8. Gaasterland, D.E., Ederer, F., Sullivan, E.K., Caprioli, J., Cyrlin, M.N.: Advanced glaucoma intervention study: 2. visual field test scoring and reliability. Ophthalmology 101, 1445–1455 (1994)
9. Garg, A., Pavlovic, V., Huang, T.S.: Bayesian networks as ensemble of classifiers. In: Proc. the 16th Int. Conf. Pattern Recogn., Quebec, Canada, pp. 779–784. IEEE Comp. Society, Los Alamitos (2002)
10. Garway-Heath, D.F.: Moorfields regression analysis. The Essential HRT Primer. Jocoto Advertising, San Ramon (2005)
11. Garway-Heath, D.F., Poinoosawmy, D., Fitzke, F.W., Hitchings, R.A.: Mapping the visual field to the optic disc in normal tension glaucoma eyes. Ophthalmology 107, 1809–1815 (2000)
12. Goldbaum, M.H., Sample, P.A., White, H., Colt, B., Raphaelian, P., Fechtner, R.D., Weinreb, R.N.: Interpretation of automated perimetry for glaucoma by neural network. Investigative Ophthalmology & Visual Science 35, 3362 (1994)
13. Hansen, L.K., Salamon, P.: Neural network ensembles. IEEE Trans. Pattern Analysis and Machine Intell. 12, 993–1001 (1990)
14. Heckerman, D.: A tutorial on learning with Bayesian networks. Tech. Report, Microsoft Research (1995)
15. Jacobs, R.A., Jordan, M.I., Nowlan, S.J., Hinton, G.E.: Adaptive mixtures of local experts. Neural Comp. 3, 79–87 (1991)
16. Johnson, C.A., Sample, P.A., Zangwill, L.M., Vasil, C.G., Cioffi, G.A., Liebmann, J.R., Weinreb, R.N.: Structure and function evaluation (SAFE): II. Comparison of optic disk and visual field characteristics. American J. Ophthalmology 135, 148–154 (2003)
17. Kirkpatrick, S., Gelatt, C.D., Vecchi Jr., M.P.: Optimization by simulated annealing. Science 220, 671 (1983)
18. Kittler, J.: Combining classifiers: A theoretical framework. Pattern Analysis & Appl. 1, 18–27 (1998)
19. Madigan, D., Raftery, A.E.: Model selection and accounting for model uncertainty in graphical models using Occam's window. J. the American Stat. Association 89, 1535–1546 (1994)
20. Pearl, J.: Probabilistic reasoning in intelligent systems: Networks of plausible inference. Morgan Kaufmann, San Francisco (1988)
21. Resnikoff, S., Pascolini, D., Etya'ale, D., Kocur, I., Pararajasegaram, R., Pokharel, G.P., Mariotti, S.P.: Global data on visual impairment in the year 2002. Bulletin of the World Health Organization 82, 844–851 (2004)
22. Sharkey, A.J.C.: On combining artificial neural nets. Connection Science 8, 299–314 (1996)
23. Tucker, A., Vinciotti, V., Liu, X., Garway-Heath, D.: A spatio-temporal Bayesian network classifier for understanding visual field deterioration. Artif. Intell. Medicine 34, 163–177 (2005)

24. Valentini, G., Masulli, F.: Ensembles of learning machines. In: Marinaro, M., Tagliaferri, R. (eds.) WIRN 2002. LNCS, vol. 2486, pp. 3–20. Springer, Heidelberg (2002)
25. Wollstein, G., Garway-Heath, D.F., Hitchings, R.A.: Identification of early glaucoma cases with the scanning laser ophthalmoscope. Ophthalmology 105, 1557–1563 (1998)
26. Woods, K., Bowyer, K., Kegelmeyer Jr., W.P.: Combination of multiple classifiers using local accuracy estimates. In: Proc. 1996 IEEE Comp. Society Conf. Comp. Vision and Pattern Recogn., San Francisco, CA, pp. 391–396. IEEE Comp. Society, Los Alamitos (1996)
27. Yanoff, M., Duker, J.S.: Ophthalmology. Mosby, St. Louis (2003)

Chapter 9
A Novel Ensemble Technique for Protein Subcellular Location Prediction

Alessandro Rozza, Gabriele Lombardi, Matteo Re, Elena Casiraghi, Giorgio Valentini, and Paola Campadelli

Abstract. In this chapter we present an ensemble classifier that performs multi-class classification by combining several kernel classifiers through Decision Direct Acyclic Graph (DDAG). Each base classifier, called K-TIPCAC, is mainly based on the projection of the given points on the Fisher subspace, estimated on the training data, by means of a novel technique. The proposed multiclass classifier is applied to the task of protein subcellular location prediction, which is one of the most difficult multiclass prediction problems in modern computational biology. Although many methods have been proposed in the literature to solve this problem all the existing approaches are affected by some limitations, so that the problem is still open. Experimental results clearly indicate that the proposed technique, called DDAG K-TIPCAC, performs equally, if not better, than state of the art ensemble methods aimed at multi-class classification of highly unbalanced data.

Keywords: Bioinformatics, protein subcellular location prediction, Fisher subspace, ensemble of classifiers.

9.1 Introduction

A cell is composed by different components, such as nucleus, mitochondrion, Golgi apparatus, endoplasmic reticulus, that correspond to different 'subcellular locations'. The primary engines of these tasks are the protein molecules, that are complex and long sequences of 20 different amino acid residues, distributed inside the cell according to their role. Since many different protein molecules are present in one or more subcellular locations, a better understanding of their location, distribution, and function is advisable to understand the complex biological systems that regulate the biological life of each cell.

Alessandro Rozza · Gabriele Lombardi · Matteo Re · Elena Casiraghi · Giorgio Valentini · Paola Campadelli
Dipartimento di Scienze dell'Informazione, Università degli Studi di Milano,
Via Comelico 39-41, 20135 Milano, Italy
E-mail: rozza@dico.unimi.it,
http://security.dico.unimi.it/∼fox721/

O. Okun et al. (Eds.): Ensembles in Machine Learning Applications, SCI 373, pp. 151–167.
springerlink.com

To this aim, the first and fundamental problem to be solved is the protein subcellular localization. To solve this problem, in the field of biochemical research various biochemical experiments have been settled; although effective, these methods are both costly and time-consuming. Furthermore, thanks to the fast advances in genomics new proteins are continuously discovered, so that the gap between the newly found protein sequences and the knowledge about their subcellular location increases. A solution to this bottleneck, which would allow to exploit the information provided by the newly discovered proteins, is an efficient automatic method for protein subcellular location prediction.

This problem can be formulated as a multi-class classification problem as follows. The training dataset, $\mathscr{P}_{Train}$, is composed of N protein vectors, $\mathscr{P}_{Train} = \{\mathbf{p}_i\}_{i=1}^{N}$, where each protein sequence can be represented as a vector $\mathbf{p} = [R_s^j]$, R_s^j being the amino acid residue whose ordered position in the sequence is $s \in \{1..S\}$ (S is the protein length, which differs in each protein), while the superscript $j \in \{1..20\}$ indicates which native amino acid is present in the s^{th} position of the sequence. The proteins in $\mathscr{P}_{Train}$ are classified into M subsets $\mathscr{P}_{Train} = \bigcup_{i=1}^{M} \mathscr{S}_i$, where each subset, $\mathscr{S}_m$ ($m \in \{1..M\}$), is composed of proteins with the same subcellular component, and the cardinality of $\mathscr{P}_{Train}$ is $|\mathscr{P}_{Train}| = N = N_1 + N_2 + \cdots + N_M$. The classifier's aim is to learn the information provided by $\mathscr{P}_{Train}$ to predict the subcellular location of a query protein $\mathbf{p}_q$.

In the past decade many authors have tried to handle this problem, and several classification methods have been proposed [12]. Nevertheless, the problem is still open due to several difficulties that make the task of protein subcellular location prediction quite challenging. At first, the protein data are usually codified with high dimensional vectors, so that the employed classifiers should be designed in order to minimize the computational complexities. Secondly, the number of subcellular locations considered in literature is about 20, and some proteins, called multiplex proteins, might be present in more than one cellular component, or they might move from one location to another. Finally, the protein subcellular distribution is highly unbalanced since some cellular components contain a significantly lower number of protein molecules.

To achieve satisfactory results in such (multiclass, high dimensional, and highly unbalanced) classification problem, a dataset of high cardinality is needed. Unfortunately at the present, for some subcellular location, the training datasets have a limited number of proteins, due to the following reasons: some proteins must be discarded since they contain less than 50 amino acids, or they are annotated as 'fragments'; to avoid homology bias proteins with $\geq 25\%$ sequence identity to any other in the same subcellular organelle must be eliminated; proteins belonging to components with less than 20 proteins are generally excluded because of lacking statistical significance; several proteins cannot be used as robust data for training a solid predictor since they have not been experimentally annotated yet. Finally, further deletions might be performed by some authors focusing on proteins with a unique subcellular location, or belonging to a specific organism.

These difficulties motivate the great deal of research work that has been devoted to the task of protein location prediction. In Sect. 9.2 we recall some state of the art

approaches that achieve promising results by coupling different protein representation methods with different learning algorithms, and eventually combine them to create ensemble classifiers. Nevertheless, noting that all these approaches are computationally expensive and they are often badly affected by unbalanced datasets with low cardinalities, which are so common in the bioinformatics field, in this paper we propose our efficient ensemble classifier technique.

The engine predictor at the basis of the ensemble classifier, called K-TIPCAC (see Sect. 9.3.1) is an extension of the originally proposed K-IPCAC algorithm [32], which projects the points on the Fisher subspace estimated on the training data. The ensemble method, described in Sect. 9.4, combines the results computed by different K-TIPCAC predictors through a DDAG technique [31].

Experimental results and the comparison to existing techniques, reported in Sect. 9.5 and Sect. 9.6, demonstrate both the effectiveness and the efficacy of the proposed ensemble classifier.

9.2 Related Works

The task of protein subcellular location prediction has gained a wide interest in the latest twenty years, and several research works have been proposed; they can be grouped according to either the data representation method, or the employed learning algorithm.

As explained in the previous section each protein molecule can be represented as a vector $\mathbf{p} = [R_1^j, R_2^j, R_3^j, \cdots, R_s^j]$, where $s \in \{1..S\}$ is the sequence order, S is the protein length, and $j \in \{1..20\}$ indicates which of the 20 native amino acids is located in the s^{th} position. A straightforward way to represent a protein $\mathbf{p}$ is to employ a vector representing its entire amino acid sequence, since this representation provides the most exhaustive description of the molecule; however, this protein coding method has the drawback of being too long, and it has proved to be misleading when the unknown proteins have not significant homology to the training proteins. Furthermore, since each protein is composed by a different number of amino acids, the training system should treat data vectors of different dimensionality.

A more compact representation is provided by the amino acid composition (AAC) protein descriptor [6], which is a 20 dimensional vector $\mathbf{p} = [f_1, \cdots, f_{20}]$ whose elements are the normalized occurrence frequencies of the 20 native amino acids. Although the AAC has been widely used for predicting several protein attributes, such as the structural class, it lacks the ability of representing the sequence order effects, that affect both the secondary and the tertiary protein structures and obviously motivate the protein structure, function, and location. A protein coding model built to capture the relations among contiguous amino acids is the pseudo-amino acid composition (PseAAC) protein model [8]; PseAAC encodes each protein with a $(20+\lambda)$ dimensional vector $\mathbf{p} = [p_1, \cdots, p_{20}, p_{20+1}, \cdots, p_{20+\lambda}]$, where the first 20 elements are associated with the AAC, while the following λ components are the correlations between all of the λ most contiguous residues. Some authors [22, 26, 27] employ a similar protein representation, the k-peptide encoding vector, which is the

normalized occurrence of the k-letter pattern that appears in a window being shifted along the sequence. Another protein representation mode, the sequential evolution (SeqEvo) protein representation [14], exploits the PseAAC coding scheme to represent the changes in the protein sequence (that are insertions, deletions, substitutions of amino acid residues) that are due to protein evolutions. More precisely, for each native amino acid, the normalized occurrence of its changes is computed, and the 20 dimensional vector thus obtained is then processed by utilizing the PseAAC scheme to recover the sequence order information.

The preceding protein representation schemes are all strictly based on the protein amino acid sequence. Different methods investigate the usage of physico-chemical properties for protein representation [1], but the achieved performances are lower than those obtained by other techniques based on protein annotations in different databases.

Among these techniques, the two protein representation models that seem to produce the most satisfactory results are the Functional domain (FunD) protein model [9] and the Gene ontology (GO) protein representation [10]. According to the content of FunD it is possible to code each protein in the form of a boolean vector indicating the presence/absence of any of the 7785 functional protein domains annotated in the database and a similar encoding scheme can be adopted by considering the annotations stored in the Cellular Component division of the Gene Ontology.

Although experiments reported in [14] prove that proteins defined in the FunD and GO space can be clustered in such a way that better reflects their subcellular location, both the FunD and the GO descriptors cannot encode all the proteins since some proteins might not be annotated in these databases. Therefore, hybrid combinations of protein representation models have been presented by researchers in the field, so that proteins that cannot be represented by one model are represented by the others. More precisely, at the state of the art the FunD-PseAA model [5], the GO-FunD-PseeAA model [10], the GO-PseAA model [11], and the GO-FunD-SeqEvo model [14] have been employed for protein subcellular localization. All the techniques, using hybrid protein representations, choose a learning algorithm to train one predictor for each protein representation, and exclusively combine them. More precisely, when a new protein is processed, if it can be represented with the FunD or GO representation mode the corresponding predictor takes the decision, otherwise the other predictors are used.

To the aim of exploiting the information carried by the training set, different classification algorithms have been proposed, which are briefly resumed below.

The covariant discriminant (CD) algorithm [7, 8] exploits a similarity function, based on the Mahalanobis distance, to compute the distance between $\mathbf{p}$ and the standard (mean) vectors of each training subset, $\bar{\mathbf{p}}_m = \langle \mathbf{p} \in \mathscr{S}_m \rangle$, where $\langle \cdot \rangle$ is the mean operator; $\mathbf{p}$ is then assigned to the subcellular location of the mean vector achieving the maximum similarity.

Methods employing the K-nearest-neighbor(KNN) technique [16] and its modified versions have also been presented [5, 27, 35]. These methods classify a protein $\mathbf{p}$ as belonging to the subcellular component containing the maximum number of the

K nearest neighbors of **p**. Usually the distance functions to compute the neighbors are the Euclidean distance, the Hamming distance, the Mahalanobis distance, and a distance function based on the normalized dot product. Due to the promising performance achieved by KNN methods, several authors [11, 37, 14] have employed its extension, called optimized evidence-theoretic KNN (OET-KNN) and initially proposed in [41]. OET-KNN is based on the Dempster-Shafer theory of belief functions [17]; in the case of protein subcellular localization a score related to the belief that **p** belongs to subset $\mathscr{S}_m$ is obtained as a combination of the evidence provided by the first K nearest neighbors of the query protein.

Support Vector Machines(SVM) [15] is a kernel method that performs classification by constructing an N-dimensional hyperplane that optimally separates the data into two categories. Due to their good classification performance, in the recent years SVMs have been widely used in several research fields; this is the reason why several protein subcellular localization systems have successfully exploited them [26, 9, 29, 28, 22].

All the afore mentioned methods are depending on critical parameters, defining both the protein representation mode, the dataset dimensionality, and different settings of the learning algorithm. To avoid any experimental setup of these parameters, ensemble methods have recently been proposed [11, 37, 38, 14]. Given an engine learning algorithm (e.g. OET-KNN or SVM), these techniques create different predictors by changing the values of the parameters, and produce the final classification result by a simple majority vote algorithm.

Finally, a completely different, recent, and interesting ensemble method approach is the one presented in [3]; the predicting engine is the Naive Bayes classifier, that computes the posterior probability of each location, $P(\mathscr{S}_m|\mathbf{p})$ (that is the probability that the query protein belongs to the m-th subcellular component, given its representation **p**), and then considers the organelle that achieves the maximum probability score as the one the protein belongs to. This method obtains promising results in multiplex protein localization too, and it is interesting since it allows to compute both the importance of each feature in the prediction, thus allowing to identify the features that influence the localization of proteins in specific locations, and a confidence score that allows to judge how reliable the prediction is.

Although promising results have been obtained, especially by the most recent ensemble methods employing hybrid protein representation modes, the computational efficiency and the classification performance of all the above mentioned techniques are highly affected both by the high unbalancing of the training set, and by its low cardinality compared to its high dimensionality. To overcome such weaknesses, in this paper we propose our ensemble method whose engine algorithm, that will be referred as K-TIPCAC in the following, is an evolution of the K-IPCAC and the O-IPCAC algorithm that have proved to be effective and computationally efficient. In the following sections both O-IPCAC and K-TIPCAC are briefly recalled. For an exhaustive description see [32, 34].

9.3 Classifiers Based on Efficient Fisher Subspace Estimation

The first version of our classifiers, called IPCAC, has been initially proposed in [32]. It is a binary classifier exploiting theoretical results presented in [4] to efficiently estimate the Fisher subspace (Fs). More precisely, in [4] it is demonstrated that, given a set of N clustered points sampled from an isotropic Mixture of Gaussians (MoG), Fs corresponds to the span of the class means; as a consequence, when a binary classification problem is considered, Fs is spanned by $\mathbf{f} = \frac{\boldsymbol{\mu}_A - \boldsymbol{\mu}_B}{\|\boldsymbol{\mu}_A - \boldsymbol{\mu}_B\|}$, being A/B the two classes, and $\boldsymbol{\mu}_{A/B}$ the class means.

IPCAC exploits this result by whitening the training set $\mathscr{P}_{Train}$, computing the unit vector $\mathbf{f}$, and then classifying a new point $\mathbf{p}$ by thresholding its projection on Fs as follows:

$$(\mathbf{W}_D^T \mathbf{f}) \cdot \mathbf{p} - \gamma = \mathbf{w} \cdot \mathbf{p} - \gamma < 0 \qquad \gamma = \left\langle argmax_{\bar{\gamma} \in \{\mathbf{w} \cdot \mathbf{p}_i\}} Score(\bar{\gamma}) \right\rangle \tag{9.1}$$

where the matrix $\mathbf{W}_D$ represents the whitening transformation estimated on the N training points, $Score(\bar{\gamma})$ computes the number of correctly classified training points when $\bar{\gamma}$ is used as threshold, and $\langle \cdot \rangle$ represents the average operator.

Unfortunately, classifiers based on the estimation of Fs cannot work on high dimensional datasets for their high computational complexity. Moreover, these techniques often fail when the training-set cardinality is equal or lower than the input space dimensionality.

To address these problems, O-IPCAC (Online IPCAC) [34] improves IPCAC, and reduces the computational complexity, by replacing the first step of data whitening by a 'partial whitening' process; if the points to be classified belong to a D dimensional space, this method whitens the data in the linear subspace $\pi_d = \mathbf{Span}\langle \mathbf{v}_1, \cdots, \mathbf{v}_d \rangle$, spanned by the first $d \ll D$ principal components, while maintaining unaltered the information related to the orthogonal subspace $(\pi_d)^{\perp} = \mathbf{Span}\langle \mathbf{v}_{d+1}, \cdots, \mathbf{v}_D \rangle$.

More precisely, the linear transformation $\mathbf{W}_D$ representing the partial whitening operator is estimated as follows. The Truncated Singular Value Decomposition (TSVD) [24] is applied to estimate the first $d = min(log_2^2 N, D)$ principal components, obtaining the low-rank factorization $\mathbf{P} \simeq \mathbf{U}_d \mathbf{Q}_d \mathbf{V}_d^T$ (where $\mathbf{P}$ is the matrix representing the training set $\mathscr{P}_{Train}$ since it contains the training vectors). The d largest singular values on the diagonal of $\mathbf{Q}_d$, and the associated left singular vectors, are employed to project the points in the matrix $\mathbf{P}$ on the subspace $\mathscr{H}_d$ spanned by the columns of $\mathbf{U}_d$, and to perform the whitening, as follows:

$$\bar{\mathbf{P}}_{\mathbf{W}_d} = q_d \mathbf{Q}_d^{-1} \mathbf{P}_{\perp \mathscr{H}_d} = q_d \mathbf{Q}_d^{-1} \mathbf{U}_d^T \mathbf{P} = \mathbf{W}_d \mathbf{P}$$

where q_d is the smallest singular value of the points projected in $\mathscr{H}_d$. Note that, to obtain points whose covariance matrix best resembles a multiple of the identity, we have chosen to set the value of the d largest singular values to q_d instead of 1, thus avoiding the gap between the d-th and the $(d+1)$-th singular value. The obtained matrix $\mathbf{W}_d$ projects and whitens the points in the linear subspace $\mathscr{H}_d$; however, dimensionality reduction during the whitening estimation might delete discriminative

information, decreasing the classification performance. To avoid this information loss, we add to the partially whitened data the residuals ($\mathbf{R}$) of the points in $\mathbf{P}$ with respect to their projections on $\mathscr{H}_d$:

$$\mathbf{R} = \mathbf{P} - \mathbf{U}_d \mathbf{P}_{\perp \mathscr{H}_d} = \mathbf{P} - \mathbf{U}_d \mathbf{U}_d^T \mathbf{P}$$
$$\bar{\mathbf{P}}_{\mathbf{W}_D} = \mathbf{U}_d \bar{\mathbf{P}}_{\mathbf{W}_d} + \mathbf{R} = \left(q_d \mathbf{U}_d \mathbf{Q}_d^{-1} \mathbf{U}_d^T + \mathbf{I} - \mathbf{U}_d \mathbf{U}_d^T \right) \mathbf{P} = \mathbf{W}_D \mathbf{P} \tag{9.2}$$

where $\mathbf{W}_D \in \Re^{D \times D}$ represents the linear transformation that whitens the data along the first d principal components, while keeping unaltered the information along the remaining components.

In case of binary classification problems, once the partial whitening step has been performed the two whitened class means, and the vector $\mathbf{f}$ estimating `Fs` in the partially whitened space, are computed; this allows the binary predictor to compute the class labels by employing the procedure described in [33].

The described approach increases the performance and guarantees a greater stability during the classification task. We note that `O-IPCAC` has been implemented to perform both batch and online training. For convenience, in this contribution, we refer to the batch method as `TIPCAC` (Truncated-whitening `IPCAC`).

9.3.1 A Kernel Version of TIPCAC

To relax the linear separability constraint imposed by the `IPCAC` algorithm, it is possible to exploit the kernel trick as in the Kernel Principal Component Analysis (`KPCA`, [39]), thus obtaining a Kernel Isotropic Principal Component Analysis Classifier (`KIPCAC`), that has been proposed in [32].

More precisely, Rozza et al. demonstrate that a given point $\mathbf{p}$ can be projected on `Fs` in the kernel space as follows:

$$proj_{\mathbf{F}}(\mathbf{p}) = \mathbf{Ker}(\mathbf{p})^T \left((N_A N_B)^{\frac{1}{2}} \tilde{\mathbf{A}} \tilde{\boldsymbol{\Lambda}}^{-1} \tilde{\mathbf{A}}^T \mathbf{N}_{A|B}^{-1} \right) = \mathbf{Ker}(\mathbf{p})^T \mathbf{w}$$

where N is the cardinality of the training set, the Kernel matrix of the training points is $\mathbf{Ker}(\mathbf{p}) = \{KerFunction(\mathbf{p}_i, \mathbf{p})\}_{i=1}^N$, $\tilde{\boldsymbol{\Lambda}}$ are the eigenvalues obtained by the decomposition of $\mathbf{Ker}(\mathbf{p})$, $\tilde{\mathbf{A}}$ are the associated eigenvectors, N_A, N_B are the cardinalities of the two classes, and $\mathbf{N}_{A|B}^{-1} = [\underbrace{N_A^{-1} \cdots}_{N_A \text{ times}} \underbrace{-N_B^{-1} \cdots}_{N_B \text{ times}}]^T$.

In this work we extended this method by exploiting the same concept at the basis of the `TIPCAC` partial whitening step. More precisely, we select the largest eigenvalues that represent a fixed amount of variance defined a-priori, and we set the remaining part of the spectrum to 1; this process reduces the overfitting problems produced by the smallest part of the spectrum without performing any kind of dimensionality reduction. The advantages of employing this modified version of `KIPCAC`, called `K-TIPCAC`, are confirmed by the performance achieved in our experimental results.

9.4 DDAG K-TIPCAC

In this section we briefly describe the DDAG technique which allows to combine different methods to create a multiclass classifier (see Sect. 9.4.1). Secondly, we describe how DDAG has been exploited to develop our technique, called DDAG K-TIPCAC (see Sect. 9.4.2).

9.4.1 Decision DAGs (DDAGs)

A Rooted Direct Acyclic Graph (DAG) is a graph whose edges have an orientation, no cycles, and only one root node. A Rooted Binary DAG has nodes which have either 0 or 2 arcs leaving them. A DDAG [31] is a method that combines the results of *one-against-one* classifiers to produce a multi-class classification. To this aim, considering a N-class problem, the DDAG is implemented using a rooted binary DAG with $K = N(N-1)/2$ internal nodes. Each node represents a classification model trained on two of the K classes, and it produces a boolean output value ($\{0,1\}$). The nodes are arranged in a binary tree with the single root node at the top, two nodes in the second layer and so on until the final layer of leaves. Considering each classifier as a boolean function, to perform classification the DDAG proceeds as follows: it starts at the root node and it evaluates the boolean function; the node is then exited via the left edge, if the binary function is zero, or the right edge, if the binary function is one; the next node binary function is then evaluated; the membership class is the final leaf node reached through this process.

9.4.2 Decision DAG K-TIPCAC

In Sect. 9.3, an efficient binary classifier (called TIPCAC) and its kernel version (called K-TIPCAC) are described, that are based on the projection of the data on the one dimensional Fs estimated in a partially whitened kernel subspace.

The ensemble classifier proposed in this chapter is a C-class classifier that projects the data on a $C-1$ dimensional Fs estimated in a partially whitened subspace, and then applies DDAG to combine many binary K-TIPCACs to obtain the final prediction.

More precisely, the first step of this method evaluates the Fs of the overall C classes by generalizing the partial whitening approach recovering residuals, used by TIPCAC; this step reduces the training time complexity.

To this aim, after the partial whitening, the whitened class means $\{\boldsymbol{\mu}_c\}_{c=1}^{C}$ are computed as follows:

$$\boldsymbol{\mu}_c = \mathbf{W}_D \hat{\boldsymbol{\mu}}_c = q_d \mathbf{U}_d \mathbf{Q}_d^{-1} \mathbf{U}_d^T \hat{\boldsymbol{\mu}}_c + \hat{\boldsymbol{\mu}}_c - \mathbf{U}_d \mathbf{U}_d^T \hat{\boldsymbol{\mu}}_c.$$

At this stage the orthonormal basis, Π_{C-1}, composed of $C-1$ vectors spanning the Fs, is computed. More precisely, Π_{C-1} is obtained by orthonormalizing the $C-1$ linearly independent $\boldsymbol{\mu}_c$ vectors through the Gram-Schmidt procedure. The partially

whitened training points $\mathscr{P}_{\mathbf{W}_D}$ are then projected on the subspace Π_{C-1}, obtaining the set of points

$$\mathscr{P}_{\Pi_{C-1}} = \left\{ \mathbf{Fs}^T \mathbf{p}_i | \mathbf{p}_i \in \mathscr{P}_{\mathbf{W}_D} \right\},$$

where **Fs** is the matrix whose columns span `Fs`.

Exploiting the points in $\mathscr{P}_{\Pi_{C-1}}$, $C(C-1)/2$ `K-TIPCAC` binary classifiers are trained, each discriminating two classes in a *one-against-one* fashion (1-vs-1), and their results are combined by means of `DDAG`.

9.5 Experimental Setting

In this section we firstly remind the multi-class classification methods employed to perform the base-line comparison (see Sect. 9.5.1); secondly, we describe in details the employed dataset (see Sect. 9.5.2); finally, we report the performance evaluation method (see Sect. 9.5.3).

9.5.1 Methods

Multiclass Support Vector Machine: Since `SVM` is a binary classifier, a problem transformation is required before the application of this method to the considered multiclass prediction problem. The existing approaches to cast a multi-class classification problem to a series of binary classification problems can be roughly divided into two main classes: *one-against-all* and 1-vs-1. We applied the latter, and thus we trained a committee of 231 probabilistic `SVM`s [30]. The probabilities produced by each classifier were then reconciled to a multiclass prediction via pairwise coupling [25] and a simple max rule over all the class probability estimates was applied to compute a final decision.

Ensemble of Nested Dichotomies (`END`): Nested dichotomies [20] is a standard statistical technique applied in polytomous classification problems where logistic regression is applied by fitting binary logistic regression models to the internal nodes composing a tree. In absence of domain knowledge it is difficult to decide, among all the possible trees of nested dichotomies, the one to be adopted. A possible solution [19] is to consider all the hierarchies of nested dichotomies equally likely, and to use an ensemble of these hierarchies for prediction. In our experiments we tuned the `END` technique across *nd* (number of dichotomies) $\in \{5, 10, 20, 40\}$.

Random Forest (`RF`): Random Forest [2] has been applied as an effective tool for biomolecular and bioinformatics research. This method grows many classification trees. Instances whose class needs to be predicted are classified using the trees composing the forest. Each tree computes its own prediction, and the forest employs a plurality voting (over all the trees in the forest) to choose the final classification. We tuned the method using a grid search over *nt* (number of trees of the forest) $\in \{10, 20, 30, 40, 50\}$ and *nf* (number of features) $\in \{10, 100\}$.

9.5.2 Dataset

We evaluated the proposed method on a publicly available dataset[1] involved in the training of the EukP-loc method described in [13].

This dataset contains 5618 different proteins, classified into 22 eukaryotic subcellular locations. Among the 5618 considered proteins, 5091 belong to one subcellular location, 495 to two locations, 28 to three locations, and 4 to four locations. None of the proteins has $\geq 25\%$ sequence identity to any other in the same subset. The collection of sequences was then evaluated to compute the Pseudo Amino Acid compositions (PseAAC) of each protein using the PseAAC web server [36]. For each protein we produced a 495-elements vector composed by 20 numbers describing the standard amino acid composition, 400 values representing the PseAAC based on the dipeptide representation of the protein and further 75 values representing three groups of 25 PseAACs values obtained by setting the λ parameter to 25 and computing the PseAACs based on three pairs of chemico-physical properties: Hydrophobicity-Hydrophilicity, pK1 (alpha-COOH)-pK2 (NH3) and Mass-pI. In this preliminary investigation we focused on the location prediction of the 5091 proteins with a single experimentally annotated subcellular location. Some characteristics of this dataset are depicted in Table 9.1. It is worth noting that the problem is highly unbalanced, ranging the number of proteins associated to a subcellular location from 13 (hydrogenosome, melanosome and synapse) to 1077 (nucleus).

Table 9.1 Protein subcellular localization prediction dataset (5091 proteins and 22 locations). This table reports the number of annotated proteins per location; labels are mutually exclusive, thus the problem is multiclass but not multilabel.

Dataset			
acrosome proteins	17	cell wall proteins	47
Golgi proteins	157	spindle pole body proteins	17
hydrogenosome proteins	13	synapse proteins	13
lysosome proteins	59	vacuole proteins	91
melanosome proteins	13	centriole proteins	45
microsome proteins	23	chloroplast proteins	497
mitochondrion proteins	488	cyanelle proteins	85
nucleus proteins	1077	cytoplasm proteins	741
peroxisome proteins	92	cytoskeleton proteins	46
plasma membrane proteins	647	endoplasmic reticulum proteins	275
extracell proteins	609	endosome proteins	39

[1] The protein sequences were downloaded in fasta format from the web site http://www.csbio.sjtu.edu.cn/bioinf/euk-multi/Supp-A.pdf

Table 9.2 Estimated performances obtained by 10 fold stratified cross validation

Performance evaluation				
Method	Parameters	Precision	Recall	F-score
DDAG_K-TIPCAC	kernel=RBF, $\sigma = 8$, $var = 0.955$	0.383	0.408	**0.390**
Multiclass SVM	$C = 10.0$ $G = 0.01$	0.369	0.409	0.368
END	$nd = 40$	0.351	0.393	0.355
RF	$nt = 50$ $nf = 100$	0.349	0.391	0.340

9.5.3 Performance Evaluation

All the compared methods were evaluated according to a canonical 10 fold stratified cross-validation scheme. Given that the considered problem is a multiclass prediction problem affected by severe unbalance, accuracy is not suitable for performance evaluation. Performances were thus collected in form of F-score (harmonic mean of Precision and Recall). All the experiments, apart those involving the DDAG K-TIPCAC, which is implemented in MATLAB, were performed using the WEKA library of Machine Learning algorithms [23].

9.6 Results

The performances achieved by the evaluated approaches averaged across all the classes are reported in Table 9.2. The table shows, for each method, the best setting of its parameters, and the achieved performance measures, that are the Precision, Recall, and F-measure. The F-scores obtained by the evaluated methods for each subcellular location averaged across the 10 stratified cross validation folds are reported in Table 9.3. In order to investigate if the differences between the collected per class performances are statistically significant we performed a Wilcoxon signed ranks sum (U) test [40]. Results are reported in Table 9.4 (direction of the comparison is row-vs-column).

Considering the performances averaged across all the classes achieved by the compared ensemble methods (see Table 9.2) the best performing approach is DDAG K-TIPCAC (weighted F-score 0.390) immediately followed by the 1-vs-1 ensemble of SVMs (weighted F-score 0.368). A closer look to this table highlights that, while all the evaluated approaches produced comparable Recall scores, on average this comes at the cost of a reduced precision, the only exceptions being represented by the DDAG K-TIPCAC ensemble.

We note that input space reduction is present in our approach and also in other types of ensembles evaluated in this experiment, as in the case of Random Forest. Nevertheless, the space reduction computed by RF might be affected by a more relevant information loss, since the input space dimensionality is reduced by means of a random selection of subsets of features of a priori defined size. We can hypothesize that the data transformation applied by our approach is able to produce a more

Table 9.3 Per class performances obtained by 10 fold stratified cross validation

Per class performance evaluation (F-score)					
END	MCSVM	RF	DDAG_K-TIPCAC	proteins	location
0.211	0.000	0.300	0.560	17	acrosome proteins
0.046	0.000	0.024	0.030	157	Golgi proteins
0.375	0.375	0.375	0.316	13	hydrogenosome proteins
0.000	0.000	0.033	0.213	59	lysosome proteins
0.632	0.000	0.556	0.522	13	melanosome proteins
0.000	0.000	0.000	0.114	23	**microsome proteins**
0.295	0.312	0.241	0.355	488	mitochondrion proteins
0.529	0.535	0.523	0.533	1077	nucleus proteins
0.000	0.000	0.000	0.047	92	**peroxisome proteins**
0.484	0.522	0.489	0.470	647	plasma membrane proteins
0.493	0.482	0.494	0.479	609	extracell proteins
0.175	0.218	0.157	0.267	47	cell wall proteins
0.000	0.000	0.000	0.306	17	**spindle pole body proteins**
0.700	0.700	0.700	0.383	13	synapse proteins
0.000	0.043	0.000	0.071	91	vacuole proteins
0.000	0.000	0.000	0.125	45	**centriole proteins**
0.424	0.504	0.459	0.518	497	chloroplast proteins
0.056	0.189	0.022	0.255	85	cyanelle proteins
0.247	0.235	0.211	0.290	741	cytoplasm proteins
0.000	0.000	0.000	0.059	46	cytoskeleton proteins
0.143	0.159	0.027	0.236	275	endoplasmic reticulum proteins
0.000	0.000	0.000	0.067	39	**endosome proteins**

Table 9.4 Statistical comparison of per class performances through Wilcoxon test (alternative hypothesis: "greater", direction of comparison: rows versus columns)

Per class performance evaluation				
	END	MCSVM	RF	DDAG_K-TIPCAC
END	–	0.6876	0.1317	0.9970
MCSVM	0.3375	–	0.1813	0.9950
RF	0.8826	0.8348	–	0.9874
DDAG_K-TIPCAC	$2.689E^{-05}$	$3.073E^{-05}$	$4.449E^{-05}$	–

informative representation of the data than feature selection, thus leading to better performances also in highly unbalanced multi-class classification problems, as the one involved in our experiments.

This interpretation is supported by the collected per class performances (see Table 9.3). As we can see, despite the multiclass SVM ensemble (MCSVM) ranks second in terms of overall F-score (after a weighted averaging of the per class F-scores), its performances are often worse that those obtained by DDAG K-TIPCAC.

Moreover, it is important to highlight that all the methods misclassify at least one class, the only exception being represented by the DDAG K-TIPCAC approach. This fact suggests that the method employed to estimate the Fisher subspace is promising, as further proved by the experiments reported in the next subsections. The hypothesis that the performances, on a per class basis, of DDAG K-TIPCAC are better than those produced by most of the other evaluated methods is also supported by the Wilcoxon signed ranks sum test (see Table 9.4).

9.6.1 DDAG K-TIPCAC Employing the Standard Multiclass Estimation of Fs

In this section we want to evaluate the effectiveness of our "truncated" approach to estimate the multiclass Fisher subspace.

To this aim, we have performed the same experiment described in Sect. 9.5 by employing the points projected on the 21 dimensional Fisher subspace. As described at length in [21], when C classes are considered the set of projection vectors $\mathbf{w}_k$, $k = 1,..,C-1$ representing the $C-1$ dimensional Fisher subspace, is the set of $C-1$ eigenvectors corresponding to the largest eigenvalues of $\boldsymbol{\Sigma}_W^{-1}\boldsymbol{\Sigma}_{Bet}$, where $\boldsymbol{\Sigma}_W$ is the within-class covariance matrix, and $\boldsymbol{\Sigma}_{Bet}$ is the between-class scatter matrix. They are defined as follows:

$$\boldsymbol{\Sigma}_W = \sum_{c=1}^{C} \boldsymbol{\Sigma}_c, \quad \boldsymbol{\Sigma}_c = \sum_{j=1}^{N_c} (\mathbf{x}_j - \boldsymbol{\mu}_c)(\mathbf{x}_j - \boldsymbol{\mu}_c)^T$$

$$\boldsymbol{\Sigma}_{Bet} = \sum_{c=1}^{C} N_c (\boldsymbol{\mu}_c - \boldsymbol{\mu})(\boldsymbol{\mu}_c - \boldsymbol{\mu})^T$$

where x_i is the point belonging to class i, and N_i is the number of points in class i.

In Table 9.5 the achieved overall performance is reported. It is possible to notice that the quality of the classification strongly decreases, obtaining results comparable with those achieved by RF (see Table 9.2). In Table 9.6, where the per class F-measures are shown, we can note that some classes are completely misclassified. This demonstrates that the estimation of the multiclass Fisher subspace described in Sect. 9.4.2 is less affected by relevant information loss.

Concluding, the results confirm the quality of the proposed approach, including the importance of the novel estimation of the multiclass Fisher subspace.

Table 9.5 DDAG_K-TIPCAC performances obtained by 10 fold stratified cross validation and employing the projection on the multiclass Fs estimated with the "standard" methodology

Performance evaluation			
Parameters	Precision	Recall	F-score
Fs = "standard" kernel=RBF, $\sigma = 8$, $var = 0.955$	0.330	0.344	0.334

Table 9.6 DDAG_K-TIPCAC per class F-measures obtained by 10 fold stratified cross validation employing the projection on the multiclass Fs estimated with the "standard" methodology

Per class performance evaluation					
F-score	proteins	location	F-score	proteins	location
0.372	17	acrosome proteins	0.289	47	cell wall proteins
0.044	157	Golgi proteins	0.081	17	spindle pole body proteins
0.363	13	hydrogenosome proteins	0.333	13	synapse proteins
0.000	59	lysosome proteins	0.027	91	vacuole proteins
0.411	13	melanosome proteins	0.110	45	centriole proteins
0.000	23	**microsome proteins**	0.456	497	chloroplast proteins
0.290	488	mitochondrion proteins	0.110	85	cyanelle proteins
0.500	1077	nucleus proteins	0.226	741	cytoplasm proteins
0.053	92	peroxisome proteins	0.027	46	cytoskeleton proteins
0.474	647	plasma membrane proteins	0.186	275	endoplasmic reticulum proteins
0.334	609	extracell proteins	0.000	39	**endosome proteins**

9.6.2 DDAG K-TIPCAC without Projection on Multiclass Fs

In this section we have presented another test using the same experimental setting described in Sect. 9.5. More precisely, we have eliminated the projection on the multiclass Fisher subspace, maintaining as engine classifier K-TIPCAC and then combining the binary classifiers to obtain the final prediction using DDAG methodology. This allows to evaluate the difference between this approach and the base ensemble method proposed in Sect. 9.4.2. The achieved overall performance is summarized in Table 9.7, while the per class results are reported in Table 9.8.

Even though the overall results obtained are slightly higher than those shown in Table 9.2, the computational cost of the technique employed in this subsection is too high. Anyhow, we would like to highlight that this performance confirms the quality of the K-TIPCAC engine algorithm.

Furthermore, considering the per class performance (reported in Table 9.8) we notice that 3 classes are completely misclassified, while the method proposed in Sect. 9.4.2 succeeds to identify all the 22 classes.

Table 9.7 DDAG_K-TIPCAC performances obtained by 10 fold stratified cross validation and without employing the projection on the multiclass Fs

Performance evaluation			
Parameters	Precision	Recall	F-score
Fs = No kernel=RBF, $\sigma = 8$, $var = 0.955$	0.398	0.419	0.394

Table 9.8 DDAG-K-TIPCAC per class F-measures obtained by 10 fold stratified cross validation without employing the projection on the multiclass Fs

Per class performance evaluation					
F-score	proteins	location	F-score	proteins	location
0.714	17	acrosome proteins	0.253	47	cell wall proteins
0.056	157	Golgi proteins	0.000	17	**spindle pole body proteins**
0.471	13	hydrogenosome proteins	0.538	13	synapse proteins
0.282	59	lysosome proteins	0.055	91	vacuole proteins
0.700	13	melanosome proteins	0.098	45	centriole proteins
0.000	23	**microsome proteins**	0.538	497	chloroplast proteins
0.344	488	mitochondrion proteins	0.167	85	cyanelle proteins
0.537	1077	nucleus proteins	0.290	741	cytoplasm proteins
0.019	92	peroxisome proteins	0.078	46	cytoskeleton proteins
0.489	647	plasma membrane proteins	0.247	275	endoplasmic reticulum proteins
0.477	609	extracell proteins	0.000	39	**endosome proteins**

9.7 Conclusion

In this contribution we proposed an ensemble method whose engine algorithm is K-TIPCAC. The K-TIPCAC method deals with the points projected on a multiclass Fisher subspace. The final multi-class classification is performed by combining the kernel classifiers through Direct Decision Acyclic Graph (DDAG).

This methodology was applied to one of the most difficult multiclass prediction problems in modern computational biology: the protein subcellular location prediction. The results achieved by the performed experimental tests show the effectiveness of the K-TIPCAC algorithm and the quality of the multiclass Fisher subspace estimation by means of the proposed approach.

It is worth noting that the ability of the proposed approach to effectively control the precision-recall trade-off also in the prediction of small classes is of paramount importance in real applications, when we need to reduce the costs associated with the biological validation of new protein locations discovered through in silico methods.

Furthermore, considering also the experiments in Sect. 9.6.1 and Sect. 9.6.2 we can affirm that the method proposed in this chapter is an efficient and effective technique. This is due to the fact that it outperforms state of the art ensemble methods, and it reduces the time cost employing a dimensionality reduction that is less affected by loss of discriminative information. Moreover, only this approach guarantees the identification of all the classes that describe the protein localization.

References

1. Bhasin, M., Garg, A., Raghava, G.P.: PSLpred: prediction of subcellular localization of bacterial proteins. Bioinformatics 21, 2522–2524 (2005)
2. Breiman, L.: Random Forests. Machine Learning 45, 5–32 (2001)
3. Briesemeister, S., Rahnenfuhrer, J., Kohlbacher, O.: Going from where to why - interpretable prediction of protein subcellular localization. Bioinformatics 26, 1232–1238 (2010)
4. Brubaker, S.C., Vempala, S.: Isotropic PCA and affine-invariant clustering. In: Proc. the 49th Annual IEEE Symp. Foundations Comp., Philadelphia, PA, pp. 551–560 (2008)
5. Cai, Y.D., Chou, K.C.: Nearest neighbor algorithm for predicting protein subcellular location by combining functional domain composition and pseudo-amino acid composition. Biochem. and Biophys. Research Communications 305, 407–411 (2003)
6. Chou, K.C.: A novel approach to predicting protein structural classes in a (20-1)-D amino acid composition space. Proteins: Structure, Function, and Genetics 21, 319–344 (1995)
7. Chou, K.C., Elrod, D.W.: Protein subcellular location prediction. Protein Engineering 12, 107–118 (1999)
8. Chou, K.C.: Prediction of protein cellular attributes using pseudo amino acid composition. Proteins: Structure, Function, and Genetics 43, 246–255 (2001)
9. Chou, K.C., Cai, Y.D.: Using functional domain composition and support vector machines for prediction of protein subcellular location. J. Biol. Chem. 277, 45765–45769 (2002)
10. Chou, K.C., Cai, Y.D.: Prediction of protein subcellular locations by GO-FunD-PseAA predictor. Biochem. and Biophys. Research Communications 320, 1236–1239 (2004)
11. Chou, K.C., Shen, H.B.: Predicting eukaryotic protein subcellular locations by fusing optimized evidence-theoretic K-nearest neighbor classifiers. J. Proteome Research 5, 1888–1897 (2006)
12. Chou, K.C., Shen, H.B.: Recent progress in protein subcellular location prediction. Analytical Biochem. 370, 1–16 (2007)
13. Chou, K., Shen, H.: Cell-Ploc: a package of web servers for predicting subcellular localization of proteins in various organisms. Nature Protocol 3, 153–162 (2008)
14. Chou, K., Shen, H.: A new method for predicting the subcellular localization of eukariotic proteins with both single and multiple sites: Euk-mPLoc 2.0. Plos One 5, e9931 (2010)
15. Cortes, C., Vapnik, V.: Support Vector Networks. Machine Learning 20, 273–293 (1995)
16. Cover, T.M., Hart, P.E.: Nearest neighbour pattern classification. IEEE Trans. Inf. Theory 13, 21–27 (1967)
17. Denoeux, T.: A K-nearest neighbor classification rule based on Dempster-Shafer theory. IEEE Trans. System, Man, and Cybernetics 25, 804–813 (1995)
18. Duda, R.O., Hart, P.E., Stork, D.G.: Pattern Recognition, 2nd edn. Wiley- Interscience, Hoboken (2001)
19. Frank, E., Kramer, S.: Ensembles of nested dichotomies for multi-class problems. In: Brodley, C.E. (ed.) Proc. the 21st Int. Conf. Machine Learning, Banff, AL. ACM Press, New York (2004)
20. Fox, J.: Applied regression analysis, linear models, and related methods. Sage, Thousand Oaks (1997)
21. Fukunaga, K.: Introduction to statistical pattern recognition, 2nd edn. Academic Press, Burlington (1990)

22. Garg, A., Bhasin, M., Raghava, G.P.: Support vector machine-based method for subcellular localization of human proteins using amino acid compositions, their order, and similarity search. J. Biol. Chem. 280, 14427–14432 (2005)
23. Hall, M., Frank, E., Holmes, G., Pfahringer, B., Reutemann, P., Witten, I.H.: The WEKA data mining software: An update. SIGKDD Explorations 11 (2009)
24. Hansen, P.C.: The truncated SVD as a method for regularization. Technical Report, Standford University, CA, USA (1986)
25. Hastie, T., Tibshirani, R.: Classification by pairwise coupling. In: Jordan, M.I., Kearns, M.J., Solla, S.A. (eds.) Proc. Neural Inf. Proc. Syst., Denver, CO, pp. 507–513. MIT Press, Cambridge (1998)
26. Hua, S., Sun, Z.: Support vector machine approach for protein subcellular localization prediction. Bioinformatics 17, 721–728 (2001)
27. Huang, Y., Li, Y.: Prediction of protein subcellular locations using fuzzy K-NN method. Bioinformatics 20, 21–28 (2004)
28. Lei, Z., Dai, Y.: An SVM-based system for predicting protein subnuclear localizations. BMC Bioinformatics 6 (2005)
29. Park, K.J., Kanehisa, M.: Prediction of protein subcellular locations by support vector machines using composition amino acid and amino acid pairs. Bioinformatics 19, 1656–1663 (2003)
30. Platt, J.: Probabilistic outputs for support vector machines and comparisons to regularized likelihood methods. In: Smola, A.J., Bartlett, P.L., Schölkopf, B., Schuurmans, D. (eds.) Advances in Large Margin Classifiers, pp. 61–74. MIT Press, Cambridge (1999)
31. Platt, C., Cristianini, N., Shawe-Taylor, J.: Large margin DAGs for multiclass classification. In: Leen, T.K., Dietterich, T.G., Tresp, V. (eds.) Proc. Neural Inf. Proc. Syst., Denver, CO, pp. 547–553. MIT Press, Cambridge (2000)
32. Rozza, A., Lombardi, G., Casiraghi, E.: Novel IPCA-based classifiers and their application to spam filtering. In: Abraham, A., Sánchez, J.M.B., Herrera, F., Loia, V., Marcelloni, F., Senatore, S. (eds.) Proc. Int. Conf. Syst. Design and Appl., Pisa, Italy, pp. 797–802. IEEE Computer Society, Washington (2009)
33. Rozza, A., Lombardi, G., Casiraghi, E.: PIPCAC: A novel binary classifier assuming mixtures of Gaussian functions. In: Proc. Artif. Intell. Appl., Innsbruck, Austria. ACTA Press, Calgary (2010)
34. Rozza, A., Lombardi, G., Rosa, M., Casiraghi, E.: O-IPCAC and its application to EEG classification. J. Machine Learning Research 11, 4–11 (2010)
35. Shen, H.B., Chou, K.C.: Virus-PLoc: A fusion classifier for predicting the subcellular localization of viral proteins within host and virus-infected cells. Biopolymers 85, 233–240 (2006)
36. Shen, H., Chou, K.: PseAAC: a flexible web server for generating various kinds of protein pseudo amino acid composition. Analytical Biochem. 373, 386–388 (2008)
37. Shen, H.B., Chou, K.C.: Hum-mPLoc: an ensemble classifier for large-scale human protein subcellular location prediction by incorporating samples with multiple sites. Biochem. and Biophys. Research Communications 355, 1006–1011 (2007)
38. Shen, H.B., Chou, K.C.: Virus-PLoc: a fusion classifier for predicting protein subcellular localization of viral proteins within host and virus-infected cells. Biopolymers 85, 233–240 (2007)
39. Schölkopf, B., Smola, A., Müller, K.R.: Nonlinear component analysis as a kernel eigenvalue problem. Neural Computing 10, 1299–1319 (1998)
40. Wilcoxon, F.: Individual comparisons by ranking methods. Biometrics 1, 80–83 (1945)
41. Zouhal, L.M., Denoeux, T.: An evidence theoretic K-NN rule with parameter optimization. IEEE Trans. Syst., Man, and Cybernetics 28, 263–271 (1999)

Chapter 10
Trading-Off Diversity and Accuracy for Optimal Ensemble Tree Selection in Random Forests

Haytham Elghazel, Alex Aussem, and Florence Perraud

Abstract. We discuss an effective method for optimal ensemble tree selection in Random Forests by trading-off diversity and accuracy of the ensemble during the selection process. As the chances of overfitting increase dramatically with the size of the ensemble, we wrap cross-validation around the ensemble selection to maximize the amount of validation data considering, in turn, each fold as a validation fold to select the trees from. The aim is to increase performance by reducing the variance of the tree ensemble selection process. We demonstrate the effectiveness of our approach on several UCI and real-world data sets.

10.1 Introduction

Many advances in Machine Learning suggest using a set of individual classifiers, or ensemble of classifiers, instead of a single predictor to address supervised classification problems [16]. A large number of studies show that ensemble of classifiers generally achieve better results compared to a single classifier in terms of misclassification error [11, 22]. This improvement of performances relies on the concept of diversity which states that a good classifier ensemble is an ensemble in which the examples that are misclassified are different from one individual classifier to another. However, the practical trade-off between diversity and accuracy of the ensemble learning is still an open question in Machine Learning [6]. Dietterich [10] states that "A necessary and sufficient condition for an ensemble of classifiers to be more accurate than any of its individual members is if the classifiers are accurate and diverse". Many methods have been proposed to generate accurate, yet diverse, sets of models. Bagging [4], Boosting [13], Random Forests [5] and their variants

Haytham Elghazel · Alex Aussem · Florence Perraud
Université de Lyon, F-69000, Lyon

Université de Lyon 1

Laboratoire GAMA, 69622 Villeurbanne, France
E-mail: haytham.elghazel@univ-lyon1.fr

O. Okun et al. (Eds.): Ensembles in Machine Learning Applications, SCI 373, pp. 169–179.
springerlink.com

are the most popular examples of this methodology. Boosting and Random Forest are comparable and sometimes better than state-of-the-art methods in classification and regression [9].

Random Forests (RF) is a popular and very efficient algorithm, based on model aggregation ideas, for both classification and regression problems [5]. The principle of RF is to combine many binary decision trees built using several bootstrap samples coming from the learning sample and choosing randomly at each node a subset of explanatory variables. We assume the reader already is familiar with details of the RF procedure. RF algorithm becomes more and more popular and appears to be computationally effective and offers good prediction performance in a lot of different applications [12]. Breiman sketches an explanation of the good performance of RF related to the good quality of each tree together with the small correlation (denoting high diversity) among the trees of the forest. However, the mechanisms that explain this good performance of RF are not clearly elucidated from a mathematical point of view [2]. Indeed, it appears that using random selection of variables during the design stage of RF makes individual trees rather weak predictors and does not always give the expected performances. In addition, Breiman observed that above a certain number of trees, adding more trees does not allow to improve the performance [5]. Precisely he stated that for an increasing number of trees in the forest, the generalization error converges to a maximum. This result indicates that the number of trees in a forest does not have to be as large as possible to produce an accurate RF. On the other hand, pruning the irrelevant trees from huge forest is not as easy as one may think. The tree selection process is subject to overfitting problems especially when the number of validation samples provided is not sufficient [1, 8]. Also, we believe there is still room for improvement.

In this work, we discuss a simple framework called *Fitselect* to improve RF under Ensemble pruning (also called Overproduce and Choose Paradigm). The main idea of our approach is to perform classifier selection from an initial pool of decision trees obtained with the RF algorithm while focusing on the trade-off between accuracy and diversity of selected trees. The proposed method works by evaluating the qualities of all obtained trees in terms of accuracy-diversity trade-off on a hillclimb (validation) set, and selectively choosing part of promising trees to build the final RF. To alleviate the overfitting problem, we wrap cross-validation around ensemble selection to maximize the amount of validation data considering, in turn, each fold as a validation fold. A distinct tree selection is performed in each RF model. Improvements are demonstrated on several classification data sets. Empirical results show that the selected subset of trees performs similar to or better than the original ensemble (RF).

The rest of this chapter is organized as follows. Section 10.2 reviews recent studies on ensemble pruning. Section 10.3 introduces the *fitselect* framework for improving Random Forest. Experiments using relevant benchmarks and real data sets are presented in Sect. 10.4. Section 10.5 concludes this chapter.

10.2 Background of Ensemble Selection

The Ensemble Selection (also called Ensemble Pruning or Overproduce and Choose paradigm) consists in selecting the ensemble members from a set of individual classifiers that are subject to less resource consumption and response time with accuracy that is similar to or better than that of the original ensemble. In supervised classification, it has been known that selective classifier ensembles can always achieve better solutions when compared with traditional ensemble methods [20, 26]. Given an ensemble of size M, the problem of finding the sub-set of ensemble members with the optimal generalization ability involves searching the space of 2^{M-1} non-empty sub ensembles, which was proved to be an NP-complete problem [18]. Like ensemble learning approaches, the performance gain of the ensemble pruning methods stems from the accuracy-diversity trade-off, where choosing only the most accurate individual classifiers to form the sub ensemble is theoretically unsound [26] and a strategy that only considers diversity for pruning does not always give the expected performances in terms of misclassification error [20]

Many pruning algorithms exist for selecting good sub ensembles to reduce the size of ensemble without compromising its performance. The paper [26] formulated the ensemble selection problem as a combinatorial optimization problem to look for a subset of classifiers that has the optimal accuracy-diversity trade-off. Their quadratic programming method was not significantly better than other metric-based pruning heuristics though. Most of the pruning approaches that appeared in the literature reorder the original ensemble members based on some predefined criteria and select a subset of ensemble members from the sorted list [8, 17, 19]. A straightforward classifiers selection method is to rank the classifiers according to their individual performance on a hillclimb (validation) set and pick the best ones. The Choose Best heuristic consists in selecting the L classifiers (among M initial classifiers) which possess the highest individual accuracy. This heuristic does not take into account diversity. To this purpose, Margineantu and Dietterich [19] use the AdaBoost algorithm to train an ensemble of decision trees which is pruned with different selection heuristics. Of them, the Kappa Pruning heuristic aims at maximizing the pair-wise difference between the selected ensemble members. In [17], the authors proposed to use the clustering algorithm to prune redundant Neural Networks for maintaining the diversity of the ensemble committee of neural networks. The major problem with the above algorithms is that they do not consider the trade-off between accuracy and diversity. To solve this limitation, Margineantu and Dietterich [19] suggest pruning the initial set of M classifiers using Kappa-error convex hull criteria that is a diagram-based heuristic targeting at a good accuracy-diversity trade-off among the selected subsets. [14] proposed a genetic algorithm to study the trade-off between accuracy and diversity for ensemble pruning. Using an iterative process, the proposed approach evaluates an accuracy-diversity trade-off measure for different sub ensemble solutions and the sub ensemble with the highest value is returned by the algorithm. This approach is often subject to overfitting problems especially when the number of validation samples provided is not sufficient. On the other hand, Ensemble selection also employs greedy forward selection to select models to add to

the ensemble [8]. Compared to previous works, ensemble selection uses many more classifiers, allows optimizing to arbitrary performance metrics, and includes refinements to prevent overfitting to the ensembles hillclimb data. Ensemble selection of classifiers from a large and diverse library of base classifiers have been shown to be most competitive learning principles in a recent world-wide KDD'09 Cup Orange Challenge [21].

Most of the methods proposed in the literature are based on a single parameter to select the ensemble members. Selection-based methods in [14, 19] consider both diversity and accuracy to train the ensemble but we currently lack effective pruning principles to consider the individual accuracy-diversity trade-off "contribution" that each ensemble member can bring to the ensemble. So it seems that there are still many unanswered questions: (1) What is a good balance between accuracy and diversity for each individual classifier in the ensemble? (2) Should different data sets have different control parameters? and (3) which refinements could be included to prevent overfitting ? We address some of these above concerns in the next section.

10.3 Contribution

In this section, we describe our algorithm, called *Fitselect*, to select the classifier ensemble under the Overproduce and Choose paradigm. We restrict our approach to the RF but it is straightforward to generalize the method to any library of general classifiers. *Fitselect* belongs to the pruning approaches that reorder the original ensemble members based on some predefined criteria and select a subset of ensemble members from the sorted list. The training data set is subdivided into "training" and "validation" subsets. The training subset serves to construct the RF and the validation set is used for ensemble selection. *Fitselect* works by evaluating the accuracy and diversity of the decision trees in the RF and selecting the promising trees. The final solution is achieved by combining all the selected trees from the original forest. To study the trade-off between accuracy and diversity, we use the fitness function employed in [14, 22] to evaluate each decision tree h_i. Given a RF $\mathscr{H}$ with M decision trees $\{h_1, h_2, \ldots, h_M\}$, the fitness function of each decision tree h_i is given by:

$$fitness(h_i) = \alpha \times \frac{a(h_i)}{m_a} + (1-\alpha) \times \frac{d(h_i)}{m_d} \tag{10.1}$$

where $a(h_i)$ and $d(h_i)$ stands respectively for the accuracy and the diversity of the tree h_i computed on the validation data set; m_a and m_d denotes respectively the maximal accuracy and diversity overall trees in the forest $\mathscr{H}$; $0 \leq \alpha \leq 1$ is a control parameter that balances the accuracy and the diversity. The accuracy $a(h_i)$ is defined as the average correct predictions of h_i on the validation set.

Two classifiers C_i and C_j are said diverse if they assign different class labels to the same examples. Various measures have been proposed to quantify the diversity between two classifiers from their respective outputs [14, 16, 19, 23, 24]. In this study, we define the diversity $d(h_i)$ to be the average Hamming distance, computed on the validation set, between the prediction of h_i and the other trees in the forest.

Accuracy and diversity values are normalized separately (using respectively the m_a and m_d factors) so that the values range from 0 to 1. Normalizing both terms allows α to have the same meaning across multiple domains. Once the fitness scores have been calculated for a given α, we rank all the trees according to their fitness values and we select the first $L < M$ trees that maximize the accuracy only of the ensemble on the validation set. In other terms, there is no $L' \neq L$ such that the L' first trees are more accurate than the L first trees in the ordered list. The search is in $O(M)$. The selected trees form the new forest. To summarize, the fitness is used for ranking only, and accuracy is used for selecting. Note that any arbitrary performance metric could be used instead of accuracy, like the area under the ROC curve [21].

As there are a large number of trees to select from, the chances of overfitting increase dramatically [7, 8]. In addition, ensemble selection is still prone to overfitting when the validation set is small. We therefore propose to wrap cross-validation around ensemble selection to maximize the amount of validation data considering, in turn, each fold as a validation fold. This has a Bagging like effect that combats overfitting. A cross-validated RF is created by training a tree in each fold. If there are K folds, there will be K individual RF models (each trained on a fraction of $K-1/K$ training points). These RF differ due to their different training samples. Tree ensemble selection is performed in each RF model. The aim is to increase performance by reducing the variance of the forward stepwise selection process. While adding cross-validation to ensemble selection is computationally expensive, the ensemble selection method is far simpler than the sequential forward selection (SFS) and sequential backward selection (SBS) discussed in [1], as well as the more complex genetic algorithm proposed in [14], since the ranking is performed once in $O(M\log(M))$. The methods is, of course, sub-optimal, however, it is very fast and simple. The final tree ensemble is obtained through combining all the selected trees obtained over the different K cross-validation steps. As the combined selected trees are obtained from K different training and model selection process, the chances of finding combinations of trees that overfit the validation sets are minimized.

The balance between diversity and accuracy is a controversial issue, so it is unclear what value α should take. We believe it should be adjusted to the data set at hand. Therefore, we perform multiple runs with increasing values of α (10% increase at each step) as done in [22]. The value of α which produces the highest *average overall accuracy* on the K different sub ensembles of selected trees $\{S_{(\alpha,1)},\ldots,S_{(\alpha,K)}\}$ is used to rank and select the trees. Note that simple majority voting is used to combine the predictions of the ensembles. The *average overall accuracy* Acc_α over the K cross-validation steps $\{S_{(\alpha,1)},\ldots,S_{(\alpha,K)}\}$ for a given value α is measured as:

$$Acc_\alpha = \frac{1}{K}\sum_{j=1}^{K} Acc_{(\alpha,j)} \tag{10.2}$$

where $Acc_{(\alpha,j)}$ corresponds to the ensemble's accuracy of tree sub ensemble $S_{(\alpha,j)}$ selected for the cross-validation step j. Algorithm below summarizes the overall approach.

Algorithm 4. Pseudo code for *FitSelect*

for each cross-validation step $j \in [1,K]$ **do**
  $\mathscr{H}_j$: Construct a RF with M decision trees $\{h_{1,j}, h_{2,j}, \ldots, h_{M,j}\}$ on the training set.
  $\{a(h_{1,j}), ..., a(h_{M,j})\}$: Calculate (on the validation set) the tree accuracies in $\mathscr{H}_j$.
  $\{d(h_{1,j}), ..., d(h_{M,j})\}$: Calculate (on the validation set) the tree diversity values using the average Hamming distance between prediction of each tree and all the other trees in $\mathscr{H}_j$
end for
for each value of $\alpha \in [0,1]$; $\alpha = \alpha + 0,1$ **do**
  for each cross-validation step $j \in [1,K]$ **do**
    $\{fitness_\alpha(h_{1,j}), \ldots, fitness_\alpha(h_{M,j})\}$: Calculate the tree fitness values as $fitness_\alpha(h_{i,j}) = \alpha \times \frac{a(h_i)}{m_a} + (1-\alpha) \times \frac{d(h_i)}{m_d}$
    Sort the trees $\{h_{1,j}, \ldots, h_{M,j}\}$ in decreasing order of the fitness
    Select the $(L < M)$ first trees $S_{(\alpha,j)} = \{h_{1,j}, \ldots, h_{L,j}\}$ that maximize, $A_{(\alpha,j)}$, the ensemble's accuracy (using majority voting) of the selected trees in $S_{(\alpha,j)}$ on the validation set
  end for
  Calculate the average overall accuracy $Acc_\alpha = \frac{1}{K} \sum_{j=1}^{K} Acc_{(\alpha,j)}$ of the K selected sub ensembles $\{S_{(\alpha,1)}, \ldots, S_{(\alpha,K)}\}$
end for
$\alpha_{opt} = argmax_{\alpha \in [0,1]}(Acc_\alpha)$
$RF^{(final)}$ = Combine $\{S_{(\alpha_{opt},1)}, \ldots, S_{(\alpha_{opt},K)}\}$

10.4 Empirical Results

10.4.1 Experiments on Benchmark Data Sets

The *Fitselect* RF selection algorithm was tested on 11 binary classification problems: Clean, Haberman, Madelon, Pima, Spamb, Transfusion, Wdbc from the UCI repository [3], Engytime [25] and Leukemia [15]. The characteristics of data sets are reported in Table 10.1. For each problem we split the data set into a training and testing sets of equal sizes. In order to guarantee the original class distribution within training and testing sets, a proportionate stratified sampling was applied. The training set was split using a 3-fold cross-validation: 3 RF models with 500 decision trees were trained on a fraction of $2/3$ training points. Selection was performed on the $1/3$ withheld data points using *Fitselect*. The testing set was used to evaluate the performance of the final tree ensemble returned by *Fitselect*. Four performance metrics were used. Three threshold metrics: accuracy (Acc), recall (Rec), F-Score (F) and one ordering/rank metric: the area under the ROC curve (AUC).

For each dataset, the performance of the classifier ensemble obtained with *Fitselect* was compared to (1) the unpruned tree ensemble obtained from learning the RF algorithm on the whole training set and (2) the forward ensemble selection method (which we will refer to as *Forward*) [8] used by the winner of the recently KDD Cup Orange Challenge (2009). To test the statistical relevancy of the results,

Table 10.1 Data sets used in the experiments

Data sets	# instance	# features
Clean	476	166
Engytime	4096	2
Haberman	306	3
Leukemia	72	7129
Madelon	2600	500
Pima	768	8
Spamb	4601	57
Transfusion	748	4
Wdbc	569	30

we used Wilcoxon signed-rank test, a non-parametric equivalent of paired t-test. Table 10.2 shows that *Fitselect* outperformed both RF and the ensemble selection algorithm proposed in [8] for the majority of the data sets (except for the recall metric for Madelon and the AUC value for Transfusion). The difference in accuracy, over all data sets, between *Fitselect* and the *Forward* selection algorithm is significant at 0.01 level using the Wilcoxon signed-rank test, at 0.04 for Recall, at 0.01 for F-Score and at 0.02 for AUC. The difference in accuracy, over all data sets, between *Fitselect* and the RF is significant at 0.01 for accuracy, at 0.04 for Recall, at 0.01 for F-Score and at 0.02 for AUC. In all cases, the test statistics were less than the critical value for a two-tailed p-value of 0.05 so the differences in performance between *Fitselect* and both RF and *Forward* approaches were significant at this level. In a way of conclusion, we suggest that adaptively trading off diversity and accuracy during the tree selection on cross-validated data sets is adequate for improving RF predictions. It seems however difficult to extract any general conclusion about the best trade-off between accuracy and diversity. The value of α_{opt} varied significantly from on data set to another, from 0.3 up to 1 (for Leukemia and Transfusion), indicating that accuracy tends to be favored more than diversity during the ensemble pruning. Although its effectiveness is confirmed for a library of heterogeneous models, our experiments suggest that the ensemble selection method proposed in [8] is not effective in the RF framework.

10.4.2 Experiments on Real Data Sets

In this section, we report very briefly on some investigations with *Fitselect* on real-world data to illustrate the usefulness of the method in a real breast cancer (BC) epidemiological study conducted by Dr. Corbex at the World Health Organization located in Cairo. The overall purpose of the study was to investigate if the psychological, economic, or socio/cultural profile of women in Egypt can be predictive of the delays between: 1) the first symptoms and the first visit to a doctor, and 2) the first visit to a doctor and the effective diagnosis. The first delay is mainly women dependent, while the second is mainly dependent on the health system. These delay values were binned into two bins according to the epidemiologist: “short delay”

Table 10.2 Performance scores on benchmark data sets. Best scores are in boldface. The number of trees returned by the *Forward* method for each data set is given in parentheses; α_{opt} and the number of trees selected by *Fitselect* are given in parentheses.

	Clean data set			**Engytime data set**		
	RF	Fwd(**37**)	Fitsel.(**0.6,80**)	RF	Fwd(**37**)	Fitsel.(**0.9,90**)
Acc	0.7322	0.7029	**0.7657**	0.9639	0.9624	**0.9663**
Rec	**0.6346**	0.5288	0.6635	**0.9600**	0.9502	**0.9600**
F	0.6735	0.6077	**0.7113**	0.9637	0.9619	**0.9661**
AUC	0.7953	0.7574	**0.8278**	0.9883	0.9840	**0.9886**
	Haberman data set			**Leukemia data set**		
	RF	Fwd(**21**)	Fitsel.(**0.7,60**)	RF	Fwd(**21**)	Fitsel.(**1,30**)
Acc	0.6883	0.7078	**0.7208**	0.8919	0.9189	**0.9459**
Rec	**0.5122**	0.3902	**0.5122**	0.6923	0.7692	**0.8462**
F	0.4667	0.4156	**0.4941**	0.8182	0.8696	**0.9167**
AUC	0.7086	0.7127	**0.7182**	0.9792	0.9744	**0.9812**
	Madelon data set			**Pima data set**		
	RF	Fwd(**163**)	Fitsel.(**0.3,230**)	RF	Fwd(**136**)	Fitsel.(**0.6,100**)
Acc	**0.7423**	0.7231	0.7408	0.7786	0.7682	**0.7865**
Rec	0.6631	**0.6923**	0.6708	0.5448	0.5448	**0.5672**
F	0.7201	0.7143	**0.7213**	0.6320	0.6213	**0.6496**
AUC	**0.8080**	0.7865	0.8077	0.8463	0.8241	**0.8569**
	Spamb data set			**Transfusion data set**		
	RF	Fwd(**54**)	Fitsel.(**0.8,70**)	RF	Fwd(**25**)	Fitsel.(**1,30**)
Acc	0.9166	0.8979	**0.9183**	0.7727	0.7701	**0.7781**
Rec	0.9261	0.9107	**0.9261**	0.1685	0.2022	**0.2135**
F	0.8974	0.8755	**0.8994**	0.2609	0.2951	**0.3140**
AUC	0.9675	0.9598	**0.9690**	0.6366	**0.6481**	0.6439
	Wdbc data set					
	RF	Fwd(**31**)	Fitsel.(**0.8,40**)			
Acc	0.9544	0.9544	**0.9719**			
Rec	0.9497	0.9609	**0.9665**			
F	0.9632	0.9636	**0.9774**			
AUC	0.9899	0.9921	**0.9931**			

(class 1) and "long delay" (class 2). 204 patients treated in Cairo were interviewed according to a questionnaire with up to 70 questions (medical journey, personal journey and socio-cultural barriers). Explanatory categorical variables included socio-economic status (education level and economic capacity), socio-economic status (age, marital status, residence, household, etc), awareness and beliefs (knowledge about BC, stigma, modesty issues, etc.), behaviors and attitudes (what women do, what they share about their disease and with who, etc.). For each explained variable, the epidemiologist has selected a subset of explanatory variables and a subset of women, see Table 10.3.

Table 10.3 The data sets description

Data sets	# instance	# features	long	short
Delay between symptoms and consultation	201	40	99	102
Delay between consultation and diagnosis	173	36	86	87

Here again, the performance of the classifier ensemble obtained, for both classification tasks, with *Fitselect* was compared to (1) the unpruned tree ensemble obtained from learning the RF algorithm on the whole training set and (2) the forward ensemble selection method. Results are reported in Table 10.4. As may be seen, *Fitselect* outperformed the other algorithms by a noticeable margin on the both classification tasks. Surprisingly, the *Fwd* method performed worse than RF. Future work will aim to extract the most important variables that explains a promising accuracy of about 67% for two tasks, from the selected trees.

Table 10.4 Performance results for the two tasks

	DELAY BETWEEN FIRST SYMPTOMS AND DOCTOR CONSULTATION			DELAY BETWEEN DOCTOR CONSULTATION AND EFFECTIVE DIAGNOSIS		
	RF	FWD(**44**)	FITSEL.(**0.6,130**)	RF	FWD(**92**)	FITSEL.(**0.7,70**)
ACC	0.6238	0.5446	0.6634	0.6437	0.5977	0.6782
REC	0.5686	0.4510	0.5686	0.5000	0.5227	0.6364
F	0.6042	0.5000	0.6304	0.5867	0.5679	0.6667
AUC	0.6425	0.5539	0.6531	0.6641	0.6414	0.6942

10.5 Conclusion

This paper introduced a tree ensemble selection method to improve efficiency and effectiveness of RF by adaptively trading off diversity and accuracy according to the data. We wrapped cross-validation around ensemble selection to maximize the amount of validation data considering, in turn, each fold as a validation fold. Tree ensemble selection was performed in each RF model. The tree selection method called *Fitselect* was shown to increase performance by reducing the variance of the ensemble selection process; however the gain in performance was relatively modest in our experiments. It would be interesting for work to be performed to ascertain the classification problems for which the *Fitselect* is most suited. Moreover, it seems difficult to extract any general conclusion about the best trade-off between accuracy and diversity in view of our experiments.

Acknowledgements. We would like to thank Grigorios Tsoumakas for his valuable comments on this chapter.

References

1. Bernard, S., Heutte, L., Adam, S.: On the selection of decision trees in random forests. In: Proc. 2009 Int. Joint Conf. Neural Networks, Atlanta, GA, pp. 302–307. IEEE Comp. Press, Los Alamitos (2009)
2. Biau, G., Devroye, L., Lugosi, G.: Consistency of random forests and other averaging classifiers. J. Machine Learning Research 9, 2039–2057 (2008)
3. Blake, C.L., Merz, C.J.: UCI repository of machine learning databases. University of California, Dept. of Information and Computer Sciences, Irvine (1998)
4. Breiman, L.: Bagging predictors. Machine Learning 26, 123–140 (1996)
5. Breiman, L.: Random forests. Machine Learning 45, 5–32 (2001)
6. Brown, G., Kuncheva, L.I.: "Good" and "bad" diversity in majority vote ensembles. In: El Gayar, N., Kittler, J., Roli, F. (eds.) MCS 2010. LNCS, vol. 5997, pp. 124–133. Springer, Heidelberg (2010)
7. Caruana, R., Munson, A., Niculescu-Mizil, A.: Getting the most out of ensemble selection. In: Proc. the 6th Int. Conf. Data Mining, Hong Kong, China, pp. 828–833. IEEE Comp. Society, Los Alamitos (2006)
8. Caruana, R., Niculescu-Mizil, A., Crew, G., Ksikes, A.: Ensemble selection from libraries of models. In: Brodley, C. (ed.) Proc. the 21st Int. Conf. Machine Learning, Banff, AB. ACM Press, New York (2004)
9. Caruana, R., Niculescu-Mizil, A.: An empirical comparison of supervised learning algorithms. In: Cohen, W.W., Moore, A. (eds.) Proc. the 23rd Int. Conf. Machine Learning, Pittsburgh, PA, pp. 161–168. ACM Press, New York (2006)
10. Dietterich, T.G.: Ensemble methods in machine learning. In: Kittler, J., Roli, F. (eds.) MCS 2000. LNCS, vol. 1857, pp. 1–15. Springer, Heidelberg (2000)
11. Dietterich, T.G.: An experimental comparison of three methods for constructing ensembles of decision trees: bagging, boosting and randomization. Machine Learning 40, 139–157 (2000)
12. Díaz-Uriarte, R., Alvarez de Andrés, S.: Gene selection and classification of microarray data using random forest. BMC Bioinformatics 7 (2006)
13. Freund, Y., Shapire, R.E.: Experiments with a new boosting algorithm. In: Saitta, L. (ed.) 1996 Proc. the 13th Int. Conf. Machine Learning, Bari, Italy, pp. 148–156. Morgan Kaufmann, San Francisco (1996)
14. Gacquer, D., Delcroix, V., Delmotte, F., Piechowiak, S.: On the effectiveness of diversity when training multiple classifier systems. In: Sossai, C., Chemello, G. (eds.) ECSQARU 2009. LNCS, vol. 5590, pp. 493–504. Springer, Heidelberg (2009)
15. Golub, T.R., Slonim, D.K., Tamayo, P., Huard, C., Gaasenbeek, M., Mesirov, J.P., Coller, H., Loh, M.L., Downing, J.R., Caligiuri, M.A., Bloomfield, C.D., Lander, E.S.: Molecular classification of cancer: Class discovery and class prediction by gene expression monitoring. Science 286, 531–537 (1999)
16. Kuncheva, L.I.: Combining pattern classifiers: Methods and algorithms. Wiley Interscience, Hoboken (2004)
17. Li, G., Yang, J., Kong, A.S., Chen, N.: Clustering algorithm based selective ensemble. J. Fudan University 43, 689–695 (2004)
18. Lu, Z., Wu, X., Bongard, J.: Ensemble pruning via individual contribution ordering. In: Rao, B., Krishnapuram, B., Tomkins, A., Yang, Q. (eds.) Proc. the 16th ACM SIGKDD Conf. Knowledge Discovery and Data Mining, Washington, DC, pp. 871–880. ACM Press, New York (2010)

19. Margineantu, D.D., Dietterich, T.G.: Pruning adaptive boosting. In: Fisher, D.H. (ed.) Proc. the 14th Int. Conf. Machine Learning, Nashville, TN, pp. 211–218. Morgan Kaufmann, San Francisco (1997)
20. Martínez-Muñoz, G., Hernández-Lobato, D., Suárez, A.: An analysis of ensemble pruning techniques based on ordered aggregation. IEEE Trans. Pattern Analysis and Machine Intell. 31, 245–259 (2009)
21. Niculescu-Mizil, A., Perlich, C., Swirszcz, G., Sindhwani, V., Liu, Y., Melville, P., Wang, D., Xiao, J., Hu, J., Singh, M., Shang, W.X., Zhu, W.F.: Winning the KDD Cup Orange Challenge with ensemble selection. J. Machine Learning Research 7, 23–34 (2009)
22. Opitz, D., Maclin, R.: Popular ensemble methods: An empirical study. J. Artif. Intell. Research 11, 169–198 (1999)
23. Partalas, I., Tsoumakas, G., Vlahavas, I.P.: An ensemble uncertainty aware measure for directed hill climbing ensemble pruning. Machine Learning 81, 257–282 (2010)
24. Tsoumakas, G., Partalas, I., Vlahavas, I.P.: An ensemble pruning primer. In: Okun, O., Valentini, G. (eds.) Applications of Supervised and Unsupervised Ensemble Methods. SCI, vol. 245, pp. 1–13. Springer, Heidelberg (2009)
25. Ultsch, A.: Fundamental clustering problems suite (2005)
26. Zhang, Y., Burer, S., Street, W.N.: Ensemble pruning via semi-definite programming. J. Machine Learning Research 7, 1315–1338 (2006)

Chapter 11
Random Oracles for Regression Ensembles*

Carlos Pardo, Juan J. Rodríguez, José F. Díez-Pastor, and César García-Osorio

Abstract. This paper considers the use of Random Oracles in Ensembles for regression tasks. A Random Oracle model (Kuncheva and Rodríguez, 2007) consists of a pair of models and a fixed randomly created "oracle" (in the case of the Linear Random Oracle, it is a hyperplane that divides the dataset in two during training and, once the ensemble is trained, decides which model to use). They can be used as the base model for any ensemble method. Previously, they have been used for classification. Here, the use of Random Oracles for regression is studied using 61 datasets, Regression Trees as base models and several ensemble methods: Bagging , Random Subspaces, AdaBoost.R2 and Iterated Bagging. For all the considered methods and variants, ensembles with Random Oracles are better than the corresponding version without the Oracles.

11.1 Introduction

Ensembles [12] are combinations of base models (also referred as ensemble members). In many situations, an ensemble gives better results than any of its members. Although they have been studied mainly for classification, there are also ensemble methods for regression.

The models to be combined have to be different, otherwise the ensemble is unnecessary. One way to have different models is to construct them with different methods. Nevertheless, there are ensemble methods that combine models obtained from the same method, but change the dataset in some way.

In Bagging [1], each base member is trained with a sample of the training data. Normally, the size of the sample is the same as the size of the original training data,

Carlos Pardo · Juan J. Rodríguez · José F. Díez-Pastor · César García-Osorio
University of Burgos
E-mail: {cpardo,jjrodriguez,jfdiez,cgosorio}@ubu.es

* This work was supported by the Project TIN2008-03151 of the Spanish Ministry of Education and Science.

O. Okun et al. (Eds.): Ensembles in Machine Learning Applications, SCI 373, pp. 181–199.
springerlink.com

but the sample is *with replacement*. Hence, some training examples will appear several times in the sample, while others will not appear. The prediction of the ensemble is the average of the predictions of its members.

In Random Subspaces [10], each member is trained with all the training examples, but with a subset of the attributes. The dimension of the subspaces is a parameter of the method. The prediction of the ensemble is also the average of the predictions.

Bagging and Random Subspaces can be used for classification and regression. AdaBoost [7] initially was a method for classification, but there are some variants for regression, such as AdaBoost.R2 [5]. In these methods, each training example has a weight. Initially, all the examples have the same weight. The construction of the ensemble members must take into account the weights of the examples. After an ensemble member is constructed, the weights of the examples are adjusted. The idea is to give more weight to the examples with greater errors in the previous iterations. Hence, in the construction of the next member, these examples will be more important. The ensemble members also have weights, they depend on their error. In AdaBoost.R2, the predicted value of the ensemble is a weighted median. In [20], this method was the one with the best results among several ensemble methods for regression.

Iterated Bagging [2] is a method for regression based on Bagging . It combines several Bagging ensembles. The first Bagging ensemble is constructed as usual. Based on the predictions of the previous Bagging ensemble, the values of the predicted variable are altered. The next Bagging ensemble is trained with these altered values. These values are the *residuals*: the difference between the real and the predicted values. Nevertheless, these predictions are not obtained using all the members in the Bagging ensemble. The error of the predictions for a training example would be too optimistic, since the majority of the ensemble methods have been trained with that example. These predictions are obtained using the *out-of-bag* estimation: the prediction for an example is obtained using only those ensemble members that were not trained with that example. The prediction of an Iterated Bagging ensemble is the sum of the predictions of its Bagging ensembles. In [17], Iterated Bagging is compared to other methods giving the best results.

Random Oracles [13] are mini-ensembles formed by two models, they can be used as base models for other ensemble methods. The objective of using Random Oracles is to have more diversity among the base models that form an ensemble. This additional diversity can improve the accuracy of the ensembles.

The rest of this chapter is organised as follows. Next section explains Random Oracles. Section 11.3 describes the experimental setting. The results are presented and discussed in Sect. 11.4. In Sect. 11.5, diversity-error diagrams are used to analyze the behaviour of the base models. Finally, Sect. 11.6 presents some concluding remarks. Appendix includes the source code.

11.2 Random Oracles

A Random Oracle model [13] is a mini-ensemble formed by a pair of models and a Random Oracle that chooses between them. It can be thought of as a random discriminant function which splits the data into two subsets with no regard of any class labels or cluster structure. Also, a Random Oracle can be used as the base model of any ensemble method. Given a base method, the training of a Random Oracle model consists of:

- Select randomly the Random Oracle.
- Split the training data in two subsets using the Random Oracle.
- For each subset of the training data, build a model. The Random Oracle model is formed by the pair of models and the oracle itself.

The prediction of a test instance is done in the following way:

- Use the Random Oracle to select one of the two models.
- Return the prediction given by the selected model.

If the computational complexity of the oracle is low, both in training and prediction, the computational complexity of a Random Oracle model is very similar to the complexity of the base method. In the prediction phase, only one of the two models is used. In the training phase, two models are built. Nevertheless, they are trained with a disjoint partition of the training examples and the training time of any method depends, at least linearly, on the number of training examples.

Different types of Oracles can be considered. In this work, the Linear Random Oracle is used. This oracle divides the space into two subspaces using a hyperplane. To build the oracle, two different training objects are selected at random, each remaining training object is assigned to the subspace of the selected training object for which is closer[1].

Algorithms 5 and 6 show the pseudo-code for the training and prediction phases of the method.

In this work, the distances are calculated according to the Euclidean distance, numerical attributes are scaled within $[0,1]$, for nominal attributes we consider that the distance is 0 or 1 depending if the two valued are different or equal.

11.3 Experiments

The experiments were conducted using 5×2 fold cross validation [4]. The performance of the different methods over different datasets was measured using *root mean squared error* (RMSE). The base models were Regression Trees. They were used pruned *P* or unpruned *U*. The method used for pruning was *Reduced Error Pruning* (REP) [6]. Ensemble size was 100.

[1] Note that a generalization of this would be to select more than two training objects, then the remaining training objects would be assigned to the Voronoi region defined by the closest selected training object.

Algorithm 5. Pseudo-code of the Random Oracle method: training phase

Input: Training dataset D; base learning method L
Output: Random Oracle Model RO
$RO.instance[1] \leftarrow \{\mathbf{x} \mid (\mathbf{x}, y)$ is a random instance from $D\}$
$RO.instance[2] \leftarrow \{\mathbf{x} \mid (\mathbf{x}, y)$ is a random instance from $D\}$
$D_1 \leftarrow \emptyset$ // The training dataset for the 1^{st} sub-model
$D_2 \leftarrow \emptyset$ // The training dataset for the 2^{nd} sub-model
Foreach $instance(\mathbf{x}, y) \in D$ **do**
  If $distance(RO.instance[1], \mathbf{x}) < distance(RO.instance[2], \mathbf{x})$ **then**
    $D_1 \leftarrow D_1 \cup (\mathbf{x}, y)$ // Add the instance to the 1^{st} subset
  else
    $D_2 \leftarrow D_2 \cup (\mathbf{x}, y)$ //Add the instance to the 2^{nd} subset
  end
end
$RO.model[1] \leftarrow L(D_1)$ // Train the 1^{st} sub-model
$RO.model[2] \leftarrow L(D_2)$ // Train the 2^{nd} sub-model

Algorithm 6. Pseudo-code of the Random Oracle method: prediction phase

Input: Trained Random Oracle RO; instance $\mathbf{x}$
Output: Predicted value
If $distance(RO.instance[1], \mathbf{x}) < distance(RO.instance[2], \mathbf{x})$ **then**
  return $RO.model[1].predict(\mathbf{x})$ // Predict with the 1^{st} sub-model
else
  return $RO.model[2].predict(\mathbf{x})$ // Predict with the 2^{nd} sub-model
end

Several ensemble methods were considered:

- Randomization. When the base method has a random element, different models can be obtained from the same training data. Randomization is an ensemble of such randomizable models in which the prediction is the average of the predictions of its members. In the case of regression trees, when pruning is used, the training data is partitioned randomly: one subset for building the tree and another for pruning. For unpruned trees, there is no random element.
- Bagging [1].
- Random Subspaces [10]. For the dimension of the subspaces, two values were considered: 50% and 75% of the number of attributes.
- AdaBoost.R2 [5]. This method can be used with different loss functions. Three are proposed in [5] and used in this work: linear, square and exponential. The suffixes "-Li", "-Sq" and "-Ex" are used to denote the used function. Moreover, methods based on AdaBoost can be used in two ways [8]. In the reweighting version, the base model is trained with all the training data, it must take into account the weights distribution. In the resampling version, the base model is trained with a sample from the training data. This sample is constructed taken into account the weights. These versions are denoted with "-W" and "-S".
- Iterated Bagging [2]. Two configurations were considered 10×10 (Bagging is iterated 10 times, the ensemble size of each Bagging is 10) and 5×20 (Bagging

is iterated 5 times, the ensemble size of each Bagging is 20). In both cases, the maximum ensemble size is 100.

For all the configurations of these methods, two versions were considered: combined or not combined with Random Oracles.

Moreover, other methods were included in the study, as a baseline for the comparisons:

- A single Regression Tree, with and without pruning.
- Linear regression. Two versions were considered: using all the features and using only the selected features with the method described in [18].
- Nearest neighbors. There are two versions, in the first one the number of neighbors is 1. In the other, the number of neighbors is selected using "leave one out".

Weka [9] was used for the experiments. It includes the base method (Regression Tree), Bagging and Random Subspaces. The rest of the methods (i.e., Iterated Bagging and AdaBoost.R2), were implemented using this library.

Table 11.1 shows the characteristics of the 61 datasets considered, of which 30 have been collected by Luis Torgo[2]. All of them are available in the format used by Weka[3].

11.4 Results

In order to compare all the configurations considered, average ranks [3] are used. For each dataset, the methods are sorted according to their performance. The best method has rank 1, the second rank 2 and so on. If there are ties, these methods have the same rank, the average value. For each method, its average rank is calculated as the average value over all the considered datasets. According to [3], "*average ranks by themselves provide a fair comparison of the algorithms*".

Table 11.2 shows the methods sorted according to their average ranks. The prefix "$*-$" denotes methods that use Random Oracles. The 12 top positions are for methods that use Random Oracles.

For a method that uses Random Oracles, the benefit is defined as the difference between the average ranks of the corresponding method without Random Oracles and the method with Random Oracles. In Table 11.2, all the benefits are positive.

When comparing two methods, the number of datasets where one method has better, equal, or worse results than the other is calculated. According to [3], using a sign test, one method is significantly better than other, with a confidence level of 0.05, if the number of wins plus half the ties is at least $N/2 + 1.96\sqrt{N}/2$ (for $N = 61$ datasets, this number is 39). Table 11.2 shows, in the columns denoted as W/T/L, the paired comparisons of methods with Random Oracles and the corresponding methods without Random Oracles. The symbol "$\bullet$" denotes significant differences.

The number of wins, ties and losses and the average ranks are calculated using a direct comparison of the results for the different methods: less, equal or greater.

[2] `http://www.liaad.up.pt/~ltorgo/Regression/DataSets.html`
[3] `http://www.cs.waikato.ac.nz/ml/weka/index_datasets.html`

Table 11.1 Datasets used in the experiments

Dataset	Examples	Numeric	Nominal
2d-planes	40768	10	0
abalone	4177	7	1
ailerons	13750	40	0
auto93	93	16	6
auto-horse	205	17	8
auto-mpg	398	4	3
auto-price	159	15	0
bank-32nh	8192	32	0
bank-8FM	8192	8	0
baskball	96	4	0
bodyfat	252	14	0
bolts	40	7	0
breast-tumor	286	1	8
cal-housing	20640	8	0
cholesterol	303	6	7
cleveland	303	6	7
cloud	108	4	2
cpu-act	8192	21	0
cpu	209	6	1
cpu-small	8192	12	0
delta-ailerons	7129	5	0
delta-elevators	9517	6	0
detroit	13	13	0
diabetes-numeric	43	2	0
echo-months	130	6	3
elevators	16599	18	0
elusage	55	1	1
fishcatch	158	5	2
friedman	40768	10	0
fruitfly	125	2	2
gascons	27	4	0
house-16H	22784	16	0
house-8L	22784	8	0
housing	506	12	1
hungarian	294	6	7
kin8nm	8192	8	0
longley	16	6	0
lowbwt	189	2	7
machine-cpu	209	6	0
mbagrade	61	1	1
meta	528	19	2
mv	40768	7	3
pbc	418	10	8
pharynx	195	1	10
pole	15000	48	0
pollution	60	15	0
puma32H	8192	32	0
puma8NH	8192	8	0
pw-linear	200	10	0
pyrimidines	74	27	0
quake	2178	3	0
schlvote	38	4	1
sensory	576	0	11
servo	167	0	4
sleep	62	7	0
stock	950	9	0
strike	625	5	1
triazines	186	60	0
veteran	137	3	4
vineyard	52	3	0
wisconsin	194	32	0

Nevertheless, they do not take into account the size of the differences. For this purpose, we use the *quantitative scoring* [16, 20]. Given the results for two methods i and j in one dataset, this score is defined as

$$S_{i,j} = \frac{RMSE_j - RMSE_i}{\max(RMSE_i, RMSE_j)}$$

where $RMSE_i$ is the root mean squared error of method i. Unless both methods have zero error, this measure will be between -1 and 1, although it is usually expressed as a percentage. The sign indicates which method is better.

Figure 11.1 shows these scores (as percentages) for the considered methods, comparing the versions with and without Random Oracles. The score is calculated for each dataset and the datasets are sorted according to its score. The number of values above and below zero corresponds to the number of wins and losses in Table 11.2.

Table 11.2 Average ranks

Average	Method	Benefit	W/T/L
13.76	∗−AdaBoost.R2-S-Ex *(P)*	8.74	•51/0/10
15.02	∗−Bagging *(U)*	9.01	•54/0/7
15.91	∗−Iterated Bagging 5x20 *(P)*	5.66	•46/1/14
16.86	∗−AdaBoost.R2-S-Li *(P)*	8.73	•49/1/11
18.30	∗−Iterated Bagging 5x20 *(U)*	8.31	•52/1/8
18.53	∗−AdaBoost.R2-S-Sq *(P)*	6.70	•47/2/12
19.35	∗−AdaBoost.R2-S-Li *(U)*	10.25	•56/0/5
19.48	∗−AdaBoost.R2-S-Ex *(U)*	11.06	•54/0/7
19.60	∗−AdaBoost.R2-W-Sq *(U)*	10.21	•55/0/6
21.03	∗−AdaBoost.R2-W-Ex *(U)*	14.98	•60/0/1
21.30	∗−Random Subspaces 75% *(P)*	13.70	•60/0/1
21.57	∗−AdaBoost.R2-S-Sq *(U)*	6.70	• 48/1/12
21.57	Iterated Bagging 5x20 *(P)*		
21.95	∗−AdaBoost.R2-W-Li *(U)*	13.07	•56/0/5
21.98	∗−Bagging *(P)*	4.15	•43/1/17
22.50	AdaBoost.R2-S-Ex *(P)*		
22.54	∗−Randomization *(U)*	24.76	•61/0/0
24.03	Bagging *(U)*		
24.07	∗−Iterated Bagging 10x10 *(P)*	2.96	• 38/2/21
24.32	∗−Randomization *(P)*	6.57	•51/1/9
25.24	AdaBoost.R2-Sq-S *(P)*		
25.43	∗−AdaBoost.R2-W-Ex *(P)*	5.29	• 44/0/17
25.59	AdaBoost.R2-S-Li *(P)*		
26.12	Bagging *(P)*		
26.61	Iterated Bagging 5x20 *(U)*		
26.76	∗−Iterated Bagging 10x10 *(U)*	5.79	•47/1/13
26.98	∗−Random Subspaces 50% *(U)*	4.56	• 47/2/12
27.02	Iterated Bagging 10x10 *(P)*		
28.26	AdaBoost.R2-Sq-S *(U)*		
28.69	∗−AdaBoost.R2-W-Li *(P)*	3.04	• 39/1/21
28.89	∗−Random Subspaces 75% *(P)*	3.32	35/2/24
29.49	∗−AdaBoost.R2-W-Sq *(P)*	3.18	38/0/23
29.61	AdaBoost.R2-S-Li *(U)*		
29.81	AdaBoost.R2-W-Sq *(U)*		
30.53	AdaBoost.R2-S-Ex *(U)*		
30.72	AdaBoost.R2-W-Ex *(P)*		
30.89	Randomization *(P)*		
31.54	Random Subspaces 50% *(U)*		
31.73	AdaBoost.R2-W-Li *(P)*		
31.79	Linear Regression (all)		
31.79	K-NN (square)		
31.90	Linear Regression (selection)		
32.21	Random Subspaces 75% *(P)*		
32.55	Iterated Bagging 10x10 *(U)*		
32.67	AdaBoost.R2-W-Sq *(P)*		
33.53	K-NN (absolute)		
34.99	Random Subspaces 75% *(U)*		
35.02	AdaBoost.R2-W-Li *(U)*		
35.50	∗−Random Subspaces 50% *(P)*	0.80	30/0/31
36.02	AdaBoost.R2-W-Ex *(U)*		
36.30	Random Subspaces 50% *(P)*		
43.43	Tree *(P)*		
46.39	1-NN		
47.30	Tree *(U)*		

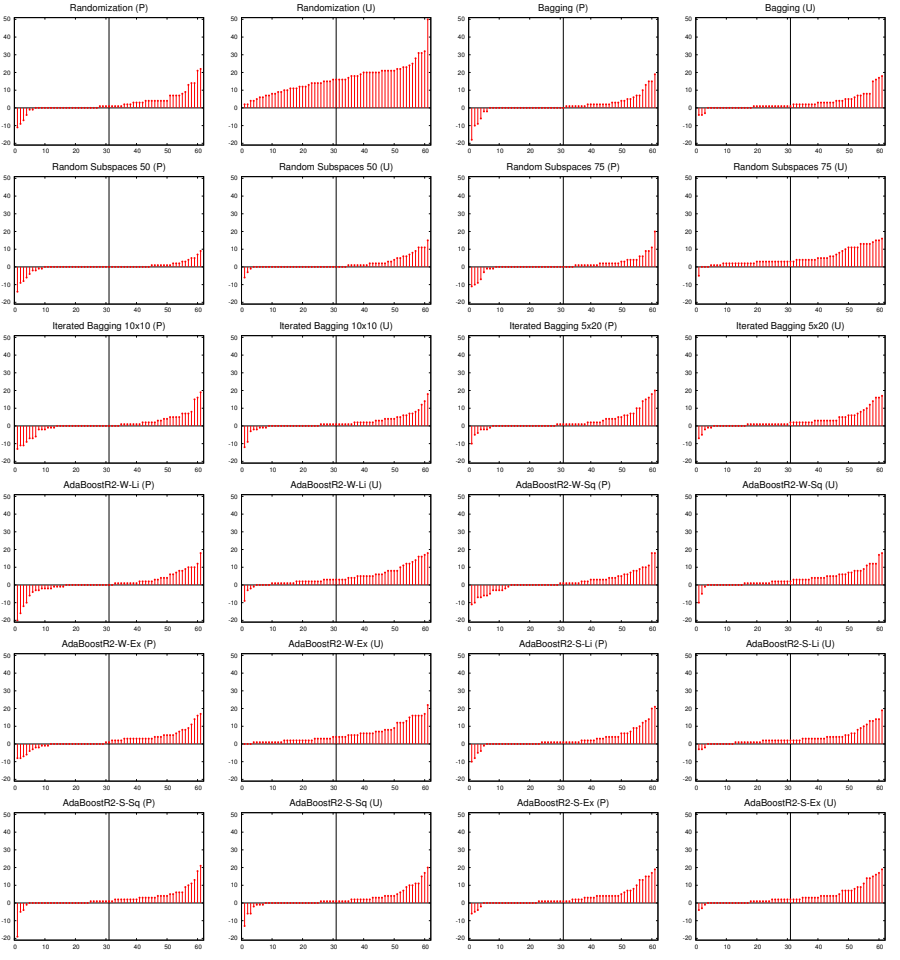

Fig. 11.1 Comparison scores

When comparing two methods with these graphs, it is desired to have more positive values than negative, but it is also desirable that the absolute values were greater for positive scores than for negative scores. For Random Oracles, there are more positive values and the greater absolute scores are also for positive values.

Results of ensemble methods depend on the ensemble size, the number of combined models. Figures 11.2 and 11.3 show the error as a function of the number iterations (from 1 to 100) for the different datasets. The graphs show the error for AdaBoost.R2-S-Ex *P* with and without Oracles. In general, the results are better with Oracles. For some datasets (e.g., echo-months, fruitfly, strike, veteran), the error increases with the number of iterations. This indicates that AdaBoost.R2 is not always robust with respect to the ensemble size. Nevertheless, the use of Oracles

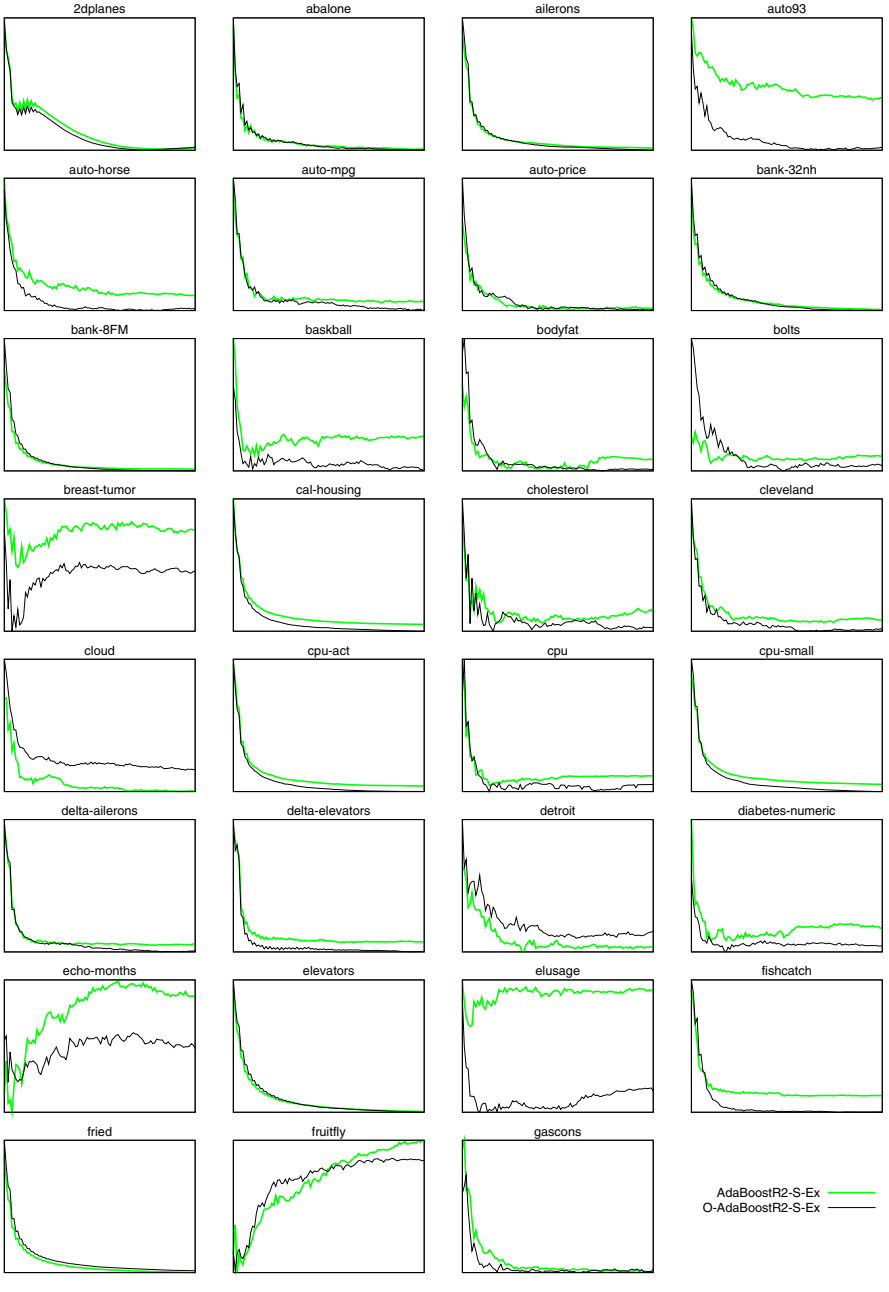

Fig. 11.2 Error as a function of the number of iterations for the different datasets, first part

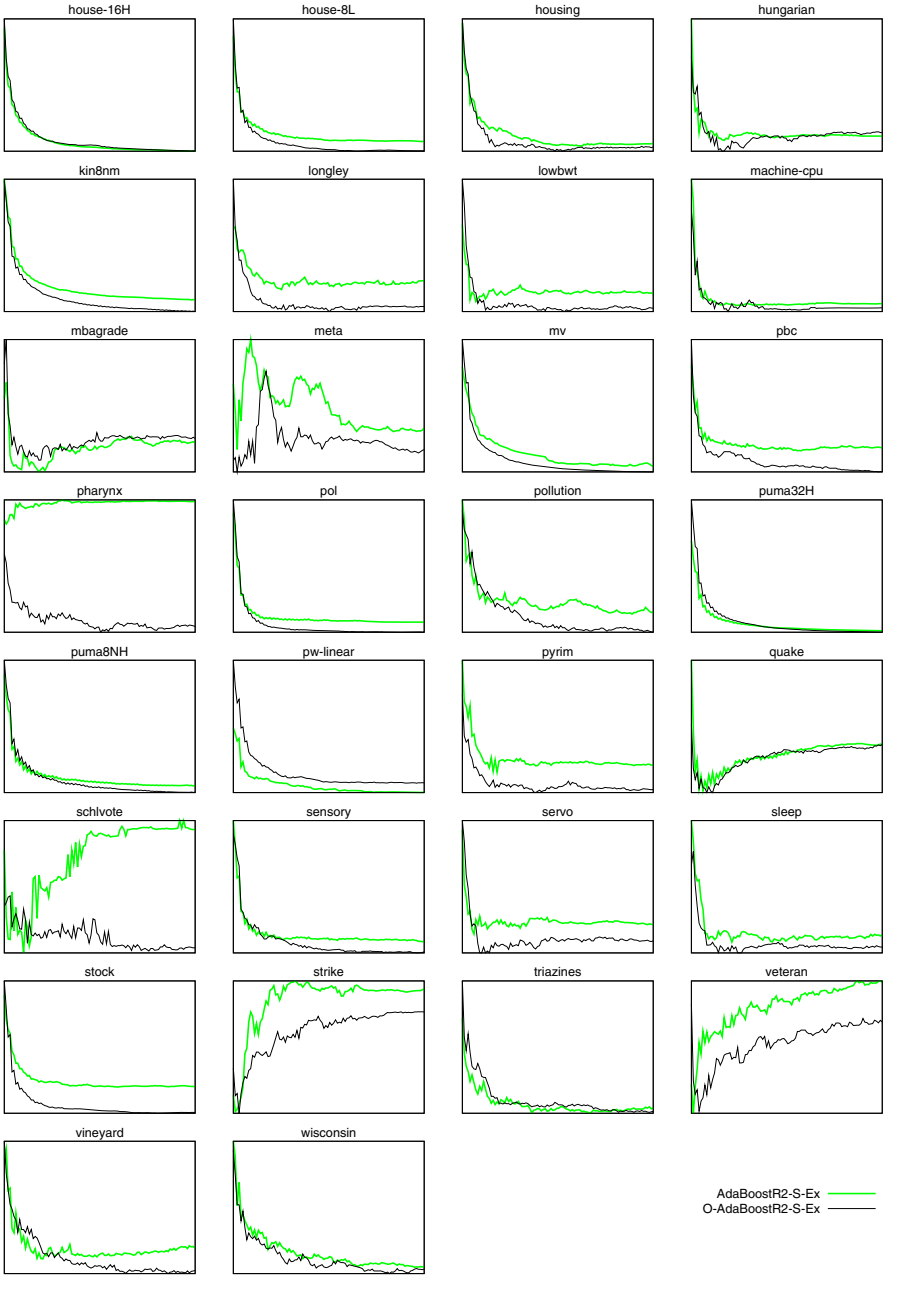

Fig. 11.3 Error as a function of the number of iterations for the different datasets, second part

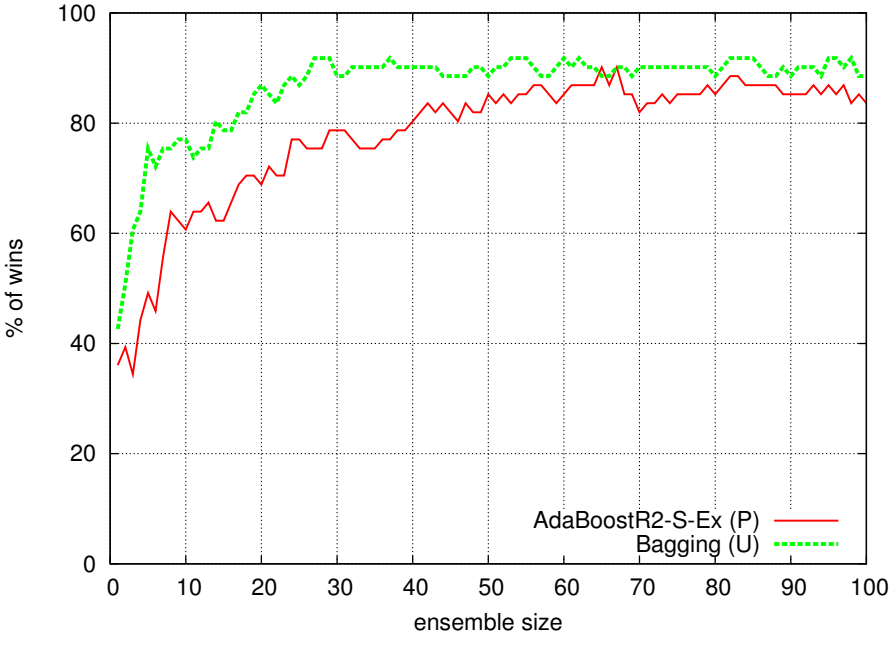

Fig. 11.4 Evolution of the percentage of wins when comparing the version with Oracle and the version without

strengthens its robustness in all the cases, in some of them, the use of Oracles is even able to change the error tendency, reducing it as the iterations increase, particularly notable are the cases of pharynx and schlvote.

Figure 11.4 shows a comparative of the versions with and without Oracles, as a function of the ensemble size. For Bagging *U* and AdaBoost.R2-S-Ex *P*, it shows the proportion of datasets where the version with Oracles is better than the version without Oracles. In the case of ties, they are considered as half a victory. If the ensemble size is very small, five or less, the version without Oracles can be better, but otherwise the advantage is for the version with Oracles.

11.5 Diversity-Error Diagrams

Successful ensembles are formed by models with low errors, but that are diverse. These two objectives are contradictory, because if the errors of two models are small, they cannot be very different. Several diversity measures had been proposed in order to analyze the behaviour of ensemble methods [11].

One of the techniques used is *diversity-error diagrams* [14]. They are scatter plots where there is a point for each pair of models. The horizontal axis represents the diversity between the two models, for classification, usually κ (kappa) is used. The vertical axis represents the average error of the two models.

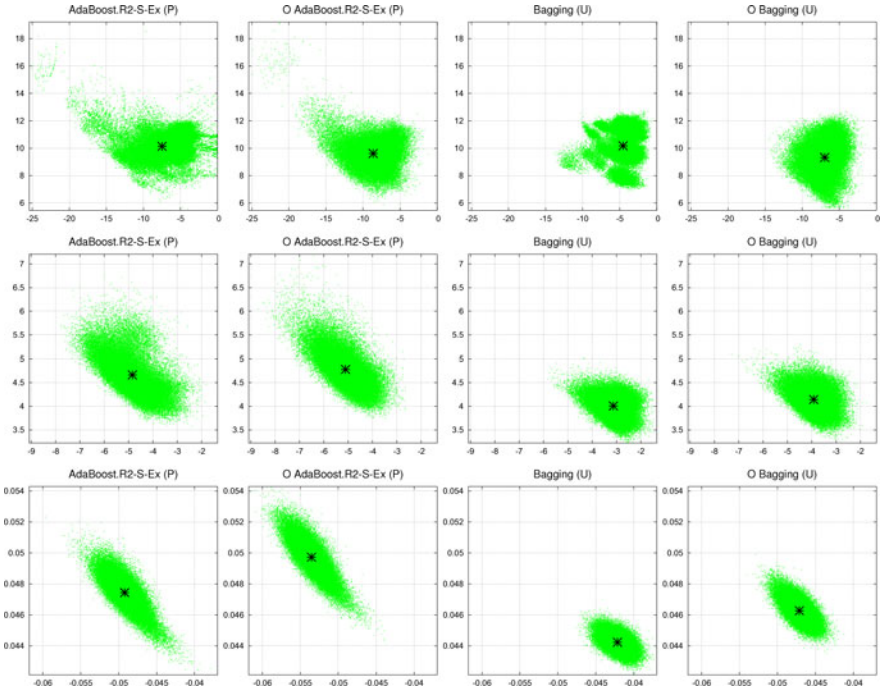

Fig. 11.5 Diversity error diagrams for "auto93" dataset (top row), "auto-mpg" dataset (middle row), and "bank-8FM" dataset (bottom row). The average point for each diagram is also shown.

In regression, several error measures can be considered, in this work RMSE was used:

$$RMSE = \sqrt{\sum_{i=1}^{n} \frac{(a_i - p_i)^2}{n}}$$

where a_i are the actual values and p_i are the predicted values.

For measuring the diversity, the negative RMSE of one of the models with respect to the other was used:

$$\text{negative } RMSE = -\sqrt{\sum_{i=1}^{n} \frac{(q_i - p_i)^2}{n}}$$

where p_i and q_i are the predictions of the two models. As with kappa, bigger values indicate less diversity.

Figure 11.5 shows, for three datasets, these diagrams for AdaBoost.R2-S-Ex P and Bagging U with and without oracles. In order to summarize these diagrams for all the datasets, *diversity-error movement diagrams* [15] are used. In these diagrams the relationship between the diversity-error diagrams of two methods for

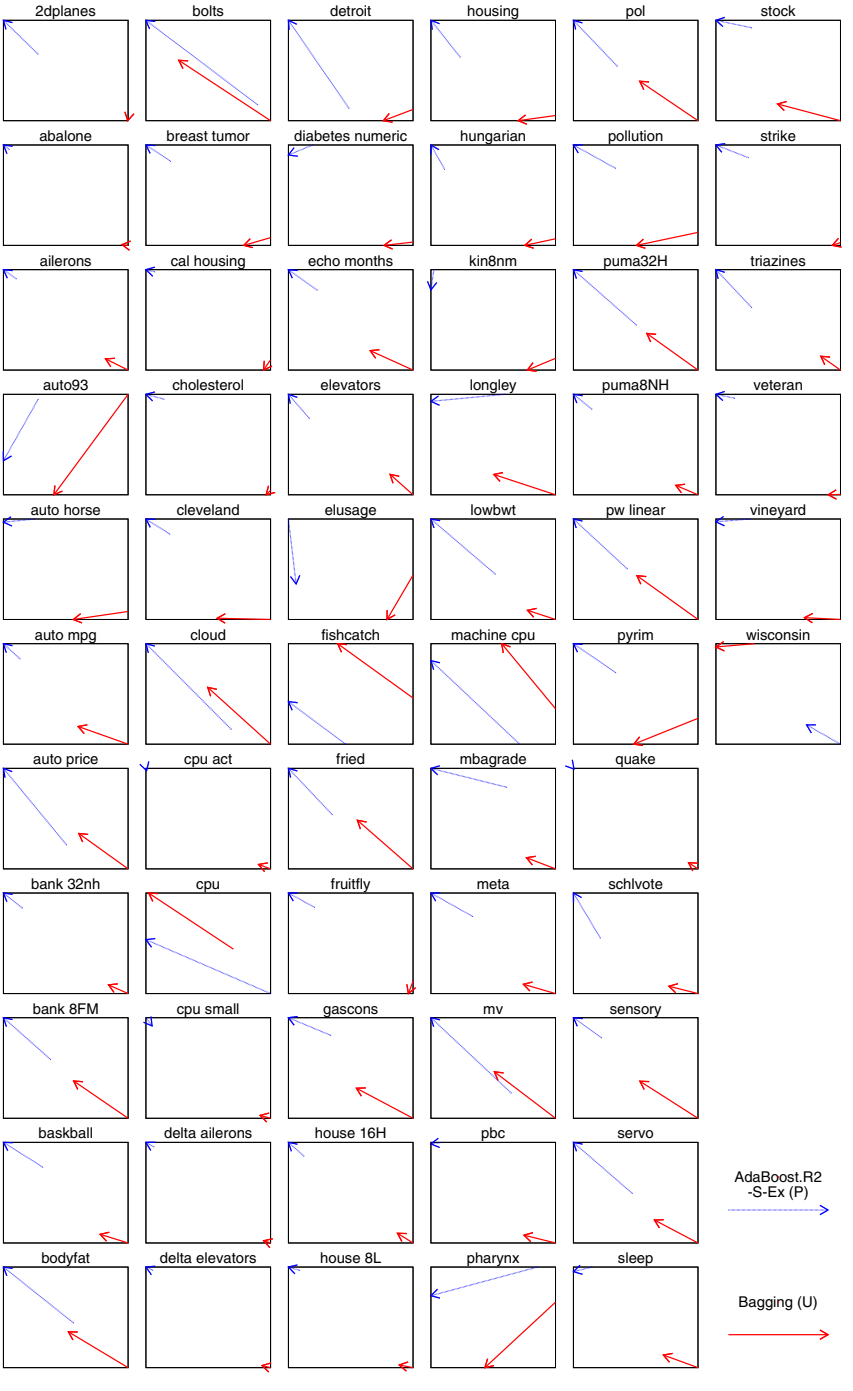

Fig. 11.6 Diversity error movement diagrams

the same dataset is represented using an arrow, the extremes of the arrow are the average points from the diversity-error diagrams. Figure 11.6 shows these diagrams for all the considered datasets. The origins of the arrows are for the methods without Random Oracles, while the heads are for the methods with Random Oracles. The majority of the arrows go to the left, this indicates that the base classifiers are more diverse when using Random Oracles. In general, the arrows go up, this means that the base classifiers have more error when using Random Oracles. The price for the increased diversity is the increased error, but in this case it is worth, because the error of the ensembles are generally smaller when using Random Oracles.

11.6 Conclusion

The performance of Random Oracles for regression ensembles have been studied, using 61 datasets and regression trees as base models. They have been combined with Bagging, Random Subspaces, AdaBoost.R2 and Iterated Bagging. For all the configurations considered using Random Oracles gives better results. The robustness of the method, as shown for AdaBoost, can be greatly increased by using Oracles as base models. The cause for these improvements is probably the increased diversity of the base models, as shown by the diversity-error diagrams.

Acknowledgements. We wish to thank the developers of Weka. We also express our gratitude to the donors of the different datasets.

Appendix: Source Code

This appendix includes the source code of the method. It is for Weka [9], version 3.7.2. The license is the GNU General Public License, version 2 or any later version.

```
package weka.classifiers.meta;

import java.util.Random;

import weka.classifiers.AbstractClassifier;
import weka.classifiers.Classifier;
import weka.classifiers.RandomizableSingleClassifierEnhancer;
import weka.core.DistanceFunction;
import weka.core.EuclideanDistance;
import weka.core.Instance;
import weka.core.Instances;
import weka.core.Randomizable;
import weka.core.WeightedInstancesHandler;

/** Random Linear Oracle. Can do classification and
 * regression depending on the base learner.
 */
```

```
public class LinearOracle
  extends RandomizableSingleClassifierEnhancer
  implements WeightedInstancesHandler {

  /** For serialization */
  static final long serialVersionUID = -9217393623430792225L;

  /** The number of sub-models */
  protected int m_NumSubModels = 2;

  /** The sub-models */
  protected Classifier [] m_SubModels = null;

  /** The distance function */
  protected DistanceFunction m_Distance = null;

  /** The selected instances */
  private Instances m_Selected;

  /**
   * Returns the corresponding region for a given instance
   *
   * @param inst the instance
   * @return the region
   * @throws Exception if there are not training instances
   */
  int region( Instance inst ) throws Exception {
    if ( m_Selected.numInstances( ) == 0 ) {
      throw new Exception( "No training instances!" );
    }

    double minDistance = m_Distance.distance( inst,
                         m_Selected.instance( 0 ) );
    int region = 0;
    for ( int i = 1; i < m_NumSubModels; i++ ) {
      Instance trainInstance = m_Selected.instance( i );
      double distance = m_Distance.distance( inst,
                        trainInstance );
      if ( distance < minDistance ) {
        minDistance = distance;
        region = i;
      }
    }
    return region;
  }
  /**
   * Calculates the class membership probabilities for the
   * given test instance.
   *
```

```
   * @param instance the instance to be classified
   * @return predicted class probability distribution
   * @throws Exception if distribution can't be computed
   * successfully
   */
  public double [] distributionForInstance( Instance
                                            instance )
    throws Exception {

    int r = region( instance );
    if ( m_SubModels[ r ] == null ) {
      // There is not a submodel for that region, a not
      // null submodel is selected
      for ( r = 0; r < m_SubModels.length; r++ ) {
        if ( m_SubModels[ r ] != null )
          break;
      }
    }

    return m_SubModels[ r ].distributionForInstance(
                            instance );
  }

  /**
   * Random Linear Oracle method.
   *
   * @param data the training data to be used for generating
   * the Random Linear Oracle model.
   * @throws Exception if the classifier could not be built
   * successfully
   */
  public void buildClassifier( Instances data )
    throws Exception {

    // Initializations
    m_Distance = new EuclideanDistance( data );
    Random random = data.getRandomNumberGenerator(
                    getSeed( ) );

    // Random selection of the instances
    m_Selected = new Instances( data, m_NumSubModels );
    int n = data.numInstances( );
    int previous = -1;
    for ( int i = 0; i < m_NumSubModels; i++ ) {
      int selected = random.nextInt( n );
      if ( previous == selected ) {
        // If the selected value if the same as for the
        // previous iteration,  we take the next one.
        // This guarantees at least two different instances.
```

```
      selected++;
      if ( selected >= n )
        selected = 0;
    }
    m_Selected.add( data.instance( selected ) );
    previous = selected;
  }

  // Initialize the data subsets
  Instances [] subDataset = new Instances[ m_NumSubModels ];
  for ( int i = 0; i < m_NumSubModels; i++ ) {
    subDataset[ i ] = new Instances( data, 0 );
  }

  // Split the instances in the subsets
  for ( int i = 0; i < data.numInstances( ); i++ ) {
    Instance inst = data.instance( i );
    subDataset[ region( inst ) ].add( inst );
  }

  // Build the sub-models
  m_SubModels = AbstractClassifier.makeCopies( m_Classifier,
                m_NumSubModels );
  boolean isRandomizable = m_Classifier instanceof
                           Randomizable;
  for ( int i = 0; i < m_NumSubModels; i++ ) {
    if ( subDataset[i].numInstances() == 0 ) {
      // If there are not instances, there is not a model
      m_SubModels[ i ] = null;
    }
    else {
      subDataset[ i ].randomize( random );
      if ( isRandomizable ) {
        ( ( Randomizable )m_SubModels[ i ] ).setSeed(
                                  random.nextInt() );
      }
      try {
        m_SubModels[ i ].buildClassifier( subDataset[ i ] );
      } catch( Exception e ) {
        // If the classifier has not ben built, there is
        // not a sub-model
        m_SubModels[ i ] = null;
      }
    }
  }
}

/**
 * Returns description of the Random Oracle model.
```

```
     *
     * @return description of the Random Oracle as a string
     */
    public String toString( ) {
      if ( m_SubModels == null )
        return "No model built yet!";
      String s = m_Classifier.toString( );
      for ( int i = 0; i < m_SubModels.length; i++ ) {
        s += "\n\nSubModel " + ( i + 1 ) + ":\n"
             + m_SubModels[ i ];
      }
      return s;
    }

    /**
     * Main method for testing this class.
     *
     * @param argv the options
     */
    public static void main( String [ ] argv )
    throws Exception {
      runClassifier( new LinearOracle( ), argv );
    }
  }
```

References

1. Breiman, L.: Bagging predictors. Machine Learning 24, 123–140 (1996)
2. Breiman, L.: Using iterated bagging to Debias regressions. Machine Learning 45, 261–277 (2001)
3. Demšar, J.: Statistical comparisons of classifiers over multiple data sets. J. Machine Learning Research 7, 1–30 (2006)
4. Dietterich, T.G.: Approximate statistical test for comparing supervised classification learning algorithms. Neural Comp. 10, 1895–1923 (1998)
5. Drucker, H.: Improving regressors using boosting techniques. In: Fisher, D.H. (ed.) Proc. the 14th Int. Conf. Machine Learning, Nashville, TN, pp. 107–115. Morgan Kaufmann, San Francisco (1997)
6. Elomaa, T., Kääriäinen, M.: An analysis of reduced error pruning. J. Artif. Intell. Research 15, 163–187 (2001)
7. Freund, Y., Schapire, R.E.: Experiments with a new boosting algorithm. In: Saitta, L. (ed.) Proc. the 13th Int. Conf. Machine Learning, Bari, Italy, pp. 148–156. Morgan Kaufmann, San Francisco (1996)
8. Freund, Y., Schapire, R.E.: A decision-theoretic generalization of on-line learning and an application to boosting. J. Comp. and Syst. Sciences 55, 119–139 (1997)
9. Hall, M., Frank, E., Holmes, G., Pfahringer, B., Reutemann, P., Witten, I.H.: The WEKA data mining software: An update. SIGKDD Explorations 11, 10–18 (2009)
10. Ho, T.K.: The random subspace method for constructing decision forests. IEEE Trans. Pattern Analysis and Machine Intell. 20, 832–844 (1998)

11. Kuncheva, L.I., Whitaker, C.J.: Measures of diversity in classifier ensembles. Machine Learning 51, 181–207 (2003)
12. Kuncheva, L.I.: Combining pattern classifiers: Methods and algorithms. John Wiley & Sons, Hoboken (2004)
13. Kuncheva, L.I., Rodríguez, J.J.: Classifier ensembles with a random linear oracle. IEEE Trans. Knowledge and Data Engineering 19, 500–508 (2007)
14. Margineantu, D.D., Dietterich, T.G.: Pruning adaptive boosting. In: Fisher, D.H. (ed.) Proc. 14th Int. Conf. Machine Learning, Nashville, TN, pp. 211–218. Morgan Kaufmann, San Francisco (1997)
15. Rodríguez, J.J., García-Osorio, C., Maudes, J.: Forests of nested dichotomies. Pattern Recognition Letters 31, 125–132 (2010)
16. Shrestha, D.L., Solomatine, D.P.: Experiments with AdaBoost.RT: An improved boosting scheme for regression. Neural Comp. 18, 1678–1710 (2006)
17. Suen, Y., Melville, P., Mooney, R.: Combining bias and variance reduction techniques for regression trees. In: Gama, J., Camacho, R., Brazdil, P.B., Jorge, A.M., Torgo, L. (eds.) ECML 2005. LNCS (LNAI), vol. 3720, pp. 741–749. Springer, Heidelberg (2005)
18. Wang, Y., Witten, I.H.: Induction of model trees for predicting continuous classes. In: van Someren, M., Widmer, G. (eds.) ECML 1997. LNCS, vol. 1224, pp. 128–137. Springer, Heidelberg (1997)
19. Witten, I.H., Frank, E.: Data mining: Practical machine learning tools and techniques. Morgan Kaufmann, San Francisco (2005)
20. Zhang, C., Zhang, J., Wang, G.: An empirical study of using Rotation Forest to improve regressors. Applied Mathematics and Comp. 195, 618–629 (2008)

Chapter 12
Embedding Random Projections in Regularized Gradient Boosting Machines

Pierluigi Casale, Oriol Pujol, and Petia Radeva

Abstract. Random Projections are a suitable technique for dimensionality reduction in Machine Learning. In this work, we propose a novel Boosting technique that is based on embedding Random Projections in a regularized gradient boosting ensemble. Random Projections are studied from different points of view: pure Random Projections, normalized and uniform binary. Furthermore, we study the effect to keep or change the dimensionality of the data space. Experimental results performed on synthetic and UCI datasets show that Boosting methods with embedded random data projections are competitive to AdaBoost and Regularized Boosting.

12.1 Introduction

Random Projections (RPs) have been widely employed as dimensionality reduction technique. RPs are based on the idea that high dimensional data can be projected into a lower dimensional space without significantly losing the structure of the data. RPs can also be viewed as a tool for generating diversity in the creation of an ensemble of classifiers. The underlying idea is the same used in various new ensemble methods such as Rotation Forest [11] or Rotboost [13]. Using RPs, the different embeddings of the original feature space provide multiple view of the original features space. This kind of diversity can be generated while projecting data into subspaces, the space having the dimensionality of the original feature space or even spaces of higher dimensionality than the original one. Here, different Random Projections are studied and applied in the construction of a Boosting ensemble.

Pierluigi Casale
Computer Vision Center, Barcelona, Spain
E-mail: pierluigi@cvc.uab.es

Oriol Pujol · Petia Radeva
Dept. of Applied Mathematics and Analysis, University of Barcelona, Barcelona, Spain
Computer Vision Center, Barcelona, Spain
E-mail: {oriol,petia}@maia.ub.es

O. Okun et al. (Eds.): Ensembles in Machine Learning Applications, SCI 373, pp. 201–216.
springerlink.com

From the point of view of incremental optimization, AdaBoost can be viewed as an additive model fitting procedure that approximates the optimization of an exponential loss function. Changing the exponential loss function with a least square loss function yields to a new model of Boosting, known as LsBoost [7]. Gradient Boosting Machines (GBMs) generalize this idea for any arbitrary loss function. In this study, RPs have been integrated into the LsBoost algorithm. The stepwise approximation is obtained by projecting data onto random spaces at each step of the optimization process and searching for the classifier that best fits the data in the new space. Nevertheless, fitting the data too closely yields to poor results. Regularization methods attempt to prevent the over-fitting by constraining the fitting procedure. For that reason, a study on the effect of the L2 penalization term has also been conducted.

The approach has been evaluated on synthetic and real problems datasets. The new method has been compared with AdaBoost and LsBoost. Results show that the new method is competitive with respect to AdaBoost and LsBoost and, for some specific problems, using RPs significantly improves the classification accuracy. Additionally, results show that the use of the L2 regularization parameter is specially justified as a way to avoid overfitting and model noise ensuring smoothness in the solutions.

This chapter is organized as follows. In the next section, previous works about RPs in the Machine Learning are briefly reported. In Sect. 12.3, GBMs and RPs are formally introduced and the proposed method for embedding RPs into GMBs is described. In Sect. 12.4, results are reported and finally, in Sect. 12.5, we give conclusions.

12.2 Related Works on RPs

Arriaga and Vempala [1] propose an algorithmic theory of learning based on RPs and robust concepts. They show how RPs are a suitable procedure for reducing dimensionality while preserving the structure of the problem. In their work, they proposed a very simple learning algorithm based on RPs mainly consisting in two steps: randomly projecting the data into a random subspace and running the algorithm in that space, taking advantage of working with a lower dimensionality. Blum [2] reports this basic algorithm showing how, if a learning problem is separable with a large margin, the problem still remains separable in a reduced random space. Moreover, even picking a random separator on data projected down to a line, provides a reasonable change to get a weak hypothesis as well. Dasgupta [3] used RPs with Gaussian mixture models for classification of both synthetic and real data. In his work, data are projected into a randomly chosen d-dimensional subspace and the learning algorithm works in this new smaller space, achieving highly accurate classification results. In the context of supervised learning, Fradkin and Madigan [5] compare the performances of C4.5, Nearest Neighbours and SVM, using both PCA and RPs as dimensionality reduction technique. The results of their experiments are always favorable to PCA. More recently, Rahimi and Recht [10] use also Random

Projections for building a weighted sum of linear separators. In their work, authors show that using Random Projections is equivalent to use the kernel trick. At the same time, Random Projections provide a faster decaying of the testing error rate with respect to the standard AdaBoost.

12.3 Methods

In this section, the formulation of both GBMs and RPs is presented. Starting from LsBoost algorithm, a particular definition of GBMs, a new method for embedding RPs into the GBMs is described. The method is a slight modification of the original LsBoost algorithm. In the modified version, training data are projected onto random spaces where the best classifier fitting the data is found.

12.3.1 Gradient Boosting Machines

In regression and classification problems, given a set of training sample $\{y_i,\mathbf{x}_i\}_1^N$, we look for a function $F^*(\mathbf{x})$ that maps $\mathbf{x}$ to y such that, over the joint distribution of all $(y,\mathbf{x})$-values, the expected value of some specified loss function $\Psi(y,F(x))$ is minimized. Usually, the function $F(\mathbf{x})$ is member of parameterized class of functions $F(\mathbf{x};\mathbf{P})$:

$$F(\mathbf{x};\mathbf{P}) = \sum_{m=0}^{M} \beta_m h(\mathbf{x};\mathbf{a}_m) \,, \tag{12.1}$$

where $\mathbf{P} = \{\beta_m, \mathbf{a}_m\}_0^M$ is a set of parameters. Nevertheless, we can consider $F(\mathbf{x})$ evaluated at each point $\mathbf{x}$ to be a parameter and minimize:

$$\Phi(F(\mathbf{x})) = E_y[\Psi(y,F(\mathbf{x})|\mathbf{x})], \tag{12.2}$$

at each individual $\mathbf{x}$, directly with respect to $F(\mathbf{x})$. The solution is of the type:

$$F^*(\mathbf{x}) = \sum_{m=0}^{M} f_m(\mathbf{x}) \,, \tag{12.3}$$

where $f_0(\mathbf{x})$ is an initial guess, and $\{f_m\}_1^M$ are incremental functions, known as "steps" or "boosts". Using steepest-descent, we get :

$$f_m(\mathbf{x}) = -\rho_m g_m(\mathbf{x}) \,, \tag{12.4}$$

where, assuming that differentiation and integration can be interchanged,

$$g_m(\mathbf{x}) = E_y\left[\frac{\partial \Psi(y,F(\mathbf{x}))}{\partial F(\mathbf{x})}|\mathbf{x}\right]_{F(\mathbf{x})=F_{m-1}(\mathbf{x})} \tag{12.5}$$

and

$$F_{m-1}(\mathbf{x}) = \sum_{i=0}^{m-1} f_i(\mathbf{x}). \tag{12.6}$$

When the joint distribution of $(y,\mathbf{x})$ is represented by a finite data sample, $E_y[\cdot|\mathbf{x}]$ cannot be evaluated accurately at each $\mathbf{x}_i$ and, if we could perform parameter optimization, the solution is difficult to obtain. In this case, given the current approximation $F_{m-1}(\mathbf{x})$ at the m-th iteration, the function $\beta_m h(\mathbf{x};\mathbf{a})$ is the best greedy step towards the minimizing solution $F^*(\mathbf{x})$, under the constraint that the step direction $h(\mathbf{x},\mathbf{a}_m)$ be a member of the parameterized class of functions $h(\mathbf{x},\mathbf{a})$. One possibility is to choose the member of the parameterized class $h(\mathbf{x};\mathbf{a})$ that is most parallel in the N-dimensional data space with the unconstrained negative gradient $\{-g_m(\mathbf{x}_i)\}_1^N$. In this case, it is possible to use $h(\mathbf{x},\mathbf{a}_m)$ instead of the unconstrained negative gradient $-g_m(\mathbf{x})$. Weights ρ_m are given by the following line search:

$$\rho_m = argmin_\rho \sum_{i=1}^{N} \Psi(y_i, F_{m-1}(\mathbf{x}_i) + \rho h(\mathbf{x}_i;\mathbf{a}_m)) \tag{12.7}$$

and the approximation updated in the following way:

$$F_m(\mathbf{x}) = F_{m-1}(\mathbf{x}) + \rho_m h(\mathbf{x};\mathbf{a}_m). \tag{12.8}$$

When $y \in \{-1,1\}$ and the loss function $\Psi(y,F)$ depends on y and F only through their product $\Psi(y,F) = \Psi(yF)$, the algorithm reduces to Boosting. If the loss function is $\Psi(y,F) = \frac{(y-F)^2}{2}$, gradient boosting produces the stagewise approach of iteratively fitting the current residuals. The algorithm, shown in Table 12.1, is called LsBoost.

Table 12.1 LsBoost Algorithm

1.	$F_0(\mathbf{x}) = argmin_\rho \sum_{i=1}^N \Psi(y_i,\rho)$
2.	For $m = 1$ to M or meanwhile $error > \varepsilon$ do:
3.	$\tilde{y}_i^m = y_i - F_{m-1}, i = 1,N$
4.	$(\rho_m,\mathbf{a}_m) = argmin_{\mathbf{a},\rho} \sum_{i=1}^N [\tilde{y}_i^m - \rho h(\mathbf{x}_i;\mathbf{a})]^2$
5.	$F_m(\mathbf{x}) = F_{m-1}(\mathbf{x}) + \rho_m h(\mathbf{x}_i;\mathbf{a}_m)$
6.	End

12.3.2 Random Projections

RPs are techniques that allow to reduce the dimensionality of a problem while still retaining a significant degree of the structure of the data. The Johnson-Lindenstrauss Lemma [8] states that, given m points in $\Re^n$, it is possible to project these points into a d-dimensional subspace, with $d = O(\frac{1}{\gamma^2} log(m))$. In this space, relative distances and angles between all pairs of points are approximately preserved up to $1 \pm \gamma$, with high probability.

Formally, given $0 < \gamma < 1$, a set X of m points in $\Re^N$, and a number $n > n_0 = O(\frac{1}{\gamma^2} log(m))$, there is a Lipschitz function $f : \Re^N \rightarrow \Re^n$ such that

$$(1-\gamma)\|u-v\|^2 \leq \|f(u)-f(v)\|^2 \leq (1+\gamma)\|u-v\|^2. \tag{12.9}$$

If m data points in a feature space are considered row-vectors of length N, the projection can be performed by multiplying all the m points by a randomly generated $N \times n$ matrix. The random matrix should be one of the following types:

- P with columns to be d pure random orthonormal vectors;
- $U_{-1,1}$ with each entry to be 1 or -1 drawn independently at random;
- $N_{0,1}$ with each entry drawn independently from a standard Normal Distribution $N(0,1)$.

While using these types of projections ensures that relative distances and angles are approximately preserved, there is no guarantee that using other types of matrices could preserve the structure of the data. Though data might be projected down to much lower dimensions or into the same space [2], projecting data onto spaces of higher dimension does not rely on any theoretical results. Here, the possibility to project data in a superspace is also taken into account.

12.3.3 Random Projections in Boosting Machine

The original algorithm of LsBoost has been slightly modified to be adapted to RPs. In the line 4 of the algorithm in Table 12.1, it is possible first searching analytically for the optimal set of weighting values for each candidate classifier and select the classifier that best approximates the negative gradient with the corresponding precomputed weight [9]. It is possible to find the optimal weighting value for each candidate classifier $h(x;a)$ by:

$$\frac{\partial[(\tilde{\mathbf{y}}^m - \rho_a^T h(x;a))^T(\tilde{\mathbf{y}}^m - \rho_a^T h(x;a))]}{\partial \rho_a} = 0 \tag{12.10}$$

solved by

$$\tilde{\mathbf{y}^m}^T h(x;a) = \rho_a^T h(x;a)^T h(x;a) = \rho_a^T N. \tag{12.11}$$

where, since $h(x;a) \in \{+1,-1\}$, the dot product $h(x;a)^T h(x;a)$ is just the number of training examples and the regularization parameter might simply be added. Therefore, the optimal set of weights is given by Eq.(12.12)

$$\rho_m = \frac{\tilde{\mathbf{y}}^m A}{N+\lambda}, \tag{12.12}$$

where $\tilde{\mathbf{y}}^m$ denotes the vector of residuals at step m, A is the matrix of training examples, N is the number of training examples and λ represents the L2 penalization

term. For $\lambda = 0$, regularization is not taken into account. Once the optimal set of values is found, a simple selection of the classifier that best approximates the negative gradient can be performed. The described procedure can be performed on training data projected onto random spaces.

Therefore, *RpBoost* is defined as Regularized Gradient Boosting where before considering the data by the weak classifiers, they are projected by a transformation represented by a specific RPs technique. Table 12.2 defines the RpBoost algorithm. In addition, the following is defined :

Definition 12.1. *Rpboost.sub* as RpBoost working of data projected into a random subspace;

Definition 12.2. *Rpboost.same* as RpBoost working of data projected into a random space of the same dimension than the original feature space;

Definition 12.3. *Rpboost.super* as RpBoost working of data projected into a random superspace.

Table 12.2 RpBoost Algorithm

Select the type of projection in $\{P, N_{0,1}, U_{-1,1}\}$
Set the dimension of the random space
Set the random matrix R_p
1. $F_0(\mathbf{x}) = argmin_\rho \sum_{i=1}^{N} \Psi(y_i, \rho)$
2. For $m = 1$ to M do:
3. $\quad \tilde{y}_i^m = y_i - F_{m-1}, i = 1, N$
4. $\quad$ Set a new R_p
5. $\quad A_r = AR_p$
6. $\quad \rho_m = \frac{\tilde{y}_m A_r}{N+\lambda}$
7. $\quad \mathbf{a}_m = argmin_{\mathbf{a}} \sum_{i=1}^{N} [\tilde{y}_i^m - \rho_m h(\mathbf{x}_i; \mathbf{a})]^2$
8. $\quad F_m(\mathbf{x}) = F_{m-1}(\mathbf{x}) + \rho_m h(\mathbf{x}_i; \mathbf{a}_m)$
9. End

12.4 Experiments and Results

In order to test the performance of RpBoost, several tests on synthetic and real problems have been performed. RpBoost is compared with AdaBoost and LsBoost. In this setting, decision stumps are used as weak classifiers. The maximum dimension of the ensemble has been set to 500 classifiers. In order to have a straightforward comparison, in all the experiments, the dimension of the subspace and of the superspace have been set equal to the half and the double of the dimension of the feature space, respectively RPs are performed using a matrix $M \in \{P, U_{-1,1}, N_{0,1}\}$. Finally, results related to the effect of regularization in the creation of the ensemble are shown in the last section.

12.4.1 Test Patterns

Test patterns are synthetic bidimensional datasets proposed by Fawcett [4] for comparing classifiers. The patterns are randomly generated on a 2-D grid of points, between [0:4] x [0:4] with a resolution of 0.05, yielding 6561 total points. The points are labeled based on where they fall in the pattern. In Table 12.3, the formal description of patterns is reported. In Fig. 12.1, examples of the patterns are presented.

Table 12.3 Test Patterns

Test Pattern	Description
Sine	$Y = 0.84sin(1.78X)$
Linear	$Y = 1.87X \pm 1.74$
Parity	9 parity circles
Annulus	Annulus at (2.00, 2.00)
Parabolic	$Y = \frac{(X-2)^2}{4*0.25+1}$
Disjunctive	4 disjoint concave polygons
Polynomial	$Y = \frac{1}{2}(x-2)^3 + \frac{1}{2}(x-2.2)^2 + 2$
Checkerboard	9 squares alternating classes

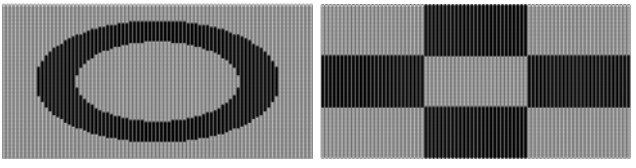

(a) (b)

Fig. 12.1 Examples of Test Patterns:(a) *Annulus* Test Pattern;(b) *Checkerboard* Test Pattern

Validation Procedure. For each test pattern, a stratified sample of 1000 points is used for training and the complete distribution as testing. The validation procedure has been performed five times and results are averaged.

Results. Comparative results of RpBoost are reported in Fig. 12.2 for P projections and in Fig. 12.3 for $U_{-1,1}$ projections. RpBoost performs slightly better than AdaBoost and LsBoost using both types of projections on some patterns. Additionally, RpBoost.sub with P projections always performs considerably worst than RpBoost.same and RpBoost.super and RpBoost.super with $U_{-1,1}$ always performs worst the RpBoost.same and RpBoost.sub. In the *parity* and in the *checkerboard* test patterns, RpBoost always performs better than the compared methods, disregarding the type of projection.

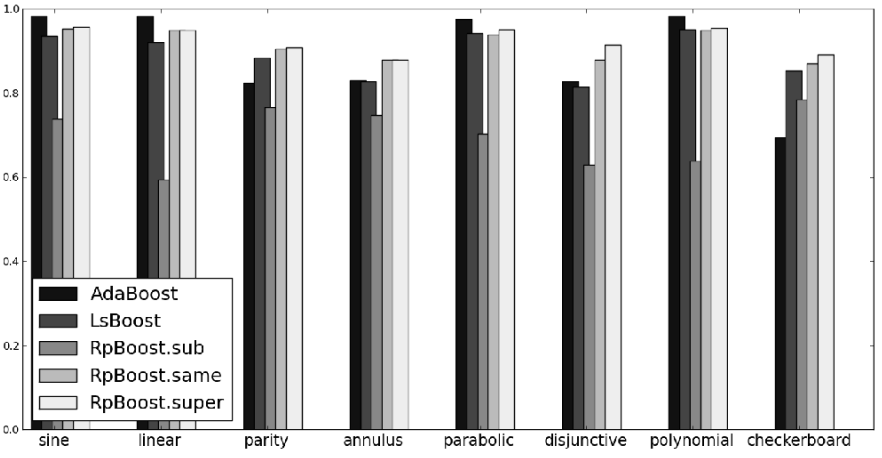

Fig. 12.2 Comparative Results of RpBoost with P projections on Test Patterns

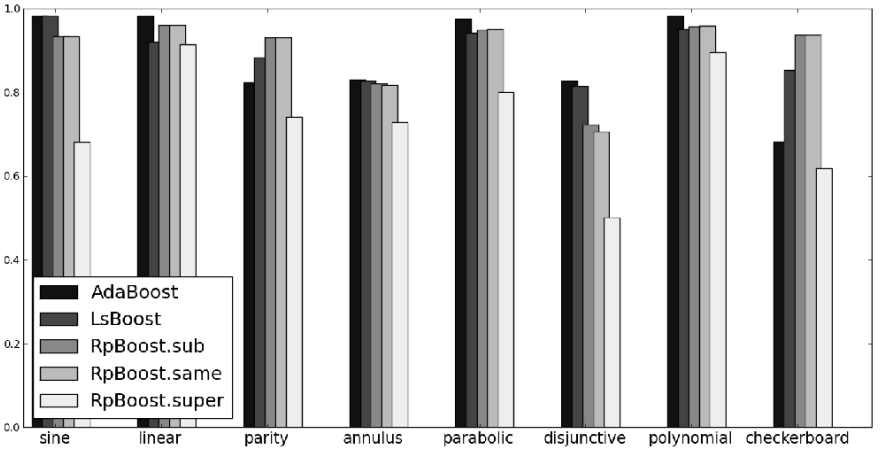

Fig. 12.3 Comparative Results of RpBoost with $U_{-1,1}$ projections on Test Patterns

In Fig. 12.4, comparative results using $N_{0,1}$ projections are shown. Numerical results are reported in Table 12.4. RpBoost.sub and RpBoost.same always provide the best performance. In particular, in the *annulus* and in the *checkerboard* pattern the classification accuracy of RpBoost is considerably improved. Even for the $N_{0,1}$ projections, projecting data to superspaces does not provide benefits for the classification.

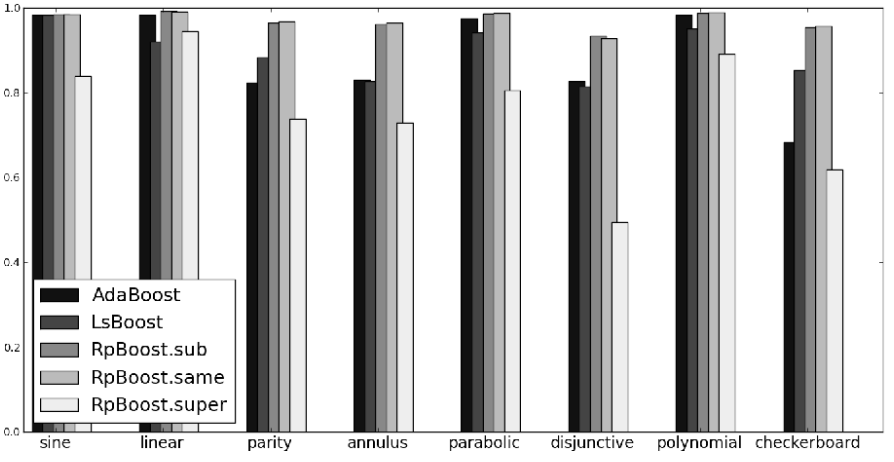

Fig. 12.4 Comparative Results of RpBoost with $N_{0,1}$ projections on Test Patterns

Table 12.4 Numerical Values of Accuracy on Test Patterns obtained with AdaBoost (Ada), LsBoost (Ls), RpBoost.sub (Sub) , RpBoost.same (Same) and RpBoost.super (Super) with $N_{0,1}$ projections

	Ada	Ls	Sub	Same	Super
sine	0.983	0.937	**0.986**	0.985	0.84
linear	0.984	0.921	**0.993**	0.992	0.946
parity	0.824	0.884	0.966	**0.968**	0.738
annulus	0.83	0.828	0.963	**0.965**	0.73
parabolic	0.976	0.943	0.987	**0.989**	0.806
disjunctive	0.827	0.816	**0.935**	0.928	0.495
polynomial	0.984	0.951	0.988	**0.99**	0.892
checkerboard	0.694	0.854	0.955	**0.957**	0.62

12.4.2 UCI Datasets

RpBoost, AdaBoost and LsBoost have been compared on eight datasets from UCI Repository [6]. The results are reported in Table 12.5, with the number of elements per class. All the datasets selected are binary classification problems.

Validation Procedure. Results have been obtained using 10-folds cross-validation. The procedure has been run two times and results have been averaged. The value of the regularization parameter has been selected using 5-fold cross validation on the training set.

Table 12.5 List of UCI Datasets

Dataset	Elements
Monks-1	272,284
Monks-2	300,301
Monks-3	275, 279
Breast	239,485
Liver	100,245
Tic-Tac-Toe	626,332
Ionosphere	126,225
Sonar	97,111

Results. Comparative results of RpBoost are reported in Fig. 12.5 for P projections and in Fig. 12.6 for $U_{-1,1}$ projections. As for synthetic data, there exist problems where RpBoost outperforms AdaBoost and LsBoost. In particular, only for P projections, RpBoost.super provides better classification accuracies. In Fig. 12.7, the mean accuracy obtained with AdaBoost, LsBoost and RpBoost using $N_{0,1}$ is shown. Numerical values are reported in Table 12.6. In Monks-1 and Monks-2 RpBoost outperforms AdaBoost and LsBoost. In Monks-3, performance is slightly improved. A slight improvement can also be noted in Breast, Sonar and Ionoshpere – the datasets having the highest dimensions; it seems that there are no benefits from the dimensionality reduction that RPs provide.

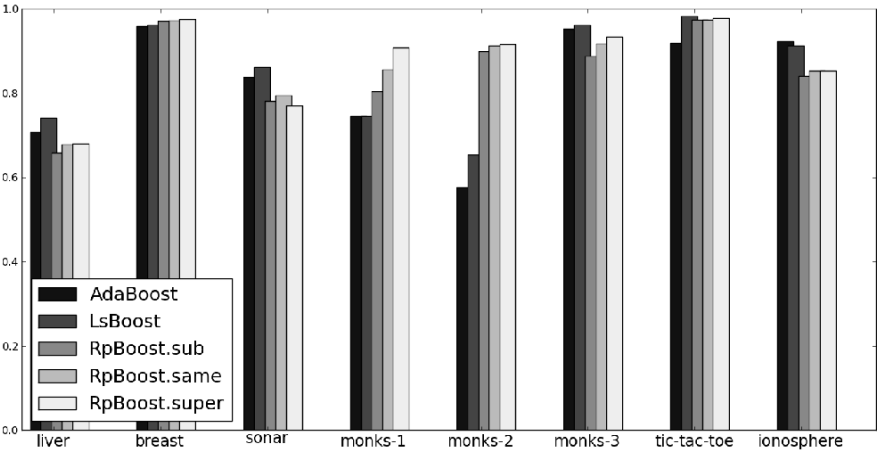

Fig. 12.5 Comparative Results of RpBoost with P projections on UCI datasets

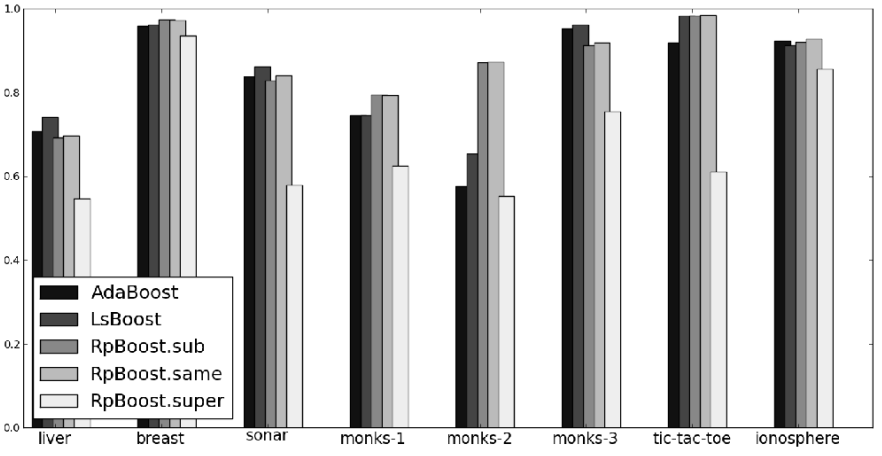

Fig. 12.6 Comparative Results of RpBoost with $U_{-1,1}$ projections on UCI datasets

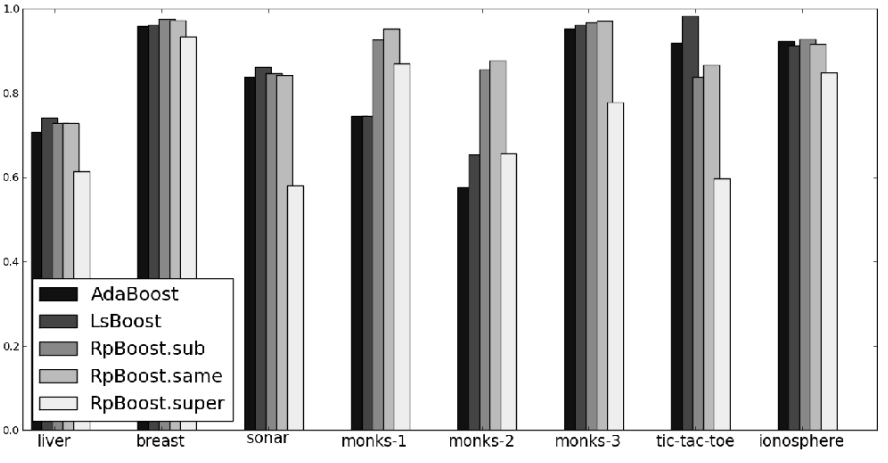

Fig. 12.7 Classification Accuracy on UCI Datasets obtained with AdaBoost, LsBoost and RpBoost with $N_{0,1}$ projections

12.4.3 The Effect of Regularization in RpBoost

In order to study the effect of the regularization parameter λ, a 10-fold cross validation over two runs of cross validation for

$$\lambda \in \{1, 5, 10, 50, 100, 500, 1000, 5000, 10000\}$$

for each dataset and for each type of projection has been performed. From the experiments, it is evident how the effect of the regularization parameter can be noted

Table 12.6 Numerical Values of Accuracy on Uci Datasets obtained with AdaBoost (Ada), LsBoost (Ls), RpBoost.sub (Sub), RpBoost.same (Same) and RpBoost.super (Super) with $N_{0,1}$ projections

	Ada	Ls	Sub	Same	Super
liver	0.708	**0.742**	0.692	0.698	0.547
breast	0.959	0.962	**0.974**	0.973	0.937
sonar	0.839	**0.862**	0.829	0.841	0.579
monks-1	0.746	0.746	**0.796**	0.794	0.625
monks-2	0.577	0.654	0.872	**0.873**	0.554
monks-3	0.953	**0.963**	0.913	0.919	0.756
tic-tac-toe	0.92	0.983	0.983	**0.986**	0.611
ionosphere	0.924	0.914	0.921	**0.928**	0.857

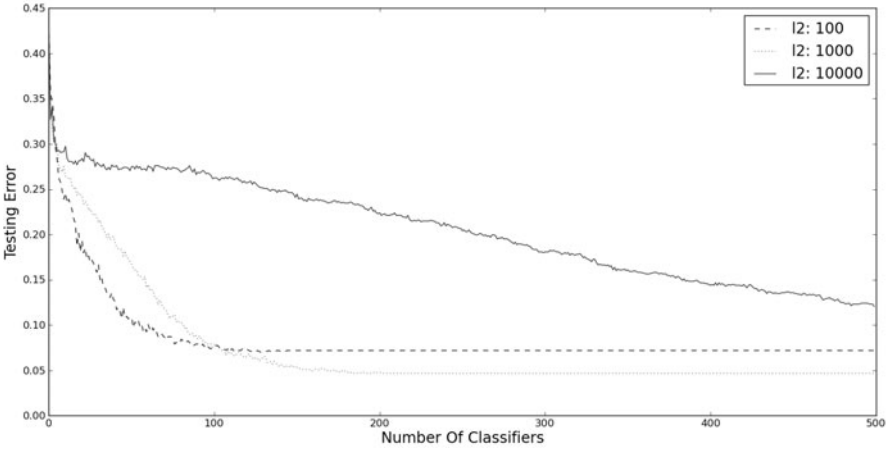

Fig. 12.8 Testing Error of RpBoost.same using $N_{0,1}$ in Monks-1 dataset for different regularization parameters.

at the initial phase of the construction of the ensemble, before the convergence of the optimization process. The principal benefits of using a proper value for λ are tied to the speed of the optimization process. In Fig. 12.8, the testing error RpBoost.same using $N_{0,1}$ projections on the Monks-1 dataset is shown. Values of λ are in $\{100, 1000, 10000\}$. Here, a typical trend is shown where it is possible to see how the optimization process converges slower when the value of λ increases. It is also evident how, in the former steps of the optimization process, λ influences the construction of the ensemble. In Fig. 12.9, the testing error RpBoost.same using $U_{-1,1}$ projections on the Liver dataset is shown. Here, it is evident how, with a proper value of λ, the testing error rapidly slows down and the overfitting is prevented. It is evident that for $\lambda = 100$, overfitting is present. In Fig. 12.10, the testing error

RpBoost.same using $U_{-1,1}$ projections on the Breast dataset is shown. In this figure, overfitting is more evident and, in particular, only for $\lambda = 10000$ the classifier does not tend to overfit. We should also note about the order of magnitude of the regularization parameter. In the last case, a very big value is needed. In Eq. (12.12) the regularization parameter is present in the denominator. This fact means that very little weights are needed in the step-wise approximation process.

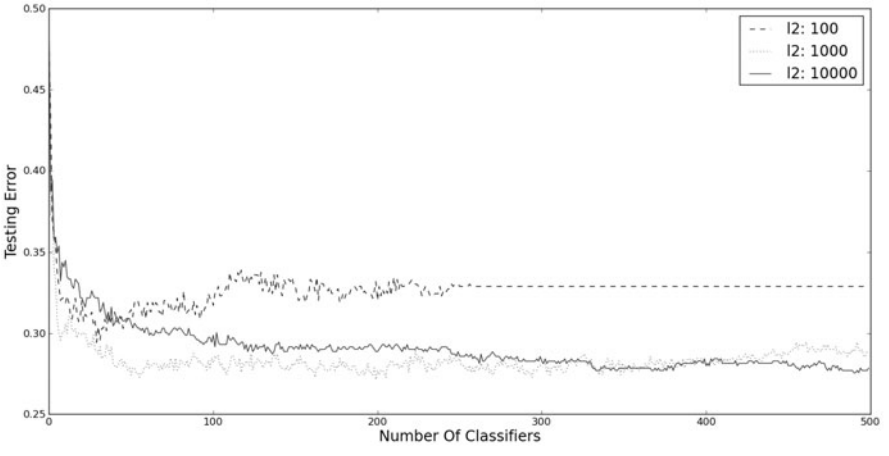

Fig. 12.9 Testing Error of RpBoost.same using $U_{-1,1}$ in Liver dataset for different regularization parameters.

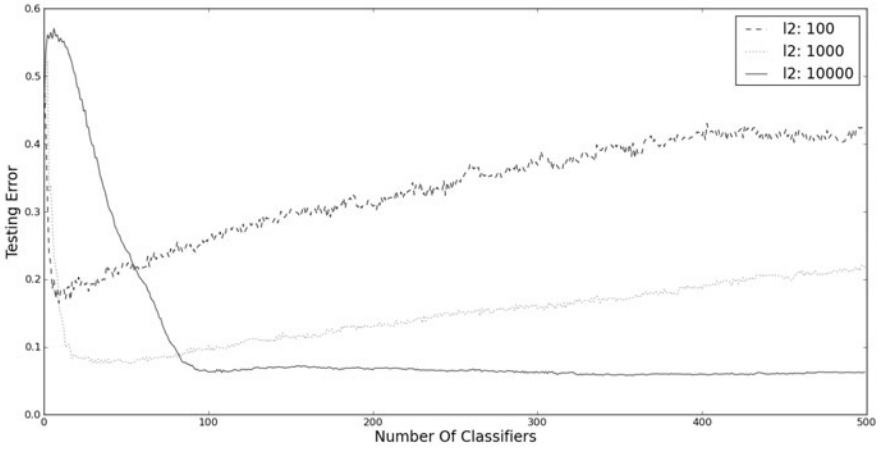

Fig. 12.10 Testing Error of RpBoost.super using $U_{-1,1}$ in Breast dataset for different regularization parameters.

12.4.4 Discussion

In Table 12.7, best classification accuracies obtained on both test patterns and Uci Datasets are reported. For each test pattern, accuracy, classifier and type of projections R_p are shown. For UCI datasets, the value of regularization parameter λ is shown too. RpBoost always performs better than AdaBoost. In addition, RpBoost always provides the best accuracy in the classification of synthetic data using projections drawn from a normal distribution. Very significant improvements are reported in the *annulus* pattern and in the *checkerboard*, *parity* and *disjunctive* patterns where performance increased by more than 10%. In Fig. 12.11, the classification of the *annulus* is shown. Although classification is not perfect, the effect of using RPs is evident. RPs allow to follow the non linear boundary even when using linear weak classifiers as decision stumps. Figure 12.12 shows the classification of the *checkerboard* pattern. Here, in contrast to the others, RpBoost is capable to

Table 12.7 Resume of Results

Test Pattern	Accuracy	Classifier	R_p	Dataset	Accuracy	Classifier	R_p	λ
Sine	98.6%	Sub	N	Liver	74.2%	Ls	-	1000
Linear	99.3%	Sub	N	Breast	97.6%	Super/Sub	P N	10000/ 10000
Parity	96.8%	Same	N	Sonar	86.2%	Ls	-	1000
Annulus	96.5%	Same	N	Monks-1	95.3%	Same	N	1000
Parabolic	98.9%	Same	N	Monks-2	91.6%	Super	P	1000
Disjunctive	93.5%	Sub	N	Monks-3	97.2%	Same	N	1000
Polynomial	99.0%	Same	N	Tic-tac-toe	98.6%	Same	U	10
Checkerboard	95.7%	Same	N	Ionosphere	92.8%	Same/Sub	U N	5000/1000

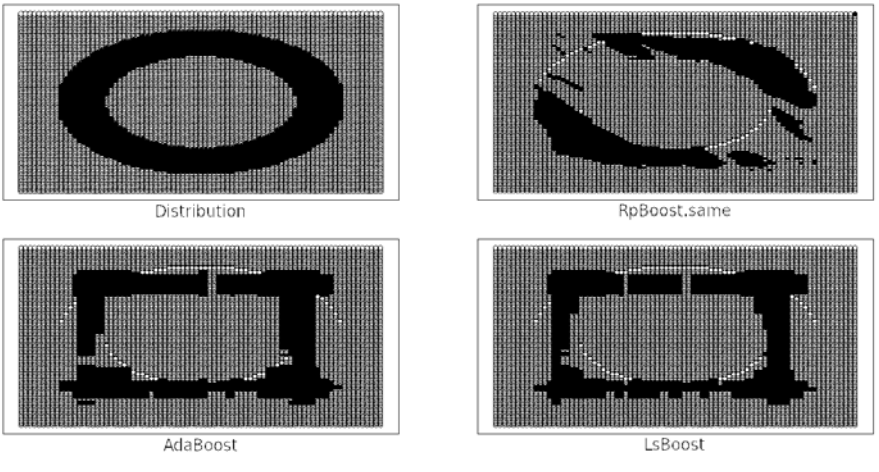

Fig. 12.11 Classification of the *annulus* test pattern using RpBoost, AdaBoost and LsBoost

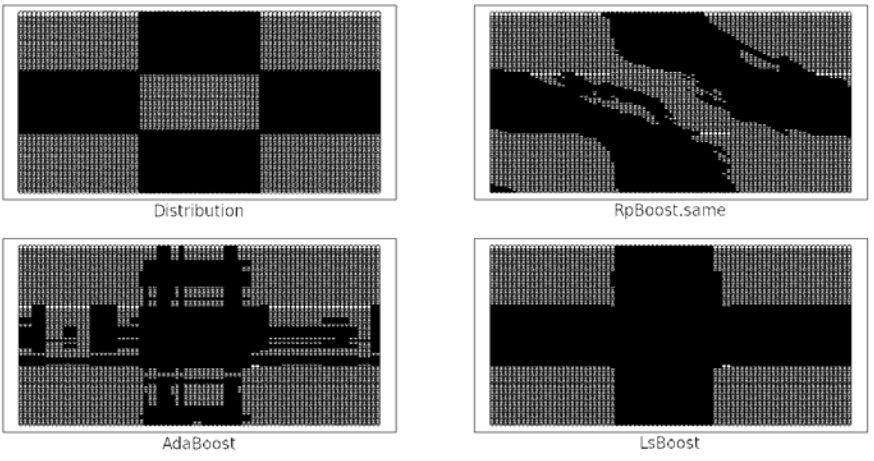

Fig. 12.12 Classification of the *checkerboard* test pattern using RpBoost, AdaBoost and LsBoost

grasp the different class in the central part of the pattern. *Checkerboard* represents a XOR-type problem. Similarly, *parity* and *disjunctive* represent XOR-type problems. On these problems, RpBoost behaves as in the case previously analyzed. This fact is confirmed in the Monks-1 and Monks-2 datasets, both representing XOR-type problems [12]. In these cases, too, the performance of RpBoost is considerably improved, compared to the performance obtained with AdaBoost or LsBoost.

12.5 Conclusion

In this work, Random Projections are used to generate diversity in the construction of regularized Gradient Boosting Machines. In particular, RPs are embedded in a modified version of LsBoost, named RpBoost. At each step of the optimization process, data are projected into a random space and, in the new space, the classifier that best fits the data is selected to be added to the ensemble. Projecting spaces can be subspaces, random spaces of the same dimension than the original feature space and random superspaces.

RpBoost always performs better than AdaBoost on synthetic data and, in the majority of the cases, performs better than LsBoost on real data especially when projections into subspaces or space of the same dimension than the original spaces are used. In these spaces, RpBoost performs well with all types of projections on most of the problems. The use of superspaces yields to better classification accuracy only when the projection is drawn completely at random. In this case, the performance appears to be slightly better than with other types of projections.

The regularization parameter influences the creation of the ensemble, in particular, when high values of regularization are provided. Finding the “optimal” value for

the regularization parameter is crucial especially when there exists a trend to overfitting. Obviously, in the cases where overfitting is present, using a small number of classifiers in the ensemble would have to provide better classification accuracy.

Finally, results clearly show that RpBoost is a promising technique and encourages future research with studies on real-world problems.

Acknowledgements. This work is partially supported by a research grant from projects TIN2009-14404-C02, La Marato de TV3 082131 and CONSOLIDER (CSD2007-00018).

References

1. Arriaga, R.I., Vempala, S.: An algorithmic theory of learning: Robust concepts and random projection. Machine Learning 63, 161–182 (2006)
2. Blum, A.: Random projection, margins, kernels, and feature-selection. In: Saunders, C., Grobelnik, M., Gunn, S., Shawe-Taylor, J. (eds.) SLSFS 2005. LNCS, vol. 3940, pp. 52–68. Springer, Heidelberg (2006)
3. Dasgupta, S.: Experiments with random projection. In: Proc. the 16th Conf. Uncertainty in Artif. Intell., Stanford, CA, pp. 143–151. Morgan Kaufmann, San Francisco (2000)
4. Fawcett, T.: Comparing patterns classifiers, http://home.comcast.net/ tom.fawcett/public_html/ML--gallery/pages/index.html
5. Fradkin, D., Madigan, D.: Experiments with random projections for machine learning. In: Proc. the 9th ACM SIGKDD Int. Conf. Knowledge Discovery and Data Mining, Washington, DC, pp. 517–522. ACM Press, New York (2003)
6. Frank, A., Asuncion, A.: UCI machine learning repository. University of California, School of Information and Computer Sciences, Irvine (2010)
7. Friedman, J.H.: Greedy function approximation: A gradient boosting machine. Annals of Stat. 29, 1189–1232 (2000)
8. Johnson, W.B., Lindenstrauss, J.: Extensions of Lipschitz maps into a Hilbert space. Contemporary Mathematics 26, 189–206 (1984)
9. Pujol, O.: Boosted geometry-based ensembles. In: El Gayar, N., Kittler, J., Roli, F. (eds.) MCS 2010. LNCS, vol. 5997, pp. 195–204. Springer, Heidelberg (2010)
10. Rahimi, A., Recht, B.: Weighted sums of random kitchen sinks: Replacing minimization with randomization in learning. In: Advances in Neural Inf. Proc. Syst., vol. 21, pp. 1313–1320. MIT Press, Cambridge (2008)
11. Rodriguez, J.J., Kuncheva, L.I., Alonso, C.J.: Rotation Forest: A new classifier ensemble method. IEEE Trans. Pattern Analysis and Machine Intell. 28, 1619–1630 (2006)
12. Thrun, S., Bala, J., Bloedorn, E., Bratko, I., Cestnik, B., Cheng, J., De Jong, K., Dzeroski, S., Hamann, R., Kaufman, K., Keller, S., Kononenko, I., Kreuziger, J., Michalski, R.S., Mitchell, T., Pachowicz, P., Roger, B., Vafaie, H., Van de Velde, W., Wenzel, W., Wnek, J., Zhang, J.: The MONK's problems: A performance comparison of different learning algorithms. Technical Report CMU-CS-91-197, Carnegie Mellon University (1991)
13. Zhang, C.-X., Zhang, J.-S.: RotBoost: A technique for combining Rotation Forest and AdaBoost. Pattern Recogn. Letters 29, 1524–1536 (2008)

Chapter 13
An Improved Mixture of Experts Model: Divide and Conquer Using Random Prototypes

Giuliano Armano and Nima Hatami

Abstract. The Mixture of Experts (ME) is one of the most popular ensemble methods used in Pattern Recognition and Machine Learning. This algorithm stochastically partitions the input space of a problem into a number of subspaces, experts becoming specialized on each subspace. To manage this process, the ME uses an expert called gating network, which is trained together with the other experts. In this chapter, we propose a modified version of the ME algorithm which first partitions the original problem into centralized regions and then uses a simple distance-based gating function to specialize the expert networks. Each expert contributes to classify an input sample according to the distance between the input and a prototype embedded by the expert. The Hierarchical Mixture of Experts (HME) is a tree-structured architecture which can be considered a natural extension of the ME model. The training and testing strategies of the standard HME model are also modified, based on the same insight applied to standard ME. In both cases, the proposed approach does not require to train the gating networks, as they are implemented with simple distance-based rules. In so doing the overall time required for training a modified ME/HME system is considerably lower. Moreover, centralizing input subspaces and adopting a random strategy for selecting prototypes permits to increase at the same time individual accuracy and diversity of ME/HME modules, which in turn increases the accuracy of the overall ensemble. Experimental results on a binary toy problem and on selected datasets from the UCI machine learning repository show the robustness of the proposed methods compared to the standard ME/HME models.

13.1 Introduction

Most real-world pattern recognition problems are too complicated for a single classifier to solve. Divide-and-conquer has proved to be efficient in many of these

Giuliano Armano · Nima Hatami
DIEE- Department of Electrical and Electronic Engineering, University of Cagliari,
Piazza d'Armi, I-09123, Italy
E-mail: {armano,nima.hatami}@diee.unica.it

O. Okun et al. (Eds.): Ensembles in Machine Learning Applications, SCI 373, pp. 217–231.
springerlink.com

complex situations, using a combination of classifiers which have complementary properties. The issues are (i) how to divide the problem into simpler subproblems, (ii) how to assign base classifiers to solve these subproblems, and (iii) how to obtain the final decision using their outputs.

In some cases the problem can be decomposed manually. However, in most real-world problems, we either know too little about the problem, or it is difficult to achieve a clear understanding of how to manually decompose it into subproblems. Thus, a method for automatically decomposing a complex problem into a set of overlapping or disjoint subproblems is desirable, assigning one or more classifiers (experts hereinafter) to each subproblem.

Jacobs et al. [5, 6] have proposed an ensemble method based on the divide-and-conquer principle called Mixture of Experts (ME), in which a set of networks referred to as *expert networks* is trained together with a *gate network*. This tight coupling mechanism (i) encourages diversity among experts by automatically localizing them in different regions of the input space and (ii) achieves good dynamic combination weights of the ensemble members by concurrently training the gate together with the experts. The Hierarchical Mixture of Experts (HME) [7] is a well-known tree-structured architecture, which can be thought of as a natural extension of the Mixture of Experts (ME) model. The expert networks form the leaves of the tree, whereas gating networks are located at the branch-points. Tasks are approached using a "recursive" divide-and-conquer strategy: complex tasks are decomposed into subtasks which in turn are themselves decomposed into sub-subtasks. Like many known classical artificial neural network ensemble methods, diversity in the standard HME is promoted by randomly initializing their weight parameters. This choice drives experts to start learning their task from different points in the search space, with the goal of getting them specialized on different subspaces.

Since Jacobs' proposal in 1991, the ME model has been widely investigated. Many of the earlier works on the ME and HME models use preprocessing to partition or transform the input space into simpler and more separable spaces. An expert is then specialized on each subspace without altering the learning rules established by the standard ME model. As a consequence, the major effort in earlier works has been spent in the task of increasing the individual accuracy of experts, so to facilitate their task on the corresponding areas of expertise. Waterhouse and Cook [11] and Avnimelech and Intrator [2] proposed to combine ME with the Boosting algorithm. Since Boosting encourages classifiers to become experts on patterns that previous experts disagree on, it can be successfully used to split the data set into regions for the experts in the ME model, thus ensuring their localization and diversity. Tang et al. [9] tried to explicitly "localize" experts by applying a cluster-based preprocessing step, aimed at partitioning their input space. In particular, they used self-organizing maps (SOM) to partition the input space according to the underlying probability distribution of the data. As a result, better generalization ability together with more stability in parameter setting is achieved. Nevertheless, as they argue at the end of the paper, the proposed method has been designed for (and validated on) only binary and low dimensional problems. Wan and Bone [10] used a mixture of radial basis function networks to partition the input space into statistically correlated

regions and learn the local covariance model of the data in each region. Ebrahimpour et al. [3] proposed a view-independent face recognition system using ME by manual decomposition of the face view space into specific angles (views), an expert being specialized on each view. Nevertheless, the proposed method is only efficient in 2D face recognition and, as argued by the authors, extending this approach to other classification problems and applications could be challenging and not always possible.

It is worth pointing out that, in the original formulation of the ME model, parameters are determined by maximum likelihood, which is prone to severe overfitting, including singularities in the likelihood function. This can be particularly problematic in a complex model such as the HME, due to the relatively large number of parameters involved in defining the distributions for experts and gating networks. Indeed, there are many singularities in the likelihood function which arise whenever one of the mixture components "collapses" onto a single data point. In any case, simultaneously training gating networks and experts in an HME architecture (with the goal of obtaining sufficiently accurate classifiers with relatively optimum parameters) continues to pose a research challenge.

Recently, Armano and Hatami have proposed a classifier selection method to be used in selection-fusion strategies [1]. The method called Random Prototype-based Oracle, RPO, splits the input domain based on some prototypes selected randomly from training data and then builds a classifier on each subset. These classifiers are used in combination with an oracle that knows the area of expertise of each classifier, thus generating a mini-ensemble. Thanks to the random nature of this splitting procedure, mini-ensembles created on a specific problem differ from one run to another. Each mini-ensemble can be used as base classifier in any ensemble strategy to improve its accuracy without increasing the computational cost required for training.

Inspired by the above mentioned idea, we decided to assign a random prototype to each expert in the ME model. In this modified ME model, called "Mixture of Random Prototype-based Experts" , the input space is partitioned according to the nearest distance from randomly-chosen prototypes. This facilitates the adoption of a weighting policy based on distances in both training and testing. In other words, instead of a complex gating network which requires a training process to adjust its weight parameters, the proposed gating function manages both training and testing using a distance-based measure.

Subsequently, we extended the idea above by embedding a set of random prototypes into each module of the HME model. Instead of specializing each expert on a stochastic and nested area in the feature space, ME experts focus on the centralized subspace defined by their corresponding prototypes. This allows to simplify the gating networks with simple distance-based measures, thus simplifying the structure of the modified HME model. Moreover, while increasing the individual accuracy of the ME modules used in the first layer of an HME architecture, their diversity is also expected to increase due to the random selection of prototypes (which makes the prototypes of a module different from those used by the others). Finally, the time required to train the proposed HME architecture dramatically decreases due to the

large saving in the training time of each ME module. Experimental results confirm the above mentioned claims.

The rest of the chapter is organized as follows. In Sect. 13.2, we briefly recall the standard ME model and its hierarchical counterpart. Section 13.3 first presents random prototype-based splitting, then introduces the proposed mixture of random prototype-based experts, and finally extends it to the hierarchical setting. Experimental results are reported and discussed in Sect. 13.4. Section 13.5 concludes the chapter and briefly outlines future research directions.

13.2 Standard Mixture of Experts Models

13.2.1 Standard ME Model

The adaptive mixture of local experts [5, 6] is a learning procedure which achieves improved generalization performance by assigning different subtasks to different experts. Its basic idea consists of concurrently training several experts and a gating network. The gating function assigns a "probability" to each expert based on the current input. In the training phase, this value denotes the probability for a pattern to appear in the training set of an expert. In the test step, it defines the relative contribution of each expert to the ensemble. The training step attempts to achieve two goals: (i) for a given expert, find the optimal gating function; (ii) for a given gating function (network), train each expert to achieve maximal performance on the distribution assigned to it by the gating function. Accordingly, the accuracy of an ME classifier is affected by the performance of both expert networks and gating network. Resulting misclassifications in this model derive from two sources: (a) the gating network is unable to correctly estimate the probability for a given input sample and (b) local experts do not learn their subtask perfectly. Let us consider the network shown in Fig. 13.1, which represents an ME model with $N = 3$ experts. The ith expert produces its output $o_i(x)$ as a generalized linear function of the input x:

$$o_i(W_i, x) = f(W_i x), \tag{13.1}$$

where W_i is the weight matrix of the ith expert and $f(.)$ is a predefined continuous nonlinearity. The gating network is also a generalized linear function, and its ith output, $g_i(V_i, x)$, is the multinomial logit or softmax function of the gating network's output, o_{g_i}.

$$g_i(V_i, x) = \frac{exp(o_{g_i})}{\sum_{j=1}^{N} o_{g_i}} \quad i = 1, ..., N, \tag{13.2}$$

where V_i is the weight vector of the gating network. Hence, the overall output of the ME architecture, $o(x)$, is

$$o(x) = \sum_i g_i(V_i, x) o_i(W_i, x). \tag{13.3}$$

Two training procedures are suggested in the literature [5, 7] for finding optimal weight parameters W_i and V_i. The first is the standard error back-propagation algorithm with gradient descent, whereas the second is based on the Expectation-Maximization (EM) method.

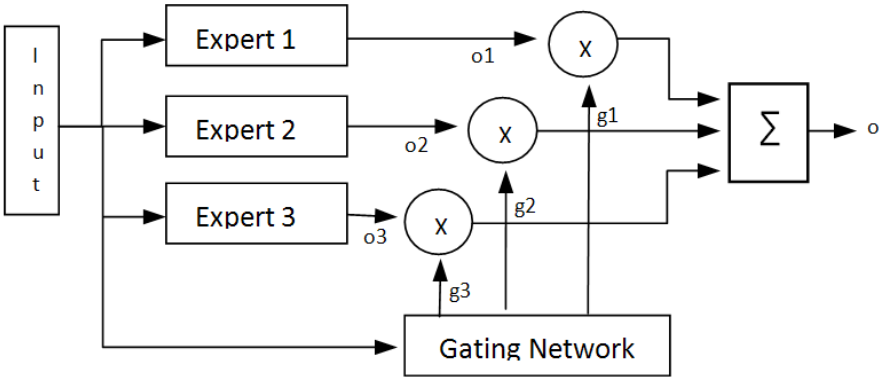

Fig. 13.1 Block diagram representing the Mixture of Experts (ME) model. The generic model shown here has three experts (N=3) and the gating network as a mediator for managing the process.

13.2.2 Standard HME Model

The HME architecture (Fig. 13.2) is a tree in which the gating networks lie at the nonterminal nodes and the expert networks lie at the leaves of the tree. Hence, it can be considered an ensemble of ME modules (as shown by dashed boxes). The task of each expert is to approximate a function over a region of the input space. Given a sample, the task of the gating network is to assign the weights to each expert. Figure 13.2 illustrates a mixture of four experts. In accordance with the typical terminology used for describing HME architectures: $\bar{x}$ is the input vector, $o_{ij}(\bar{x})$ is the output (expected value) of the ijth expert, $g_i(\bar{x})$ is the output of the top gating network, denoting the prior probability for the pattern to be generated by the left or right branch of the root, and $g_{j|i}(\bar{x})$ is the output of the ith bottom gating network, denoting the prior probability that the pattern is generated by the ijth expert. In addition, t is the target (desired output) and $P_{ij}(t|\bar{x})$ is the probability associated with the ijth expert.

Assuming that experts are mutually exclusive, the overall probability, $P(t|\bar{x})$ and the expected value at the network output, $o(\bar{x})$, are given by:

$$P(t|\bar{x}) = \sum_i g_i(\bar{x}) \sum_j g_{j|i}(\bar{x}) P_{ij}(t|\bar{x}), \tag{13.4}$$

$$o(\bar{x}) = \sum_i g_i(\bar{x}) \sum_j g_{j|i}(\bar{x}) o_{ij}(\bar{x}). \tag{13.5}$$

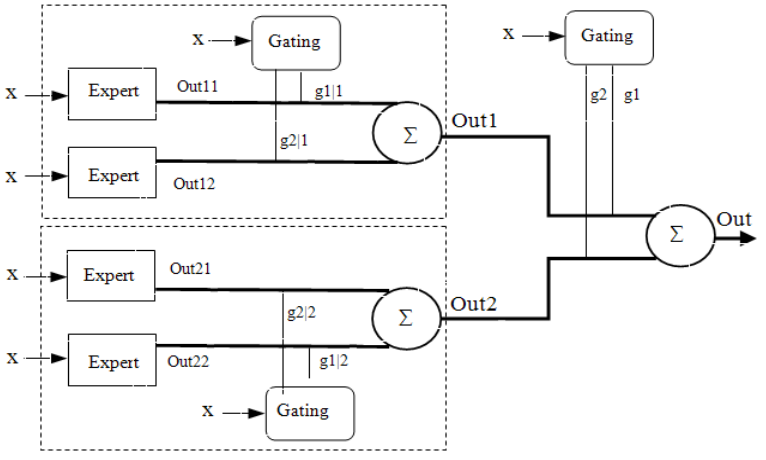

Fig. 13.2 Block diagram representing a two-layer HME. The generic model shown here has four experts (two ME modules, each embedding two experts) and three gating networks which act as mediators.

Note that the notations defined for the two-level depth tree shown in Fig. 13.2 can be easily extended to larger HME networks with a binary tree architecture.

Two training procedures are suggested in the literature [3, 9, 10] for finding optimal weight parameters of the HME architecture. The first is the standard error back-propagation algorithm with gradient descent and the second procedure is based on the Expectation-Maximization (EM) method.

13.3 Mixture of Random Prototype-Based Experts (MRPE) and Hierarchical MRPE

13.3.1 Mixture of Random Prototype-Based Local Experts

In this section, we illustrate the proposed mixture of random prototype-based experts with more detail. The key underlying idea is to randomly partition the input space of the problem into subspaces and then specialize each expert on each subspace by means of "soft" competitive learning. First of all, the input space is partitioned according to some prototypes randomly chosen from the training set, so that the input samples are weighted during the training and testing phases based on their distances from the selected prototypes. The main advantage of this method is that, instead of a complex gating network which must be trained concurrently with other experts, the generated gating function has no parameters (weights) to adjust – as

it simply enforces a distance-based weighting policy. This modification improves three important aspects of the standard ME model. First, it reduces the training time by decreasing the number of parameters to be estimated. Secondly, as simple distance measures used by the gating function are more robust with respect to errors in determining the area of expertise of an expert, errors in the proposed ME model are mainly limited to the error made by the expert networks, thus improving the overall accuracy of the classifier. Lastly, the region of expertise for each expert in the standard ME model is nested, which makes the problem difficult to learn. In the proposed method, each expert's area of expertise is more centralized, which makes the subproblem easier to learn. The latter property also makes the rules embedded by an expert easy to analyze, which is vital in some applications that need to make explicit the information about the area of expertise of each expert.

For the sake of simplicity and ease of comprehension, we describe this approach for the synthetic two-class problem shown in Fig. 13.3a. We used two different partitioning methods, i.e. disjoint and overlapping, shown in Figs. 13.3b and 13.3c respectively. In case of disjoint partitioning, we first measure the distance between each training sample and the prototypes, and then assign a fixed value, η_j, to the h_i of the expert proportional to these distances. h_i is an estimate of the "a posteriori" probability for the ith expert to generate the desired output o and used as the coefficient of the learning rate for updating the weight parameters of the expert (static strategy). This implies that the weight update on the expert network whose prototype is nearest to the current input sample will be stronger than those performed on the others (the closer the expert, the stronger the update is). Similarly, in the testing phase, the expert whose prototype is nearest to the input sample will contribute to a greater extent to the final output.

Unlike disjoint partitioning, where the learning rate coefficients are fixed for each partition and change sharply from one to another, in the overlapping method they change smoothly, proportional to the distances (dynamic strategy). Similarly, the amount of d_i for the ith expert depends on how close the prototype is to the current input sample x. In other words, for disjoint learning, the amount of expertise and contribution of experts is fixed for each partition, whereas, for overlapping learning, their expertise smoothly vary with the distance d_i from the prototypes embedded in the experts. It is worth pointing out that the proposed method is general enough to be applied for building ME classifiers using both standard error back-propagation and EM learning rules. Algorithm 7 reports the procedure to be used for training and testing a mixture of random prototype-based experts, using both disjoint and overlapping partitioning rules for any chosen learning method.

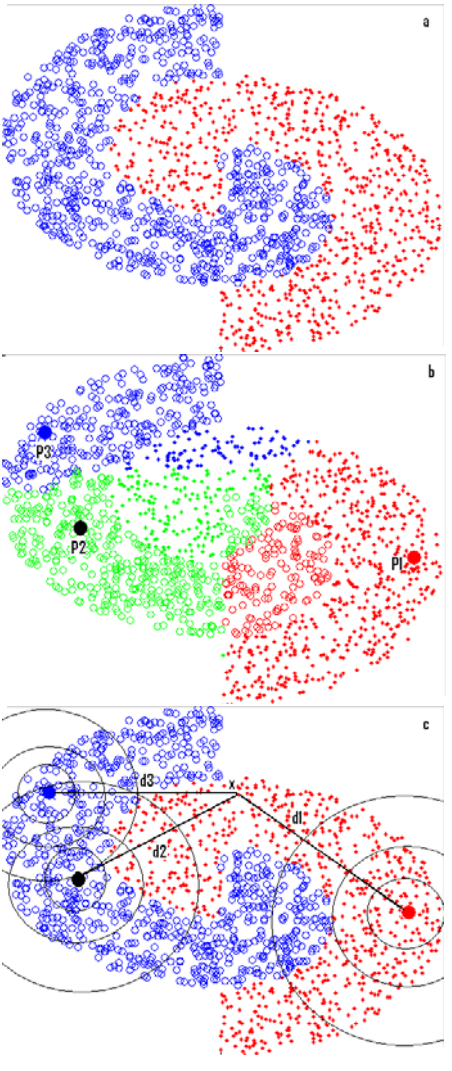

Fig. 13.3 Partitioning of a 2-class semantic classification problem using N=3 random prototypes (bold points denote prototypes selected from training data): a) original problem, b) partitioning into three disjoint regions based on the nearest distance from the prototypes, c) partitioning into three overlapping subspaces.

Algorithm 7. Mixture of Random Prototype-based Experts

PARAMETERS:

- $strategy = \{static, dynamic\}$
- N number of experts in an ME classifier
- $E = \{\eta_j \in (0,1) \mid j = 1..N\}$ such that: $\eta_k \leq \eta_{k+1}; k = 1..N-1$ and $|E| = \sum_j \eta_j = 1$

WITH:

- $\Psi = \{\varepsilon_i \mid i = 1..N\}$ set of experts
- $P = \{p_i \in LS \mid i = 1..N\}$ set of randomly chosen prototypes, each assigned to an expert
- LS/TS = Learning/Training Set

TRAINING:

For $x \in$ LS Do:

- $D(x) = \{d_i(x) \mid i = 1..N\}$ where
  $d_i(x) = \|x - p_i\|$
- $H(x) = \{h_i(x) \mid i = 1..N\}$ where
  $h_i(x)$ represents the expected capability of ε_i to deal with the given input x
  $[strategy = static] : h_i(x) = \eta_r, \quad r = Rank(\varepsilon_i, D(x))^*$
  $[strategy = dynamic] : h_i(x) = 1 - \frac{d_i}{\|D(x)\|}, \quad \|D(x)\| = \sum_j d_j(x)$
- update each expert ε_i $(i = 1..N)$ according to the standard learning rule for ME

TESTING:

Given an $x \in$ TS Do:

- $D(x) = \{d_i(x) \mid i = 1..N\}$
- $G(x) = \{g_i(x) \mid i = 1..N\}$ where
  $[strategy = static] : g_i(x) = \eta_r, \quad r = Rank(\varepsilon_i, D(x))^*$
  $[strategy = dynamic] : g_i(x) = 1 - \frac{d_i}{\|D(x)\|}, \quad \|D(x)\| = \sum_j d_j(x)$
- calculate the overall output:
  $o_j(x) = \sum_i^N g_i(x) \cdot o(x, W_i)$
- select the class label c_k such that
  $k = argmax_j\ (o_j(x))$

* $r = Rank(\varepsilon_i, D(x))$ returns the rank of expert ε_i (i.e. a number in [1,N]) according to the distance $D(x)$ evaluated on the input x (the lower the distance, the highest the ranking).

13.3.2 Hierarchical MRPE Model

This section presents the proposed hierarchical mixture of random prototype-based experts (HMRPE) with more detail. The key underlying idea is to randomly partition the input space of the problem into subspaces and then pushing each expert to specialize on its subspace by means of "soft" competitive learning.

13.3.2.1 RP-Based Splitting for HME

For each ME module of an HME architecture, the input space is partitioned according to some prototypes randomly chosen from the training set (Fig. 13.4).

Let us note that the learning rules of the first-layer gating networks (gating of the ME modules) change with respect to the standard HME model, whereas the gating networks of the other layers (second, third, and so on) do not.

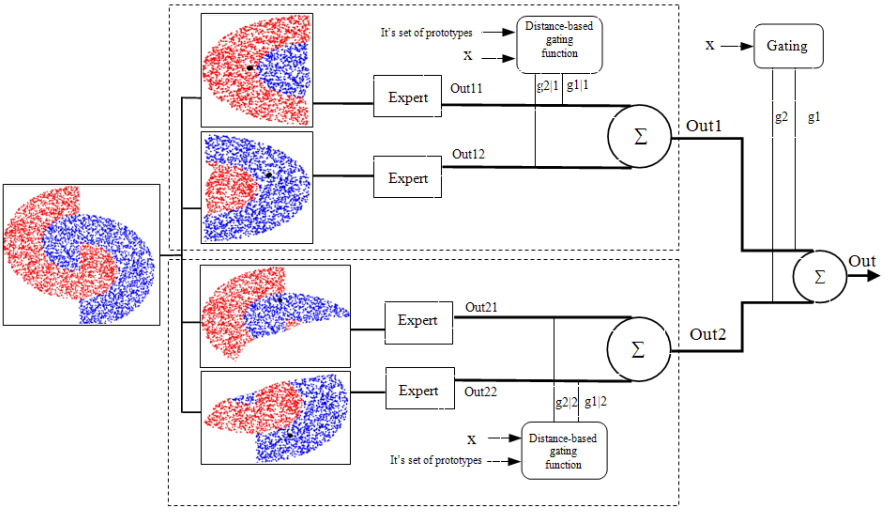

Fig. 13.4 Block diagram representation of the proposed HMRPE model operating on a typical binary toy problem (bold block points denote randomly-selected prototypes)

13.3.2.2 Why Does HMRPE Work?

Notwithstanding the amount of empirical studies proving that diversity and individual accuracy of ensemble members are two primary factors that affect the overall classification accuracy, theoretical studies clearly show that they are not independent [8]. Hence, the success of the proposed HMRPE approach can be attributed to three factors as follows:

1. Splitting the input space into N centralized parts makes the subproblems easier to learn for the expert network. As a consequence, the individual accuracy of the ensemble members is expected to be better than, or at least not worse than, the one exhibited by sets of experts specialized over the nested and stochastic subspaces. It is worth noting that, although expected, higher individual accuracy is not guaranteed by any means, since it depends on the complexity of classification boundaries, on the adopted learning algorithm, as well as on the position of the selected prototypes. Figure 13.5 compares the regions of expertise of an

ME module, embedded in both the standard HME and the HMRPE models, on a four-class toy problem. The figure (first row, first column) shows the original problem, and the next three figures report the nested areas of expertise for the three experts in the standard ME module. The figure (third row, first column) shows how the problem is partitioned using three random prototypes, and the next three figures highlight the centralized areas of expertise of three experts in the proposed HMRPE module.

2. Since each ME module embedded in the HMRPE architecture has its own set of prototypes (which are different from those embedded by the other ME modules), experts are specialized on very different data subsets, thus enforcing diversity.
3. The accuracy of an HME classifier is affected by the performance of both experts and gating networks. Accordingly, resulting misclassifications in this model derive from two sources: (a) the gating networks are unable to correctly estimate the probability for a given input sample and (b) local experts do not learn their subtask perfectly. Since simple distance rules used by the gating function are more robust with respect to errors in determining the area of expertise of an expert, errors in the proposed HMRPE model are mainly limited to the error made by the expert networks, thus improving the overall accuracy of the classifier.

13.4 Experimental Results and Discussion

Some UCI machine learning data sets [12] have been used to check the validity of the proposed method. These data sets include real-world and synthetic problems, with variable characteristics. Table 13.1 shows the selected datasets.

Table 13.1 The main characteristics of the selected UCI datasets

Problem	# Train	# Test	# Attributes	# Classes
Glass	214	-	9	7
Iris	150	-	4	3
Letter	20000	-	16	26
Pendigits	7494	3498	16	10
Satimage	4435	2000	36	6
Segment	210	2100	19	7
Vowel	990	-	11	11
Yeast	1484	-	8	10

For the datasets with no train/test partitioning, the classification performance assessed by the 10-fold cross-validation provides realistic generalization accuracy for unseen data. To build the standard HME and the proposed HMRPE models, we used a Multi-Layer Perceptron (MLP) architecture with one hidden layer, trained with the back-propagation learning rule [4]. To determine the best value for the N partitions, which is equal to the number of experts, we varied it from 2 to 10 for each

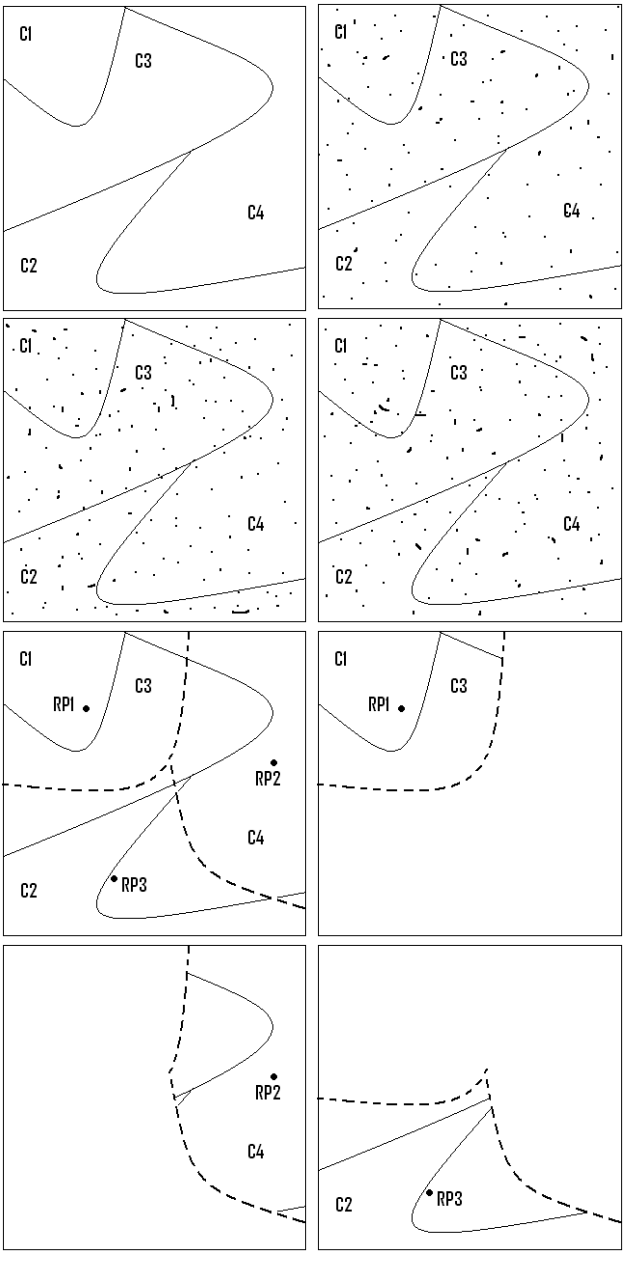

Fig. 13.5 Comparison between the input space partitioning performed by the standard HME (top 4 figures) model and the HMRPE model (bottom 4 figure) for a 4-class toy problem

Table 13.2 The mean and standard deviation of accuracy for the ME vs. the proposed mixture of random prototype-based experts on the selected UCI datasets (in percentage)

	Standard ME	Disjoint partition	Overlapping partition
Glass	87.7 ± 0.61	89.3±0.43	89.6±0.40
Iris	88.7 ± 1.05	90.9±0.80	91.1±0.78
Letter	88.0 ± 0.43	89.5±0.44	90.2±0.31
Pendigits	71.5±0.94	73±0.73	73.8±0.82
Satimage	60.9±1.55	63.8±1.0	64.4±1.21
Segment	79±0.85	82.2±0.68	82.9±0.79
Vowel	72.1±1.75	75.8±1.77	76.9±1.44
Yeast	50.6±2.22	52.7±1.56	54.0±1.45

Table 13.3 The mean and standard deviation of accuracy for the HME vs. the proposed HMRPE on the selected UCI datasets (in percentage)

	Standard HME	Disjoint partition	Overlapping partition
Glass	88.7±0.59	89.3±0.55	90.5±0.49
Iris	87.6±1.1	90.2±0.7	91.3±0.7
Letter	89.0±0.81	89.0±0.45	90.2±0.4
Pendigits	70.9±0.44	72.9±1.1	73.1±1.05
Satimage	61.5±2.05	62.3±2.0	64.1±2.3
Segment	78.5±0.95	82.9±0.78	83.8±0.8
Vowel	73.3±1.8	76.8±1.87	77.0±1.65
Yeast	50.0±2.35	53.7±2.6	54.1±2.6

Table 13.4 Training time of the standard ME and HME vs. the proposed MRPE and HMRPE models (seconds)

	Glass	Iris	Letter	Pendigits	Satimage	Segment	Vowel	Yeast
Standard ME	50	232	351	324	59	49	30	41
MRPE	28	158	221	258	39	32	21	29
Standard HME	84	324	451	604	99	71	44	67
Hierarchical MRPE	198	311	451	451	63	53	30	42

dataset. We also varied the number of hidden neurons in expert networks to experimentally find the optimal architecture of the MLP experts for each problem. The results of these experiments (shown in Tables 13.2 and 13.3) highlight that the proposed method outperforms the standard ME and its hierarchical counterpart for all selected datasets, no matter whether disjoint or overlapping partitions are adopted.

The time required for training the different datasets is shown in Table 13.4 for further comparison. Table 13.4 highlights that the training time of the proposed method is considerably shorter than the standard version. Simulations are performed

using an Intel CPU with 2.83GHz and 4GB RAM memory. Note that the results presented here which compare standard HME and the proposed method, use the same parameters and architecture.

13.5 Conclusion

In this chapter, a modified version of the popular ME algorithm has been presented. Unlike the standard ME, which specializes expert networks on nested and stochastic regions of the input space, the proposed method partitions the sample space into subspaces based on similarities with randomly-selected prototypes. This strategy enables to define a simple rule for the gating network for both training and testing. As shown by experimental results, despite its simplicity, the proposed method improves the accuracy of the both standard ME and HME models while reducing the training time.

Future work will be focused on defining a light procedure for automatically determining the number of experts for a given problem, without resorting to complex preprocessing and time consuming methods. Adapting this method to simple distance-based classifiers (instead of artificial neural networks) is another interesting future research direction, concerned with reducing the training time of the overall network while maintaining high accuracy.

We are also experimenting with heuristics able to help in the process of partitioning the input space (instead of using random prototypes).

References

1. Armano, G., Hatami, N.: Random prototype-based oracle for selection-fusion ensembles. In: Proc. the 20th Int. Conf. Patt. Recogn., Istanbul, Turkey, pp. 77–80. IEEE Comp. Society, Los Alamitos (2010)
2. Avnimelech, R., Intrator, N.: Boosted mixture of experts: An ensemble learning scheme. Neural Comp. 11, 483–497 (1999)
3. Ebrahimpour, R., Kabir, E., Yousefi, M.R.: Teacher-directed learning in view-independent face recognition with mixture of experts using overlapping eigenspaces. Comp. Vision and Image Understanding 111, 195–206 (2008)
4. Haykin, S.: Neural networks: A comprehensive foundation. Prentice Hall, Upper Saddle River (1999)
5. Jacobs, R., Jordan, M.I., Barto, A.: Task decomposition through competition in a modular connectionist architecture: The what and where vision tasks. Technical Report 90-44, Univ. Massachusetts, Amherst (1991)
6. Jacobs, R., Jordan, M.I., Nowlan, S., Hinton, G.: Adaptive mixtures of local experts. Neural Comp. 87, 79–87 (1991)
7. Jordan, M.I., Jacobs, R.A.: Hierarchical mixtures of experts and the EM algorithm. Neural Comp. 6, 181–214 (1994)
8. Kuncheva, L.I.: Combining pattern classifiers: Methods and algorithms. John Wiley & Sons, Hoboken (2004)

9. Tang, B., Heywood, M., Shepherd, M.: Input partitioning to mixture of experts. In: Proc. the 2002 Int. Joint Conf. Neural Networks, Honolulu, HI, pp. 227–232. IEEE Comp. Society, Los Alamitos (2002)
10. Wan, E., Bone, D.: Interpolating earth-science data using RBF networks and mixtures of experts. In: Mozer, M., Jordan, M.I., Petsche, T. (eds.) Advances in Neural Inf. Proc. Syst., vol. 9, pp. 988–994. MIT Press, Cambridge (1997)
11. Waterhouse, S., Cook, G.: Ensemble methods for phoneme classification. In: Mozer, M., Jordan, M.I., Petsche, T. (eds.) Advances in Neural Inf. Proc. Syst., vol. 9, pp. 800–806. MIT Press, Cambridge (1997)
12. UCI Repository of Machine Learning Databases, Dept. of Inf. and Comp. Sci., Univ. of California, Irvine, http://archive.ics.uci.edu/ml/

Chapter 14
Three Data Partitioning Strategies for Building Local Classifiers

Indrė Žliobaitė

Abstract. Divide-and-conquer approach has been recognized in multiple classifier systems aiming to utilize local expertise of individual classifiers. In this study we experimentally investigate three strategies for building local classifiers that are based on different routines of sampling data for training. The first two strategies are based on clustering the training data and building an individual classifier for each cluster or a combination. The third strategy divides the training set based on a selected feature and trains a separate classifier for each subset. Experiments are carried out on simulated and real datasets. We report improvement in the final classification accuracy as a result of combining the three strategies.

14.1 Introduction

Divide-and-conquer approach has been recognized in multiple classifier systems. The idea is to build and maintain individual classifiers with local specialization [3, 6, 7, 9, 11]. As an illustration, consider the task of evaluating scientific research proposals for funding. Given a research proposal in accordion music we would like to assign it to an expert in music rather than biology.

There are two main design issues when constructing such systems of local classifiers. The first is how to partition the data to form the clusters of local expertise. In the research funding example, the tracks for submissions may be defined in different ways: based on the area (biology, music, literature, physics), theoretical versus

Indrė Žliobaitė
Smart Technology Research Centre, Bournemouth University
Poole House, Talbot Campus, Fern Barrow, Poole, Dorset, BH12 5BB, UK

Eindhoven University of Technology, P.O. Box 513, 5600 MB Eindhoven, the Netherlands
E-mail: izliobaite@bournemouth.ac.uk

O. Okun et al. (Eds.): Ensembles in Machine Learning Applications, SCI 373, pp. 233–250.
springerlink.com

industrial projects, based on the size of a requested budget or combination of all criteria. In multiple classifier systems, this corresponds to different ways to train local experts to ensure local specialization.

The second design issue is how to assign the incoming data to one or several available experts for a decision making. In the research proposal example, suppose that there is no annotation, only the proposal text itself is available. A secretary reads through the incoming proposals and determines to which track to assign it. In multiple classifier systems, this corresponds to associating an incoming instance with a particular cluster of expertise.

A popular design of such locally specialized systems is to cluster the training data and train a separate classifier on each cluster. In such systems the incoming instance is directed to one of the classifiers for decision making based on its cluster membership (e.g. [3, 7, 11, 12]). Depending on the data, this approach may lead to high class imbalance within clusters and raise challenges for training individual classifiers. We introduce one modification and one alternative partitioning strategy to overcome this problem.

We experimentally analyze the three strategies for data partitioning to build local classifiers. The effects to the final classification accuracy are demonstrated using a synthetic dataset and six real datasets. We experimentally show under what circumstances these strategies are beneficial. We report improvement in final classification accuracy as a result of combining the three strategies.

The paper is organized as follows. In Sect. 14.2 we present three alternatives for training local classifiers. In Sect. 14.3 we illustrate the alternatives by analyzing a synthetic dataset. In Sect. 14.4 we present and analyze experimental results using six real datasets. Section 14.5 concludes the study.

14.2 Three Alternatives for Building Local Classifiers

Multiple classifier systems with local expertise can be designed in two different ways. The first way is to train local classifiers on random subsets of data and then control the diversity by fusion rules (e.g. Bagging [1], see also a review [2]). The second way is to partition the data in a directed manner to form clusters of similar data (e.g. using clustering as in [3, 7, 11]). In such a case an individual classifier (a local expert) is trained on each cluster; we call this approach *a directed diversity*.

Our study concerns the second type of approaches. Intuitively, expert based decision making is meaningful if we can train competent experts. We investigate strategies how to build competent local experts in classification. More specifically, we look how to divide the input space into regions of competence, so that each region represents a local classification problem.

Regions of competence can be defined using all or selected features of the input data, and the label information. We study three alternatives for partitioning the training data, based on: all features without label information, all features with label information and one selected feature.

14.2.1 Instance Based Partitioning

A straightforward way to form local experts is to cluster the input data [3, 7, 11]. In such a case no label information is used for partitioning the data. Let $\mathbf{X}$ be the input data. The instance space is partitioned into k regions by applying a selected clustering algorithm on $\mathbf{X}$. Let $R_1, R_2, \ldots, R_k$ be the sets of indices of the instances, belonging to one of k regions. An ensemble of classifiers $\mathscr{L} = L_1, L_2, \ldots, L_k$ is constructed using each subset for training one classifier: $L_i : y = f_{R_i}(X)$. Note that for partitioning the unlabeled data is used, while for training local classifiers the class labels are needed. We refer to this partitioning strategy as CLU.

Two design decision needs to be made for CLU. First, the number of clusters k needs to be fixed as close as possible to the nature of the data. Second, a clustering algorithm with a distance metric needs to be chosen. Recall the research proposal example. Suppose we have a pile of historical not annotated documents, but we know (domain knowledge) that the proposals came from three departments: biology, physics and music. Thus, we can choose to partition the documents into $k = 3$ clusters. If we do not have the background knowledge, we need to guess k.

After we decided how to train local classifiers, we need to decide in what way to assign the incoming instances to those classifiers. Typically in CLU they are assigned to the classifier, 'in charge' for the closest cluster center. The same distance metric as in the original clustering needs to be used.

In the proposal example the ultimate task is to classify the new incoming document to 'accept' or 'reject' class. Given a new document we do not know its label, but we can extract the content features the same way we did for the historical data. Based on these features we can assign the document to one of the existing clusters. Based on the cluster assignment we ask the local expert to decide 'accept' or 'reject'. The procedure for CLU is summarized in Fig. 14.1.

CLUSTERING (CLU)
input: training dataset $\mathbf{X}$ with labels $\mathbf{y}$; number of partitions k.
output: trained multiple classifier system $\mathscr{L}$.

1. Cluster the input data $(R_1, R_2, \ldots, R_k) = clust(\mathbf{X}, k)$,
   where $clust(.,k)$ is any distance based clustering algorithm,
   R_i is a set of indices, assigned to cluster i.
2. For each cluster $i = 1 \ldots k$
   train a local expert $L_i : y = f_{R_i}(X)$,
   where f_{R_i} is a classifier trained on R_i instances.
3. Form an ensemble $\mathscr{L} = L_1, L_2, \ldots, L_k$,
   where an unseen instance X' is assigned to the classifier
   L_i: $i = \arg\min_{i=1\ldots k} dist\,(X', center(R_i))$.

Fig. 14.1 Clustering strategy (CLU) to form local classifiers

14.2.2 Instance Based Partitioning with Label Information

The problem with clustering approach to build local classifiers is that it may produce clusters with high class imbalance. This happens as clusters may capture some of the actual class membership ('accept' or 'reject') information. This distorts prior distributions of the classes, for instance, we may get many 'accepts' in one cluster, while many 'rejects' in the other. Training an accurate classifier on such distorted subsets may be challenging.

We propose an alternative to overcome capturing class discriminative information. The idea is to cluster the classes separately and then use all possible combinations selecting one cluster from each class. Let $X^{(1)}, X^{(2)}, \ldots, X^{(c)}$ be the partitioning of historical data based on the class membership, where c is the number of the classes. First we cluster each $X^{(j)}$ to obtain k_j subsets $R_1^{(j)}, R_2^{(j)}, \ldots, R_{k_j}^{(j)}$. Then we build a multiple classifier system, consisting of $k_1 \times k_2 \times \ldots \times k_c$ classifiers: $L_{i_1 i_2 \ldots i_c}$: $y = f_{R_{i_1}^{(1)} \cup \ldots \cup R_{i_c}^{(c)}}(X)$. One classifier is trained on a combination of c subsets of the training data, where each class is represented by one subset. Such an approach allows to handle the problem of class imbalance within one cluster. As the data is partitioned within each class separately, class discriminatory information does not affect the partitioning. Note, that the subsets $R_1^{(1)}, R_2^{(1)}, \ldots, R_{k_1}^{(1)}, \ldots, R_1^{(c)}, R_2^{(c)}, \ldots, R_{k_c}^{(c)}$ do not intersect, and together form an input data X. We refer to this strategy as CL2.

We assign a new incoming instance for a decision making based on the proximity to the cluster centers, in a similar way to CLU. However in CL2 an instance is assigned to c nearest clusters (one from each class), since we do not know the true class membership.

CL2 approach requires the number of clusters $k_1, k_2, \ldots, k_c$ to be given as parameters.

For the intuition behind the approach recall the proposal example. We know the labels of the historical documents, i.e. which of them were 'accepted', which were 'rejected'. The 'rejected' proposals in biology may happen to be similar in content to the 'accepted' proposals in physics. Thus we are interested to learn the peculiarities to distinguish between the two. We first cluster all the 'accepted' documents. Then we cluster all the 'rejected' documents independently. Then build a local classifier using the two closest clusters as a training set. We illustrate CL2 in Fig. 14.2 and summarize the procedure in Fig. 14.3.

14.2.3 Partitioning Using One Feature

The result of data partitioning using clustering may differ depending on which clustering algorithm and distance measure are used. We propose an alternative way to form local experts, which is expected to be more robust. We propose to select a feature and slice the data based on that feature. We will call the selected feature *the slicing feature*

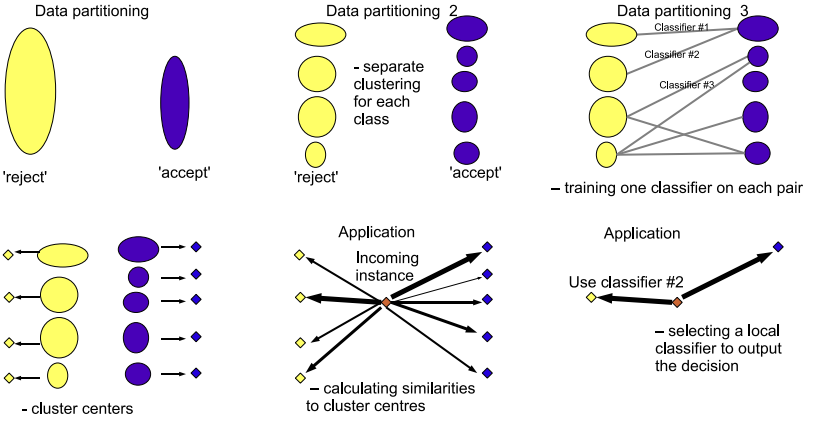

Fig. 14.2 Illustration of CL2 partitioning

CLUSTERING WITH LABELS (CL2)
input: training dataset $\mathbf{X}$ with labels $\mathbf{y}$;
numbers of partitions $(k_1, k_2, \ldots, k_c)$ for each class.
output: trained multiple classifier system $\mathscr{L}$.

1. Split the historical data based on class membership into $X^{(1)}, X^{(2)}, \ldots, X^{(c)}$,
   where $X^{(j)}$ is a set of all instances labeled as class j.
2. For each class $j = 1 \ldots c$
   cluster the input data $(R_1^{(j)}, R_2^{(j)}, \ldots, R_{kj}^{(j)}) = clust(\mathbf{X}, k_j)$.
3. For all combinations $(i_1 i_2 \ldots ic)$, where $i_j \in (1, 2, \ldots, k_j)$,
   train a local expert $L_{i_1 i_2 \ldots i_c} : y = f_{R_1^{(c)}, R_2^{(c)}, \ldots, R_{k_c}^{(c)}}(X)$.
4. Form an ensemble $\mathscr{L} = L_{11\ldots1}, L_{11\ldots2}, \ldots, L_{k_1 k_2 \ldots k_c}$,
   where an unseen instance X' is assigned to the classifier
   $L_{i_1 i_2 \ldots i_c}$: for j=1:c, $i_j = \arg\min_{i_j = 1 \ldots k_j} dist\left(X', center(R_{i_j}^{(j)})\right)$
   .

Fig. 14.3 Clustering with label information (CL2) to form local classifiers

The training data needs to be partitioned into k subsets. We select a feature x_s, where $s \in p$, p is the number of features. We split the range of the feature x_s into k equal intervals. Let $\delta_k = \frac{\max x_s - \min x_s}{k}$. Then the i^{th} interval is r_i : $[\min x_s + (i-1)\delta_k, \min x_s + i\delta_k)$[1]. The historical data is partitioned into subsets $R_1^{(F)}, R_2^{(F)}, \ldots, R_k^{(F)}$, where an instance $X^j \in R_i^{(F)}$ is assigned to the i^{th} subset, if the value of its slicing feature $x_s^j \in r_i$ is in the range of that partition. One local

[1] The value $\min x_s + k\delta_k = \max x_s$ for the last interval r_k is inclusive.

classifier is trained on each subset. An incoming instance will be assigned to a classifier based on the value of its feature x_s the same way. We call this approach FEA.

In the research proposal example there may be experts that are good in evaluating short and concise proposals and another experts that are good in long detailed proposals. Suppose we have a feature in the feature space that records the number of words in the document. The partitions may be formed conditioning on that feature, e.g. if the number of words is less than 2000 then assign it to the first cluster, otherwise to the second cluster.

There are two parameters to be specified for FEA: k and x_i. A simple way is to select x_i using domain expertise or visual inspection of the data. We will elaborate more on selecting the slicing feature in Sect. 14.4.4.4.

The procedure for FEA is summarized in Fig. 14.4.

ONE FEATURE BASED PARTITIONING (FEA)
input: training dataset $\mathbf{X}$ with labels $\mathbf{y}$;
number of partitions k; slicing feature x_s.
output: trained multiple classifier system $\mathscr{L}$.

1. For $i = 1 \ldots k$, calculate slicing intervals:
   $r_i : [\min x_s + (i-1)\delta_k, \min x_s + i\delta_k)$,
   where $\delta_k = \frac{\max x_s - \min x_s}{k}$.
2. Partition the input data into $R_1^{(F)}, R_2^{(F)}, \ldots, R_k^{(F)}$,
   where $X^j \in R_i^{(F)}$ if $x_s^j \in r_i$.
3. For $i = 1 \ldots k$ each partition
   train a local expert $L_i : y = f_{R_i^{(F)}}(X)$,
   where $f_{R_i^{(F)}}$ is a classifier trained on $R_i^{(F)}$ instances.
4. Form an ensemble $\mathscr{L} = L_1, L_2, \ldots, L_k$,
   where an unseen instance X' is assigned to classifier L_i if
   ${x'}_s^j \in r_i$.

Fig. 14.4 Slicing based on one feature (FEA) to form local classifiers

14.3 Analysis with the Modeling Dataset

For exploring CLU, CL2 and FEA partitioning strategies we construct a modeling dataset. We generate dataset in 2D, where four cluster centers are fixed at $(0,0)$, $(4.5,3)$, $(1,3)$, $(3,0.1)$. We label two centers as 'class 1' and the other two as 'class 2'. We generate 5000 normally distributed instances for each center. The data is illustrated in Fig. 14.5. As it is seen from the plot, the data is linearly inseparable. We will demonstrate how a multiple classifier system, consisting of locally specialized linear classifiers classifies this data.

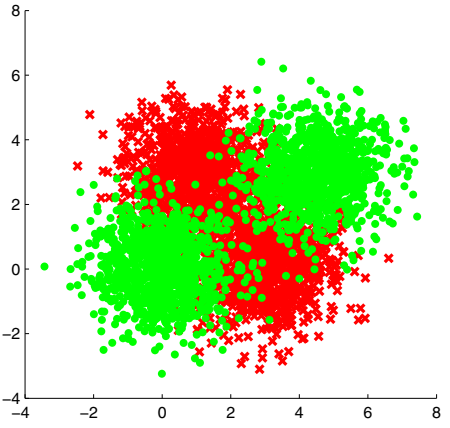

Fig. 14.5 Modeling dataset, green and red colors represent two classes

14.3.1 Testing Scenario

We generate an independent testing set using the same distribution as for training. We generate a testing set of 20000 instances in total.

14.3.1.1 Performance Metrics

We compare testing errors of the alternative strategies that indicate their generalization performance. We use the mean absolute error measure. A standard error is calculated assuming Binomial distribution over testing errors $SE = \sqrt{\frac{E \times (1-E)}{N}}$, where E is the observed error and N is the testing sample size.

14.3.1.2 Alternative Strategies

We experimentally compare the performance of CLU, CL2 and FEA. Figure 14.6 gives an example of the partitions by the three strategies on the modeling data. '$\times$' indicates an instance under consideration. We plot the areas of local expertise around this instance (a) for CLU, in (b) for CL2 and in (c) for FEA.

In addition to the three discussed strategies, we experiment the strategy that averages the outputs of the three. We will refer to it as MMM. Let $\hat{Y}_{CLU}$, $\hat{Y}_{CL2}$ and $\hat{Y}_{FEA}$ be the labels output by the three respective strategies. Then $\hat{Y}_{MMM} = \frac{\hat{Y}_{CLU} + \hat{Y}_{CL2} + \hat{Y}_{FEA}}{3}$. The intuition is to combine the diverse views on the same instance obtained by the respective strategies.

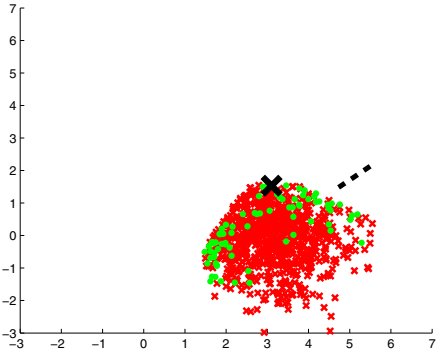

(a)

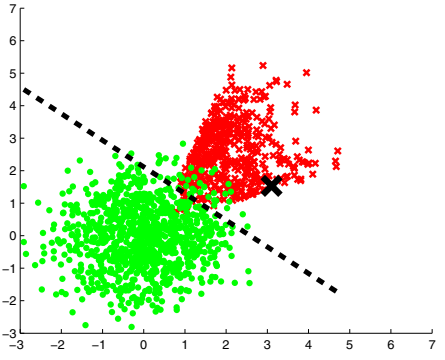

(b)

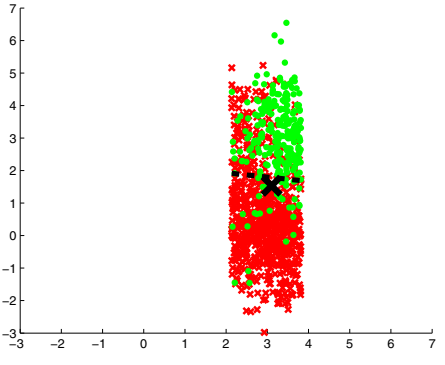

(c)

Fig. 14.6 Illustration of data partitioning: (a) CLU, (b) CL2 and (c) FEA

This strategy can be viewed as an ensemble of ensembles, where classifier selection is used in the first level and then classifier fusion is applied on top of that. This combination is similar to the random oracle [10]. The principal difference is that random oracle uses the same partitioning strategy for all mini-ensembles. In this experimental study we investigate the performance of alternative partitioning strategies rather than ensemble building strategies, thus we do not include oracles in our experiments.

In addition, we include two benchmark strategies in our experiments. With the first strategy we test the benefits of specialization. Here the instances to train local classifiers are assigned at random instead of employing a directed procedure. In this case the classifiers are expected to have no specialization, since it will be trained on a random subset of the historical data. We refer to this strategy as RSS.

The second benchmark strategy does not do any partitioning of the data. It trains a single classifier on all the available historical data. We call it ALL. Comparing to this strategy allows us to investigate the effects of reduced training sample size towards the prediction accuracy.

Finally, we include a baseline strategy, which assigns all the labels according to the highest prior probability. We refer to it as NAY.

14.3.1.3 Number of Clusters

In the modeling dataset four clusters can be identified visually. We investigate the strategies of building local classifiers under two scenarios: A) the number of subclasses fits correctly (in our modeling dataset $k = 4$) and B) the number of classes is incorrect (we use $k = 9$). That means for CLU, FEA and RSS we test $k = 4$ and $k = 9$ respectively. For CL2 we test $k_1 = k_2 = 2$ and $k_1 = k_2 = 3$. The latter case leads to $k = 3 \times 3 = 9$ local experts for CL2.

14.3.1.4 Base Classifier

We choose logistic regression as the base classifier. The motivation for this choice is twofold. First, the weights can be interpreted as the importance score of each feature. Thus it is popular in application tasks, such as credit scoring. Second, it is a parametric classifier, thus rearranging the training subsets changes the local expert rules significantly.

We already mentioned that partitioning strategies are likely to distort prior probabilities of the classes within each subset as compared to the whole set of historical data. Logistic regression uses prior information in training, thus *a correction for priors* is required. We use a prior correction for rare events [8]. The regression coefficients are statistically consistent estimates, while the correction for an intercept is as follows: $\beta_0 = \hat{\beta}_0 - \log\left[\left(\frac{1-\tau}{\tau}\right)\left(\frac{\pi}{1-\pi}\right)\right]$, where $\hat{\beta}_0$ is an intercept estimated from the training sample, τ is the population prior for the 'class 1' and π is the sample prior for the 'class 1'.

14.3.2 Results

In Table 14.1 we provide the testing errors of the discussed strategies on the modeling dataset. We run two experiments with different number of clusters. In the first experiment $k = 4$ is the same as in our modeling data. In the second experiment $k = 9$ the number of partitions we are going to make is different from the number of clusters in the original data. The best results are indicated in **bold**. In both cases MMM outperforms the baseline strategies by a large margin. In case when the number of clusters is correct ($k = 4$), CLU has a comparable performance, however it performs much worse if k is set incorrectly.

Table 14.1 Testing errors using the modeling dataset

	A: $k = 4$ error, standard error	B: $k = 9$ error, standard error
CLU	10.6% (±0.2)	12.1% (±0.2)
CL2	13.9% (±0.2)	14.3% (±0.2)
FEA	17.1% (±0.3)	14.1% (±0.2)
MMM	**10.5**% (±0.2)	**10.5**% (±0.2)
RSS	49.7% (±0.4)	49.8% (±0.4)
ALL	49.7% (±0.4)	49.8% (±0.4)
NAY	50.0% (±0.7)	50.0% (±0.7)

Interestingly, we observe an improvement in the performance of FEA when the number of subsets is increased to $k = 9$. This can be explained by the nature of the modeling data. It is not linearly separable, thus the slices of the data selected by FEA are not separable as well, see Fig. 14.6(c). But the smaller are the slices in this case, the more linearly separable are the subsets.

14.4 Experiments with Real Data

We analyze the performance of the three strategies using six real datasets.

14.4.1 Datasets

The characteristics of the six datasets used in the experiments are presented in Table 14.2. All datasets present a binary classification task for simplicity and computational issues; however, the tested strategies are not restricted to the binary tasks. For Shuttle data we aggregated the classes into a binary task (‘class 1’ against all the

others). In Marketing data we transformed the categorical features to numerical by expanding the feature space. We constructed Chess dataset[2] using the statistics from Chess.com, the task is to predict the outcome of a game given the players and game setup characteristics. Elec2 dataset is known to be non-stationary. In these settings non-stationarity is expected to be handled directly by local learners.

Table 14.2 Real datasets used in the experimental evaluation

	size	dimensionality	class balance	source
cred	1000	23	70% – 30%	(German credit) [13]
shut	43500	9	22% – 78%	(Shuttle) [13]
spam	4601	57	39% – 61%	(Spam) [5]
marc	8993	48	47% – 53%	(Marketing) [5]
elec	44235	7	43% – 57%	(Elec2) [4]
chess	503	8	39% – 61%	author collection

14.4.2 Implementation Details

Testing sets were formed using the holdout testing procedure. Each dataset was split into two equal parts at random, one was used for training, the other for testing.

The parameters and experimental choices were fixed as follows, unless reported otherwise. The number of partitions was fixed to $k = 4$ in all partitioning strategies (CLU, CL2, FEA, RSS). We chose to use simple and intuitive k-means clustering algorithm.

For FEA we chose the slicing feature to be the first feature in a row having 4 or more distinct values. The selected feature may be different across the datasets, but the procedure for choosing it is the same for all.

14.4.3 Experimental Goals

The goal of these experiments is to compare the classification accuracies when using the three partitioning strategies (CLU, CL2, FEA) and a combination of those (MMM) and analyze the underlying properties of the data leading to these accuracies.

We aim to be able to assign the credits for a better accuracy. Thus, two benchmarks (ALL, RSS) and a baseline (NAY) are included for control reasons. We look at the following guidelines for control:

- We expect the partitioning strategies (CLU, CL2, FEA) to do better than no partitioning (ALL) in order for partitioning to make sense.

[2] The dataset is available at
http://sites.google.com/site/zliobaite/resources-1

- We expect random partitioning (RSS) not to perform much worse than no partitioning (ALL). Much worse accuracy would indicate that a small sample size within each partitioning causes problems.
- NAY gives the error of classification if all the instances are predicted to have the same label; given equal costs of mistakes we expect all the intelligent predictors to do better.

In addition, we aim to analyze the effect of directed diversity to the accuracy of MMM achieved by our strategies for building local classifiers.

We present two sets of experimental results. First we present and discuss the accuracies of each strategy. Second, we analyze the relationship between outputs of the four strategies (CLU, CL2, FEA, MMM).

14.4.4 Results

In Table 14.3 we compare the testing errors of the alternative partitioning strategies. Clustering strategies (CLU, CL2) and the feature based partitioning (FEA) do not show significant effect on accuracies individually. However, blending all three (MMM) leads to significant improvement in accuracy and dominates in five out of six datasets.

Table 14.3 Testing errors using the real datasets

	cred	shut	marc	spam	elec	chess
testing errors						
CLU	31.8%	3.9%	30.5%	11.0%	29.3%	22.2%
CL2	32.8%	2.2%	32.1%	11.6%	32.5%	27.0%
FEA	28.7%	**1.6**%	28.8%	11.5%	32.4%	28.3%
MMM	**28.2**%	2.1%	**24.8**%	**8.4**%	**24.7**%	**19.3**%
RSS	32.7%	5.3%	34.5%	11.5%	32.1%	27.9%
ALL	31.2%	5.4%	32.2%	11.7%	32.7%	26.9%
NAY	31.0%	21.4%	46.5%	38.7%	42.6%	42.1%
standard error	(±2.0)	(±0.1)	(±0.7)	(±0.7)	(±0.3)	(±3.0)

14.4.4.1 Accuracies

RSS performs worse than ALL in all six datasets. The difference in errors quantifies the effect of reducing the training sample size when training local classifiers. When we partition the input space into non overlapping regions to gain on specialization of classifiers, as a result we lose on sample size. We can see from the table that the deterioration in accuracy is not that drastic. However, smaller sample sizes can partially explain the mediocre performance of the individual partitioning strategies (CLU, CL2, FEA).

14.4.4.2 Diversity

Averaging over three strategies leads to the significant improvement in accuracy. We look at how diverse are the individual outputs. In Fig. 14.7 we picture pairwise correlations between classifier outputs. Black corresponds to perfect correlation (1) and white denotes independence (0). 'Spam' and 'shut' are nearly black because overall accuracy on these datasets is higher. We see that different partitioning strategies lead to diverse outputs of individual classifiers.

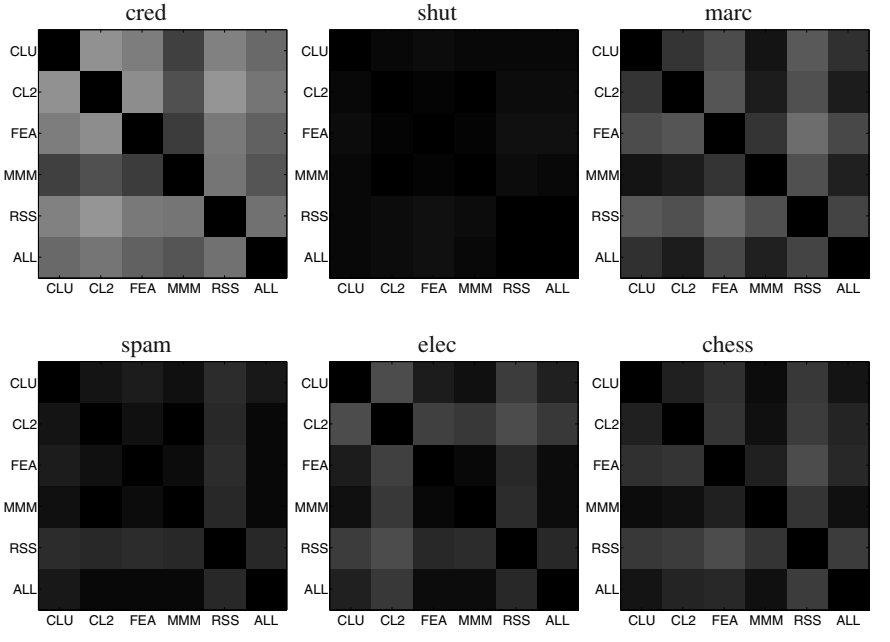

Fig. 14.7 Correlations of the classifier outputs

14.4.4.3 How Many Partitions?

In the experiments we used fixed number of clusters ($k = 4$). In order to see the effect of local specialization we look at the sensitivity of the results to the number of clusters. For that test we choose the two largest datasets 'shut' and 'elec', as they have the sufficient number of instances for a large number of partitions. Figure 14.8 plots the relationship between the number of clusters and testing error for the strategies.

The performance of the partitioning strategies is slightly improving with increasing number of clusters and then stabilizes. The results indicate that directed classifier specialization is not that sensitive to knowing or guessing the correct number of partitions in the data.

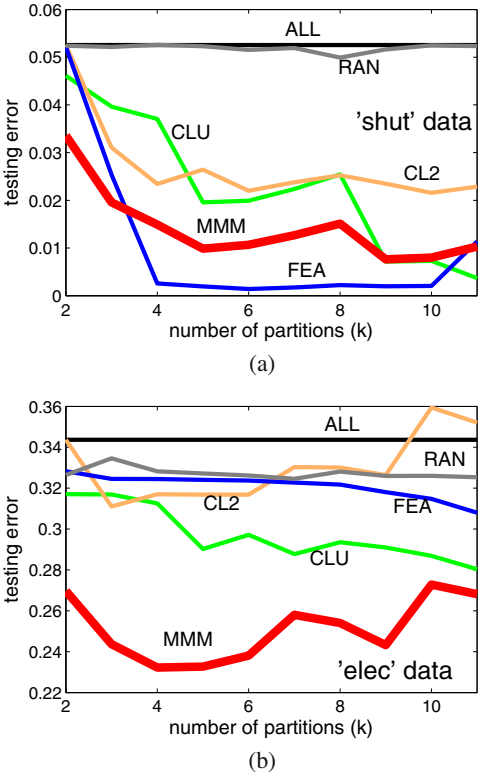

Fig. 14.8 Sensitivity of testing accuracy to the number of clusters: (a) 'shut', (b) 'elec'

14.4.4.4 Which Slicing Feature to Select for FEA?

In the experiments we fixed the procedure for choosing the slicing feature for FEA strategy. Let us investigate how sensitive the results are to the choice of the slicing feature on 'shut' and 'elec' datasets. In Fig. 14.9 we plot the relationship between the number of clusters and testing error.

The results indicate that the performance of the ensemble (MMM) is quite stable, no matter which feature is used for partitioning. In 'shut' dataset CLU and CL2 have a good consent, thus the vote of FEA is not essential. One can see that MMM follows CLU and CL2 very closely in 'shut' dataset. However, the performance of FEA itself in 'shut' dataset is interesting to analyze. It shows notable volatility along different choices of the slicing feature.

The accuracy of FEA is exceptionally good when using the first feature in 'shut' dataset. Let us look closer what makes this set up to perform so well. In Fig. 14.10 we plot the sizes of partitions for each choice of the slicing feature. Each bar represents full dataset, and each sector shows the size of one partition within that run. Recall, that for each run we use four partitions ($k = 4$).

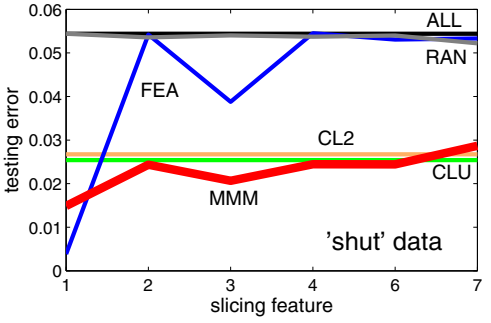

(a)

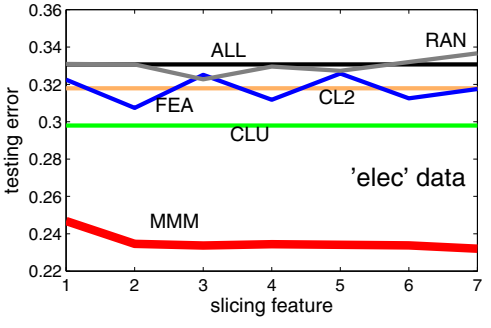

(b)

Fig. 14.9 Sensitivity of testing accuracy to choice of the slicing feature in FEA: (a) 'shut', (b) 'elec'

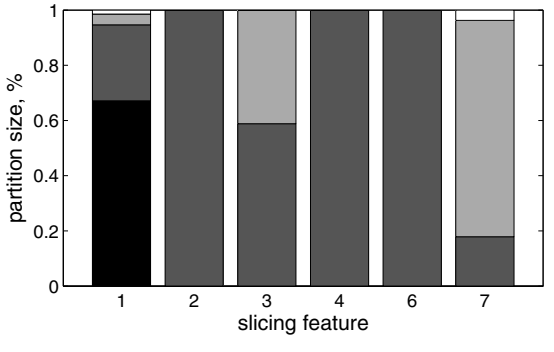

Fig. 14.10 Sizes of partitions in FEA, 'shut' data

The plot shows that for slicing feature 2, 4 and 6 a single partition dominates in size. It means that most of the data fall in one cluster, which is nearly the same as using a single classifier. That is not desirable, since we are aiming to build a multiple classifier system. Not surprisingly, in those cases (feature 2, 4 or 6) the accuracy of

FEA is nearly the same as ALL, see Fig. 14.9. On the other hand, choosing slicing features 1, 3 or 7 gives at least two clusters of distinctive size. In two of these cases (1 and 3) FEA stand alone gives better accuracy than ALL. Why the slicing feature 7 is not performing that well? Let us have a closer look.

In Fig. 14.11 we plot the regression coefficients of local classifiers built using FEA strategy. Each subplot represents different slicing feature, thus different experimental run. Each line represents one trained regression model. We plot only the models resulting from the two largest partitions. The plot suggests that in case when slicing feature 7 is used, both local models (green and blue) follow the global model ALL (black) very closely. That means that the partitions we get in that case are not that different from all training set. Such partitions can be regarded as random subsamples of the whole data, thus do not give much value added for building local models. On the other hand, in cases of slicing features 1 and 3 the resulting local models (green and blue) are quite distinct from the global models (black), that is the value added to the partitioning approach.

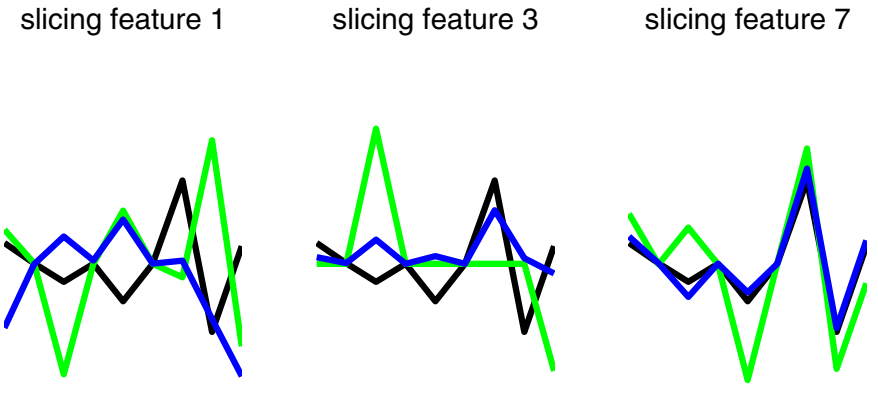

Fig. 14.11 Regression coefficients of FEA local classifiers (green and blue) and ALL classifier (black)

To answer the question, which slicing feature to select for FEA, let us look at the relations between features in 'shut' dataset. In Table 14.4 we present the correlation matrix of the training data. We depict only the features that we analyzed in this section as well as the class label.

The slicing features that lead to good partitioning (1, 3 and 7) also have high correlation with the label. Features that lead to bad accuracy (features 2, 4, 6, recall Fig. 14.9) show low correlation with the label and with the other features, suggesting that these features are not informative for the classification task at hand. Correlations are calculated on the training data and they can be used as an indication, which feature to choose for slicing. We recommend selecting a feature, that is strongly correlated with label and other features. We also recommend to inspect whether the resulting partitions have volume, i.e. ensure that the data is distributed among the

Table 14.4 Correlation matrix of 'shut' training data (high correlations in **bold**)

feature	1	2	3	4	6	7	label
1	-	0.06	**0.26**	-0.01	0	**-0.75**	**-0.66**
2	0.06	-	-0.01	-0	-0	-0.06	0
3	**0.26**	-0.01	-	0.02	-0	**0.43**	**-0.13**
4	-0.01	-0	0.02	-	0	0.03	0
6	0	-0	-0	0	-	-0.01	0.01
7	**-0.75**	-0.06	**0.43**	0.03	-0.01	-	**0.54**
label	**-0.66**	0.00	**-0.13**	0.00	0.01	**0.54**	-

clusters. Finally, we recommend to inspect the resulting local classifiers, to ensure that they represent different data distributions. This can be done by inspecting the parameters of the trained models, or by monitoring the diversity of the classifier outputs.

14.5 Conclusion

We experimentally investigated three approaches of building local classifiers. Each partitioning strategy individually often does not give significant improvement in accuracy as compared to a single classifier. However, blending the three strategies demonstrates significant improvement in accuracy as compared to the baseline and benchmarks.

This approach can be viewed as a two level ensemble. The first level uses deterministic classifier selection from a pool of local classifiers. The second level averages over individual classifiers selected from different partitions of the input space.

We identify several properties of the partitions that lead to improvement in overall accuracy as compared to a single classifier. We recommend partitioning using a feature that is strongly correlated with the labels and other features. We also recommend to inspect whether the resulting partitions have sufficient data volume as well as to monitor that the resulting local classifiers output diverse predictions.

A natural and interesting extension of this study would be to look at partitioning strategies, not limited to distance in space as clustering. One relevant direction for further research is developing meta features to describe subsets of instances and use them for nominating the classifiers (experts) that make the final decision.

Acknowledgements. The research leading to these results has received funding from the European Commission within the Marie Curie Industry and Academia Partnerships and Pathways (IAPP) programme under grant agreement no. 251617. The author thanks Dr. Tomas Krilavičius for feedback on the experimental setting.

References

1. Breiman, L.: Bagging predictors. Machine Learning 24(1996), 123–140 (1996)
2. Brown, G., Wyatt, J., Harris, R., Yao, X.: Diversity creation methods: a survey and categorization. Inf. Fusion 6, 5–20 (2005)
3. Frosyniotis, D., Stafylopatis, A., Likas, A.: A divide-and-conquer method for multi-net classifiers. Pattern Analysis and Appl. 6, 32–40 (2003)
4. Harries, M.: Splice-2 comparative evaluation: Electricity pricing. Technical Report UNSW-CSE -TR-9905, Artif. Intell. Group, School of Computer Science and Engineering, The University of New South Wales, Sidney (1999)
5. Hastie, T., Tibshirani, R., Friedman, J.: The elements of statistical learning: data mining, inference and prediction. Springer, Heidelberg (2005)
6. Jacobs, R., Jordan, M., Nowlan, S., Hinton, G.: Adaptive mixtures of local experts. Neural Computation 3, 79–87 (1991)
7. Katakis, I., Tsoumakas, G., Vlahavas, I.: Tracking recurring contexts using ensemble classifiers: an application to email filtering. Knowledge and Inf. Syst. 22, 371–391 (2009)
8. King, G., Zeng, L.: Logistic regression in rare events data. Political Analysis 9(2001), 137–163 (2001)
9. Kuncheva, L.: Clustering-and-selection model for classifier combination. In: Proc. the 4th Int. Conf. Knowledge-Based Intell. Eng. Syst. and Allied Technologies, Brighton, UK, pp. 185–188 (2000)
10. Kuncheva, L.I., Rodriguez, J.J.: Classifier ensembles with a random linear oracle. IEEE Trans. Knowledge and Data Eng. 19, 500–508 (2007)
11. Lim, M., Sohn, S.: Cluster-based dynamic scoring model. Expert Systems with Appl. 32, 427–431 (2007)
12. Liu, R., Yuan, B.: Multiple classifiers combination by clustering and selection. Inf. Fusion 2, 163–168 (2001)
13. Newman, D.J., Asuncion, A.: UCI machine learning repository, http://archive.ics.uci.edu/ml/

Index